

Multi-scale variability in phytoplankton populations of the North Atlantic basin: from eddies to global change

by

Sophie C. Leterme

A thesis submitted to the University of Plymouth in partial fulfilment for the degree of

DOCTOR OF PHILOSOPHY

School of Biological Sciences
Faculty of Science

In collaboration with:

Sir Alister Hardy Foundation for Ocean Science

University of Plymouth	
Item No.	9007291097
Shelfmark:	S77-7631
THESIS:	

WET

Multi-scale variability in phytoplankton populations of the North Atlantic basin: from eddies to global change

Sophie C. Leterme

Abstract

The Continuous Plankton Recorder (CPR) survey has been deployed since 1931 to describe and analyze plankton variability in the North Atlantic and North Sea. This survey measures the presence and abundance of 437 phytoplankton and zooplankton taxa and provides an assessment of phytoplankton biomass, the Phytoplankton Colour Index (PCI). The diatoms and dinoflagellates are the two main phytoplankton groups identified by the CPR survey. The first part of this work provides insights into the space-time dynamics of phytoplankton communities through an analysis of diatom and dinoflagellate populations in the whole North Atlantic basin. Because the North Atlantic Ocean includes many different biotopes, the second part focuses on the mesoscale variability of phytoplankton species. The long-term fluctuations of the phytoplankton species are studied in the NW and in the NE Atlantic, the two best sampled areas of the CPR survey. In the NE Atlantic, the aim is to determine the contribution of the diatoms and dinoflagellates to the PCI, their fluctuations over 45 years of sampling and their geographical variations. Because local variability in environmental conditions is thought to play a dominant role in temporal fluctuations of phytoplankton biomass, the next part takes advantage to define small areas around the British Isles. This allowed me to study more precisely the processes influencing the long-term variation of phytoplankton assemblages. The North Atlantic Current transports water across the Northern basin of the Atlantic Ocean, along the shelf of Ireland and from the Norwegian current which corresponds to the inflow of oceanic waters into the Norwegian Sea and the North Sea. In this highly hydrodynamic region attention is focused on the fluctuations of plankton species in relation to the currents. The aim of this part is therefore to investigate the fluctuations of phytoplankton biomass, diatoms and dinoflagellates, their geographical distribution and abundance within the area and their relationship with physical processes. The intense hydrodynamic activity observed in the Northwestern Atlantic Shelves Province (NWCS) makes this region especially intriguing from the point of view of physical-biological interactions. The relationship between spatial and temporal structures of eddies (via Sea Surface Heights) and chlorophyll *a* (from the Sea-viewing Wide Field-of-view Sensor, SeaWiFS) was assessed along the Gulf Stream axis. In particular, the physical structures identified were followed and compared with phytoplankton distribution. In addition, the impact of the ISW changing flow along the Scotian Shelf and the influence of Gulf Stream rings along the George Bank is determined. This work demonstrated that changes are occurring in pelagic ecosystems at different temporal and spatial scales. These changes have been illustrated by the spatial variability induced by eddies and/or currents but also by the regional variability of the hydro-climatic processes, influencing in different ways Sea Surface Temperature, wind-regimes and mixing of local environments. Several different aspects of the North Atlantic Oscillations impact on pelagic ecosystems have been highlighted. In the northeast Atlantic, NAO fluctuations imply changes in (i) SST in northern Europe, (ii) wind regimes, (iii) Atlantic Water inflow into the North Sea. In contrast, in the northwest Atlantic, the variations of NAO imply changes in (i) SST on the Scotian Shelf, (ii) coastal currents, and (iii) inflow of Labrador Sea Slope Water (LSSW) towards the Scotian Shelf and Georges Bank. These changes in environmental process impact phytoplankton production, abundance, spatial distribution, community structure phenology and ultimately would impact trophodynamics processes. It is, however, still difficult to explain unambiguously all the mechanisms that are involved in the control of the observed patterns.

Table of contents

1. Introduction	1
2. General Methodology of the Continuous Plankton Recorder survey	10
2.A. SAMPLING AND ANALYSIS	11
2.A.1. <i>The survey</i>	11
2.A.2. <i>Continuous Plankton Recorder</i>	13
2.A.3. <i>Sample analysis</i>	16
2.B. PHYTOPLANKTON	20
2.B.1. <i>The Phytoplankton Colour Index</i>	20
3. Decadal basin-scale changes in diatoms, dinoflagellates, and phytoplankton colour across the North Atlantic	26
3.A. INTRODUCTION	27
3.B. MATERIALS AND METHODS	28
3.B.1. <i>The data</i>	28
3.B.2. <i>Statistical analysis</i>	29
3.C. RESULTS	31
3.D. DISCUSSION	38
3.D.1. <i>Phytoplankton variability in the Eastern Atlantic: towards sea surface temperature and nutrient control</i>	38
3.D.2. <i>Phytoplankton fluctuations in the Western Atlantic: basin-scale circulation control</i>	40
3.D.3. <i>Phytoplankton changes in the Central Atlantic: meteorological control</i>	41
3.D.4. <i>Differential contribution of phytoplankton taxonomic groups to the Phytoplankton Colour Index</i>	42
4. Differential contribution of diatoms and dinoflagellates to phytoplankton biomass in the NE Atlantic and the North Sea	43
4.A. INTRODUCTION	44
4. B. MATERIALS AND METHODS	45
4.C. RESULTS	47
4.C.1. <i>The Northeast Atlantic</i>	47
4.C.2. <i>The North Sea</i>	51
4.D. DISCUSSION	54
4.D.1. <i>Multiple ecosystem states in the NE Atlantic and the North Sea</i>	54
4.D.2. <i>Phytoplankton communities and regime shift in the North Sea</i>	55
4.D.3. <i>Phytoplankton composition and ecosystem structure and function</i>	56
5. Decadal fluctuations of the inflow of North Atlantic Water into the North Sea between 1958-2003 and its impact on plankton assemblages	58
5.A. INTRODUCTION	59
5.B. DATA AND METHODS	60
5.B.1. <i>Phytoplankton data</i>	60

5.B.2. Zooplankton data.....	60
5.B.3. Plankton species indicative of the inflow of oceanic water.....	61
5.B.4. Hydrological and climatic data.....	61
5.B.5. North Atlantic Waters inflow into the North Sea.....	61
5.B.6. Statistical analysis.....	62
5.C. RESULTS.....	65
5.C.1. Long-term changes in the environment.....	65
5.C.2. Decadal fluctuations of phytoplankton in the North Sea.....	69
5.C.3. Decadal fluctuations of zooplankton in the North Sea.....	72
5.C.4. Fluctuations in plankton species indicators of oceanic inflow.....	72
5.C.5. Decadal changes in the North Sea pelagic community composition.....	75
5.D. DISCUSSION.....	78
5.D.1. Long-term fluctuations of Atlantic Waters inflow into the North Sea.....	78
5.D.2. Decadal changes in species indicative of Atlantic inflow.....	81
5.D.3. Long-term fluctuations in the plankton community.....	82
5.D.4. Decadal changes and regime shifts in the North Sea pelagic community composition.....	84
6. Impact of climate and mesoscale physical processes on phytoplankton distribution in the Northwest Atlantic Ocean.....	86
6.A. INTRODUCTION.....	87
6.B. THE GULF STREAM, RINGS AND NORTH ATLANTIC EDDY STRUCTURES FROM REMOTE SENSING (ALTIMETER AND SEAWIFS).....	88
6.B.1. Introduction.....	88
6.B.2. Methods and data.....	88
6.B.3. Results.....	93
6.B.4. Discussion.....	105
6.C. IMPACT OF CLIMATE AND MESOSCALE PHYSICAL PROCESSES ON PHYTOPLANKTON (CONTINUOUS PLANKTON RECORDER AND SEAWIFS) ALONG THE E-ROUTE.....	108
6.C.1. Introduction.....	108
6.C.2. Methods and data.....	108
6.C.3. Results.....	111
6.C.4. Discussion.....	119
6.D. CONCLUSION.....	123
7. General Discussion.....	126
Literature cited.....	138

Number of pages: 152
Words count: 32 896 words

List of abbreviations

- ALACE: Autonomous Lagrangian Circulation Explorer
ANOSIM: ANalysis Of SIMilarities
ANOVA: ANalysis Of Variance
ARGOS: Airborne Remote Geographic/Oceanographic System
ARIMA: AutoRegressive Integrated Moving Average
ATSW: Atlantic Temperate Slope Water
AVISO: Archiving, Validation and Interpretation of Satellite Oceanographic data
BIOENV: correlation-based procedures that define the environmental variables that best explain patterns in the underlying biotic matrix
CALCOFI: CALifornia Cooperative Oceanic Fisheries Investigations
Chl *a*: Chlorophyll *a*
CLS: Collecte Localisation Satellites
CPR: Continuous Plankton Recorder
CZCS: Coastal Zone Color Scanner
DEFRA : Department for Environment, Food and Rural Affairs
DNMI: Norwegian Meteorological Institute
ERS: European Remote Sensing
GPS: Global Positioning System
HadISST: Hadley centre sea Ice and SST data set
HAB: Harmful Algae Bloom
HMS: Her Majesty's Ship (UK)
ICES: International Council for the Exploration of the Sea
LSSW: Labrador Subarctic Slope Water
LSW: Labrador Sea Water
MDS: Multi-Dimensional Scaling
NAO: North Atlantic Oscillation
NC: North Central
NCC: Norwegian Coastal Current
NE: NorthEast
NODS: NON-metric multi-Dimensional Scaling
NORWECOM: NORWegian ECOlogical Model system
NW: NorthWest
PCI: Phytoplankton Colour Index
PRIMER5: Plymouth Routines in Multivariate Ecological Research version 5

SAHFOS: Sir Alister Hardy Foundation for Ocean Science

SC: South Central

SE: SouthEast

SeaDAS: SeaWiFS Data Analysis System

SeaWiFS: Sea-viewing Wide Field-of-view Sensor

SLA: Sea Level Anomaly

SOOP: Ship Of OPportunity

SSH: Sea Surface Height

SST: Sea Surface Temperature

SW: SouthWest

UK: United Kingdom

USA: United States of America

XBT: eXpendable BathyThermograph

List of tables

Table 2.1. Phytoplankton analysis: calculating abundance of a particular taxonomic entity in a CPR sample. The total number of fields out of 20 in which the taxon was present is converted to a value representing the total number of cells of that taxon present in those 20 fields. This is then multiplied by 10,000 to give the abundance per sample and compressed into 10 values to give the recorded abundance per sample in the database. (from Richardson *et al.* 2006).

Table 2.2. Diatom taxa identified since 1958 by the CPR survey (from CPR database)

Table 2.3. Dinoflagellate taxa identified since 1958 by the CPR survey (from CPR database).

Table 3.1. Results of Kendall's statistical test for the whole time series of PCI, total diatoms and total dinoflagellates over the period 1958-2002. Significant ($p < 0.05$) results are in bold.

Table 3.2. Proportion of significant correlation over the period 1958-2002 between the monthly time series of PCI, total dinoflagellates and total diatoms and SST across the North Atlantic.

Table 3.3. Kendall's statistical test performed on monthly time series of PCI (A), total diatoms (B) and total dinoflagellates (C) over the period 1958-2002. Significant ($p < 0.05$) results are in bold.

Table 3.4. Results of Spearman's correlation analysis between the monthly time series of PCI, diatoms and dinoflagellates and the NAO winter index over the period 1958-2002. Significant ($p < 0.05$) results are in bold.

Table 4.1. Kendall's τ estimated from the time series of PCI, diatoms and dinoflagellates abundance over the period 1958-2002. *5% significance level

Table 4.2. Kendall's τ estimated for the contribution of diatoms and dinoflagellates toward the PCI and their residuals over the period 1958-2002. *5% significance level

Table 4.3. Spearman's ρ estimated between PCI and diatoms and dinoflagellates abundance and (i) the North Atlantic Oscillation index and (ii) the Sea Surface Temperature over the period 1958-2002. *5% significance level

Table 4.4. Spearman's ρ estimated between the contribution of diatoms and dinoflagellates and (i) the North Atlantic Oscillation index and (ii) the Sea Surface Temperature over the period 1958-2002. *5% significance level

Table 5.1. Results of Kendall's statistical test for the yearly time series of Sea Surface Temperature, salinity, nutrients, Phytoplankton Colour Index (PCI), dinoflagellates, diatoms, phytoplankton indicator species and copepod species over the period 1958-2003. * 5% confidence level. Due to missing data, nutrients time series have not been analysed for regions 11 to 13 (-).

Table 5.2. Results of Spearman's correlation analysis between the cumulative sums of the time series of phytoplankton indicator species, copepods and the northern inflow (at 59°17'N) over the period 1958-2003. The analysis was performed only in the areas potentially influenced by the northern inflow (regions 1-8). Black and grey areas represent significant ($p < 0.05$) positive and negative correlations, respectively.

Table 5.3. Results of Spearman's correlation analysis between the cumulative sums of time series of phytoplankton indicator species and copepods and the southern inflow (through the English Channel) over the period 1958-2003. The analysis was performed only in the areas possibly influenced by the southern inflow (regions 8-13). Black and grey areas represent significant ($p < 0.05$) positive and negative correlations, respectively.

Table 5.4. Results of Spearman's correlation analysis between the cumulative sums of time series of plankton species indicators of oceanic inflow and the (N) northern and (S) southern inflow over the period 1958-2003. Black and grey areas represent significant ($p < 0.05$) positive and negative correlations, respectively. White areas correspond to non-significant correlations. Due to the scarce observation of some species in the North Sea, when there were only zeros in the area the analysis was not performed (-). * The considered inflow does not influence this region.

Table 5.5. Result of BIOENV analysis between environmental/hydrologic variables (i.e. SST, NAO, salinity, phosphate, nitrate and inflows of Atlantic waters), phytoplankton indicator species and copepods. The single variable best explaining the patterns within the biotic matrix is underlined and the corresponding weighted Spearman correlation coefficient is indicated.

Table 6.1. Spearman correlation analysis between the monthly time series of PCI and SeaWiFS (original data) and between seasonal cycles of PCI and SeaWiFS over the period 1997-1998. *5% significance level.

Table 6.2. Results of Spearman correlation analysis between the monthly time series of PCI and NAO and both original and residual (seasonal cycle removed) time series of PCI and SST over the period 1995-1998. *5% significance level.

Table 6.3. Structure of the seasonal cycles of Phytoplankton Colour Index (PCI) and SeaWiFS chlorophyll a over the period 1997-1998.

List of figures (abbreviated titles)

Figure 1.1. Stommel diagram, modified from ICES Zooplankton Methodology Manual, Harris *et al.* (eds., 2000), overlaid to show the scales that can be sampled with various platforms, and features such as fronts (from Kaiser *et al.* 2005).

Figure 1.2. Scales of phytoplankton ecology. Horizontal and vertical scales are determined respectively by coefficients of horizontal and vertical diffusion. The time scales for algae are determined by the growth time-scale, μ , (grey band). The processes of importance at each scale are specified in colour (modified from Harris 1986).

Figure 2.1. Continuous Plankton Recorder survey sampling routes between 1958 and 2004

Figure 2.2. A Continuous Plankton Recorder towed behind a ship of opportunity (from SAHFOS archives)

Figure 2.3. The Continuous Plankton Recorder

Figure 2.4.A, B Launch of the Continuous Plankton Recorder (from SAHFOS archives).

Figure 2.5. Lance Gregory (Marine Technician at SAHFOS) removing the internal mechanism from the CPR body on board a ship of opportunity (from SAHFOS archive).

Figure 2.6. The silk is cut into sections (samples), representing 10 nautical miles of tow

Figure 2.7. Paul Tranter (analyst at SAHFOS) undertaking routine analysis of the silk under microscope in the laboratory (from SAHFOS archive).

Figure 2.8. Layout of silk sample showing the 20 phytoplankton fields

Figure 3.1. The North Atlantic basin divided into 6 regions identified on bathymetric criteria and separated according to a north-south axis: Northwest (NW), Southwest (SW), North Central (NC), South Central (SC), Northeast (NE) and Southeast (SE). CPR samples used in this chapter are illustrated in grey.

Figure 3.2. Hovmöller diagrams of PCI, total diatoms abundance and total dinoflagellates abundance over the period 1958-2002 in the different regions of the North Atlantic basin.

Figure 3.3 Cumulative sums of the PCI (A), total diatoms abundance (B) and total dinoflagellates abundance (C) for each month over the period 1958-2002 (540 data points) in the Northeast (black) and the Southeast Atlantic (grey).

Figure 3.4. Fluctuations of the Spearman correlation coefficient (bold lines) obtained between SST and PCI, total diatoms and total dinoflagellates over the period 1958-2002 in the Southwest, Central and Eastern North Atlantic. The Central and the Eastern areas have been divided in two parts: North (orange) and South (blue). The thin lines represent the significant limits at $p < 0.05$.

Figure 3.5. Contribution to the PCI of total diatoms (orange) and total dinoflagellates (green) in the Northeast (A) and Southeast (B) North Atlantic.

Figure 4.1. The NE Atlantic divided into two regions separated according to a North-South axis: North NE (NE) and South NE (SE) and the North Sea divided into three regions:

Northern (N), central (C) and Southern (S) from a North-South axis following the limits of the CPR Standard Areas. CPR samples used in this study are illustrated in grey.

Figure 4.2. Variation of the annual cells concentration of both diatoms (black squares) and dinoflagellates (grey open dots) and PCI (black line) in the North NE Atlantic (A) and the South NE Atlantic (B) and the cumulative sum analysis for each parameters in the North NE Atlantic (C) and the South NE Atlantic (D).

Figure 4.3. Dinoflagellates (grey open dots) and diatoms (black triangles) contribution to the Phytoplankton Colour Index (PCI) for each year over the period 1958-2002 in the north NE Atlantic (A) and the south NE Atlantic (B). The bold lines represent the 5-years running mean illustrating the trends in the time series. Cumulative sums of dinoflagellates (grey) and diatoms (black) contribution to the PCI were determined in the north NE Atlantic (C) and the south NE Atlantic (D).

Figure 4.4. Variation of the annual cells concentration of both diatoms (black squares) and dinoflagellates (grey open dots) and PCI (black line) in the Northern (A), Central (B) and the Southern North Sea (C) and the cumulative sum analysis for each parameters in the Northern (D), Central (E) and the Southern North Sea (F).

Figure 4.5. Dinoflagellates (grey open dots) and diatoms (black triangles) contribution to the Phytoplankton Colour Index (PCI) for each year over the period 1958-2002 in the northern North Sea (A), Central North Sea (B) and southern North Sea (C). The bold lines represent the 5-years running mean illustrating the trends in the time series.

Figure 5.1. Study area divided into 13 regions identified using hydrodynamic (i.e. stratified, mixed and frontal) and bathymetric criteria.

Figure 5.2. Cumulative sums of the North Atlantic Oscillation (NAO) and (A) northern and (B) southern oceanic inflows over the period 1958-2003. The NAO is represented in black and the Atlantic inflow in grey.

Figure 5.3. Decadal means of Sea Surface Temperature for the whole North Sea from 1958 to 2003.

Figure 5.4. Cumulative sums of Sea Surface Temperature (SST) in the different regions of the North Sea and English Channel. Regions 1 and 4, showing different patterns to the other regions are shown in black.

Figure 5.5. Kendall's rank correlation coefficient identifying long-term trends in phytoplankton indicator species (5% significant level: $\tau > 0.201$).

Figure 5.6. Kendall's rank correlation coefficient identifying long-term trends in zooplankton indicator species (5% significant level: $\tau > 0.201$).

Figure 5.7. Second stage Multi-Dimensional Scaling ordinations for similarity matrices of (A) environmental variables, (B) phytoplankton indicator species and (C) copepods in each region of the North Sea (R1-R10).

Figure 5.8. Wind-driven residual currents resulting from a uniform southwest and southeast wind stress of $1.6 \text{ dynes cm}^{-2}$. The length of a current vector determines the strength of the current at its central point. The current arrows are slightly curved to conform to the direction of current flow (after Pingree & Griffiths 1980).

Figure 6.1. Annual Sea Level amplitude (mm) in the North Atlantic. The Gulf Stream route selected (marked black) starts along the continental slope off Cape Hatteras and then follows the maximum amplitude region.

Figure 6.2. Topography of the studied area and Gulf Stream axis (marked orange) adopted in this present study.

Figure 6.3. SeaWiFS Chl *a* patterns observed in the North Atlantic Ocean during the spring bloom in April 1999. Black line contour shows 2000m depth. Plumes extending southward along the spring bloom boundary are labelled a to e (see Fig. 6.4). In the Gulf Stream region, cyclonic structures labelled 1 to 7 (see also Fig. 6.4) are associated with higher levels of Chl *a*. Anticyclonic eddies to the north of the Gulf Stream axis labelled A to G (see Fig. 6.4) are generally associated with lower Chl *a* levels. Low values of Chl *a* near the Gulf Stream route are marked with – sign (these correspond with warm core rings marked with + in Fig. 4)

Figure 6.4. Sea level anomalies (cm) for the North Atlantic Ocean for April 1999. Positive and negative anomalies match the spring bloom boundary near 35°N. Labels a to e correspond to the plumes on chlorophyll frontal boundary and are associated with the south component of an adjacent cyclonic eddy.

Figure 6.5. Seasonal cycles of SeaWiFS Chl *a* ($\text{mg}\cdot\text{m}^{-3}$ Chl *a*) at 34.5°N, 52°W and mean annual cycle over a 5 year data period. Start of the year and first letter of alternate months annotated. The time window corresponding to the buoy track in March (M) and April 1999 is indicated.

Figure 6.6. Variance (annual component removed) of Sea Level Anomalies (cm^2) along the route of the Gulf Stream for an 8 years period.

Figure 6.7. Mean of SeaWiFS Chl *a* ($\text{mg}\cdot\text{m}^{-3}$ Chl *a*; black) and variance (seasonal cycle removed) of SeaWiFS Chl *a* ($[\text{mg}\cdot\text{m}^{-3}$ Chl *a*] 2 ; grey) along the route of the Gulf Stream for a 5 years period.

Figure 6.8. Hovmöller of SLA residuals along the route of the Gulf Stream between September 1997 and December 2000. Negative sign indicates position of a low SLA associated with elevated Chl *a* anomaly (+ in Fig. 6.10). Positive sign indicates position of a high SLA associated with lower Chl *a* anomaly (- in Fig. 6.10).

Figure 6.9. SeaWiFS Chl *a* ($\text{mg}\cdot\text{m}^{-3}$ Chl *a*) seasonal cycle (determined with 5 years of data) from different water masses identified along the Gulf Stream route. The results for stations 1-17 are in grey and for stations 18-92 in black.

Figure 6.10. Hovmöller of SeaWiFS Chl *a* residuals along the route of the Gulf Stream between September 1997 and December 2000. Positive sign indicates position of elevated Chl *a* anomaly associated with low SLA (- in Fig. 6.8). Negative sign indicates position of lower Chl *a* anomaly associated with high SLA (+ in Fig. 6.8).

Figure 6.11. Correlation between SeaWiFS Chl *a* and SLA residuals in the different water masses sampled along the route. Black triangles represent stations 1–17 and stations 18-92 are in white dots.

Figure 6.12. Monthly correlation coefficient between SeaWiFS Chl *a* anomalies and SLA residuals in the different water masses sampled along the route. The results for stations 1–17 are in grey and in black for stations 18-92.

Figure 6.13. Examples of (A) SeaWiFS and (B) SLA structures for August 2001. Warm-core rings are labelled A, B, C, D and cold core rings E, F, G and weaker negative anomalies H, I, J. The arrows represent the currents associated with eddy structure and the sea level slopes between eddies C, G, D have been used to determine the velocity of the flow between the eddies

Figure 6.14. Bottom topography of the study area and the 15 stations sampled along the CPR route (black dots). Stations A and B have been chosen as representative of the shelf and the open ocean, respectively, in order to determine the fluctuations in geostrophic flow along the Shelf Break.

Figure 6.15. Seasonal cycles of Phytoplankton Colour Index (A, B, C) and SeaWiFS chlorophyll *a* ($\text{mg}\cdot\text{m}^{-3}$ Chl *a*; D, E, F) along the CPR route (15 stations). The cycles that were significantly correlated were observed on Georges Bank (stations 2 and 3), Shelf Break (Stations 6 and 7), Sable Island (stations 8 and 9) and St Pierre Bank (stations 13 and 14); see Table 6.C.2.

Figure 6.16. Mean seasonal cycles of PCI (black triangles) and SeaWiFS chlorophyll *a* ($\text{mg}\cdot\text{m}^{-3}$ Chl *a*; open dots) over the period 1997-1998 along the CPR route. The error bars are the standard deviation.

Figure 6.17. Hovmöller diagram of original data (A), seasonal cycle (B) and anomalies after removing the seasonal cycle (C) of Phytoplankton Colour Index (PCI) for the 15 stations sampled on the CPR route between January 1995 and December 1998. Cumulative sum analysis was performed on PCI anomalies for all the stations (D), over the period 1995-1998.

Figure 6.18. Hovmöller diagram of original data (A), seasonal cycle (B) and anomalies after removing the seasonal cycle (C) of Sea Surface Temperature (SST) for the 15 stations sampled on the CPR route between January 1995 and December 1998. Cumulative sum analysis was performed on SST anomalies for all the stations (D), over the period 1995-1998.

Figure 6.19. Hovmöller diagram of original data (A), seasonal cycle (B) and anomalies after removing the seasonal cycle (C) of Sea Surface Heights (SSH) for the 15 stations sampled on the CPR route between January 1995 and December 1998. Cumulative sum analysis was performed on the residuals of Sea Level Anomalies (SLA) for all the stations (D), over the period 1995-1998.

Figure 6.20. Cumulative NAO (index month; black triangles) and cumulative geostrophic current (white triangles) derived from altimeter sea level anomaly (km) over the period 1995-1998.

Figure 7.1. Mechanisms linking the positive (A) and negative (B) phases of the North Atlantic Oscillation (NAO) to the variability in physical processes and planktonic ecology. Red/green arrows imply an increase/decrease in the parameter. The dashed arrows illustrate the relationship between NAO and Sea Surface Temperature (SST) via the currents in Northeast and Northwest Atlantic.

Figure 7.2. Schematisation of eddy formation from the Gulf Stream meanders and mechanism of plankton and nutrient exchange across the frontal boundary between Subtropical Waters (light blue) and both Slope and Subpolar origin waters (dark blue).

Acknowledgements

I wish to thank Dr. Peter Cotton and Prof. Patrick Holligan for examining this thesis.

I am very grateful to my director of studies Prof. Martin Attrill, for his support and advice even when I was on this other side of the globe! Many thanks for your comments and help during the PhD.

I also thank my two other supervisors Dr. Chris Reid and Dr. Martin Edwards for their support over the three years I spent at SAHFOS and their advice as co-authors of several publications.

I am thankful to Prof. R.D. Pingree without whom half of this work would not have been possible. I thank him for providing the Sea Level Anomalies and SeaWiFS data, as well as figures 6.1, 6.3 and 6.4. I also thank him for his time and patience as well as for the nice discussions and the afternoon swims in summer.

Thanks to Anthony John for helping me so much with the identification of all those plankton species, thanks for the advice, the pleasant discussions and the phone calls when I was the only one working during bank holidays.

I wish to thank Dr. M.D. Skogen from the Institute of Marine Research of Bergen (Norway) for giving me access to the NORWECOM data used in chapter 5.

I am also grateful to Dr. L. Seuront for his help with statistic analysis (chapters 3 and 4) and for his valuable comments on the discussion.

I would also like to thank the Hadley Centre, UK MetOffice for providing Sea Surface Temperature data (HadISST Version 1.1), ICES for salinity and nutrient data, and the SeaWiFS Project Office for providing high resolution of SeaWiFS data. Altimeter data were received from AVISO, CLS and European Space Agency (grant A02.UK121). This research was funded by a DEFRA contract (CSA 6193/AE1147): "Environmental change and biodiversity".

I express gratitude to my friend and flat mate Marie who shared the expatriation on the other side of "La Manche" with me; and to Kiki and Yaginobaka who kept in touch even if we only managed to see each other once a year.

I thank Angie for her friendship, support and help "all over the world".... Please tell me again the story of the Indian women.... And teach me new words!

I also thank my friends from the BEACH group at Plymouth University (Antonio, Cathy, Cécile, Chutamad, Colin, Fay, Frank, Garry, Gerald, Jin Bo, Laura, Simon....) and from SAHFOS (Darren, Debbie, Jean....), you made my stay in England very enjoyable.

I am also grateful to the Albion Ladies Rugby team for giving me the opportunity to play rugby with them during two seasons and allowing me to forget Marine Biology after hard working days.

I finally thank my parents and sister for always being there for me and for their constant support during those three years. I am grateful to Lozza for being available 24/24, for his friendship, patience, humour and support.

Author's declaration

At no time during the registration for the degree of Doctor of Philosophy has the author been registered for any other University award.

This study was financed with the aid of a studentship from the DEFRA contract (CSA 6193/AE1147): "Environmental change and biodiversity" and carried out in collaboration with the Sir Alister Hardy Foundation for Ocean Science.

Relevant scientific seminars and conferences were regularly attended at which work was often presented; external institutions were visited for consultation purposes and several papers prepared for publication.

Publications 2003-2006:

1. **Leterme S.C.**, Seuront L. & Edwards M. (2006) Differential contribution of diatoms and dinoflagellates to phytoplankton biomass in the NE Atlantic and the North Sea. *Marine Ecology Progress Series* 312: 57-65.
2. Edwards M., Johns D.G., **Leterme S.C.**, Svendsen E. & Richardson A.J. (2006) Regional climate change and meso-scale Harmful Algal Bloom 'hotspots' in the northeast Atlantic. *Limnology & Oceanography* 51(2): 820-829.
3. **Leterme S.C.**, Edwards M., Seuront L., Attrill M.J., Reid P.C. & John A.W.G. (2005) Decadal basin-scale changes in diatoms, dinoflagellates, and phytoplankton colour across the North Atlantic. *Limnology & Oceanography* 50(4): 1244-1253.
4. **Leterme S.C.** & Pingree R.D. (in press) The Gulf Stream, Rings and North Atlantic Eddy structure from remote sensing (Altimeter and SeaWiFS). *Journal of Marine Systems*.
5. Gieskes W.W.C., **Leterme S.C.**, Peletier H., Edwards M. & Reid P.C. (accepted) Annual variation of *Phaeocystis* colonies Atlantic-wide since 1948, and influence of Atlantic Ocean water in the eutrophic "hotspot" North Sea. *Biogeochemistry*.
6. Kesaulya I., Seuront L., **Leterme S.C.** & Mitchell J.G. The impact of *Phaeocystis globosa* derived-foam formation on chlorophyll concentration and seawater viscosity in the inshore and offshore waters of the Eastern English Channel. *Journal of Plankton Research* (submitted).
7. **Leterme S.C.** & Pingree R.D. Structure of phytoplankton (Continuous Plankton Recorder and SeaWiFS) and impact of climate in the Northwest Atlantic Shelves. *Ocean Science* (submitted).
8. **Leterme S.C.**, Attrill M.J., Pingree R.D., John A.W.G. & Skogen M.D. Decadal fluctuations of Atlantic Water inflow into the North Sea and its impact on plankton between 1958-2003. *Limnology & Oceanography* (submitted).

Presentation and Conferences attended 2003-2006: (Presenter underlined)

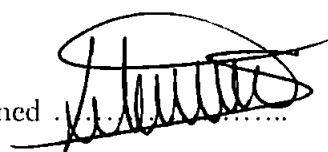
1. Mendes J.C. & **Leterme S.C.** (2006) Decadal changes in North Atlantic Harmful Algae Blooms: a long-term study from the Continuous Plankton Recorder (CPR) survey. 41st *European Marine Biology Symposium, September 2006, Cork, Ireland.*

2. **Leterme S.C.**, Pingree R.D., Attrill M.J., John A.W.G & Skogen M.D. (2006) Decadal Fluctuations of Plankton species in the North Sea: Relation with Physical and Hydrological Parameters. *AGU-ASLO-TOS Ocean Sciences Meeting, February 2006, Honolulu, Hawaii, USA.*
3. **Edwards M.**, Johns D.G., **Leterme S.C.**, Svendsen E. & Richardson A.J. (2006) Regional Climate Change and Harmful Algal Blooms in the Northeast Atlantic. *AGU-ASLO-TOS Ocean Sciences Meeting, February 2006, Honolulu, Hawaii, USA.*
4. **Leterme S.C.** (2006) Multi-scale variability in phytoplankton populations, from eddies to global change. *February 2006, School of Biological Sciences, Flinders University, Adelaide, South Australia.*
5. **Leterme S.C.** (2005) Large scale climate variability, physical processes and plankton. *November 2005, Port Lincoln Marine Science Center, South Australia.*
6. **Gieskes W.W.C.**, **Leterme S.C.**, Peletier H., Edwards M. & Reid P.C. (2005) Variability in the contribution of *Phaeocystis* to phytoplankton biomass in the North Sea and the North Atlantic between 1948 and 2005: causes and consequences. *Phaeocystis, major Link in the Biogeochemical Cycling of Climate-relevant Elements, August - September 2005, University of Groningen, Haren, The Netherlands.*
7. **Leterme S.C.** (2005) How plankton reflects climate change. *Tamar Coastal Festival, Talks on Climate Change, July 2005, Plymouth, United Kingdom.*
8. **Leterme S.C.** & Pingree R.D. (2005) Impact of mesoscale physical processes on phytoplankton distribution in the Northwest Atlantic Ocean. *ASLO Summer Meeting, June 2005, Santiago de Compostela, Spain.*
9. **Leterme S.C.** & Pingree R.D. (2005) Phytoplankton in the Northwest Atlantic: physical-biological interactions. *May 2005, Marine Biological Association, Plymouth, UK.*
10. **Leterme S.C.** & **Mendes J.C.** (2004) Harmful Algae Blooms occurrence in the North Atlantic: a long-term study from the Continuous Plankton Recorder (CPR) survey. *11th Conference on Harmful Algae, November 2004, Cape Town, South Africa.*
11. **Edwards M.**, Johns D., **Leterme S.C.** & Richardson A. (2004) Decadal spatial and temporal patterns of Harmful Algae Blooms in the northeast Atlantic. *ICES-IOC, Working Group on HAB dynamics Meeting, September 2004, Norway.*
12. **Leterme S.C.**, Edwards M., Seuront L., Attrill M.J. & Reid P.C. (2004) Decadal changes in phytoplankton biomass in the North Atlantic. *Postgraduate Marine Biology Workshop, April 2004, University of Wales, Bangor, UK.*
13. Kesaulya I., **Seuront L.**, **Leterme S.C.** & Mitchell J.G. (2004) Phytoplankton biomass and seawater viscosity during a spring bloom of *Phaeocystis*. *1st General Assembly of the European Geosciences Union, 25-30 April 2004, Nice, France.*
14. **Seuront L.**, **Leterme S.C.**, Seymour J.R., Mitchell J.G. & Waters R.L. (2004) Sampling the sampling unit: a world in a bottle. *ASLO/TOS Ocean Research Conference. 15-20 February 2004, Honolulu, Hawaii, USA.*

External Contacts:

- Dr. Winfried W.G. Gieskes, Department of Marine Biology, University of Groningen, Haren, The Netherlands.
- Dr. Irma Kesaulya, Fisheries Faculty, Pattimura University, Jl. Martha Alphons, PO BOX 97211, Ambon, Indonesia.

- Prof. Jim G. Mitchell, School of Biological Sciences, Flinders University, GPO BOX 2100, Adelaide 5001, Australia.
- Prof. Robin D. Pingree, Marine Biological Association of the UK, The Laboratory, Citadel Hill, PL1 2PB Plymouth, United Kingdom.
- Dr. Laurent Seuront, CNRS – ELICO, Université des Sciences and Technologies de Lille, 28 Avenue Foch, 62930 Wimereux, France.
- Dr. Morten D. Skogen, Institute of Marine Research, P.O.Box 1870 Nordnes, N-5817 Bergen, Norway.
- Prof. Hidekatsu Yamazaki, Department of Ocean Sciences, Tokyo University of Marine Science and Technology, 4-5-7 Konan, Minato-ku, Tokyo 108-8477 Japan.

Signed 

Date. 28/09/2005

Chapter 1

INTRODUCTION

All marine organisms are affected to some extent by the movement of ocean currents, but plankton, because of its minute size and short growth rates, is most directly coupled to the physical environment. Being at the base of the marine food-web, information on phytoplankton is an absolute prerequisite to the understanding of biological responses to natural variability within this environment. Small fluctuations in plankton biomass at short time and space scales may have equal or greater importance in determining ecosystem structure and function than larger fluctuations, such as climatic cycles (Haury *et al.* 1978). In addition, interactions between physical (Fig. 1.1) and biological (Fig. 1.2) processes result in variability over a wide range of temporal and spatial scales (Kaiser *et al.* 2005). Physical processes are the basis of many perturbations that are critical for the ecology of organisms (Harris 1986). The spatial and temporal patchiness in the physical environment arises from the interaction of solar heating and wind mixing in all bodies of water. As the wind induces motion in surface waters, both horizontal and vertical water motions are observed (*i.e.* processes called turbulent advection and diffusion), and dissolved and suspended materials (*e.g.* plankton) are then carried around by the water masses. Small to large scale events can then be observed from 10^{-2} to 10^6 meters, from microscale vortices to regional scale horizontal motions like the Gulf Stream. Those events then create patchiness in the ocean at the corresponding scale. In temperate climates, it is believed that the primary mechanism initiating the spring phytoplankton bloom is the alteration between vertical mixing and stratification of the water column and the availability of light; the penetration of light being mainly limited by the turbidity of the water (Edwards 2001).

Consistent patterns of ecological succession in the phytoplankton have been observed as a result of the degree of vertical stability of the water column, consequently influencing nutrient ratios and life history strategies adopted by specific groups of phytoplankton (Holligan 1987). The increase in the intensity of stratification and nutrient depletion/loading impacts the community composition and leads to a shift from diatoms to dinoflagellates, as dinoflagellates prefer these conditions (Margalef 1975). Due to the intrinsic nature of pelagic ecosystems, there are two types of abiotic component which influence phytoplankton community structure: (i) geographically-dependent component, including solar energy flux, bottom topography and current direction, and (ii) geographically-independent components associated with the hydrodynamics of the system (*e.g.* eddy structure), including temperature, salinity and nutrients (van der Spoel 1994). As Tomczak and Godfrey (1994) pointed out, the Atlantic basin is by far the longest latitudinally-extended ocean basin (*i.e.* 21,000 km from the Bering

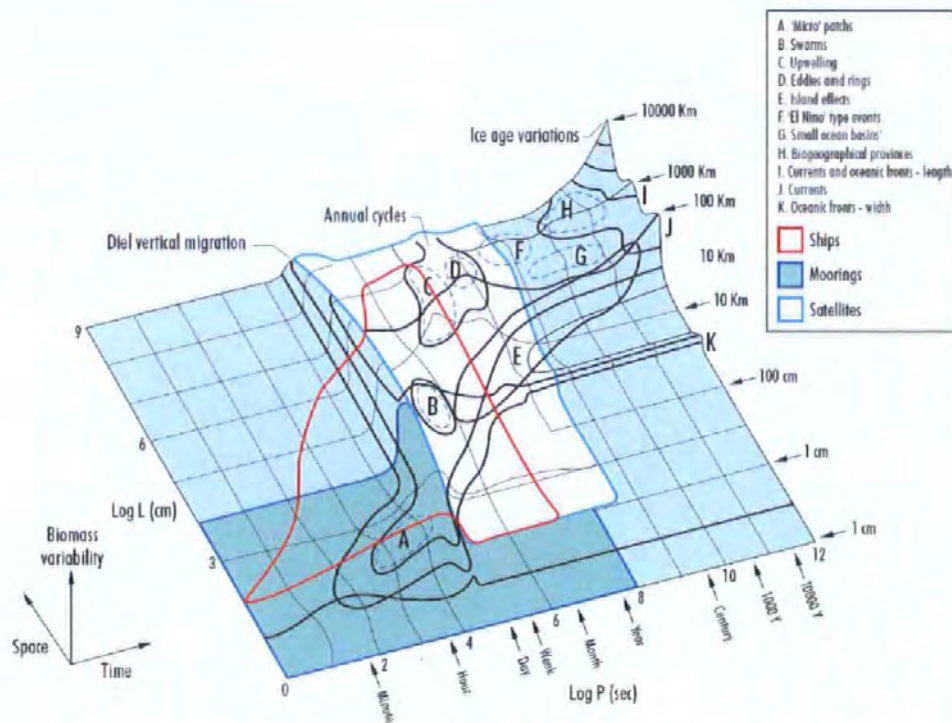


Figure 1.1. Stommel diagram, modified from ICES Zooplankton Methodology Manual, Harris *et al.* (eds., 2000), overlaid to show the scales that can be sampled with various platforms, and features such as fronts (from Kaiser *et al.* 2005).

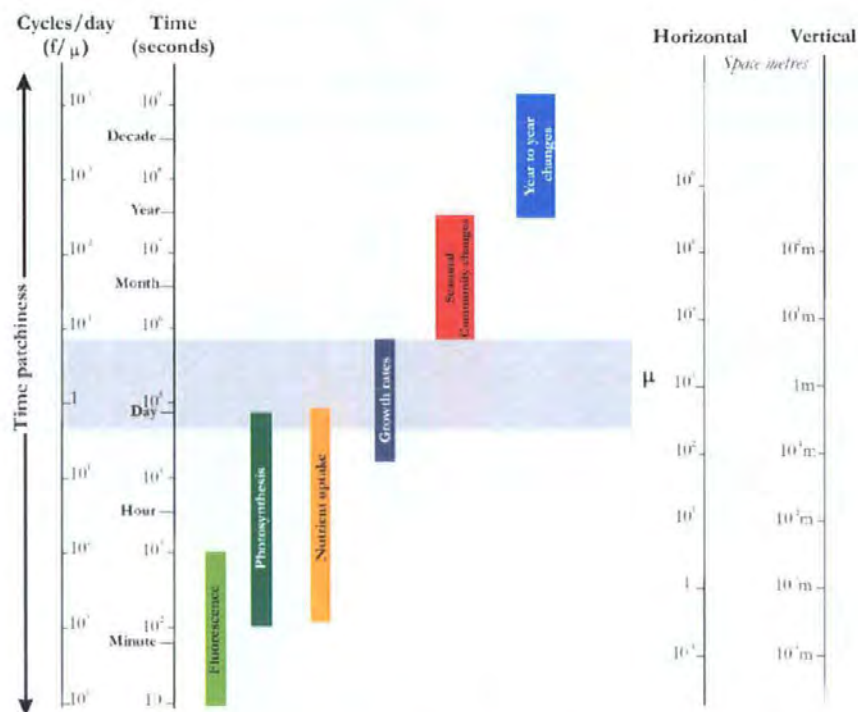


Figure 1.2. Scales of phytoplankton ecology. Horizontal and vertical scales are determined respectively by coefficients of horizontal and vertical diffusion. The time scales for algae are determined by the growth time-scale, μ , (grey band). The processes of importance at each scale are specified in colour (modified from Harris 1986).

Straits over the pole and down to Antarctica) and regroups different provinces that can be considered individually due to their physical and biological characteristics. Here, I focus on the North Atlantic basin, within which the seasonal chlorophyll anomaly has the greatest spatial coverage of any region of the World Ocean (Longhurst 1998). The only plankton monitoring programme that comes close to this scale is the Continuous Plankton Recorder (CPR) survey, which is the only long-term biological monitoring program providing a systematic coverage of the Northeast Atlantic and the North Sea in both space and time. The survey measures the presence and abundance of ca. 500 phytoplankton and zooplankton taxa and provides a visual assessment of phytoplankton biomass: the Phytoplankton Colour Index (PCI, Colebrook & Robinson 1965). The PCI has been extensively used to describe the seasonal and long-term patterns of phytoplankton abundance in various regions of the North Atlantic (*e.g.* Reid 1978, Edwards *et al.* 2001, Johns *et al.* 2003, Batten *et al.* 2003a). Each region of the North Atlantic basin accommodates a characteristic seasonal production within its boundaries; seasonality is not, however, identical from year to year. The amplitudes of these year-to-year fluctuations may appear to be minor, but are associated with changes in weather patterns that are very significant (Longhurst 1998). The temporal and spatial scales that are particularly examined in this study range from years to decades and cover environmental processes such as currents (*e.g.* the European Continental Slope Current and the Gulf Stream), advection (*e.g.* eddies) and climatic oscillations (*i.e.* the North Atlantic Oscillation).

At large scales, atmospheric forcing (*i.e.* North Atlantic Oscillation) is the dominant environmental factor driving fluctuations of phytoplankton populations (Drinkwater *et al.* 2003). The North Atlantic Oscillation (NAO) refers to a redistribution of atmospheric mass between the Arctic and the subtropical Atlantic. Switches from one NAO phase to another produce large changes in the mean wind speed and direction over the Atlantic, the heat and moisture transport between the Atlantic and the neighbouring continents, and the intensity and number of storms, their paths, and their weather (Hurrell *et al.* 2003). Walker and Bliss (1932) constructed the first index of the NAO using a linear combination of surface pressure and temperature measurements from weather stations on both sides of the Atlantic basin. Most modern NAO indices are derived from the simple difference in surface pressure anomalies between various northern and southern locations (Hurrell *et al.* 2003). Several indices have been developed to quantify the state of the NAO, but the most widely used is Hurrell's NAO index (Hurrell 1995a). Hurrell (1995a) analysed the wintertime variability in Sea Level Pressure and surface temperature over the North Atlantic basin, between Lisbon,

Portugal and Stykkisholmur, Iceland. It is thought that the recent increasing number of studies related to the NAO has been motivated by a trend toward a more positive phase over the past 30 years. The magnitude of this recent trend appears to be unprecedented in the observational record (Hurrell 1995b), and probably over the past several centuries as shown by paleoclimate data (Stockton & Glueck 1999). The most pronounced anomalies have occurred since the winter of 1989 (Hurrell 1995a, Walsh *et al.* 1996, Thompson & Wallace 1998) when record positive values of an index of the NAO have been recorded. Moreover, the trend in the NAO accounts for several remarkable changes recently in the climate and weather over the middle and high latitudes of the Northern Hemisphere, in both marine and terrestrial ecosystems. The atmospheric shifts associated with the NAO have been linked to (i) changes in sea-ice cover in both the Labrador and Greenland Seas as well as over the Arctic (Chapman & Walsh 1993), (ii) transport by the Labrador Current (Marshall *et al.* 1997) and the iceberg flux past Newfoundland (Drinkwater *et al.* 1999), (iii) pronounced decreases in mean sea level pressure over the Arctic (Walsh *et al.* 1996) and changes in the physical properties of Arctic sea water (Sy *et al.* 1997), (iv) changes in North Atlantic surface wave heights (Kushnir *et al.* 1997), (v) evaporation and precipitation patterns (Hurrell 1995a), (vi) changes in the paths of Atlantic storms and their intensity (Rogers 1990, Hurrell 1995a), and (vii) the latitude of the Gulf Stream (Taylor & Stephens 1998). Part of the response from the pelagic environment is local and rapid (*e.g.* Sea Surface Temperature (SST), mixed-layer depth or surface Ekman transport). However, the geostrophically balanced large-scale horizontal and overturning circulation can take several years to adjust to changes in the NAO forcing (Visbeck *et al.* 2003).

Major long-term changes in pelagic ecosystems have been apparent in the North Sea (Aebischer *et al.* 1990, Reid & Edwards 2001) and across the North Atlantic Ocean as a whole (Planque & Taylor 1998, Greene & Pershing 2000, Beaugrand *et al.* 2003). At the regional to oceanic scale (and at the sampling scale of the CPR survey), climate variability and regional climate warming appear to play a dominant role in the long-term changes in phytoplankton assemblages and biomass (Reid *et al.* 1998, Edwards *et al.* 2002, Richardson & Schoeman 2004). Barton *et al.* (2003) showed that the positive PCI trends observed in many areas are similar to the long-term trend in the NAO index and they provided hypotheses about the NAO-dependent physical factors underlying the long-term pattern of phytoplankton variability. In addition, zooplankton species from warmer waters have been observed recently in the North Sea (Beaugrand *et al.* 2002), the changes observed being related to variations at higher levels in the food chain or by bottom-up control via phytoplankton.

The CPR survey has been used to describe and analyse plankton variability in the North Atlantic and North Sea and to interpret this variability in relation to fisheries and atmospheric climate events (Robinson & Hiby 1978, Batten *et al.* 2003a). Recent studies have shown an increase in phytoplankton biomass in the North Atlantic via the analysis of the PCI (Barton *et al.* 2003). In the same way, an increasing trend in phytoplankton biomass has been shown in the North Sea (Reid & Edwards 2001, Lancelot *et al.* 1997, Cadée & Hegeman 1993, Hickel *et al.* 1995) and in the area west of the British Isles (Edwards *et al.* 2001). Different explanations have been suggested to explain those increase, *e.g.* hydro-climatic processes (Edwards *et al.* 2001) and/or eutrophication (Lancelot *et al.* 1997, Cloern 2001). Furthermore, non-indigenous phytoplankton species (*i.e.* *Coscinodiscus wailesii*, Edwards *et al.* 2001) have been observed in the North Sea.

This work will focus on the changes that are occurring in pelagic ecosystems at different temporal and spatial scales. These changes will be illustrated by the spatial variability induced by eddies and/or currents but also by the regional variability of the hydro-climatic processes, influencing Sea Surface Temperature, wind-regimes and mixing of local environments. In particular, attention will be focused on the impact of the North Atlantic Oscillation on phytoplankton via the changes in the physical and hydrological properties of the pelagic environment. The structure of the present work follows a progression from the macroscale (*i.e.* North Atlantic basin) to the mesoscale (*i.e.* eddies), and from phytoplankton biomass to the phytoplankton community.

Chapter 2 provides an overview of the sampling strategy and sample analysis of the CPR survey. The analysis of phytoplankton biomass and indicator species (*i.e.* species most regularly identified during the survey) is subsequently introduced in relation to hydro-climatic and physical parameters, at different spatial and temporal scales, across the North Atlantic basin.

In Chapter 3, phytoplankton biomass is analysed from the CPR samples using the Phytoplankton Colour Index (PCI), together with the total count of diatoms and dinoflagellates (important groups of primary producers of the North Atlantic Ocean (Lalli & Parsons 1997) and the two main groups of phytoplankton taxa identified by the CPR survey) across the whole North Atlantic basin. Diatom and dinoflagellate species with a frequency of occurrence greater than 1% in the samples were used as indicator taxa to provide more information on the processes linking climate to changes in the phytoplankton community.

This chapter investigates (i) long-term fluctuations of phytoplankton biomass, total diatoms, and total dinoflagellates, (ii) geographical variation of patterns, (iii) the relative contribution of diatoms and dinoflagellates to the PCI, and (iv) the fluctuations of the dominant species over the period of the survey to provide more information on the processes linking climate to changes in the phytoplankton community. Five dinoflagellate species (*Ceratium furca*, *C. fusus*, *C. horridum*, *C. lineatum*, and *C. tripos*) and six diatom taxa (*Proboscia alata alata*, *Rhizosolenia hebetata semispina*, *R. styliformis*, *Thalassionema nitzschioides*, *Thalassiosira* spp., and *Thalassiothrix longissima*) have thus been investigated further. Due to the differences in microscopic analytical methods prior to 1958, the analyses have been conducted only over the period 1958-2002, with the North Atlantic basin divided into six sub-regions identified through bathymetric criteria and separated along a North-South axis.

However, because local variability in environmental conditions has been shown to play a critical role in temporal fluctuations of phytoplankton biomass (Hasegawa *et al.* 2004), the subsequent chapters are based on the consideration of smaller areas inside these sub-regions in order to study more precisely the processes influencing the long-term variation of phytoplankton assemblages. These chapters will focus on the variability of the phytoplankton species at the mesoscale in the Northeast (NE; chapter 4) and Northwest (NW; chapter 6) Atlantic Ocean as well as in the North Sea (Chapter 5).

As outlined above, sampling by the CPR survey over the North Atlantic and the North Sea has enabled long-term studies of phytoplankton biomass. Analysis of an index of phytoplankton biomass, the PCI, has previously shown an increase in phytoplankton biomass in the NE Atlantic. In Chapter 4, further investigations are conducted to determine the contribution of diatoms and dinoflagellates cell counts to the PCI, their fluctuations over the last 45 years and their geographical variations in the eastern North Atlantic and the North Sea. The relative contributions of diatom and dinoflagellate to the PCI could lead to the identification of different regimes in the diatom/dinoflagellate dynamics of the NE Atlantic and the North Sea.

Within the North Sea, intricate relationships are apparent between physical conditions (*i.e.* waves, tides, currents), water chemistry (*i.e.* nutrients, oxygen, trace metals), sediment (*i.e.* in suspension and on the bottom), living organisms and human activities (Eisma 1987). The circulation of Atlantic waters along the European continental slope, and more precisely the inflow of Atlantic waters into the North Sea, highly influences North Sea water characteristics,

with any changes in temperature, salinity and nutrient concentration affecting the biology and ecology of plankton organisms (Reid 1978, Eisma 1987, Reid *et al.* 1992, Reid *et al.* 2003). Changes in temperature, salinity and nutrient concentration in North Sea waters are then likely to have a strong impact on the space-time dynamics of planktonic organisms. Anomalous high salinity (Otto *et al.* 1990) and Atlantic plankton indicator species (Corten 1999) observed in the North Sea are particularly indicative of Atlantic inflow. The variability in the source and volume of oceanic water inflow has been shown by Corten (1986, 1990), with a reduction of Atlantic inflow into the northwestern North Sea in the 1960s and 1970s, and an increased inflow after 1980. Because temporal fluctuations of phytoplankton biomass might also be critically influenced by local variability (Hasegawa *et al.* 2004), Chapter 5 defines a set of smaller regions around the British Isles and assesses the long-term (1958-2003) impact of changing oceanographic conditions on the North Sea planktonic ecosystem, with a particular focus on (i) fluctuations in Atlantic inflow to the North Sea from two sources over the 45-yr study period, (ii) the influence of changes in inflow on North Sea salinity, temperature and nutrient levels between 1958 and 2003, (iii) the identification of long-term changes in the North Sea plankton assemblage (copepod abundance, phytoplankton biomass, diatom and dinoflagellate abundances) in different regions of the North Sea and (iv) the potential causal relationships between the observed environmental fluctuations and changes in inflow rate.

As previously stressed, physical parameters, such as currents, have a strong influence on the dynamics of plankton species. As a consequence, in Chapter 6, the effect of eddies and currents on the dynamics and distribution of phytoplankton are specifically investigated. The intense hydrodynamic activity observed in the NW Atlantic Shelves Province makes this region especially intriguing from the point of view of physical-biological interactions (Longhurst 1998). This zone is under the influence of the cold southward inflow of Labrador Sea Water (LSW) and the warm northward inflow of the Gulf Stream. The Gulf Stream is the largest current in the western North Atlantic, it flows from the continental slope off Cape Hatteras and travels eastward meandering until the tail of the Grand Banks (Stommel 1958). The NW Atlantic includes contrasted, well-studied regions like the Grand Banks, the Scotian shelf and the Georges Bank (Petrie & Yeats 2000, Campbell *et al.* 2001, Greene *et al.* 2003, Thomas *et al.* 2003). In this hydrodynamically driven region, a specific attention has been given to the influence of the physical processes on the distribution and fluctuations of phytoplankton biomass.

Firstly, the influence of the Gulf Stream and its rings (generated from the cut-off of Gulf Stream meanders) on phytoplankton biomass distribution is investigated. No CPR data are used in this part, as there is no continuous sampling done by the CPR survey in this area. Instead, Sea-viewing Wide Field-of-view Sensor (SeaWiFS) Chlorophyll *a* images are used as a proxy of phytoplankton biomass. Gulf Stream warm and cold core rings have been shown to influence surface phytoplankton distributions via the entrainment of the surrounding water masses around and into the rings (Kennelly *et al.* 1985, Garcia-Moliner & Yoder 1994, Ryan *et al.* 1999, Ryan *et al.* 2001). In order to determine the relationship between spatial and temporal structures of phytoplankton and eddies along the Gulf Stream axis, the first part of the chapter 6 examines and compares: (i) the spatial and seasonal structure of SeaWiFS chlorophyll *a* along the spring bloom boundary in the North Atlantic near 35°N in relation to eddy structure, (ii) the seasonal cycles of SeaWiFS Chl *a* along a mean Gulf Stream path, (iii) the speed and propagation of Gulf Stream rings and (iv) eddy and SeaWiFS Chl *a* spatial structures along the Gulf Stream route.

Secondly, Gulf Stream rings have been observed as being partially responsible for the warm SST in slope water (Fox *et al.* 2005). In particular, a Gulf Stream warm-core ring has been shown as strongly influencing water mass and chlorophyll distributions along the southern flank of Georges Bank (Ryan *et al.* 2001). This area, as well as the Scotian Shelf and the Grand Banks, is also under the influence of the North Atlantic Oscillation through the modification of the inflow of Labrador Sea Water (LSW). More specifically, fluctuations in the inflow of LSW along the Scotian shelf have been associated with changes in coastal water characteristics (i.e. SST, salinity and nutrient concentration) and in zooplankton (Greene & Pershing 2000). In this context, the second part of this chapter assesses the impact of the LSW changing flow along the Scotian Shelf and the influence of Gulf Stream rings along the George Bank. A specific CPR route (E-route; between Norfolk (Virginia, USA; 39°N, 71°W) and Argentia (Newfoundland; 47°N, 54°W) has then be used to investigate over the period 1995-1998 (i) the consistency between PCI and SeaWiFS Chl *a* measurements in this area, (ii) the fluctuations of phytoplankton biomass and their geographical distribution, (iii) the possible links between PCI, SST and NAO, and (iv) the relation between phytoplankton and altimetry (i.e. Sea Level Anomalies and eddies).

The final chapter (Chapter 7) critically assesses the potential limitation of the CPR survey in monitoring large scale changes in phytoplankton communities and discusses the main processes that have been observed as influencing the variations of phytoplankton in the North Atlantic basin at different temporal and spatial scales during this project.

Chapter 2

GENERAL METHODOLOGY OF THE CONTINUOUS PLANKTON RECORDER SURVEY

2.A. Sampling and Analysis

2.A.1. The survey

The Continuous Plankton Recorder (CPR) survey is one of the longest running marine biological surveys in the world [others include: CALifornia Cooperative Oceanic Fisheries Investigations (CALCOFI; Moser *et al.* 2001), Virginia Fishery Independent Seine and Trawl Survey (Bonzek *et al.* 1995), Caribbean Conservation Corporation Research and monitoring of sea turtle (Godfrey 1999), Running Wildlife Monitoring Program for Contaminants in Herring Gull Eggs (Bishop *et al.* 1992)] and the only one providing a systematic coverage of the NE Atlantic and the North Sea in space and time. This upper layer plankton monitoring programme has regularly collected samples, at monthly intervals, in the North Atlantic and the North Sea since 1931 (Fig. 2.1). The wide geographical coverage of the survey has been possible through the contribution of the many voluntary 'ships of opportunity' (Fig. 2.2, SOOP) that have towed CPR machines, involving close to 250 vessels from more than 30 nations. The vessels have included weather, naval, hydrographical and research ships, ferries and a wide range of other merchant ships.

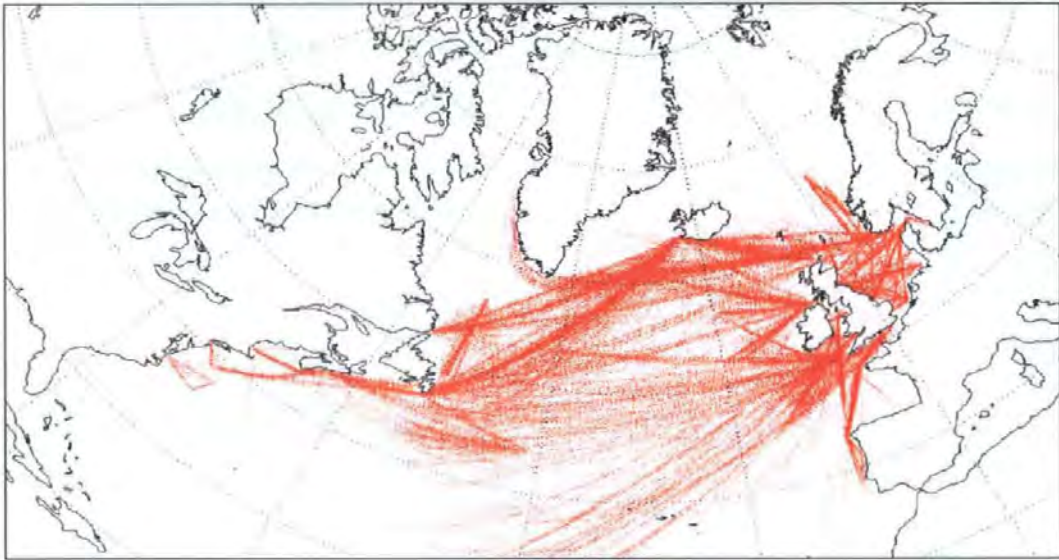


Figure 2.1. Continuous Plankton Recorder survey sampling routes between 1958 and 2004

The prototype CPR was used for the first time during the Discovery expedition in the Antarctic between 1925 and 1927. Since the first CPR tow in the North Sea in 1931 by Alister Hardy, the methodology (Warner & Hays 1994) has been used in all the oceans of the world, as well as in the North Sea, the Mediterranean, the Baltic, and in freshwater lakes. However,

the core CPR programme of monthly, synoptic sampling has focused on the NW European Shelf and in the NE and NW Atlantic Ocean. More than four million miles of CPR tows have been carried out since 1931, with the highest concentration of sampling in the North Sea and NE Atlantic Ocean. Close to 190,000 samples have been analysed under microscopes, when phytoplankton and zooplankton are counted and identified into ~ 500 different taxa. The computerised database for this unique survey contains observations from an average of ~ 20 ship routes per month since 1946.

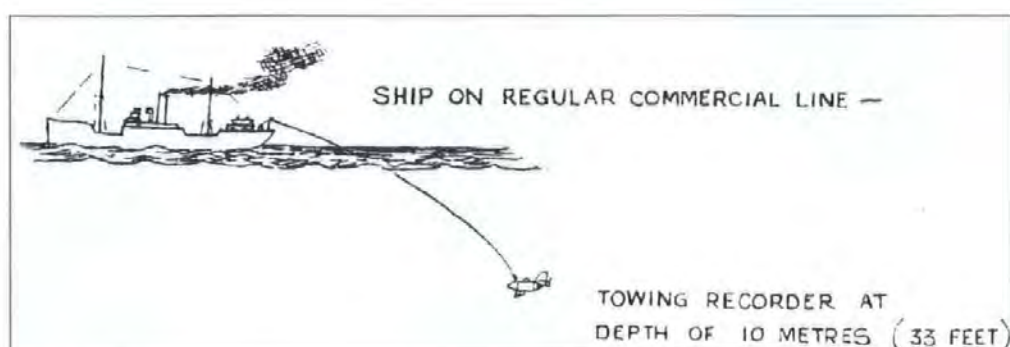


Figure 2.2. A Continuous Plankton Recorder towed behind a ship of opportunity (from SAHFOS archives)

For the last 50 years of sampling, the equipment used and procedures applied have barely varied. However, over that time there have been changes, beyond the control of the agencies operating the CPR survey which might have influenced the sampling characteristics. The most obvious change has been the increase in the mean operating speed of the SOOP used to tow the CPR. Hays and Warner (1993) calculated the mean annual towing speed and showed that after an initial decline between 1946 and 1952 from 11.8 to 10.5 knots, there was a steady increase until 1991 to 14.2 knots. A significant amount of work has been carried out over the years to investigate possible effects of this increase in speed on the consistency of the CPR time series (Batten *et al.* 2003a). Even if the operating speed of the vessels that tow CPRs has increased over the duration of the survey, this has not affected the depth at which the CPR is towed (Batten *et al.* 2003a). In addition, there is no effect of increased speed on the mechanical efficiency of the sampler, but at highest speeds flow through the machine might be reduced (Batten *et al.* 2003a).

2.A.2. Continuous Plankton Recorder

The CPR is towed at between 10-18 knots, ca 20-36 km h⁻¹, behind voluntary merchant ships at a standard depth of ca 6.5 m (Hays & Warner 1993). An impeller mounted at its rear drives the internal sampling mechanism (Fig. 2.3). Water flows through a ~1.62 cm² aperture in the CPR nose cone, down a tunnel which expands to a cross-sectional dimension of 5 x 10 cm, where it is filtered by a moving band of silk with an average mesh size of 270 μm. The filtering silk is covered by a second layer of silk and wound together into a storage tank filled with 4% formaldehyde for fixation and preservation of the plankton. This mechanism is analogous to that used in a camera. The two bands of silk move continuously across the tunnel at a speed adjusted according to the speed of the ship, via the impeller and gearbox, to 10 cm per 10 nautical miles (18.5 km). The water exits through a rectangular aperture at the rear of the CPR. The 10 cm of filtered silk equates approximately to the sampling of 3 m³ of seawater.

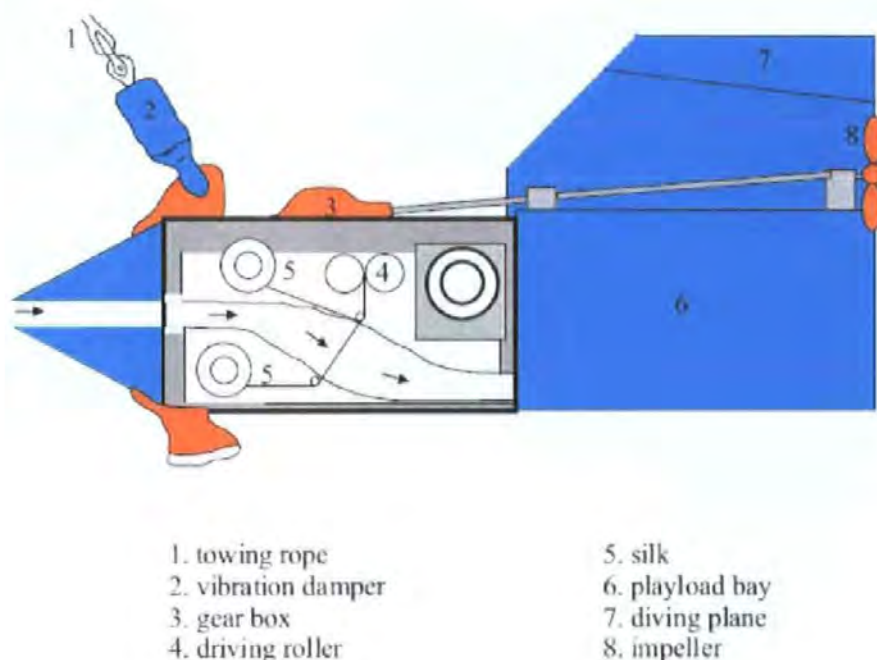


Figure 2.3. The Continuous Plankton Recorder

The CPR is launched at the rear of the SOOP (Fig. 2.4). After the tow, the internal mechanism is removed from the CPR body (Fig. 2.5) and returned to the laboratory for the routine analysis of the silk band. Then the silks, representing a continuous record of the plankton on that tow, are removed from the internal mechanism and unwound (typically a 500 nautical mile tow will use about 5 m of silk). For ease of plankton counting, the silk is then divided into samples representing 10 nautical miles of tow (Fig. 2.6). The start and end cutting



Figure 2.4.A, B. Launch of the Continuous Plankton Recorder (from SAHFOS archives).



Figure 2.5. Lance Gregory (Marine Technician at SAHFOS) removing the internal mechanism from the CPR body on board a ship of opportunity (from SAHFOS archive).



Figure 2.6. The silk is cut into sections (samples), representing 10 nautical miles of tow

points for each sample are calculated from the exact length of the filtering silk, the speed of the silk advance through the mechanism, and from information on a log sheet completed by the officers of the towing vessel. The log sheet records the exact time and position of CPR deployment and recovery, in addition to intermediate times and positions of alterations in the course. Calculations assume the vessel does not alter course or speed between successive points on the log sheet. Position (latitude and longitude) and local time for each sample are also calculated, corresponding to the geographical position of the CPR when the mid-point of the sample is in the middle of the filtering tunnel (Richardson *et al.* 2006). Comparison between the calculated position and data from vessels where a GPS record was available suggests the position assigned to CPR samples is accurate to within 10–20 nautical miles.

2.4.3. *Sample analysis*

Colebrook (1975), Warner & Hays (1994) and Richardson *et al.* (2006) have described methods of counting and data processing. Despite the near-surface sampling, studies have shown that the CPR gives a satisfactory representation of plankton dynamics in the epipelagic zone (Lindley & Williams 1980, Williams & Lindley 1980, Batten *et al.* 1999). There are four steps in the analysis:

- The first step is a visual estimation of the total phytoplankton biomass, known as the Phytoplankton Colour Index (PCI), determined for each sample prior to the cutting of the silk (Robinson & Hiby 1978). This index has four levels of colour from 'nil' to 'green':
 - 'Nil': no phytoplankton.
 - 'Very pale green': low biomass of phytoplankton.
 - 'Pale green': medium biomass of phytoplankton.
 - 'Green': high biomass of phytoplankton.

These ordinal values have been assigned numerical values (0, 1, 2 and 6.5) based on the work of Colebrook and Robinson (1965).

- The second step involves the identification of phytoplankton species following a well-established protocol (Colebrook 1960). Following the assessment of PCI, the silk is cut into sections (samples), representing 10 nautical miles of tow (Fig. 2.6). Each sample is then laid out on a purpose-built stage (Fig. 2.7) and 10 fields on each of two diagonals of the filtering silk are counted at 450x magnification for phytoplankton (using the Watson Bactil microscopes), consisting of 20 microscope fields of 0.295 mm diameter (Fig. 2.8). These 20



Figure 2.7. Paul Tranter (analyst at SAHFOS) is undertaking routine analysis of the silk under microscope in the laboratory (from SAHFOS archive).

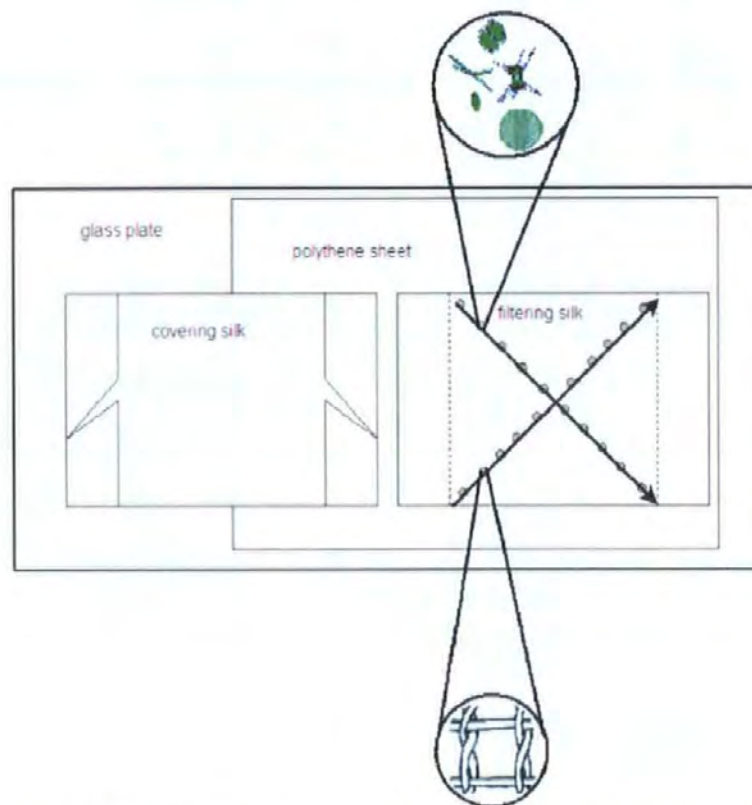


Figure 2.8. Layout of silk sample showing the 20 phytoplankton fields

fields amount to 1/10,000 of the area of the filtering silk. The analyst centres the field of view on a grid square of the mesh and records the taxa present and the total number of individuals of each species per field. This is repeated for 20 fields, giving the total number of fields (20 abundance "categories") in which each taxon has been seen. Each of these 20 categories has an associated accepted value, representing the total number of individuals of a species that are likely in the fields examined (Richardson *et al.* 2006). This has been derived from the Poisson distribution, which assumes organisms are randomly distributed on the silk (Colebrook, 1960). The statistic $h = -\ln(k/20)$ is used as an estimate of the mean number of cells per field, where k equals the number of empty fields observed (Robinson & Hiby 1978). If no empty fields are observed the value 4.5 is used for h . If a species is randomly distributed over the silk with a mean density of m cells per field, the probability that a species is absent from a field is e^{-m} , independently for each field, so k has a binomial distribution $B(20, e^{-m})$. Then for k not equal to 0, h is the maximum likelihood estimator for m (Robinson & Hiby 1978). These accepted values are then multiplied by 10,000 to estimate the phytoplankton abundance on the filtering silk. Unfortunately, because of historical data storage limitations before computers were used, these 20 abundance values are compressed into 10 by averaging (Table 2.1). Phytoplankton abundance values are thus restricted to 10 discrete values and can be considered semi-quantitative estimates. Different groups of phytoplankton taxa are identified, many to the level of species, *e.g.* diatoms, dinoflagellates, coccolithophores and silicoflagellates.

The third step is the analysis of zooplankton taxa and/or species with a size up to 2 mm called 'zooplankton traverse'. The microscopic analysis is a stepped traverse of the CPR filtering silk and covering silk at 54x magnification using the Watson Bactil microscopes. The field of view is 2.06 ± 0.05 mm and all zooplankton organisms <2 mm total length are counted. Although it is assumed that retained organisms are uniformly distributed on the silk, the design of the phytoplankton analysis and zooplankton traverse procedures ensures all areas of the silk receive equal weighting. The zooplankton traverse procedure examines 1/50 of the silk. The main types of zooplankton encountered in this traverse are small copepods and decapods.

The final step of the CPR analysis procedure counts all zooplankton greater than *Metridia lucens* stage V in size (>2 mm total length: Rae, 1952). Individuals are removed from the filtering silk and covering silk for identification. Generally all individuals are counted, but for particularly dense samples a sub-sample may be counted.

Plankton identification at the Survey is a trade-off between providing the highest taxonomic identification possible and the time taken to analyse the large number of CPR samples each year (currently totalling >5000). Copepods, diatoms and dinoflagellates are the groups most commonly recorded in the database because their members are common in the plankton and are robust, remaining relatively intact during CPR sampling. Within these groups, specimens are usually identified to species or at least to genus. Other common and robust crustaceans such as decapods and euphausiids are not speciated. This is partly because of factors such as the high diversity, but also because of the susceptibility to damage of the prominent spines of many larval decapods and the damage to larger adult euphausiids and post-larval decapods (Richardson *et al.* 2006).

Table 2.1. Phytoplankton analysis: calculating abundance of a particular taxonomic entity in a CPR sample. The total number of fields out of 20 in which the taxon was present is converted to a value representing the total number of cells of that taxon present in those 20 fields. This is then multiplied by 10,000 to give the abundance per sample and compressed into 10 values to give the recorded abundance per sample in the database. (from Richardson *et al.* 2006).

Total number of fields	Accepted value	Abundance per sample	Recorded abundance per sample
1	1	10,000	15,000
2	2	20,000	15,000
3	3	30,000	35,000
4	4	40,000	35,000
5	6	60,000	65,000
6	7	70,000	65,000
7	9	90,000	95,000
8	10	100,000	95,000
9	12	120,000	130,000
10	14	140,000	130,000
11	16	160,000	170,000
12	18	180,000	170,000
13	21	210,000	225,000
14	24	240,000	225,000
15	28	280,000	300,000
16	32	320,000	300,000
17	38	380,000	420,000
18	46	460,000	420,000
19	60	600,000	750,000
20	90	900,000	750,000

The size and compact morphology of most copepods usually makes identification reasonably straightforward despite specimens being partially flattened (Richardson *et al.* 2006). By contrast, many gelatinous and delicate taxa are damaged irrevocably and are not easily

identifiable in CPR samples. These include “Coelenterata tissue”, “Doliolidae”, “Salpidae”, “Siphonophores” and to a lesser extent “Chaetognatha” (Richardson *et al.* 2006). The nature of CPR sampling therefore unfortunately reinforces the traditional bias towards copepods and away from gelatinous taxa in zooplankton ecological research (Richardson *et al.* 2006).

All taxa in the CPR database are counted numerically except for two that are only ever recorded as present: *i.e.* *Phaeocystis pouchetii* and “Coelenterata tissue”. The colonial Prymnesiophyte *Phaeocystis pouchetii* appears as a dense mass of nondescript cells under the microscope, making abundance estimates very difficult. Unusually, *Phaeocystis* is most easily identified on CPR samples by its slimy, mucilaginous feel when gently brushing a finger across the silk. Coelenterates are delicate and extremely damaged during CPR sampling and consequently cannot be speciated or given a numerical abundance other than percentage of occurrence. They are only recorded as present under “Coelenterata tissue”. Coelenterates are identified by a combination of their appearance as acellular tissue strewn over the silk in zooplankton eyecount, and the presence of nematocysts during phytoplankton analysis and zooplankton traverse.

2.B. Phytoplankton

2.B.1. *The Phytoplankton Colour Index*

The visual estimation of the total phytoplankton biomass, known as the Phytoplankton Colour Index (PCI), is determined for each sample prior to the cutting of the silk (Robinson & Hiby 1978). The green coloration of the silk mesh has been used as an index of chlorophyll concentration (Reid 1975, 1978) to describe seasonal and long-term patterns of phytoplankton abundance. A number of studies have examined relationships between the PCI and other types of estimates of phytoplankton abundance. The first comparison between PCI and fluorometrically measured chlorophyll was undertaken by Hays & Lindley (1994). Their results showed a good relationship between PCI and chlorophyll, but only when the number of cells retained by the CPR mesh was small. Batten *et al.* (2003b) compared simultaneous fluorometric measurements of chlorophyll *a*, phytoplankton cell abundance and PCI from the Iberian margin, western Europe. The relationships between fluorometrically determined chlorophyll, cell abundance and PCI were all positive and significant, with PCI showing a better relationship to chlorophyll than cell abundance. This tends to support the hypothesis

(Reid 1978) that small phytoplankton cells that are not well preserved in formaldehyde, or are too small to be enumerated under the microscope, contribute to the green coloration of the sampling mesh. The study also compared PCI and fluorometer data with chlorophyll values obtained from satellite imagery (SeaWiFS) for the Iberian margin. Significant correlations exist between these three estimates of phytoplankton concentration. This estimation of phytoplankton biomass can be used to study bloom dynamics between 1936 and now. The last comparison of the PCI with another estimate of phytoplankton abundance was achieved by Raitso *et al.* (2005) using Sea-viewing Wide Field-of-view Sensor (SEAWIFS) data. They found a significant relationship between PCI and SeaWiFS data and made available data on the monthly variation of plant biomass (Chl-a) in the NE Atlantic and the North Sea since 1948.

2.B.2. Phytoplankton species

Cells are identified to species where practicable or to other taxonomic groups. The phytoplankton species identified by the plankton analysts of SAHFOS are listed below by systematic order. The two main groups of phytoplankton taxa sampled by the CPR are the diatoms and the dinoflagellates.

Division Chromophyta	Dinophyceae (dinoflagellates)
	Prymnesiophyceae/Haptophyta (coccolithophorids)
	Dictyochophyceae (silicoflagellates)
	Bacillariophyceae (diatoms)

2.B.2.a. Diatoms

The diatoms belong to a class of algae called the Bacillariophyceae. They are among the best studied of the planktonic algae and are often the dominant phytoplankton in temperate and high latitudes. Diatoms are unicellular, with cell sizes ranging from about 2 μm to over 1000 μm (Lalli & Parsons 1997). Some species form large chains or aggregates in which individual cells are held together by mucilaginous threads or spines. All species have an external skeleton, or frustule, made of silica and are fundamentally composed of two valves. Diatoms may be divided into two main classes, the centric diatoms, or Centrobacillariophyceae, which are

Table 2.2. Diatom taxa identified since 1958 by the CPR survey (Thomas 1997)

<i>Actinocyclus octonarius ralfsi</i>	<i>Encampia zodiacus</i>	<i>Rhizosolenia acuminata</i>
<i>Actinoptychus</i> spp.	<i>Fragilaria</i> spp.	<i>Rhizosolenia alata alata</i>
<i>Amphidoma caudata</i>	<i>Gossleriella tropica</i>	<i>Rhizosolenia alata curvirostris</i>
<i>Amphiprora hyperborea</i>	<i>Guinardia flaccida</i>	<i>Rhizosolenia alata indica</i>
<i>Asterionella bleakeleyi</i>	<i>Gyrosigma</i> spp.	<i>Rhizosolenia alata inermis</i>
<i>Asterionella glacialis</i>	<i>Hemianulus</i> spp.	<i>Rhizosolenia bergonii</i>
<i>Asterionella kariana</i>	<i>Hemidiscus cuneiformis</i>	<i>Rhizosolenia calcar-avis</i>
<i>Asteromphalus</i> spp.	<i>Hexasterias problematica</i>	<i>Rhizosolenia cylindrus</i>
<i>Aulacodiscus avigus</i>	<i>Lauderia borealis</i>	<i>Rhizosolenia delicatula</i>
<i>Bacillaria paxillifera</i>	<i>Leptocylindrus danicus</i>	<i>Rhizosolenia fragilissima</i>
<i>Bacteriastrium</i> spp.	<i>Lithodesmium undulatum</i>	<i>Rhizosolenia hebetata semispina</i>
<i>Bacteriosira fragilis</i>	<i>Melosira arctica</i>	<i>Rhizosolenia imbrica shrubsolei</i>
<i>Bellerochea malleus</i>	<i>Melosira lineata</i>	<i>Rhizosolenia robusta</i>
<i>Biddulphia alternans</i>	<i>Navicula planamembranacea</i>	<i>Rhizosolenia setigera</i>
<i>Biddulphia biddulphiana</i>	<i>Navicula</i> spp.	<i>Rhizosolenia stollerfothii</i>
<i>Campylosira cymbelliformis</i>	<i>Neodenticula seminae</i>	<i>Rhizosolenia styliformis</i>
<i>Cerataulina pelagica</i>	<i>Nitzschia delicatissima</i>	<i>Schroederella delicatula</i>
<i>Chaetoceros (Hyalochaete) spp</i>	<i>Nitzschia longissima</i>	<i>Skeletonema costatum</i>
<i>Chaetoceros (Phaeoceros) spp</i>	<i>Nitzschia seriata</i>	<i>Stauroneis membranacea</i>
<i>Climacodium frauenfeldianum</i>	<i>Nitzschia sigma rigida</i>	<i>Stephanopyxis</i> spp.
<i>Corethron criophilum</i>	<i>Odontella aurita</i>	<i>Streptotheca tamesis</i>
<i>Coscinodiscus concinnus</i>	<i>Odontella mobiliensis</i>	<i>Thalassionema nitzschioides</i>
<i>Coscinodiscus wailesii</i>	<i>Odontella obtusa</i>	<i>Thalassiosira</i> spp.
<i>Cylindrotheca closterium</i>	<i>Odontella regia</i>	<i>Thalassiothrix longissima</i>
<i>Dactylosolen antarcticus</i>	<i>Odontella rhombus</i>	<i>Triceratium favius</i>
<i>Dactylosolen mediterraneus</i>	<i>Odontella sinensis</i>	
<i>Defonula conferracea</i>	<i>Paralia sulcata</i>	Unidentified sub-species
<i>Diploneis</i> spp.	<i>Planktoniella sol</i>	<i>Nitzschia</i> spp.
<i>Ditylum brightwellii</i>	<i>Podosira stelliger</i>	<i>Coscinodiscus</i> spp.
<i>Encampia groenlandica</i>	<i>Rhaphoneis amphiveros</i>	

Table 2.3. Dinoflagellate taxa identified since 1958 by the CPR survey (Thomas 1997).

<i>Actiniscus pentasterias</i>	<i>Ceratium karstenii</i>	<i>Exuviaella</i> spp.
<i>Amphisolenia</i> spp.	<i>Ceratium lamellicorne</i>	<i>Glenodinium</i> spp.
<i>Blepharocysta paulsenii</i>	<i>Ceratium limulus</i>	<i>Goniodoma polyedricum</i>
<i>Centrodinium</i> spp.	<i>Ceratium lineatum</i>	<i>Gonyaulax</i> spp.
<i>Ceratium arcticum</i>	<i>Ceratium longipes</i>	<i>Gyrosigma</i> spp.
<i>Ceratium arietinum</i>	<i>Ceratium longirostrum</i>	<i>Hemiaulus</i> spp.
<i>Ceratium azoricum</i>	<i>Ceratium lunula</i>	<i>Histioneis</i> spp.
<i>Ceratium belone</i>	<i>Ceratium macroceros</i>	<i>Katodinium</i> spp.
<i>Ceratium breve</i>	<i>Ceratium massiliense</i>	<i>Murrayella</i> spp.
<i>Ceratium bucephalum</i>	<i>Ceratium minutum</i>	<i>Noctiluca scintillans</i>
<i>Ceratium buceros</i>	<i>Ceratium pentagonum</i>	<i>Ornithocercus</i> spp.
<i>Ceratium candelabrum</i>	<i>Ceratium platycorne</i>	<i>Ocyropsis</i> spp.
<i>Ceratium carriense</i>	<i>Ceratium pulchellum</i>	<i>Parahistioneis</i> spp.
<i>Ceratium compressum</i>	<i>Ceratium ranipes</i>	<i>Phalacroma</i> spp.
<i>Ceratium contortum</i>	<i>Ceratium setaceum</i>	<i>Podolampas</i> spp.
<i>Ceratium declinatum</i>	<i>Ceratium symmetricum</i>	<i>Polykrikos schwartzii</i> cysts
<i>Ceratium falcatifforme</i>	<i>Ceratium teres</i>	<i>Pronoctiluca pelagica</i>
<i>Ceratium extensum</i>	<i>Ceratium trichoceros</i>	<i>Prorocentrum</i> spp.
<i>Ceratium falcatum</i>	<i>Ceratium tripos</i>	<i>Protoceratium reticulatum</i>
<i>Ceratium furca</i>	<i>Ceratium vultur</i>	<i>Protoperidinium</i> spp.
<i>Ceratium susus</i>	<i>Ceratocorys</i> spp.	<i>Ptychodiscus noctiluca</i>
<i>Ceratium geniculatum</i>	<i>Cladopyxis</i> spp.	<i>Pyrocystis</i> spp.
<i>Ceratium gibberum</i>	<i>Corythodinium</i> spp.	<i>Pyrophacus</i> spp.
<i>Ceratium hexacanthum</i>	<i>Dinoflagellate</i> cysts	<i>Scrippsiella</i> spp.
<i>Ceratium horridum</i>	<i>Dinophysis</i> spp.	
<i>Ceratium inflatum</i>	<i>Dissodinium pseudolunula</i>	

generally radially symmetrical and the pennate diatoms, members of the Pennatibacillariophyceae, showing a typical bilateral symmetry. Members of both classes may be found in either fresh or salt water, although centric forms tend to predominate in marine habitats, while pennate diatoms are associated with benthic sediments or typical of freshwater environments. The main diatom taxa observed during the CPR survey are listed below in alphabetic order (Table 2.1).

2.B.1.b. Dinoflagellates

The dinoflagellates are the second most important group of primary producers identified in CPR samples, following the diatoms (Table 2.2). Dinoflagellates are unicellular protists that exhibit a great diversity of form. Only some dinoflagellates are strictly autotrophic, building organic materials and obtaining all their energy from photosynthesis. Other species carry out heterotrophic production; they meet their energy needs by feeding on phytoplankton and small zooplankton. The genus *Noctiluca*, for example, is large enough to eat fish eggs and is able to swallow protists larger than itself. Finally, some dinoflagellates are mixotrophic, and are capable of both autotrophic and heterotrophic production (Lalli & Parsons 1997). A number of photosynthetic dinoflagellates take up residence within other organisms as symbiotic partners (Lalli & Parsons 1997). These zooxanthellae may be found in many marine invertebrates, including sponges, corals, jellyfish, as well as within protists, such as ciliates or foraminifera. The majority of planktonic dinoflagellate species form the Dinophyceae, and the majority of them are thecate. Common thecate genera include *Ceratium*, *Protoperidinium*, *Gonyaulax* and *Dinophysis*.

2.B.1.c. Other taxa

Others taxa identified by the CPR survey are listed below.

- **Coccolithophorids:** they belong to a class of algae called the Prymnesiophyceae/Haptophyta, and have been recorded as present or absent in the CPR database between 1965 and 1993. Since 1993, they are counted in the CPR samples. Records are weighted toward larger species such as *Coccolithus pelagicus*, but 7 other species, including *Emiliana huxleyi*, and holococcolithophorids have been recorded (Hays *et al.*,

1995). Hays *et al.* (1995) suggested that these small species are present on CPR samples due to plankton clogging up the silk.

- ***Oscillatoria* spp.:** this species are now called *Trichodesmium* spp., belong to the class of Cyanophyceae and has been identified and counted in the CPR samples since 1958.
- ***Pachysphaera* spp.:** this species belong to the division Chlorophyta and the class of Prasinophyceae and has been identified and counted in the CPR samples since 1958.
- ***Phaeocystis pouchetii*:** this species belong to the class of Prymnesiophyceae/Haptophyta. Its presence recorded since 1958. This species has been found to be toxic to cod larvae in Norway (Moestrup 2004).
- ***Pterosperma* spp.:** this species belong to the division Chlorophyta and the class of Prasinophyceae and has been counted in the CPR samples since 1958.
- **Silicoflagellates:** they belong to a class of algae called the Dictyochophyceae and have been recorded as present or absent between 1965 and 1993 and have been counted in the CPR samples since 1993.

Chapter 3

DECADAL BASIN-SCALE CHANGES IN DIATOMS, DINOFLAGELLATES, AND PHYTOPLANKTON COLOUR ACROSS THE NORTH ATLANTIC

Part of this chapter has been included in the following:

Leterme S.C., Edwards M., Seuront L., Attrill M.J., Reid P.C. & John A.W.G. (2005) Decadal basin-scale changes in diatoms, dinoflagellates, and phytoplankton colour across the North Atlantic. *Limnology & Oceanography* 50(4): 1244-1253.

Leterme S.C., Edwards M., Seuront L., Attrill M.J. & Reid P.C. (2004) Decadal changes in phytoplankton biomass in the North Atlantic. Postgraduate Marine Biology Workshop, April 2004, University of Wales, Bangor, United Kingdom.

3.A. Introduction

The Phytoplankton Colour Index (PCI) and phytoplankton species determined by the CPR survey gives estimates of phytoplankton populations over large areas of the North Atlantic Ocean. This chapter will focus on the determination of long-term changes in phytoplankton at a basin-scale. In this context, a recent study based on CPR samples showed that much of the North Atlantic exhibited an increase in the Phytoplankton Colour Index during the period 1948–2000 (Barton *et al.* 2003). Barton *et al.* (2003) showed that the positive PCI trends observed in many areas are similar to the long-term trend in the North Atlantic Oscillation (NAO) index and provided hypotheses about the NAO-dependent physical factors underlying the long-term pattern of phytoplankton variability. Recent studies in fjords reported positive correlations between the NAO and both phytoplankton biomass and the abundance of three species of toxic dinoflagellates (Belgrano *et al.* 1999). A similar relationship has been shown in the English Channel for diatoms (Irigoien *et al.* 2000) and *Phaeocystis* sp. abundance (Seuront & Souissi 2002). Barton *et al.* (2003), however, based their analysis only on yearly mean PCI anomalies and whilst the PCI has been shown to be a relevant index of *in situ* chlorophyll concentration (Batten *et al.* 2003b), it has several limitations. First, it does not provide relevant information on the structural changes occurring in phytoplankton communities that are likely to influence phytoplankton biomass. A first step that would provide further insights into the space-time dynamics of phytoplankton communities is an analysis of diatom and dinoflagellate populations. These data can be used as corollary variables of phytoplankton biomass, allowing comparison of potential differences in the space-time dynamics of the PCI, diatom and dinoflagellate abundance. Finally, it is also critical to determine how the PCI compares to cell counts and to understand what is causing the observed large increase in phytoplankton biomass with time.

The aim of this chapter is thus to investigate over the period 1958-2002 (i) the long-term fluctuations of phytoplankton biomass, diatoms and dinoflagellates, (ii) their geographical variation within the North Atlantic basin, (iii) their relationship with climate forcing, (iv) the contribution of both diatoms and dinoflagellates to the PCI and (v) the fluctuations of the dominant species over the period of survey to provide more information on the processes linking climate to changes in the phytoplankton community.

3.B. Materials and methods

3.B.1. The data

Most of the diatom and dinoflagellate species have been identified and counted in the same way since 1958. Two taxa – coccolithophores and silicoflagellates – have only been counted since 1993; previously they were merely recorded as present or absent. Consequently, only diatoms and dinoflagellates are taken into account in the present work as they have complete time series. First, all species identified by the CPR survey (Warner & Hays 1994), and belonging to diatoms or dinoflagellates, were grouped by summing the number of cells identified to determine the overall trends of these two groups. Second, diatom and dinoflagellate species with a frequency of occurrence greater than 1% of the samples were used as indicator species to provide more information on the processes linking climate to changes in the phytoplankton community. Five dinoflagellate species (*i.e.* *Ceratium furca*, *C. fusus*, *C. horridum*, *C. lineatum*, and *C. tripos*) and six diatom taxa (*i.e.* *P. alata alata*, *Rhizosolenia hebetata semispina*, *R. styliformis*, *Thalassionema nitzschioides*, *Thalassiosira* spp., and *Thalassiothrix longissima*) have thus been investigated further.

The analysis is based on monthly time series to take into account the effect of seasonal variability. The area of study was divided into six regions, identified on bathymetric criteria (*i.e.* continental shelf boundaries) and divided according to a north-south axis. The six sub-regions of the North Atlantic Ocean considered here are as follows (Fig. 3.1): Northwest (51.5-74.5°N, 79.5-45°W), Southwest (29.5-51.5°N, 79.5-45°W), North Central (51.5-74.5°N, 45-20°W), South Central (29.5-51.5°N, 45-20°W), Northeast (51.5-74.5°N, 20°W-15°E), and Southeast (29.5-51.5°N, 20°W-15°E). In each area, the data obtained for the estimates of phytoplankton biomass (*i.e.* PCI) and phytoplankton abundance (*i.e.* total diatoms, total dinoflagellates and indicator species), have been averaged every month over the period 1958-2002; this period was chosen because analytical methodology has been consistent since 1958.

To identify the relationship between phytoplankton and climate forcing, two climatic indices have been used, the Sea Surface Temperature (SST) and the North Atlantic Oscillation (NAO). Several indices have been developed to quantify the state of the North Atlantic Oscillation, but the most widely used is Hurrell's NAO index (Hurrell 1995a). This index computes the pressure difference based on measurements from Lisbon, Portugal and Stykkisholmur, Iceland. In particular, NAO index values averaged from December to March

inclusive have been used as a climatic index (Hurrell 1995a). This index corresponds to the NAO winter index (see www.cdg.ucar.edu/~jhurrell/nao.html) which is used in this chapter. The Sea Surface Temperature (SST; see The British Atmospheric Data Centre, <http://badc.nerc.ac.uk/home>) data were used to provide additional climatic information likely to influence phytoplankton growth and abundance.

3.B.2. Statistical analysis

The normality of the data was assessed using a Kolmogorov-Smirnov statistical test. Where data did not correspond to a normal distribution, non-parametric statistics were used for further analysis. The stationarity of time series obtained in each of the six sub-regions was tested by calculating Kendall's coefficient of rank correlation, τ , between the series and the x-axis values in order to detect the presence of a linear trend. We thus eventually detrended the time series by fitting regressions to the original data by least squares and used the regression residuals in further analysis. As our samples are independent, Bonferroni's correction was not performed.

To detect changes, intensity and duration of any changes in the value of a given parameter, the cumulative sums method (Ibañez *et al.* 1993) has been used. The calculation consists of subtracting a reference value (here the mean of the series) from the data; these residuals are then successively added, forming a cumulative function. Successive positive residuals produce an increasing slope, whereas successive negative residuals produce a decreasing slope. A succession of values similar to the mean shows no slope. This method has only been applied on the NE and SE phytoplankton time series (*i.e.* PCI, total diatoms and total dinoflagellates) due to missing values in the other regions.

Autocorrelation was tested on each time series using ARIMA (AutoRegressive Integrated Moving Average); absence of any significant autocorrelation in the hydroclimatic indices ensures the relevance of further statistical analysis between these series and other data (Legendre & Legendre 1998). The relationship between phytoplankton and climate forcing was tested through Spearman correlation analysis performed between the phytoplankton estimators (*i.e.* abundance of the indicator species, total diatoms, total dinoflagellates, and PCI), the NAO winter index and SST. This test was conducted between 45 twelve-month series of SST, PCI, total diatom, total dinoflagellate and indicator species abundance over the

period 1958-2002. To test the relationship with the NAO, six time-series from March to August (which correspond to the main period of occurrence of the diatoms and the dinoflagellates) have been correlated with the NAO winter index of the previous winter. In order to infer potential differences in the effect of climate forcing on phytoplankton, correlation analyses were systematically conducted on non-detrended and detrended time series.

To identify the phytoplankton group and/or species that contributed to the PCIs in each month over the time period, multiple linear-regression models were constructed on the monthly time series. However, in order to assess complete time series, this analysis has been conducted only on the eastern part of the North Atlantic, which is the most continuously sampled over the study period. Not enough samples had been obtained in the NW North Atlantic over the period 1958-2002 to allow the relevant application of statistical analyses. No quantitative results are thus available for this area.

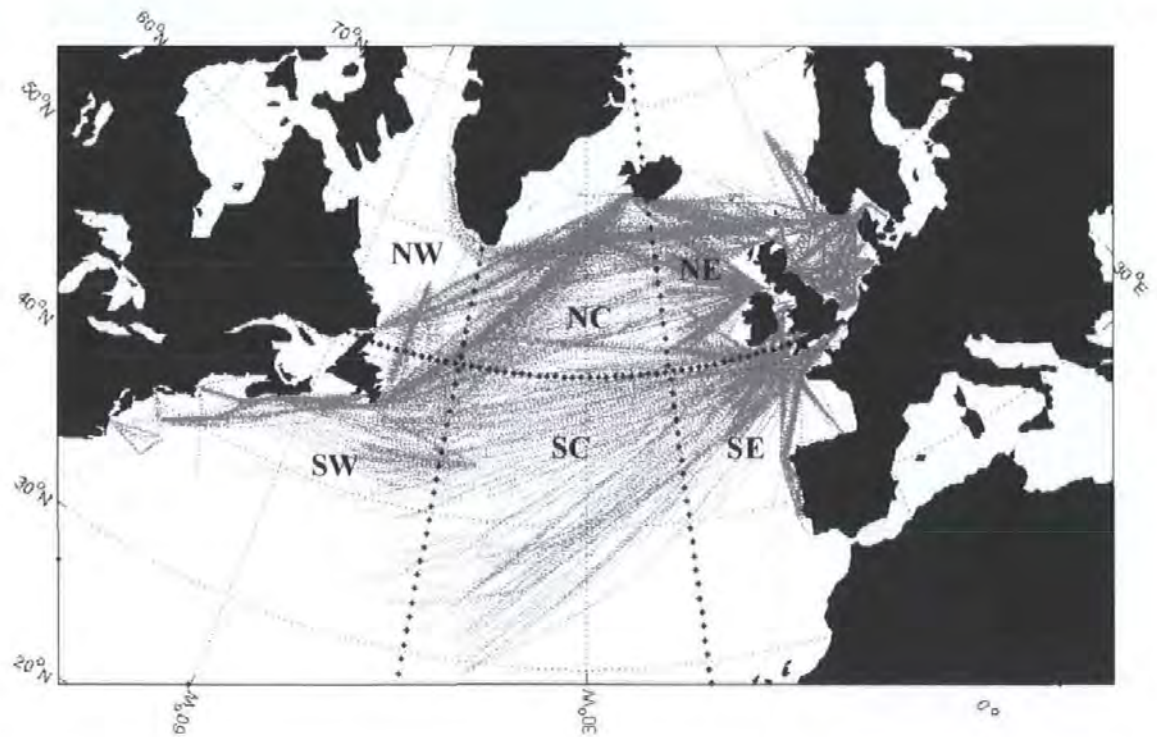


Figure 3.1. The North Atlantic basin divided into 6 regions identified on bathymetric criteria and separated according to a north-south axis: Northwest (NW), Southwest (SW), North Central (NC), South Central (SC), Northeast (NE) and Southeast (SE). CPR samples used in this chapter are illustrated in grey.

3.C. Results

Positive long-term trends have been observed for PCI within the five sub-regions of the North Atlantic (Fig. 3.2, Table 3.1), these trends are significant in the NE, SW and SC for the PCI. Total dinoflagellates and *Ceratium furca* have shown significant positive trend in the SW. Apart from the SW North Atlantic, where there is significant positive correlation between SST and both PCI and total dinoflagellates, there is no significant relationship between phytoplankton estimators and the SST. The cumulative sums obtained in the Eastern North Atlantic have shown different phases to the long-term trends (Fig. 3.3). For the PCI, there is an initial decreasing phase until 1979 and 1987 in the SE and in the NE, respectively. Subsequent increases in PCI have been observed. In the SE, the increasing trend is stronger than in the NE (Fig. 3.3). For diatoms (Fig. 3.3) there is an initial increasing trend until 1968 in the NE and 1970 in the SE, then a succession of decreasing trends has been observed. *Thalassionema nitzschioides*, *Thalassiosira* spp. and *Thalassiothrix longissima* exhibit the same patterns as the one observed for total diatoms. Dinoflagellates (Fig. 3.3) exhibit a combination of small-scale fluctuations around a succession of positive and negative phases. The same pattern has been observed with *Ceratium fusus*, *C. horridum* and *C. tripos*, which were also the most abundant species in the samples.

Table 3.1. Results of Kendall's statistical test for the whole time series of PCI, total diatoms and total dinoflagellates over the period 1958-2002. Significant ($p < 0.05$) results are in bold.

	Northeast	Southeast	North central	South central	Southwest
PCI	0.229	0.183	0.097	0.196	0.282
Total dinoflagellates	-0.035	0.040	0.016	0.046	0.240
Total diatoms	-0.080	-0.071	-0.049	0.003	0.107

Correlation analyses conducted between the 45-year time series of SST, PCI and phytoplankton species have shown positive relationships across the whole North Atlantic (Fig. 3.4). However, most significant correlations between SST, PCI and dinoflagellates (*i.e.* total dinoflagellates and indicator species) have been observed in the eastern, rather than in the western part of the North Atlantic Ocean (Table 3.2). The relationship between SST and diatoms showed a different pattern, as more significant correlations have been observed in the western than in the eastern part of the North Atlantic Ocean for total diatoms as well as for *T. nitzschioides*, *Thalassiosira* spp. and *T. longissima* (Table 3.2). Conversely, two of the indicator species (*i.e.* *P. alata alata* and *R. styliformis*) have shown the same pattern as the one observed

for dinoflagellates in the NE and NC Atlantic. The indicator species that have shown the same pattern as their taxonomic group (*i.e.* total diatoms) are the species that are the most abundant in the samples: *T. nitzschioides*, *Thalassiosira* spp. and *T. longissima*.

Table 3.2. Proportion (%) of significant correlations (Spearman correlation analysis) over the period 1958-2002 between 45 twelve-month time series of PCI, total dinoflagellates and total diatoms and SST across the North Atlantic.

	Northeast	Southeast	North central	South central	Southwest
PCI	64	29	53	18	18
Total dinoflagellates	100	89	69	31	22
<i>Ceratium furca</i>	100	64	47	20	4
<i>Ceratium fusus</i>	100	80	60	16	31
<i>Ceratium horridum</i>	98	44	29	0	9
<i>Ceratium lineatum</i>	100	47	44	2	7
<i>Ceratium tripos</i>	100	91	33	13	9
Total diatoms	4	11	53	16	33
<i>Proboscia alata alata</i>	96	71	31	2	7
<i>Rhizosolenia hebetata semispina</i>	4	24	13	0	4
<i>Rhizosolenia styliformis</i>	76	24	51	0	9
<i>Thalassionema nitzschioides</i>	18	13	38	2	31
<i>Thalassiosira</i> spp.	0	2	33	9	27
<i>Thalassiothrix longissima</i>	36	22	49	4	38

More detailed analyses of the 12 monthly time series have highlighted that the significance of trends observed for the PCI depends on the month and the geographical area (Table 3.3). Similar results have been found for dinoflagellates and diatoms. In the NE and NC, dinoflagellates have shown negative trends (Table 3.3), while positive trends have been observed in the other regions. On the other hand, positive trends have been observed for total diatoms in the SW, but trends are negative in the other regions of the North Atlantic (Table 3.3). Alternatively, in the NC, for total diatoms, significant negative trends have been observed in July and September. Correlation analyses conducted between the monthly time series and the NAO winter index (Hurrell 1995a) have also shown different results related to the time period and the study area. Positive relationships have been observed between the NAO and dinoflagellates during April (*i.e.* total dinoflagellates, *C. furca* and *C. horridum*) and May (*i.e.* total dinoflagellates and all the indicator species) and between NAO and PCI during April, May and June in the NE (Table 3.4).

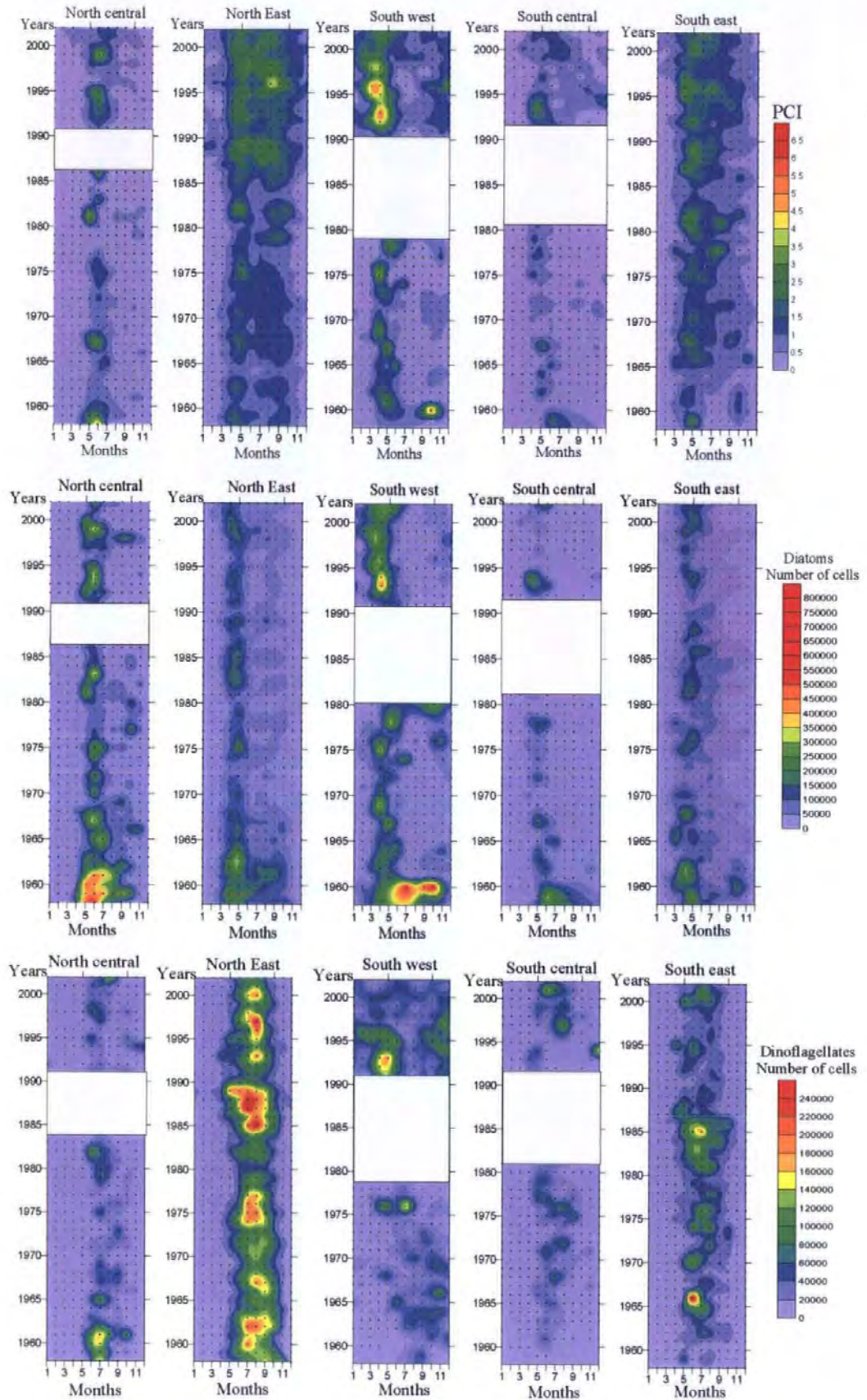


Figure 3.2. Hovmöller diagrams of PCI, total diatoms abundance and total dinoflagellates abundance over the period 1958-2002 in the different regions of the North Atlantic basin.

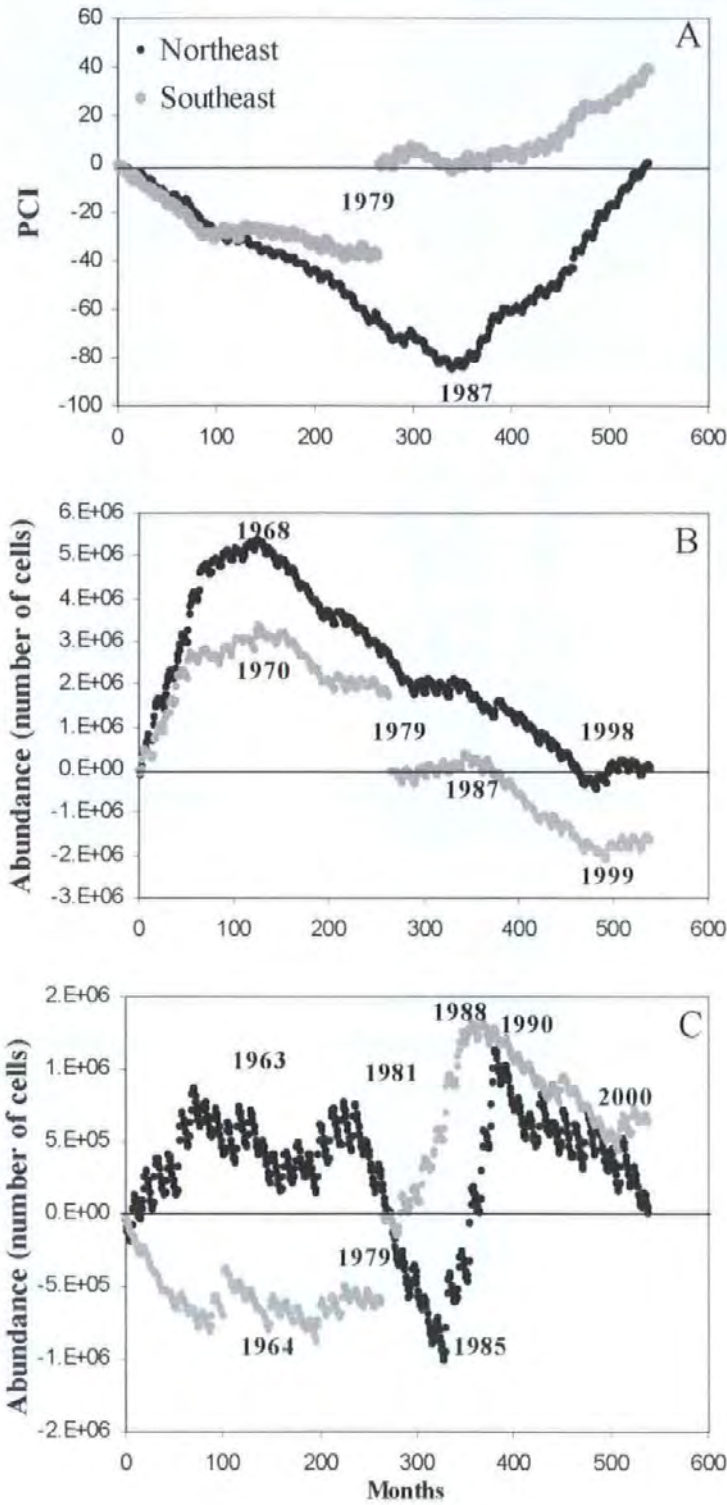


Figure 3.3 Cumulative sums of the PCI (A), total diatom abundance (B) and total dinoflagellate abundance (C) for each month over the period 1958-2002 (540 data points) in the Northeast (black) and the Southeast Atlantic (grey).

Table 3.3. Kendall's statistical test performed on monthly time series of PCI (A), total diatoms (B) and total dinoflagellates (C) over the period 1958-2002. Significant ($p < 0.05$) results are in bold.

	Northeast			Southeast			North central			South central			Southwest		
	A	B	C	A	B	C	A	B	C	A	B	C	A	B	C
January	0.362	0.101	-0.125	0.446	0.130	0.097	0.337	0.289	0.223	-0.099	0.053	0.145	0.370	0.394	0.362
February	0.339	0.122	-0.079	0.353	-0.070	-0.087	0.249	0.196	0.192	0.252	0.154	0.089	0.424	0.397	0.382
March	0.145	-0.203	-0.029	0.187	-0.200	0.197	0.249	0.019	0.172	0.229	-0.010	0.053	0.344	0.391	0.412
April	0.298	-0.074	0.108	0.251	-0.126	0.190	0.102	-0.097	0.214	0.267	0.226	0.180	0.354	0.212	0.465
May	0.434	-0.351	0.087	0.226	-0.105	0.187	-0.088	-0.165	-0.185	0.219	0.136	0.276	0.124	0.032	0.301
June	0.509	-0.210	0.067	0.516	0.106	0.090	0.019	-0.190	0.081	0.102	-0.261	-0.155	0.151	-0.056	0.374
July	0.313	-0.250	-0.059	0.485	-0.163	0.048	0.12	-0.383	-0.228	0.384	0.006	0.179	0.210	0.037	0.144
August	0.547	0.224	0.040	0.542	-0.171	0.157	0.184	-0.307	-0.177	0.278	0.124	0.277	0.312	0.237	-0.084
September	0.378	-0.177	-0.348	0.361	-0.212	0.204	-0.08	-0.344	-0.214	0.236	-0.091	0.153	0.304	-0.008	0.028
October	0.197	-0.296	-0.444	0.131	-0.181	-0.119	0.307	-0.142	0.022	0.171	0.004	0.038	0.243	-0.028	0.039
November	0.281	-0.038	-0.271	0.162	-0.230	-0.104	0.121	-0.053	-0.013	0.493	-0.215	0.192	0.494	0.246	0.153
December	0.409	0.003	-0.084	0.339	-0.021	-0.016	0.361	0.192	0.179	0.214	0.113	-0.062	0.489	0.228	0.246

Table 3.4. Results of Spearman's correlation analysis between the monthly time series of PCI, diatoms and dinoflagellates and the NAO winter index over the period 1958-2002. Significant ($p < 0.05$) results are in bold.

months	PCI					Diatoms					Dinoflagellates				
	April	May	June	July	August	April	May	June	July	August	April	May	June	July	August
Northeast	0.388	0.371	0.482	0.176	0.234	0.074	-0.259	-0.027	-0.131	-0.109	0.389	0.546	0.109	0.084	-0.139
Southeast	0.172	0.218	0.295	0.189	0.297	-0.008	0.078	0.070	-0.146	0.042	0.207	0.183	0.039	0.070	0.143
North central	0.010	0.408	0.380	0.029	0.146	-0.210	0.272	0.213	-0.274	-0.356	0.025	0.182	0.111	-0.143	-0.139
South central	0.285	0.237	0.029	0.331	0.195	0.300	0.242	-0.144	-0.134	0.030	0.191	0.202	-0.360	0.046	0.025
Southwest	0.328	0.395	-0.015	0.249	0.145	0.076	0.137	-0.110	0.080	0.281	0.368	0.178	0.418	-0.151	-0.148

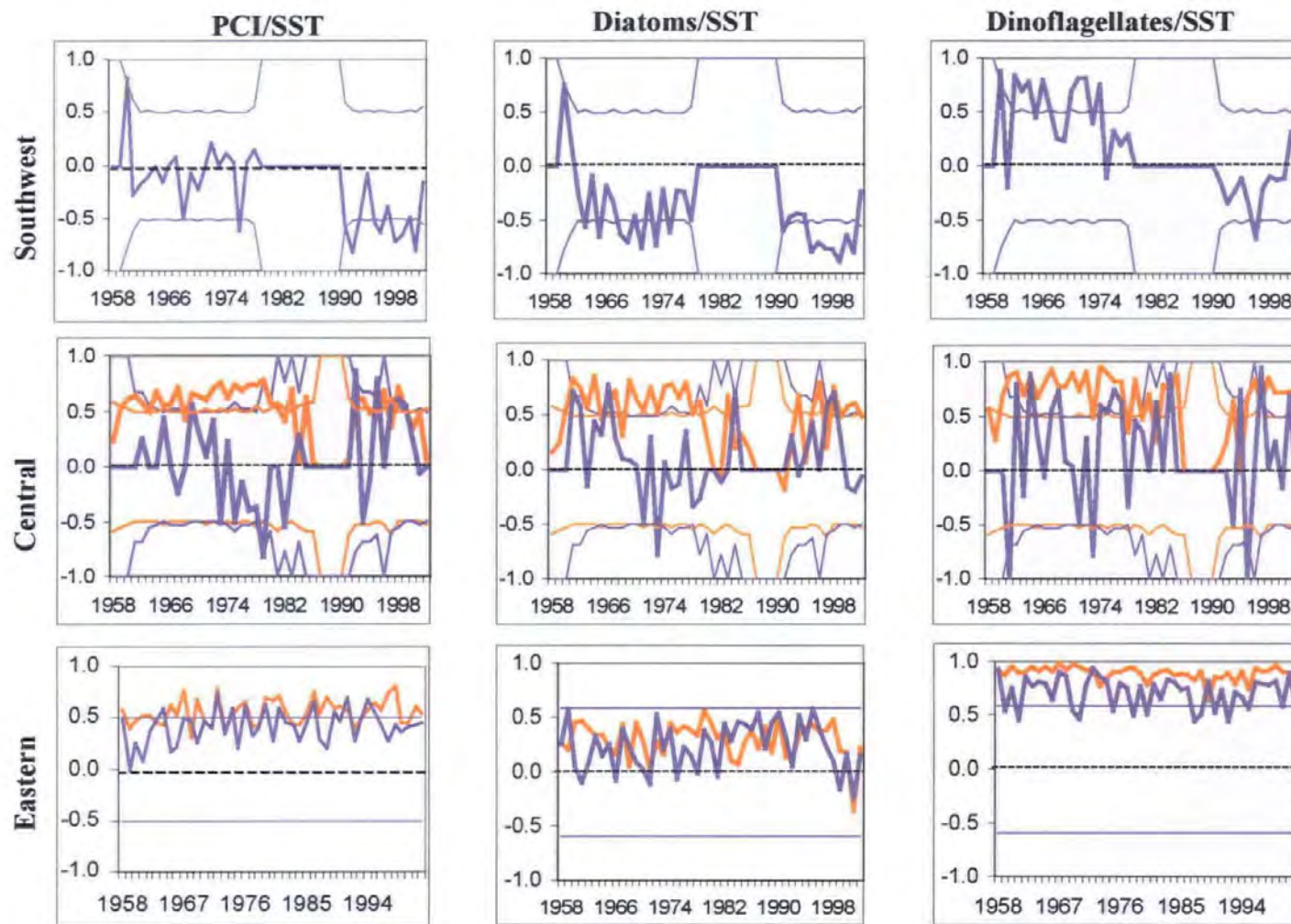


Figure 3.4. Fluctuations of the Spearman correlation coefficient (bold lines) obtained between SST and PCI, total diatoms and total dinoflagellates over the period 1958-2002 in the Southwest, Central and Eastern North Atlantic. The Central and the Eastern areas have been divided in two parts: North (orange) and South (blue). The thin lines represent the significance limits at $p < 0.05$.

In the SE, NAO and PCI have shown a positive correlation in June and August (Table 3.4). In the NC positive relationships have been observed between NAO and PCI in May and June even though diatoms and NAO have shown negative correlation in July (*i.e.* total diatoms, *Thalassiosira* spp. and *T. nitzschoides*) and August (*i.e.* total diatoms and *T. nitzschoides*) and a positive relationship in May (*i.e.* total diatoms, *R. hebetata semispina*, *Thalassiosira* spp. and *T. longissima*) and June (*i.e.* total diatoms, *R. hebetata semispina* and *Thalassiosira* spp.).

In the SC, the NAO shows a positive relationship with PCI in April and July, with diatoms in April and a negative relationship with dinoflagellates in June (*i.e.* total dinoflagellates, *C. fusus* and *C. lineatum*). In the SW, positive relationships have been observed between the NAO and PCI in April and May (Table 3.4), with dinoflagellates in April (*i.e.* total dinoflagellates, *C. lineatum* and *C. tripos*) and June (*i.e.* total dinoflagellates) and with diatoms in August (*i.e.* total diatoms, *P. alata alata*, *R. hebetata semispina* and *T. nitzschoides*). The analyses conducted on the detrended time series led to similar results, but only during the spring as no significant correlations were observed for other months.

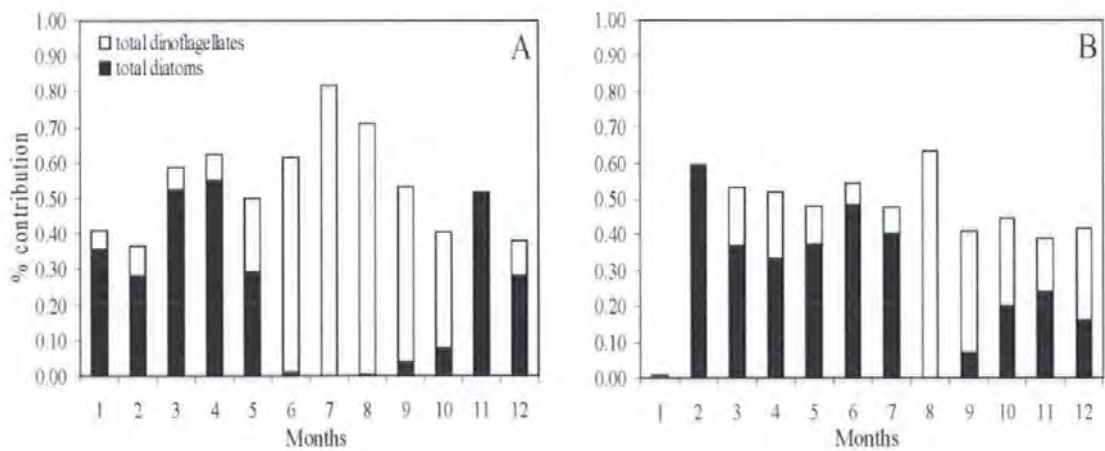


Figure 3.5. Contribution to the PCI of total diatoms and total dinoflagellates in the Northeast (A) and Southeast (B) North Atlantic.

Finally, the results of the multiple linear-regression conducted on the monthly time series to identify the contributions of diatoms and dinoflagellates to the PCI in the Eastern North Atlantic are shown in Fig. 3.5. These contributions are variable depending on the month. In the NE, the main contribution of diatoms occurs between January and May and during November and December (Fig. 3.5). For the dinoflagellates the main contribution is between June and October (Fig. 3.5). In contrast, in the SE the contribution of diatoms and dinoflagellates to PCI

is more variable over the whole year. The main contribution of diatoms to the PCI thus occurred from February to July and in November and from August to October and in December for the dinoflagellates (Fig. 3.5). No significant contribution of diatoms and dinoflagellates to the PCI has been identified in January.

3.D. Discussion

In the North Atlantic Ocean, between 1958 and 2002 there are evident overall trends of increasing Phytoplankton Colour and dinoflagellates and a decrease of diatoms (Fig. 3.4). This increasing trend of the PCI has already been shown in the North Sea (Reid & Edwards 2001), in the area west of the British Isles (Edwards *et al.* 2001), over the Scotian Shelf and Georges Bank in the NW Atlantic (Sameoto 2001) and recently over all the North Atlantic basin (Barton *et al.* 2003). In the framework of this chapter, the use of diatoms and dinoflagellates allowed a better understanding of the processes leading to the long-term trends observed for the PCI.

3.D.1. Phytoplankton variability in the Eastern Atlantic: towards sea surface temperature and nutrient control

In the Southern North Sea, the increase in phytoplankton biomass has been attributed to an increase in nutrient inputs from the major European rivers during the past decades (Richardson 1997). However, eutrophication has mainly an effect on phytoplankton biomass in the coastal margins and, in particular, those areas that have limited water exchange (Edwards *et al.* 2001). In the offshore waters of the North Sea, variability in environmental conditions is thought to play a dominant role in temporal fluctuations of phytoplankton biomass (Edwards *et al.* 2001). In this chapter, the NE North Atlantic area brings together different types of environment like the North Sea, the English Channel, the Celtic Sea, the Irish Sea and the area west of the British Isles (which corresponds to oceanic waters). In such open waters, eutrophication is highly unlikely to explain the fluctuations in phytoplankton biomass.

It is possible, however, to relate phytoplankton fluctuations to hydrometeorological processes characterizing the Northern hemisphere. These processes are thus likely to control physical parameters that affect phytoplankton growth (*e.g.* temperature and turbulence). Temperature determines the rate at which phytoplankton cells divide; nutrient supply and wind-induced turbulent mixing control the onset of the spring phytoplankton bloom (Sverdrup 1953). All these parameters have also been shown to be influenced by the NAO, the atmospheric

variables exerting strong forcing on the ocean leading to changes in sea surface temperature, seawater salinity, vertical mixing, circulation patterns and, in northern areas, ice formation (Visbeck *et al.* 2003).

More specifically, the present work showed that the relationship between PCI, dinoflagellates, diatoms and the SST varies depending on the area, there being a stronger relationship between SST and PCI or dinoflagellates in the eastern part of the ocean (see Table 3.2). The inverse has been observed for diatoms (*i.e.* *T. nitzschioides*, *Thalassiosira* spp. and *T. longissima*), with a stronger correlation in the Western North Atlantic. These observations can be linked to the influence of the NAO through the North Atlantic basin, as Drinkwater *et al.* (2003) have shown that the physical response to NAO forcing varies spatially across the North Atlantic. Furthermore, the main factors likely to affect phytoplankton dynamics and community structure (besides light, temperature and salinity) are turbulence and the related nutrient supply (Li 2002, Rodriguez *et al.* 2001).

Different adaptive strategies are required to deal with different combinations of these factors, embodied mainly in the differences between diatoms and dinoflagellates (Margalef 1975). Dinoflagellates possess an undulating flagellum that keeps the cell turning and accelerates the flow of water over the cell body that improves the chances for nutrient absorption (Margalef 1997). In stratified and low turbulence water, it pays to invest energy in swimming and so to be able to position the cell in the most favourable environment. This optimisation can be useless in turbulent water where the nutrients are more easily redistributed in the water column and where non-motile diatoms frequently flourish. Warmer surface temperatures related to the increasing NAO winter index promote earlier, or more intense, stratification of the upper water-column (Drinkwater *et al.* 2003). According to Margalef's (1975) hypothesis, all these factors would create an environment favouring the growth of dinoflagellates (*e.g.* *C. tripos*, a typical species of mixed Atlantic waters) over the growth of diatoms (*e.g.* *R. styliformis*) in both parts of the eastern North Atlantic. This is fully congruent with our observations regarding the differential relationships found between dinoflagellates, diatoms and the NAO (see Table 3.3, 4).

3.D.2. Phytoplankton fluctuations in the Western Atlantic: basin-scale circulation control

Bathymetry, coupled with the differences in the relative strength and/or seasonality of advection, tidal mixing and stratification lead to a strong spatial heterogeneity in the oceanographic environment that phytoplankton encounter in the Gulf of Maine (Thomas *et al.* 2003). Georges Bank, on the other hand, remains relatively well vertically mixed throughout the year, eliminating much of the influence of stratification on the timing of phytoplankton seasonality (Thomas *et al.* 2003). In this chapter, PCI, dinoflagellates and diatoms have all shown significant increasing trends in this area, but during different periods. Diatoms have shown an increase between January and March and dinoflagellates increased in spring. These observations correspond to an increase in the occurrence of these two taxa during the first months of the period in which they are usually present, leading to an earlier presence of these taxa during the year. Similar conclusions have been drawn for the dinoflagellates in the NE. Furthermore, positive relationships have been observed between the winter NAO and spring values for both dinoflagellates (*i.e.* *C. lineatum* and *C. tripos*) and the PCI and on the other hand with diatoms (*i.e.* *P. alata alata*, *R. hebetata semispina* and *T. nitzschioides*) during August.

Thomas *et al.* (2003) suggest that basin-scale forcing associated with the NAO, through its influence on hydrographic structure, has also the potential to induce interannual variability in phytoplankton dynamics in the Gulf of Maine. During positive NAO phases, this area is subjected to warmer, drier and milder conditions (Hurrell 1995a, Visbeck *et al.* 2003). The NAO also affects the shallow and deepwater circulation patterns of the North Atlantic. During positive phases of the NAO, convection is deeper and more intense in the Labrador Sea and a relatively cool, fresh and thick layer of Labrador Sea Water (LSW) is formed (Dickson *et al.* 1996). This results in higher salinity and temperature on the Scotian Shelf and in the Gulf of Maine (Petrie & Drinkwater 1993) and in higher nutrient concentration (Gatien 1976). The observed increase of the PCI can then be linked to the increase in nutrients in the Gulf of Maine and the Scotian Shelf. Higher salinity and temperature associated with higher nutrient concentration can also create favourable conditions for the growth of dinoflagellates such as *C. lineatum* and *C. tripos*, typical of mixed Atlantic waters, in spring. Diatom species typical of oligotrophic waters, such as *Rhizosolenia* spp., thus encounter favourable conditions at the end of the summer when low nutrient conditions prevail.

3.D.3. Phytoplankton changes in the Central Atlantic: meteorological control

Few studies have focused on the central part of the North Atlantic Ocean (Kushnir *et al.* 1997, Hurrell *et al.* 2003). Here, long-term increasing trends in PCI have been observed over the whole area and only in the SC for the dinoflagellates. In contrast, positive then negative trends have been observed for diatoms in the NC (Table 3.3). These observations correspond to a decrease in the occurrence of these two taxa for the last months of their bloom period, leading to a shortening of their presence during the year and/or to an earlier bloom. The same situation has been observed for the dinoflagellates in the SC area. Their abundance at the beginning of the bloom significantly increased, suggesting an earlier presence of dinoflagellates during the year. In addition, the relationship between NAO and phytoplankton is clearly different, whether it relates to different taxonomic groups or to PCI. A positive relationship has been observed between both PCI and diatoms (*i.e.* *R. hebetata semispina*, *Thalassiosira* spp. and *T. longissima*) and NAO in the North and South of the central area. In the opposite sense, a negative relationship has been identified in the NC between diatoms (*i.e.* *T. nitzschoides*, a typical species in the Central North Atlantic Ocean) and NAO in August and between dinoflagellates (*i.e.* *C. fusus* and *C. lineatum*) and NAO in June in the SC (see Table 3.4).

While it is still difficult to clearly identify the processes driving the patterns discussed above, it should be noted that changes in the mean circulation patterns over the North Atlantic associated with the NAO are also associated with changes in the intensity and number of storms. During winter, a well-defined storm track connects the North Pacific and North Atlantic basins, with maximum storm activity over the oceans (Hurrell *et al.* 2003). As the ocean integrates the effects of storms in the form of surface waves, the recent upward trend towards more positive NAO index winters could be associated with increased wave heights over the northeast Atlantic and decreased wave heights south of 40°N (Kushnir *et al.* 1997). As the increase in storms will lead to an increase in wind-induced vertical mixing, during positive NAO phases a larger area in the centre of the North Atlantic is expected to be less stratified and cooler than normal. As these parameters strongly influence phytoplankton growth and species succession, it is believed that their complex interactions might play a role in the timing and temporal patterns of diatom and dinoflagellate occurrence, abundance and succession. Further information relating to the specific hydrometeorological conditions characterizing our sampling would nevertheless be necessary to infer the previous hypothesis.

3.D.4. Differential contribution of phytoplankton taxonomic groups to the Phytoplankton Colour Index

In the NE Atlantic, the main contributors to the Phytoplankton Colour Index are diatoms (*i.e.* *Thalassiosira* spp. and *T. longissima*) between January and May and dinoflagellates (*i.e.* *C. furca* and *C. fusus*) between June and October. These periods correspond to the characteristic bloom periods of these groups. However, whilst from March to September and in November, 52 to 82% of the PCI can be explained respectively by the contribution of diatoms and dinoflagellates, during other months they explain only up to 40% of the PCI (Fig. 3.5). The same pattern occurs in the SE area, where 39 to 64% of the PCI is explained by diatoms and dinoflagellates between February and December. Diatoms (*i.e.* *P. alata alata*, *T. nitzschoides* and *Thalassiosira* spp.) and dinoflagellates (*i.e.* *C. furca* and *C. tripos*) are the main contributors to the PCI between February and July and between August and December respectively in the SE. During January, only 1% of the PCI is explained by these groups (Fig. 3.3). Other categories of phytoplankton must also be involved in the fluctuations of the PCI. Other taxa identified by the CPR survey have not been taken into account in this chapter and some taxa are too small to be counted and identified by the CPR survey. Microflagellates, for instance, would not be identifiable in the CPR samples, as they disintegrate in formalin, but their chloroplasts would survive to add to the coloration of the silks. Future studies would then benefit from more in depth investigations of the relative contribution of other taxonomic groups identified by the CPR survey to the PCI, in order to improve the ecological relevance of this index.

Chapter 4

DIFFERENTIAL CONTRIBUTION OF DIATOMS AND DINOFLAGELLATES TO PHYTOPLANKTON BIOMASS IN THE NE ATLANTIC AND THE NORTH SEA

Part of this chapter has been included in the following:

Leterme S.C., Seuront, L. & Edwards M. (2006) Differential contribution of diatoms and dinoflagellates to phytoplankton biomass in the NE Atlantic and the North Sea. *Marine Ecology Progress Series* 312: 57-65.

4.A. Introduction

Interannual fluctuations in phytoplankton species composition and abundance have received less attention in the NE Atlantic than those of higher trophic groups such as zooplankton (Planque & Taylor 1998, Hays *et al.* 2001, Lindley & Batten 2002) and fish (Fromentin *et al.* 1998, Sims & Reid 2002, Lindley *et al.* 2003). Since 1958, several studies have shown an increase in phytoplankton biomass in the North Atlantic (Barton *et al.* 2003, Leterme *et al.* 2005), the NE Atlantic (Reid *et al.* 1987) and the North Sea (Reid 1978, Reid & Edwards 2001). The overall phytoplankton abundance in the NE Atlantic has been shown to be driven mainly by variations in sea surface temperature (Richardson & Schoeman 2004).

Changes in phytoplankton abundance and/or community composition may impact zooplankton population structure and their predator abundance. This is especially true in a complex marine ecosystems including different types of environments from open oceanic waters to epicontinental basins and neritic coastal regions such as the NE Atlantic and the North Sea. In particular, the North Sea is hydrographically divided into different regions, from seasonally stratified waters in the north to tidally mixed waters in the south. Edwards and Richardson (2004) have shown that the response of the marine pelagic community to climate changes in the central North Sea, leading to a mismatch between trophic levels and taxonomic groups.

The Continuous Plankton Recorder (CPR) survey provides records of the abundance of 500 phytoplankton and zooplankton taxa and provides a visual assessment of phytoplankton biomass, *i.e.* the Phytoplankton Colour index (PCI, Colebrook & Robinson 1965). Within the phytoplankton, diatoms and dinoflagellates are the main taxonomic groups identified by the survey, consisting of 178 species or taxa. Most phytoplankton taxa have been enumerated and identified following a procedure that has remained consistent since 1958. The PCI has been extensively used to describe the seasonal and long-term patterns of phytoplankton abundance (Reid 1978, Edwards *et al.* 2001, Batten *et al.* 2003a, Johns *et al.* 2003) in various regions of the North Atlantic. An increasing trend in phytoplankton biomass has been shown in the North Sea (Lancelot *et al.* 1997, Cadée & Hegeman 1993, Hickel *et al.* 1995, Reid & Edwards 2001), and in the area west of the British Isles (Edwards *et al.* 2001). Such increases have been lately observed in different region of the globe. Different explanations have been formulated to explain this increase, *e.g.* hydro-climatic processes (Edwards *et al.* 2001, Richardson & Schoeman 2004) and eutrophication (Lancelot *et al.* 1997, Cloern 2001). However, to our

knowledge, this increase has not been investigated in relation to the two most abundant taxonomic groups within the phytoplankton assemblage, the diatoms and dinoflagellates.

The aim of this chapter is thus to determine: (i) the long-term trends of PCI and diatom and dinoflagellate abundance, (ii) the contribution of the diatoms and dinoflagellates to the PCI, (iii) their fluctuations over 45 yr of sampling, (iv) their geographical variations in the NE Atlantic and (v) how they may be linked to hydro-climatic variables such as the North Atlantic Oscillation (NAO) and sea surface temperature (SST).

4. B. Materials and methods

Different groups of phytoplankton taxa have been identified by the CPR survey (*e.g.* diatoms, dinoflagellates, coccolithophores and silicoflagellates), many to the species level. Diatom and dinoflagellate species have been identified and counted in the same way since 1958, while coccolithophores and silicoflagellates have only been enumerated since 1993. It is thus impossible to conduct the same analyses on those taxa. Consequently, only diatoms and dinoflagellates (*i.e.* a total of 131 species) were taken into account in the present chapter, to consistently investigate the period from 1958 to 2002. The abundance of all diatom and dinoflagellate species (75 and 56, respectively) identified in the NE Atlantic (Warner & Hays 1994) was derived by summing the number of cells identified to determine the overall trends of these 2 groups (Leterme *et al.* 2005).

The potential influence of hydro-climatic variables on phytoplankton fluctuations was investigated using the NAO winter index and the SST. Hurrell's NAO winter index (Hurrell 1995a) computes the pressure difference based on measurements from Lisbon, Portugal, and Stykkisholmur, Iceland, from December to March. The SST (Hadley Centre Sea Ice and SST data set (HadISST) Version 1.1) data were provided by the Hadley Centre, UK Met Office.

The study area (Fig. 4.1) corresponds to 2 regions identified along a north–south axis: the North NE Atlantic (51 to 64°N, 20°W to 15°E) and the South NE Atlantic (37 to 51°N, 20°W to 15°E). Even if the North NE Atlantic includes the epicontinental North Sea, the latter was considered separately for the purposes of this study and divided into 3 regions along a north–south axis following the limits of the CPR 'Standard Areas' (Colebrook 1975) to take into

account the different hydrographical forcing processes (e.g. the northern inflow of Atlantic waters between Scotland and Norway and the southern inflow via the English Channel).

Using the 108,951 samples available from 1958 to 2002, annual means of PCI, diatom and dinoflagellate abundance were generated as a preliminary step to detect long-term trends. More specifically, monthly means of PCI, diatom and dinoflagellate abundance were calculated to investigate details of the relationship between the PCI and diatom and dinoflagellate abundance in the 5 above mentioned areas. To determine the contribution of diatoms and dinoflagellates to the PCI and their variations during the period of study, multiple linear regression analysis (Sokal & Rohlf 1995, Zar 1996) was conducted between monthly means of PCI, diatom and dinoflagellate abundance for each sampling year. This analysis was performed only on the complete time series of data (i.e. 12 monthly means yr^{-1}). As a consequence, when the time series were not complete, our analysis generated missing values in the contribution time series. Thus, 4 and 20% of the values are missing in the contribution time series for the central and southern North Sea, respectively. We also stress that because large dinoflagellate species (e.g. *Ceratium* spp.) and chain-forming diatoms (e.g. *Chaetoceros* spp.) were undersampled (Warner & Hays 1994, Edwards *et al.* 2006), the sum of the contributions of total diatoms and total dinoflagellates did not always reach 100%.

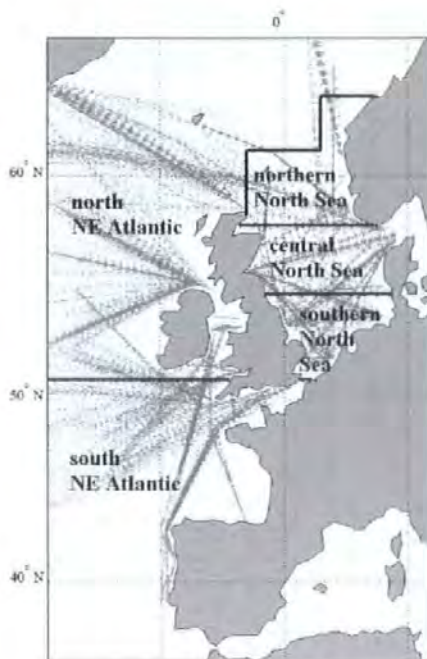


Figure 4.1. The NE Atlantic divided into two regions separated according to a North-South axis: North NE (NE) and South NE (SE) and the North Sea divided into three regions: Northern (N), central (C) and Southern (S) from a North-South axis following the limits of the CPR Standard Areas. CPR samples used in this study are illustrated in grey.

The residuals of the diatom/dinoflagellate contribution were analysed in order to infer the contribution of other groups to the PCI. Long-term trends in abundance and in the contribution of diatoms and dinoflagellates to the PCI were examined in each region by calculating Kendall's coefficient of rank correlation, τ , between the series and the time in years in order to detect the presence of a linear trend (Kendall & Stuart 1966). Kendall's coefficient of correlation is used in preference to Spearman's coefficient of correlation, ρ , although the latter was recommended in Kendall (1976), because Spearman's ρ gives greater weight to pairs of ranks that are further apart, while Kendall's τ weights each disagreement in rank equally (see Sokal & Rohlf 1995 for further developments).

To detect changes and the intensity and duration of any changes in the value of a given parameter, the cumulative sums method (Ibañez *et al.* 1993) has been used. The calculation consists of subtracting a reference value (here the mean of the series) from the data; the anomalies are then successively added, forming a cumulative function. Successive positive anomalies produce an increasing slope, whereas successive negative anomalies produce a decreasing slope. Succession of values with little difference from the mean show no slope. This analysis was performed on the time series of annual means in all the areas, but it was performed on the time series of contributions only in the NE Atlantic, due to the excess of missing data for the North Sea.

The relationship between phytoplankton and climate indices was tested through Spearman correlation analysis performed for the NE and SE North Atlantic between the abundance and contribution of diatoms and dinoflagellates and (i) the NAO winter index and (ii) the SST. As stated above, these tests were not performed for the North Sea, due to the excess of missing data.

4.C. Results

4.C.1. The Northeast Atlantic

4.C.1.a. The North Northeast Atlantic

In the North NE Atlantic, there is a significant increase in PCI and a significant decrease in diatom and dinoflagellate abundances (Fig. 4.2.A, Table 4.1). The cumulative sums revealed different short-term trends in PCI and diatom abundance, but none for dinoflagellate

abundance (Fig. 4.2.C). The cumulative sums of PCI decreased and increased, respectively, before and after 1986, while it increased and decreased, respectively, before and after 1967 for diatoms. This suggests a shift in phytoplankton biomass and diatom abundance before and after 1986 and 1967, respectively.

Over the period of study, the contribution of diatoms significantly decreased (Table 4.2) from 66 to 37%. In contrast, the contribution of dinoflagellates did not exhibit any significant trend. The residuals of the diatom/dinoflagellate contribution significantly increased (Table 4.2) from 22 to 36%. In addition, a shift was observed in the phytoplankton community between 1986 and 1996, when dinoflagellates become more dominant than diatoms in the community Fig. (4.3.A). This is specified by the cumulative sums, which suggests a period of relative stability in diatom and dinoflagellate contributions from 1958 to 1985, followed by antisymmetric short-term trends from 1985 to 2002 (Fig. 4.3.C). This suggests a stability of the phytoplankton community composition before 1985.

PCI and diatom abundance have shown a significant positive correlation with NAO and SST, respectively, but no relationships were observed between the climatic parameters and dinoflagellate abundance (Table 4.3). No relationship was observed between the NAO winter index and the diatom/dinoflagellate contribution to the PCI (Table 4.4). Conversely, the contribution of dinoflagellates resulted in a significant negative relationship with SST (Table 4.4). No significant long-term trend was observed for the SST over the period of study (Kendall's $\tau = 0.034$, $p < 0.05$).

However, no significant decadal trend was identified for dinoflagellate abundance (Table 4.1). The cumulative sums revealed different short-term trends in PCI, with a decrease and increase, respectively, before and after 1984 (Fig. 4.2.D). As observed in the North NE Atlantic, the cumulative sums of diatom abundance increased before 1967 and globally decreased after 1967, with a short-term increase between 1979 and 1985 (Fig. 4.2.D). In contrast, the cumulative sums of dinoflagellate abundance were relatively constant from 1958 to 1979, followed by an increase until 1985 and a decrease until 2002 (Fig. 4.2.D).

Table 4.1. Kendall's τ estimated from the time series of PCI, diatom and dinoflagellate abundances over the period 1958-2002. *5% significance level

	PCI	diatoms	dinoflagellates
North NE Atlantic	0.378 *	-0.337 *	-0.297 *
South NE Atlantic	0.535 *	-0.248 *	0.085
Northern North Sea	0.624 *	-0.020	0.364 *
Central North Sea	0.386 *	-0.200	-0.085
Southern North Sea	0.329 *	-0.158	-0.242 *

Table 4.2. Kendall's τ estimated for the contribution of diatoms and dinoflagellates toward the PCI and their residuals over the period 1958-2002. *5% significance level

	diatoms	dinoflagellates	residuals
North NE Atlantic	-0.236 *	0.190	0.232 *
South NE Atlantic	0.039	0.206 *	-0.177
Northern North Sea	-0.204 *	0.253 *	0.114
Central North Sea	-0.038	-0.054	0.104
Southern North Sea	0.011	-0.059	0.075

Table 4.3. Spearman's ρ estimated between PCI and diatom and dinoflagellate abundances and (i) the North Atlantic Oscillation index and (ii) the Sea Surface Temperature over the period 1958-2002. *5% significance level

Abundance	North Atlantic Oscillation			Sea Surface Temperature		
	diatoms	dinoflagellates	PCI	diatoms	dinoflagellates	PCI
North NE Atlantic	-0.114	-0.031	0.378*	0.372*	0.250	0.281
South NE Atlantic	-0.207	0.161	0.263	-0.017	-0.054	0.170
Northern North Sea	-0.008	0.153	0.399*	-0.028	0.076	0.155
Central North Sea	-0.143	0.018	0.179	-0.119	-0.028	0.302*
Southern North Sea	-0.153	-0.193	0.082	-0.067	-0.173	0.466*

Table 4.4. Spearman's ρ estimated between the contribution of diatoms and dinoflagellates and (i) the North Atlantic Oscillation index and (ii) the Sea Surface Temperature over the period 1958-2002. *5% significance level

Contribution	North Atlantic Oscillation		Sea Surface Temperature	
	diatoms	dinoflagellates	diatoms	dinoflagellates
North NE Atlantic	-0.193	0.133	0.271	-0.302 *
South NE Atlantic	0.055	0.096	0.368 *	-0.119

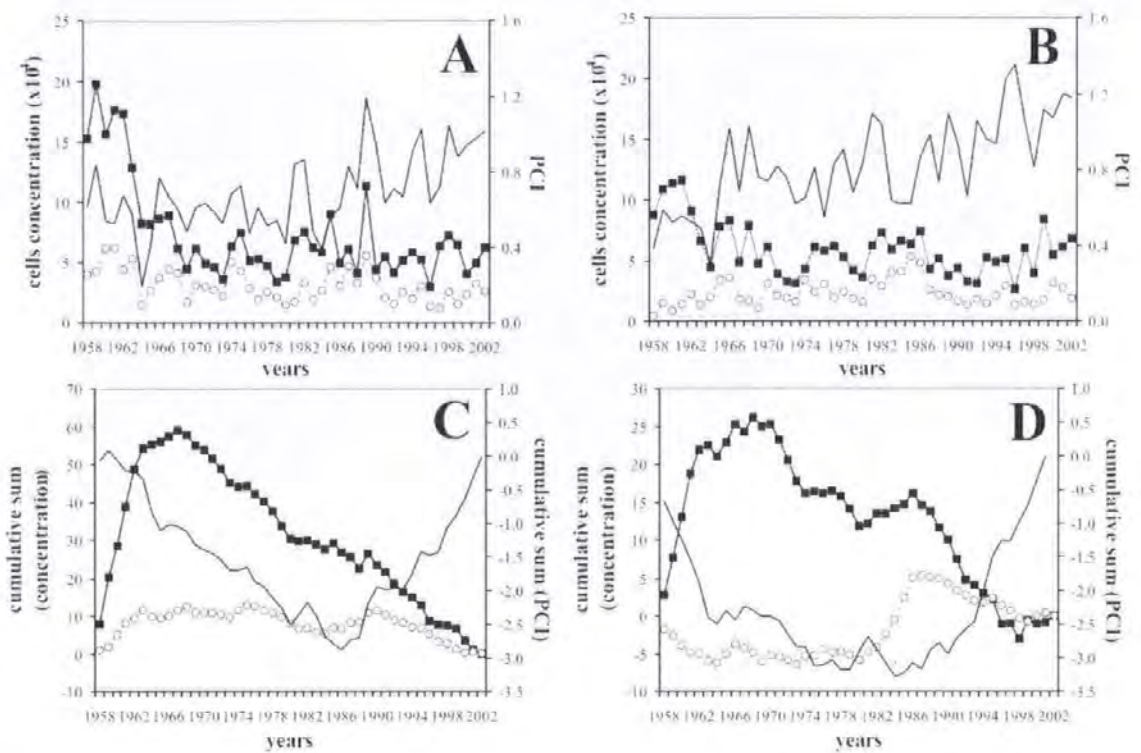


Figure 4.2. Variation of the annual cell concentrations of both diatoms (black squares) and dinoflagellates (grey open dots) and PCI (black line) in the North NE Atlantic (A) and the South NE Atlantic (B) and the cumulative sum analysis for each parameter in the North NE Atlantic (C) and the South NE Atlantic (D).

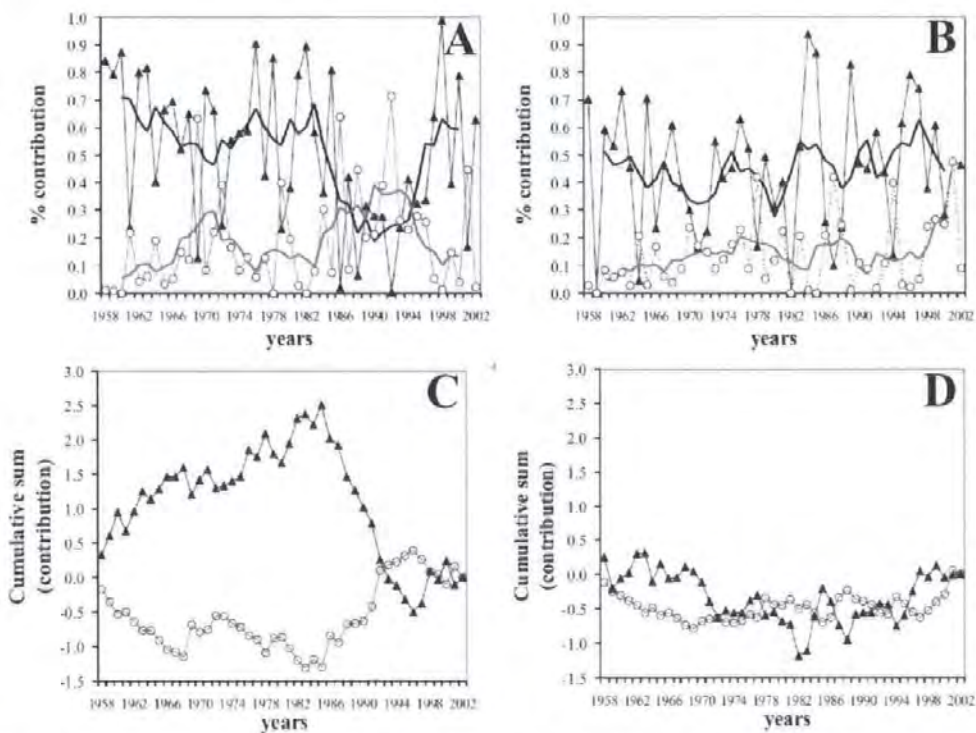


Figure 4.3. Dinoflagellate (grey open dots) and diatom (black triangles) contributions to the Phytoplankton Colour Index (PCI) for each year over the period 1958-2002 in the north NE Atlantic (A) and the south NE Atlantic (B). The bold lines represent the 5-year running means illustrating the trends in the time series. Cumulative sums of dinoflagellate (grey) and diatom (black) contributions to the PCI were determined in the north NE Atlantic (C) and the south NE Atlantic (D).

4.C.1.b. The South Northeast Atlantic

As previously seen in the North NE Atlantic, there was a significant increase in PCI and a significant decrease in diatom abundance (Fig. 4.2.B, Table 4.1). Only the contribution of dinoflagellates to the PCI significantly varied over the period of study (Table 4.2, Fig. 4.3.B), with an increase from 7 to 19%. The residuals of the diatom/dinoflagellate contribution did not exhibit any significant trend (Table 4.2). In addition, cumulative sum analysis did not show any significant short-term trend over the period of study (Fig. 4.3.D). In contrast to what was observed for the NE Atlantic, this suggests that the ecosystem is still in evolution, with a constant contribution of diatoms to the PCI and an increasing contribution of dinoflagellates.

No relationship was observed between PCI and diatom and dinoflagellate abundance and the NAO winter index (Table 4.3). The same observation was true of the SST. There was no significant relationship between diatom and dinoflagellate contributions and the NAO winter index (Table 4.4). On the contrary, there was a significant positive correlation between the contribution of diatoms and SST (Table 4.4). As observed in the North NE Atlantic, no significant long-term trend was observed for the SST over the period of study in this area (Kendall's $\tau = 0.188, p < 0.05$).

4.C.2. The North Sea

In the northern North Sea, PCI and dinoflagellate abundance increased significantly (Fig. 4.4.A, Table 4.1) and exhibited short-term trends (Fig. 4.4.D). Diatom abundance did not exhibit any long-term trend. More specifically, the PCI cumulative sums decreased until 1985 and increased afterwards. Dinoflagellate cumulative sums decreased before 1984 and subsequently increased, while diatom cumulative sums remained roughly steady (Fig. 4.4.D). The contribution of diatoms and dinoflagellates significantly decreased from 71 to 50% and increased from 10 to 24%, respectively (Table 4.4, Fig. 4.5). The residuals of diatom/dinoflagellate contributions did not significantly vary over the period of study. These results suggest an evolution of the ecosystem towards a balance between diatoms and dinoflagellates over the last 45 yr, with the overall diatom/dinoflagellate contribution decreasing from 97 to 72% from 1958 to 2002. In the central and southern North Sea, PCI significantly increased, while dinoflagellate abundance significantly decreased in the southern North Sea, and diatom abundance did not show any long-term trend in either area (Fig. 4.4.B, C, Table 4.1). In addition, PCI and diatom abundance revealed short-term trends in both areas

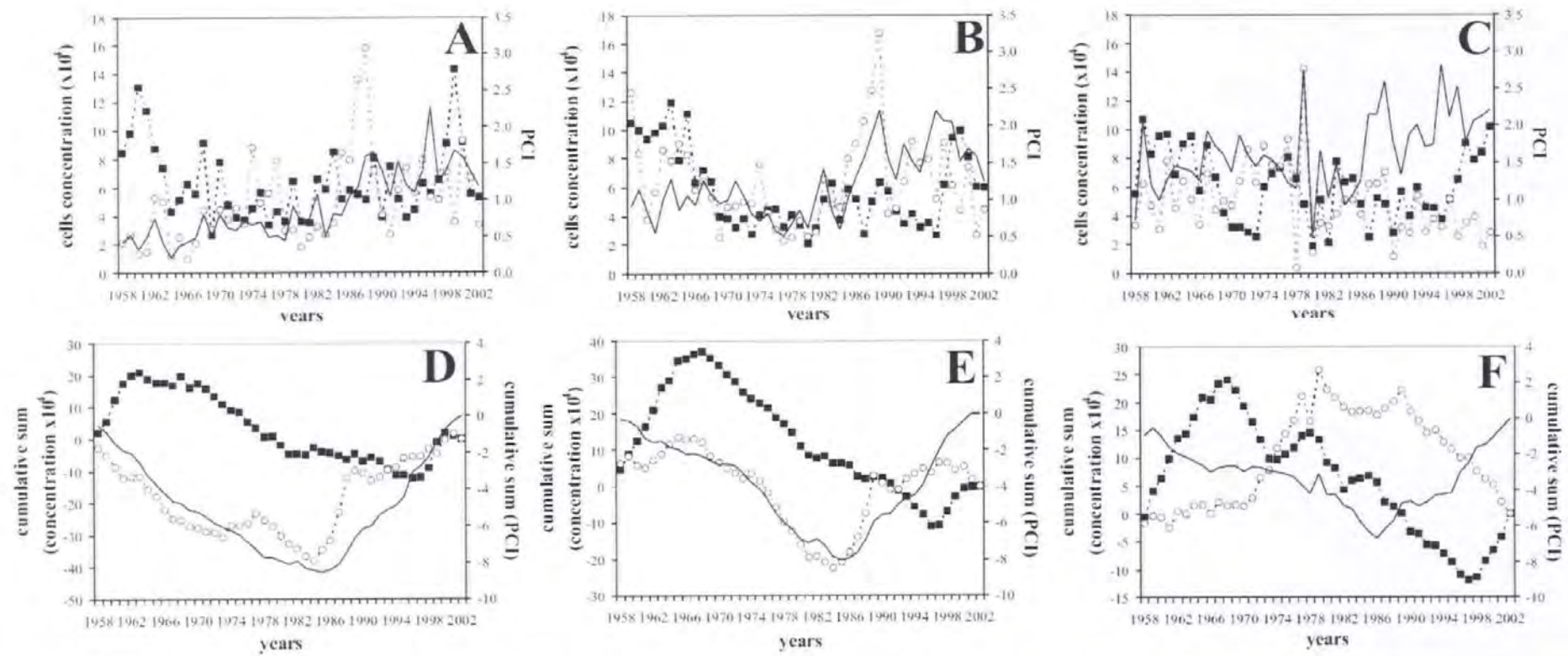


Figure 4.4. Variation of the annual cells concentration of both diatoms (black squares) and dinoflagellates (grey open dots) and PCI (black line) in the Northern (A), Central (B) and the Southern North Sea (C) and the cumulative sum analysis for each parameters in the Northern (D), Central (E) and the Southern North Sea (F).

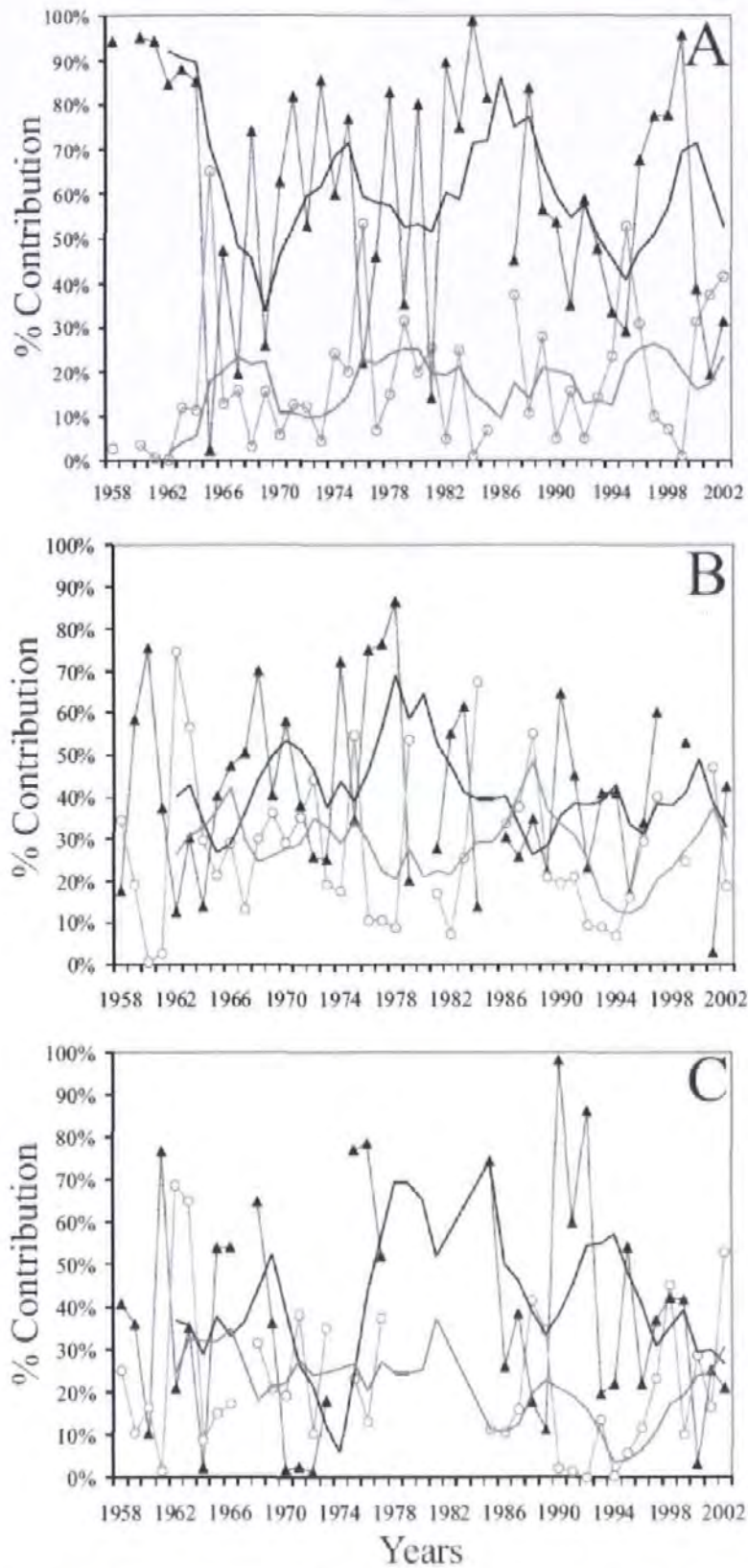


Figure 4.5. Dinoflagellate (grey open dots) and diatom (black triangles) contributions to the Phytoplankton Colour Index (PCI) for each year over the period 1958-2002 in the Northern North Sea (A), Central North Sea (B) and Southern North Sea (C). The bold lines represent the 5-year running means illustrating the trends in the time series.

(Fig. 4.4.E, F). Diatom cumulative sums increased until 1968 and decreased afterwards, and PCI cumulative sums decreased until 1985 and subsequently increased. In the central North Sea, dinoflagellate cumulative sums were roughly steady over the period of study, with a drop between 1974 and 1989, while in the southern North Sea dinoflagellate cumulative sums increased until 1979 and decreased afterwards.

The contributions of diatoms and dinoflagellates as the residuals did not vary over the period of study in the central and southern North Sea (Table 4.4). In these areas, the ecosystem can thus be regarded as being in a stable state, in which diatoms dominate the phytoplankton community. The mean diatom and dinoflagellate contributions were 41.4 and 37.8% and 27.7 and 21.6% in the central and southern North Sea, respectively (Fig. 4.5). The mean diatom/dinoflagellate contribution residuals were 30.92 and 40.60% in the central and southern North Sea, respectively.

There was a significant relationship between the NAO winter index and PCI in the northern North Sea (Table 4.3), but no relationship was observed between the NAO and diatom and dinoflagellate abundance in this area. Moreover, no significant relationship was observed between PCI, diatom and dinoflagellate abundance and NAO winter index in the central and southern North Sea (Table 4.3). SST and PCI were significantly correlated in the central and southern North Sea (Table 4.3), but no relationship was observed between SST and diatom and dinoflagellate abundance in these areas. In addition, no significant relationship was observed between PCI, diatom and dinoflagellate abundance and SST in the northern North Sea (Table 4.3). There was a significant, positive, long-term trend for the SST over the period of study in the central and southern North Sea (Kendall's $\tau = 0.267$ and $\tau = 0.380$, respectively, $p < 0.05$). By contrast, no significant long-term trend was observed for the SST in the northern North Sea (Kendall's $\tau = 0.137$, $p < 0.05$).

4.D. Discussion

4.D.1. Multiple ecosystem states in the NE Atlantic and the North Sea

Three states of the phytoplanktonic ecosystem have been identified throughout the NE Atlantic, suggesting differential temporal and spatial dynamics of the phytoplankton communities in geographically adjacent oceanic domains.

Firstly, a stable ecosystem was observed in the southern and central North Sea, where diatoms dominated the phytoplankton community. These areas belong to an epicontinental basin, where the influence of the North Atlantic water inflow is much weaker than in the northern North Sea (e.g. Turrell *et al.* 1992, Corten 1999). The southern area is also characterised by strong tidal mixing and is increasingly impacted by eutrophication (Lancelot *et al.* 1997), two factors more favourable for diatoms than for dinoflagellates (e.g. Margalef 1975) and thus fully compatible with our observations.

Secondly, an evolving ecosystem was determined in the South NE Atlantic and the northern North Sea, with an increasing contribution of dinoflagellates contrasting, respectively, with a stable diatom population in the former region and a decreasing contribution of diatoms in the latter. These patterns can be related to the specific circulation patterns characterising these areas. The South NE Atlantic and the northern North Sea are indeed both highly influenced by the North Atlantic water inflow (Reid *et al.* 1992, Corten 1999). During the late 1980s, the NAO index was strongly positive and the strength of the westerly winds increased in the NE Atlantic, leading to an increase in the oceanic inflow into the North Sea (Drinkwater *et al.* 2003). Turrell *et al.* (1992) suggested that the Atlantic inflow makes a major contribution to the input of generally warmer, nutrient-rich water into the northern North Sea. The resulting relatively warmer surface temperatures promote earlier, or more intense, stratification of the upper water column (Drinkwater *et al.* 2003), which, according to Margalef's (1975) hypothesis, would create an environment favouring the growth of dinoflagellates over the growth of diatoms.

Finally, the north NE Atlantic is an ecosystem that has moved from one state to another, to reach a balanced state over the last decade. More specifically, our results suggest evolution from a diatom-dominated ecosystem to a more even distribution between diatoms and dinoflagellates and an increase in the proportion of other taxonomic groups such as phytoflagellates, as recently observed in coastal ecosystems (Cloern 2001).

4.D.2. Phytoplankton communities and regime shift in the North Sea

The different ecosystem states discussed in the above section are clearly related to a shift in the abundance and/or composition of phytoplankton communities. However, in our analyses, only the PCI provided evidence for the regime shift (defined as an abrupt shift from one dynamic

regime to another, *sensu* Scheffer *et al.* 2001) observed in the North Sea during the period 1982 to 1988 (Reid *et al.* 2001, Beaugrand 2004). Dinoflagellates showed a shift in 1985, but only in the northern North Sea, and diatoms did not exhibit any evidence of a regime shift over this period. The observed discrepancy then suggests that the changes seen in PCI do not reflect changes in the community structure.

In addition, the features suggested to explain the regime shift in the North Sea by Beaugrand (2004) are acknowledged to influence the whole North Sea. shown here, however, that the dynamics of the northern North Sea clearly differ from those of the central and southern North Sea. This suggests that different driving processes might control the dynamics of the phytoplankton community. While this question needs to be addressed through in-depth investigations of the temporal fluctuations in the phytoplankton taxonomic composition, it is (i) beyond the scope of the present work and (ii) still unfeasible, considering that the different taxonomic groups have not been surveyed over the same period. Thus, pico- and nanoplankton that contribute to the PCI cannot be identified in the samples (Reid 1978). As a consequence, their potential contribution to the PCI space–time patterns is intrinsically not determinable, and might ultimately drive PCI variability and/or obfuscate the variability of the contributions of identifiable groups.

Finally, the decreasing contribution of diatoms/dinoflagellates along a north–south gradient could possibly be related to the increasing contribution of other taxonomic groups or smaller size fractions of phytoplankton, such as naked flagellates, which either break up when they impact the silk or disintegrate in formaldehyde (Batten *et al.* 2003b), and thus contribute to PCI without being identifiable.

4.D.3. Phytoplankton composition and ecosystem structure and function

The fluctuations in the two phytoplankton taxonomic groups studied here are likely to impact the dynamics of the whole food web. The space–time differences in taxonomic group contributions could, for instance, have an effect on zooplankton populations through their trophodynamics. Richardson & Schoeman (2004) have thus shown a dominant bottom-up control within the plankton community in the NE Atlantic over time and space as the result of sea surface warming. However, this study shows that: (1) the SST only exhibited a significant long-term trend in the central and southern North Sea from 1958 to 2002, (2) the PCI, the

abundance of diatoms and dinoflagellates and the contribution of diatoms and dinoflagellates to the PCI were barely correlated to the NAO and SST (cf. Tables 4.3 & 4.4), and (3) the significant correlations did not exhibit any distinct spatial pattern (cf. Tables 4.3 & 4.4). As a consequence, it is suggested that: (i) the so-called hydro-meteorological forcing is likely to have short-term rather than long-term effects on phytoplankton communities in the eastern North Atlantic and the northern North Sea, (ii) SST is likely to have long-term effects on phytoplankton communities in the central and southern North Sea and (iii) the potential causal relationships between hydro-meteorological variables and phytoplankton abundance and community composition are strongly affected by the spatial location.

More detailed investigations of the relationships between changes in phytoplankton composition and their potential effects on zooplankton communities are needed to achieve a deeper understanding of the mechanisms driving the observed patterns. Phytoplankton composition and thus zooplankton diet have indeed already been shown to influence hatching success (Laabir *et al.* 2001, Irigoien *et al.* 2002), growth and development (Koski *et al.* 1999) of calanoid copepods. As the production of copepods supports most food webs, directly affecting higher trophic levels and the biological pump of carbon (Ohman & Hirche 2001), elucidation of the interplay between phytoplankton and zooplankton communities is vital for the future. The global relevance of this inter-relationship is clear, considering the importance of these organisms in the context of climate change, anthropogenic impacts on ecosystems and the consequences on management of aquatic living resources.

Chapter 5

DECADAL FLUCTUATIONS OF THE INFLOW OF NORTH ATLANTIC WATER INTO THE NORTH SEA BETWEEN 1958-2003 AND ITS IMPACT ON PLANKTON ASSEMBLAGES

Part of this chapter has been included in the following:

Leterme S.C., Pingree R.D., Attrill M.J., John A.W.G, Reid P.C. & Skogen M.D. (submitted) Decadal fluctuations of plankton species in the North Sea: relation with physical and hydrological parameters. *Limnology and Oceanography*.

Leterme S.C., Pingree R.D., Attrill M.J., John A.W.G & Skogen M.D. (2006) Decadal fluctuations of plankton species in the North Sea: relation with physical and hydrological parameters. AGU-ASLO-TOS Ocean Sciences Meeting, February 2006, Honolulu, Hawaii, USA.

5.A.Introduction

As a semi-enclosed basin, the North Sea is characterized by complex interactions between physical conditions (*i.e.* waves, tides, currents), water chemistry, suspended sediments, living organisms, and human activities (Eisma 1987). In particular, the circulation of Atlantic waters along the European continental slope, and more precisely the inflow of Atlantic waters into the North Sea, highly influences its water characteristics, with consequent changes in temperature, salinity, and nutrient concentration affecting the biology and ecology of plankton organisms. Atlantic waters flow into the North Sea along two pathways: the continental slope flow enters the northern North Sea through the Fair Isle Channel and along the east side of the Shetland Islands (Turrell *et al.* 1990), while a smaller flow enters from the south through the Straits of Dover, with warmer and saltier properties that influence the temperature and salinity distributions of the Southern Bight of the North Sea (Pingree 2005). The resulting outflow of North Sea water, called the Norwegian coastal current (NCC), is concentrated along the western coast of Norway. This current is a combination of wind-driven coastal water from the southern North Sea, saline water from the western North Sea, freshwater Baltic outflow (Lee 1970).

The possibility that large-scale ecological changes in the North Sea are related to variations in the Atlantic inflow has been mentioned by several authors (*e.g.* Fraser 1952, Turrell *et al.* 1996, Witbaard *et al.* 1997, Reid *et al.* 2003). High salinity water masses (Otto *et al.* 1990) and Atlantic plankton 'indicator species' (Fraser 1969, Reid *et al.* 1992, Corten 1999, Edwards *et al.* 1999, Lindley & Batten 2002) observed in the North Sea are particularly indicative of Atlantic inflow. The composition of copepod species undertaking ontogenic migration (*e.g.* *Calanus finmarchicus*) in shelf seas is also largely dependent upon the input of inter-annually varying pulses of oceanic water (Corten 1999, Heath *et al.* 1997).

The inflow of Atlantic waters to the North Sea is highly variable in both source and volume (Corten 1986, 1990), and is strongly linked to climate variability mainly through the North Atlantic Oscillation (Corten 1990). A decrease and an increase in the Atlantic inflow into the northwestern North Sea has been identified in the 1960s and 1970s, and in the 1980s, respectively. In this context, the objective of this chapter is to assess the long-term (1958-2003) impact of inflow fluctuations in North Atlantic water on the North Sea plankton ecosystem. Special attention will be given to (i) the relative fluctuations in the two sources of Atlantic waters inflow (*i.e.* through the northern North Sea and English Channel) over a 45-year period,

(ii) the impact of these fluctuations on salinity, temperature, and nutrient levels between 1958 and 2003, (iii) the related long-term changes in North Sea plankton, including copepod abundance, phytoplankton biomass, and diatom and dinoflagellates abundances, in different regions of the North Sea (Fig. 5.1), and (iv) the assessment of the contribution of Atlantic inflow fluctuations to the observed changes.

5.B. Data and methods

5.B.1. Phytoplankton data

Only diatoms and dinoflagellates are taken into account in the present work, as they are the most regularly identified phytoplankton groups in the CPR survey. Firstly, the abundance of every species identified as belonging to the diatoms or dinoflagellates were grouped by summing the number of cells identified to determine the overall trends in these two groups. Secondly, diatom and dinoflagellate species with a frequency of occurrence greater than 1% in the samples were used as indicator species to provide more information on the processes linking climate to changes in the phytoplankton community (Leterme *et al.* 2005). Five dinoflagellate species (*i.e.* *Ceratium furva*, *C. fusus*, *C. horridum*, *C. lineatum*, and *C. tripos*) and six diatom taxa (*i.e.* *Proboscia alata alata*, *Rhizosolenia hebetata semispina*, *R. styliformis*, *Thalassionema nitzschoides*, *Thalassiosira* spp., and *Thalassiothrix longissima*) have thus been considered.

5.B.2. Zooplankton data

The most frequently recorded zooplankton organisms within the CPR survey are calanoid copepods. Here the most common species identified in the North Sea are taken into account: *Acartia* spp., (mainly *A. clausi* and some *A. longiremis*, Colebrook (1982)), *Calanus finmarchicus*, *C. helgolandicus*, *Para-Pseudocalanus* spp. (includes all stages of *Paracalanus* spp. and of *Pseudocalanus* spp. and any unidentifiable small (*i.e.* <2 mm) copepods), and *Temora longicornis*. *Acartia* spp., *Para-Pseudocalanus* spp. and *T. longicornis* have been identified as representative of the North Sea neritic community (Oceanographic Laboratory Edinburgh 1973, Fransz *et al.* 1991). Abundance estimates from individual plankton samples are inherently imprecise because of variable zooplankton behaviour such as diel vertical migration and local weather conditions that can concentrate or disperse fine-scale patches (Robertson 1968). The potential biases related to this fine-scale variability have been discarded through spatial and temporal averaging of CPR data over areas and periods of interest (Richardson *et al.* 2006).

5.B.3. Plankton species indicative of the inflow of oceanic water

Some of the plankton species identified by the CPR survey have previously been associated with the inflow of oceanic water into the North Sea. These include calanoid copepods such as: *Aetideus armatus*, *Subeucalanus crassus*, *Paraeuchaeta hebes*, *Metridia lucens*, *Rhincalanus nasutus*, and *Candacia armata* (Lindley *et al.* 1990, Corten 1999, Edwards *et al.* 1999). These species were included in the analyses. *C. armata* and *M. lucens* have already been identified as indicator species for Atlantic waters in the northwestern North Sea in several studies (Farran 1910, Rae & Fraser 1941, Rae & Rees 1947, Corten 2001). A few other species that appear occasionally in the northwestern North Sea, and are also likely to be related to the Atlantic inflow (A.W.G. John, personal communication), *i.e.* the dinoflagellate *Ceratium hexacanthum* and the calanoid copepods *Clausocalanus* spp. and *Pleuromamma* spp., have also been taken into account.

5.B.4. Hydrological and climatic data

ICES have provided data on hydrological parameters such as salinity and nutrient concentration (*e.g.* nitrate and phosphate) on a monthly basis over the period 1958-2003. These data were collected for all years from 1958 to 2003 to obtain yearly time series and averaged for the top 20 meters of the water column to be consistent with the CPR sampling conducted at ~10 meters. The climatic indices used in this study are the North Atlantic Oscillation (NAO) winter index and Sea Surface Temperature (SST). Several indices have been developed to quantify the state of the NAO, but the most widely used is Hurrell's NAO Index (Hurrell 1995a). This index computes the pressure difference based on measurements from Lisbon, Portugal and Stykkisholmur, Iceland. In particular, the NAO winter index (NAO) values averaged from December to March inclusive have been used as a climatic index (Hurrell 1995a). Sea Surface Temperature (SST; see The British Atmospheric Data Centre, <http://badc.nerc.ac.uk/home>) data were used to provide additional climatic information that is likely to impact phytoplankton growth and abundance.

5.B.5. North Atlantic Waters inflow into the North Sea

The NORWegian ECOlogical Model System (NORWECOM) is a coupled physical, chemical, and biological model designed to study primary production, nutrient budgets, and dispersion of particles such as fish larvae and pollution (Skogen *et al.* 1995, Skogen & Soiland 1998). The forcing variables are six-hourly hindcast atmospheric pressure fields and wind stress from the

Norwegian Meteorological Institute (DNMI), four tidal constituents at the lateral boundaries, and freshwater runoff. Due to a lack of data on the surface heat fluxes, evaporation, and precipitation, a climatology method is used for the surface layer (Cox & Bryan 1984). Validation of the model system has been achieved by comparison with field data in the North Sea and the Skagerrak (Svendsen *et al.* 1995, Skogen *et al.* 1997, Soiland & Skogen 2000). The circulation module is based on the wind and density driven primitive equation Princeton Ocean Model (Blumberg & Mellor 1980). A 20-km horizontal grid covering the whole shelf area from Portugal to Norway, including the North Sea has been used. Each simulation was started on December 15th and, after a 2-weeks spin-up time, model results were stored from January 1st to December 31st. The model was then re-initialized and run for the next year.

Based on the modelled current fields, average monthly inflows through an east-west section from Utsira (Norway) to the Orkney Islands along 59°17'N (*i.e.* northern inflow) in the northern North Sea and a longitudinal section through the English Channel in the Dover Straits along 0°E (*i.e.* southern inflow), were computed for all years from 1958 to 2003 and averaged for the whole water column. The outflow and net flow (*i.e.* the sum of Baltic outflow, river runoff, and fluxes through the Channel via the Dover Straits) were also computed over the same period. Data from the NORWECOM model were provided by Dr. M.D. Skogen (Institute of Marine Research, Bergen, Norway).

5.B.6. Statistical analysis

In each region, the data obtained for the estimates of phytoplankton biomass (*i.e.* PCI), phytoplankton abundance (*i.e.* total diatoms, total dinoflagellates, and phytoplankton indicator species), zooplankton species, plankton species indicative of oceanic water inflow, salinity, and nutrients have been averaged every year over the period 1958-2003. The climatic index (*i.e.* SST), as well as the estimated northern and southern inflows from the Atlantic, were also computed as yearly means.

Any temporal trends within the time series obtained for each of the 13 regions delimited within the North Sea (Fig. 5.1) were tested by calculating Kendall's coefficient of rank correlation, τ , between the yearly time series of the physical and biological parameters and the x-axis values in order to detect the presence of an underlying linear trend.

To detect changes, intensity, and duration of any variation in the value of a given parameter, the cumulative sum method (Ibañez *et al.* 1993) which enhances the trends in data anomalies and the presence of a regime shift has been used. The calculation consists of subtracting a reference value (here the mean of the series) from the original data; these anomalies are then successively added, forming a cumulative function. Successive positive anomalies produce an increasing slope, whereas successive negative anomalies produce a decreasing slope; a succession of values similar to the mean shows no slope. This analysis has only been applied to the environmental variables (*i.e.* SST, NAO and inflow of Atlantic waters) and plankton variables, but not to the hydrological parameter dataset (salinity and nutrient concentration) as there were too many missing data in the time series.

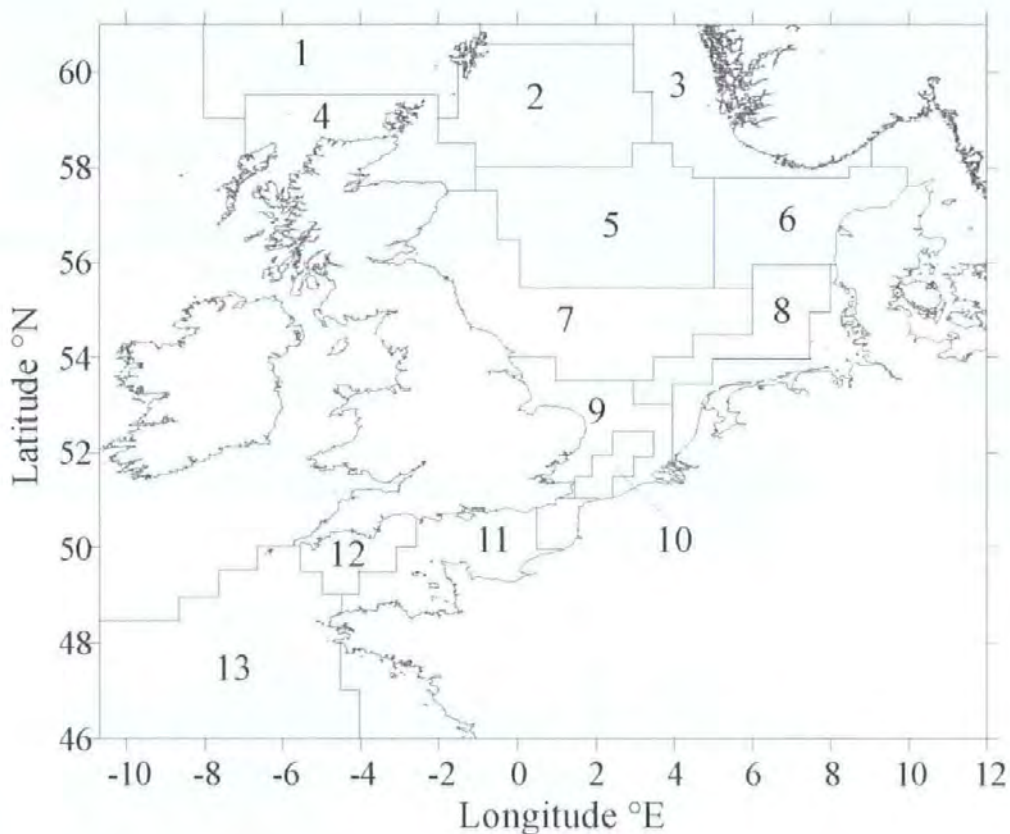


Figure 5.1. Study area divided into 13 regions identified using hydrodynamic (*i.e.* stratified, mixed and frontal) and bathymetric criteria.

The association between the northern and southern inflows of Atlantic waters and other large-scale variables (*i.e.* climatic forcing (NAO and SST), hydrological parameters (salinity and nutrient concentration), and biological measures (copepod species, phytoplankton groups and plankton species indicative of oceanic inflow) was tested through Spearman rank correlation

analysis. The analysis was performed between residual monthly time series (*i.e.* seasonal cycle removed) of both northern and southern inflows of Atlantic waters and residual monthly time series SST in order to test the long-term effect of oceanic inflow. Because of the scarcity of values other than zero in some plankton time series, the traditional methods of correlation were not appropriate (Scherrer 1984). In order to have homogeneity in the statistical methods applied, the relationship between the oceanic inflow and plankton species has been investigated by applying Spearman's correlation to cumulative sums of the variables. The same method was applied to climatic forcing data such as SST and NAO. However, as the cumulative sum method could not be performed on the hydrological parameters, Spearman's correlation analysis was not conducted between inflow of Atlantic waters and salinity and nutrient concentration.

To investigate changes in the whole assemblage composition of the plankton, a suite of multivariate analyses were employed utilizing the PRIMER 5 (Plymouth Routines in Multivariate Ecological Research version 5) software. These are similarity-based analyses designed to visualize, and test the significance of, changes in community composition in time and space and they have been particularly widely utilized in the marine environment (see Clarke & Warwick 2001). Three procedures were employed in this analysis:

1. NON-metric multi-Dimensional Scaling (NODS), producing a 2-dimensional ordination to visualize differences in community composition, supplemented by creating second-stage MDS ordinations of regions to assess similarity of temporal trends (Sommerfield & Clarke 1995);
2. ANOSIM (Analysis of Similarities, Clarke 1993), a formal significance test of differences in composition between *a priori* defined groupings
3. BIOENV (Clarke & Ainsworth 1983), correlation-based procedures that define the environmental variables that best explain patterns in the underlying biotic matrix.

Separate analyses were undertaken on zooplankton and phytoplankton species matrices, plus 2nd-stage MDS on environmental variables, in order to identify significant differences between decades (*i.e.* from 1960 to 2000) and/or presence of regime shifts. The term 'regime shift' has been used to describe large, decadal-scale switches in the abundance and composition of plankton and fish (Reid *et al.* 2001). First, Bray-Curtis similarity indices were calculated between each pair of samples, to form a similarity matrix, using Log (X+1) transformations to smooth out the influence of abundant plankton species. Multi-Dimensional Scaling (MDS; 10 runs) was then undertaken on the similarity matrix for each region, resulting in 2-dimension ordination

plots. Using the similarity matrices produced for all North Sea regions, a 2nd-stage MDS was computed for copepods, phytoplankton and environmental variables. This method calculates a similarity value between all pairs of matrices, using rank correlation (here, Kendall). The results give a graphical indication of the similarity of change within the regions on a second stage MDS ordination plots. To formally test differences in assemblage composition between decades (to investigate major changes in the plankton) and pre- and post-regime shift, analysis of similarities (ANOSIM, a multivariate randomisation procedure broadly analogous to ANOVA) was applied to similarity matrices for each region. Finally, in order to determine which environmental and hydrological variables (i.e., SST, NAO, salinity, phosphate, nitrate, and inflows of Atlantic waters) best explained the changes observed in zooplankton/phytoplankton, the BIOENV algorithm was applied on a joint matrix of copepods, environmental and hydrological variables, and on a plankton similarity matrix from the same region. Combinations of the environmental variables were considered at steadily increasing levels of complexity, i.e., k variables at a time ($k = 1, 2, 3$), to yield the best matches of biotic and abiotic similarity matrices for each k , as measured by Spearman rank correlation ρ_s . This method then selects the variables that best explain the phytoplankton community pattern by maximizing a Spearman rank correlation between their respective similarity matrices. Here, BIOENV analysis selects the variable that best explains the fluctuations of plankton species. The best three explanatory variables are also taken into account to determine which combination of environmental factors induces the changes observed (or not) in plankton species.

5.C. Results

5.C.1. Long-term changes in the environment

Between 1958 and 2003, based on modelled data, the southern inflow of Atlantic Waters into the North Sea significantly increased ($\tau = 0.22$, $p < 0.05$). However, no significant long-term trend in the northern inflow was identified ($p > 0.05$). A significant relationship was observed between NAO and the northern inflow ($\rho_r = 0.581$, $p < 0.05$). The cumulative sums revealed short-term trends within the long-term changes identified above (Fig. 5.2). The northern inflow decreased until 1988, then increased until 1995, and finally decreased until 2003. A decreasing trend was observed in the southern inflow until 1982, followed by an increase until 2003. This suggests differential shifts in the inflow of Atlantic Waters through the northern and southern

North Sea. However, the regimes identified are similar, with a low and high inflow characterized respectively by the decrease and increase in cumulative sums. In addition, a significant relationship was observed between cumulative sums of NAO and the cumulative sums of northern inflow ($\rho_t = 0.85, p < 0.05$, Fig. 5.2). Despite a similar trend, the relationship between NAO and the southern inflow was weaker ($\rho_t = 0.66, p < 0.05$, Fig. 5.2). This was primarily due to a decoupling of the inflow trend from the NAO after 1980.

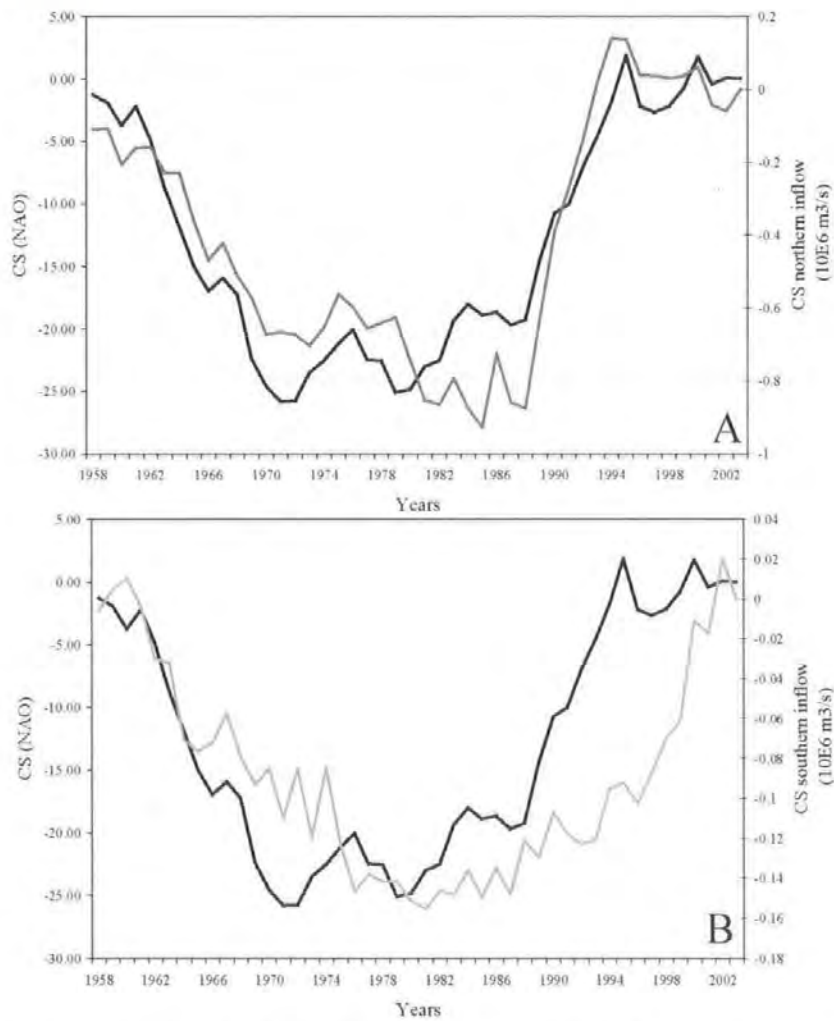


Figure 5.2. Cumulative sums of the North Atlantic Oscillation (NAO; black) and (A) northern and (B) southern oceanic modelled inflows (grey) over the period 1958-2003. The NAO is represented in black and the Atlantic inflow in grey.

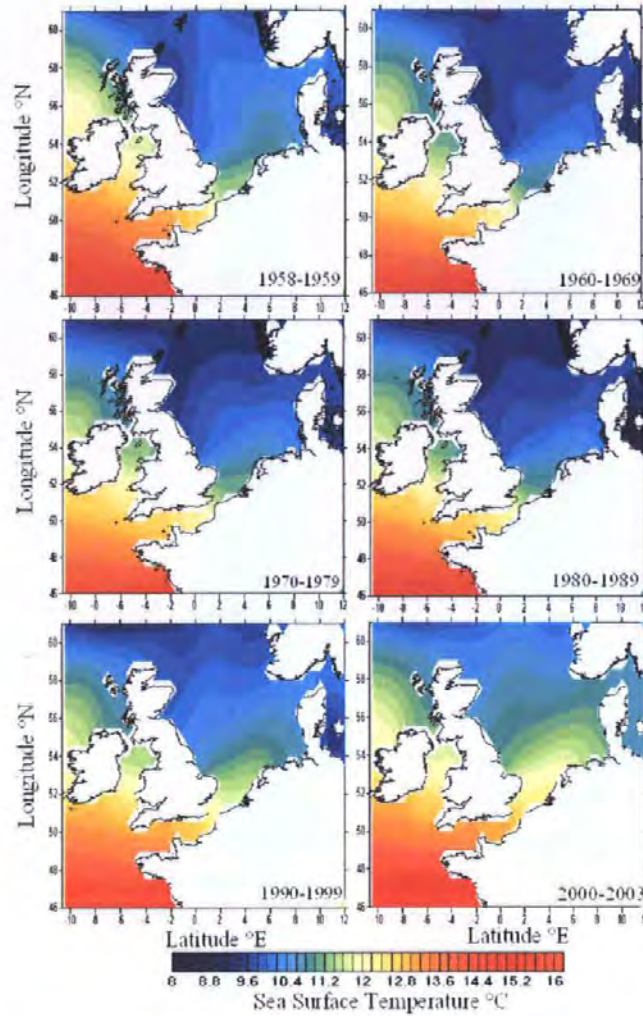


Figure 5.3. Decadal means of Sea Surface Temperature for the whole North Sea from 1958 to 2003 (from ICES and UK MetOffice dataset).

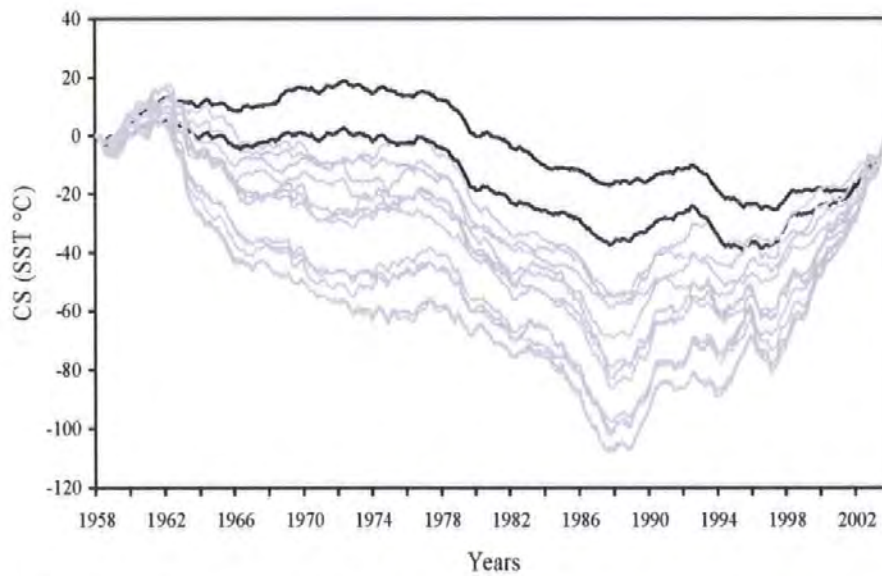


Figure 5.4. Cumulative sums of Sea Surface Temperature (SST) in the different regions of the North Sea and English Channel. Regions 1 and 4, showing different patterns to the other regions are shown in black.

Across most of the North Sea, long-term changes have been observed in SST (Table 5.1, Fig. 5.3). Apart from regions 1 and 4, the cumulative sums of SST increased until 1962, then slowly decreased until 1987 (Fig. 5.4), and finally increased until 2003. This suggests that regions 1 and 4 have not been constrained by the same forcings as the other regions of the North Sea. In the same way, the relationship between SST and the inflow of Atlantic Waters differed depending on the origin of the flow. In regions 5 to 10, there was a significant positive relationship between annual time series of SST and northern inflow ($0.36 \leq \rho_i \leq 0.44$, $p < 0.05$). However, significant positive relationships between annual time series of SST and the southern inflow were only observed in region 10 ($\rho_i = 0.30$, $p < 0.05$). This suggests a long-term effect of oceanic inflow on the SST of the North Sea, supported by a significant correlation observed between cumulative sums of SST and cumulative sums of northern inflow in region 1 ($\rho_i = -0.38$, $p < 0.05$) and in regions 7 to 13 ($0.32 \leq \rho_i \leq 0.43$, $p < 0.05$). For areas 8 to 12, significant correlations were also apparent between cumulative sums of SST and cumulative sums of southern inflow ($0.47 \leq \rho_i \leq 0.79$, $p < 0.05$). In addition, except in region 1, 4 and 13, significant positive correlations were observed between annual time series of SST and NAO ($0.31 \leq \rho_i \leq 0.62$, $p < 0.05$). However, significant correlations between cumulative sums of SST and cumulative sums of NAO were only observed in region 1 ($\rho_i = -0.57$, $p < 0.05$), 7 to 10 ($0.29 \leq \rho_i \leq 0.33$, $p < 0.05$), and 13 ($\rho_i = 0.30$, $p < 0.05$).

Table 5.1. Results of Kendall's statistical test for the yearly time series of Sea Surface Temperature, salinity, nutrients, Phytoplankton Colour Index (PCI), dinoflagellates, diatoms, phytoplankton indicator species and copepod species over the period 1958-2003. + 5% confidence level. Due to missing data, nutrients time series have not been analysed for regions 11 to 13 (-).

Areas	1	2	3	4	5	6	7	8	9	10	11	12	13
SST	-0.02	0.23 ⁺	0.20 ⁺	0.17	0.30 ⁺	0.26 ⁺	0.36 ⁺	0.32 ⁺	0.36 ⁺	0.33 ⁺	0.23 ⁺	0.22 ⁺	0.23 ⁺
Salinity	-0.18	-0.14	-0.14	0.29 ⁺	-0.06	-0.07	-0.14	-0.14	-0.17	0.18	-0.21	-0.10	0.21
Nitrate	0.25 ⁺	0.22	0.02	0.05	-0.08	0.51 ⁺	0.07	0.32 ⁺	0.36 ⁺	-0.02	-	-	-
Phosphate	0.14	0.35 ⁺	-0.08	0.02	-0.07	0.34 ⁺	0.07	0.18	0.23 ⁺	0.11	-	-	-
PCI	0.03	0.04	0.15	0.20 ⁺	0.13	0.22 ⁺	0.13	0.08	0.11	-0.02	0.19	0.22 ⁺	-0.01
Dinoflagellates	-0.27 ⁺	0.05	0.41 ⁺	-0.28 ⁺	-0.14	-0.23 ⁺	-0.19	-0.17	-0.26 ⁺	-0.02	0.03	0.26 ⁺	0.12
Diatoms	-0.42 ⁺	0.03	0.33 ⁺	-0.33 ⁺	-0.18	-0.24 ⁺	-0.25 ⁺	-0.07	-0.17	-0.10	-0.24 ⁺	0.07	-0.10

5.C.2. Decadal fluctuations of phytoplankton in the North Sea

Between 1958 and 2003, decadal-scale changes have been observed in the phytoplankton community. These trends, however, were not consistent across the whole North Sea, indicating the importance of smaller spatial scale processes. Hereafter the name of the diatom and dinoflagellates indicator species exhibiting the same trends as their taxa are given in parenthesis. The Phytoplankton Colour Index (PCI) significantly increased in regions 4, 6, and 12 (Table 5.1). Significant increases have also been observed for diatoms (*T. longissima*) in region 3, and for dinoflagellates (*Ceratium* spp.) in regions 3 and 12. However, significant decreases have been observed in regions 1, 4, 6, 7, and 11 for diatoms (*P. alata alata*) and in regions 1, 4, 6, and 9 for dinoflagellates (*C. fusus*, *C. lineatum*, and *C. tripos*). Some indicator species, however, did not follow the same trend as their major taxonomic group. *Rhizosolenia* spp., *Thalassiosira* spp., *T. nitzschoides*, and *P. alata alata* significantly increased in region 8, but *Rhizosolenia* spp. and *P. alata alata* significantly decreased in region 5 (Fig. 5.5). In addition, *T. nitzschoides* significantly decreased in region 1 and increased in region 10, whilst significant increases were observed for *Thalassiosira* spp. in regions 2, 3, 8, 9, 12, and 13.

Significant correlations were also observed between cumulative sums of phytoplankton and cumulative sums of both Atlantic Water inflows. For the northern inflow, there were significant negative correlations with diatoms (*P. alata alata* and *T. nitzschoides*) in regions 1 and 4 to 8 (Table 5.2) and with dinoflagellates (*C. fusus*, *C. lineatum*, and *C. tripos*) in regions 1, 4, and 6 (Table 5.2). Conversely, positive correlations were apparent between northern inflow and diatoms (*T. longissima* and *Thalassiosira* spp.) in regions 2 and 3 (Table 5.2) and with dinoflagellates (*C. furca* and *C. tripos*) in regions 2, 3, and 8 (Table 5.2). For the southern inflow, there was a significant negative correlation with diatoms (*P. alata alata*, *R. bebetata semispina*, and *T. longissima*) in regions 8 to 11 (Table 5.3), and with dinoflagellates (e.g. *C. fusus*, *C. horridum*, *C. lineatum*, and *C. tripos*) in region 9 (Table 5.3).

The relationship between phytoplankton indicator species and Atlantic inflow differed between regions and did not always reflect the relationship observed as a whole for their taxa. In contrast to most other diatom indicators, significant positive correlations were mostly recorded between *Thalassiosira* spp. and northern inflow (Table 2), similarly observed for three dinoflagellate indicator species: *C. furca*, *C. fusus*, and *C. horridum* (Table 5.2). The relation observed between *R. styliformis* and the southern inflow was highly polarized with positive correlation in regions 8, 12, and 13, and negative correlation in region 9 (Table 5.3). In

Table 5.2. Results of Spearman's correlation analysis between the cumulative sums of the time series of phytoplankton indicator species, copepods and the modelled northern inflow (at 59°17'N) over the period 1958-2003. The analysis was performed only in the areas potentially influenced by the northern inflow (regions 1-8). Black and grey areas represent significant ($p < 0.05$) positive and negative correlations, respectively.

Areas	1	2	3	4	5	6	7	8
total Diatoms	Grey	Black	Black	Black	Black	Black	Black	Black
<i>Proboscia alata alata</i>	Grey	Black	Black	Black	Black	Black	Black	Black
<i>Rhizosolenia hebetata semispina</i>	Black	Black	Black	Black	Black	Black	Black	Black
<i>Rhizosolenia styliformis</i>	Black	Black	Black	Black	Black	Black	Black	Black
<i>Thalassionema nitzschioides</i>	Black	Black	Black	Black	Black	Black	Black	Black
<i>Thalassiosira</i> spp.	Black	Black	Black	Black	Black	Black	Black	Black
<i>Thalassiothrix longissima</i>	Black	Black	Black	Black	Black	Black	Black	Black
total Dinoflagellates	Black	Black	Black	Black	Black	Black	Black	Black
<i>Ceratium furca</i>	Black	Black	Black	Black	Black	Black	Black	Black
<i>Ceratium fusus</i>	Black	Black	Black	Black	Black	Black	Black	Black
<i>Ceratium borridum</i>	Black	Black	Black	Black	Black	Black	Black	Black
<i>Ceratium lineatum</i>	Black	Black	Black	Black	Black	Black	Black	Black
<i>Ceratium tripos</i>	Black	Black	Black	Black	Black	Black	Black	Black
<i>Acartia</i> spp.	Black	Black	Black	Black	Black	Black	Black	Black
<i>Calanus finmarchicus</i>	Black	Black	Black	Black	Black	Black	Black	Black
<i>Calanus belgolandicus</i>	Black	Black	Black	Black	Black	Black	Black	Black
<i>Para-Pseudocalanus</i> spp.	Black	Black	Black	Black	Black	Black	Black	Black
<i>Temora longicornis</i>	Black	Black	Black	Black	Black	Black	Black	Black

Table 5.3. Results of Spearman's correlation analysis between the cumulative sums of time series of phytoplankton indicator species and copepods and the modelled southern inflow (through the English Channel) over the period 1958-2003. The analysis was performed only in the areas possibly influenced by the southern inflow (regions 8-13). Black and grey areas represent significant ($p < 0.05$) positive and negative correlations, respectively.

Areas	8	9	10	11	12	13
total Diatoms	Black	Black	Black	Black	Black	Black
<i>Proboscia alata alata</i>	Black	Black	Black	Black	Black	Black
<i>Rhizosolenia hebetata semispina</i>	Black	Black	Black	Black	Black	Black
<i>Rhizosolenia styliformis</i>	Black	Black	Black	Black	Black	Black
<i>Thalassionema nitzschioides</i>	Black	Black	Black	Black	Black	Black
<i>Thalassiosira</i> spp.	Black	Black	Black	Black	Black	Black
<i>Thalassiothrix longissima</i>	Black	Black	Black	Black	Black	Black
total Dinoflagellates	Black	Black	Black	Black	Black	Black
<i>Ceratium furca</i>	Black	Black	Black	Black	Black	Black
<i>Ceratium fusus</i>	Black	Black	Black	Black	Black	Black
<i>Ceratium borridum</i>	Black	Black	Black	Black	Black	Black
<i>Ceratium lineatum</i>	Black	Black	Black	Black	Black	Black
<i>Ceratium tripos</i>	Black	Black	Black	Black	Black	Black
<i>Acartia</i> spp.	Black	Black	Black	Black	Black	Black
<i>Calanus finmarchicus</i>	Black	Black	Black	Black	Black	Black
<i>Calanus belgolandicus</i>	Black	Black	Black	Black	Black	Black
<i>Para-Pseudocalanus</i> spp.	Black	Black	Black	Black	Black	Black
<i>Temora longicornis</i>	Black	Black	Black	Black	Black	Black

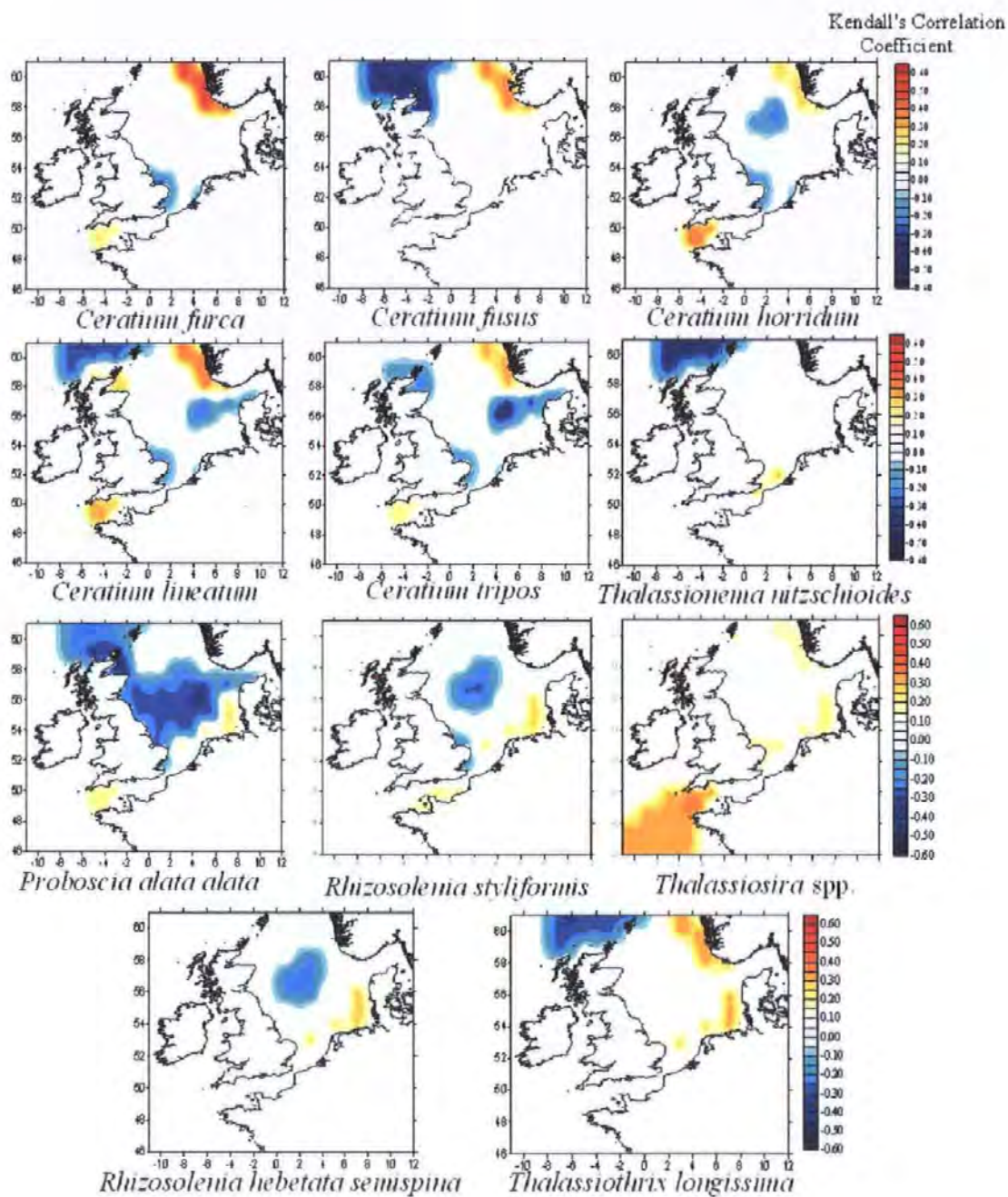


Figure 5.5. Kendall's rank correlation coefficient identifying long-term trends in phytoplankton indicator species over the period 1958-2003 (5% significant level: $\tau > 0.201$).

addition, the relationship between *T. longissima* and the southern inflow was variable, with positive correlation in region 8, and negative correlation in regions 9 to 12. *Ceratium horridum* and the southern inflow also showed opposite relationships, with positive correlation in regions 11 and 12, and negative correlation in regions 8 to 10. Moreover, the relation between *C. furca* and the southern inflow was mainly positive in the southern North Sea and English Channel regions, (Table 5.3). On the contrary, the relation between *R. hebetata semispina* and the southern inflow was negative in the southern regions of the North Sea (Table 5.3).

5.C.3. Decadal fluctuations of zooplankton in the North Sea

As observed with phytoplankton indicator species, differential long-term trends have been identified for copepod species dependent on the region. *Acartia* spp. showed a marked split in response within the North Sea, significantly increasing in regions 2, 3, 5, and 6 (Fig. 5.6) yet decreasing in regions 4, 7, and 8. Similarly, *T. longicornis* significantly increased in regions 3, 6, and 11 and decreased in regions 4 and 7 (Fig. 5.6). Significant decreases of *C. finmarchicus* and *Para-Pseudocalanus* spp. populations occurred in most regions, except in regions 1 (far NW) and 12 (far SW) respectively, where they significantly increased (Fig. 5.6). Finally, *C. helgolandicus* significantly increased in most regions.

The relationship between oceanic inflows and copepod species varied geographically. Significant negative relationships were identified between copepod species (*Acartia* spp., *C. finmarchicus*, *Para-Pseudocalanus* spp., and *T. longicornis*) and southern inflow in the southern North Sea (Table 5.3). Some of these copepods (*Acartia* spp., *Para-Pseudocalanus* spp., and *T. longicornis*), however, were also positively correlated to the northern inflow (Table 5.3) in the northern and central North Sea. In contrast, the relationship observed between *C. helgolandicus* and northern (Table 5.2) and southern (Table 5.3) inflows was mainly positive over all the regions of the North Sea.

5.C.4 Fluctuations in plankton species indicators of oceanic inflow

The decadal changes in the inflow reported earlier are expected to be related to the occurrence of plankton species indicative of oceanic waters. Two such species of calanoid copepods (*i.e.* *Metridia lucens* and *Candacia armata*) usually associated with the inflow from the northern North Sea (Lindley *et al.* 1990) demonstrated long-term trends between 1958 and 2003. Whilst both

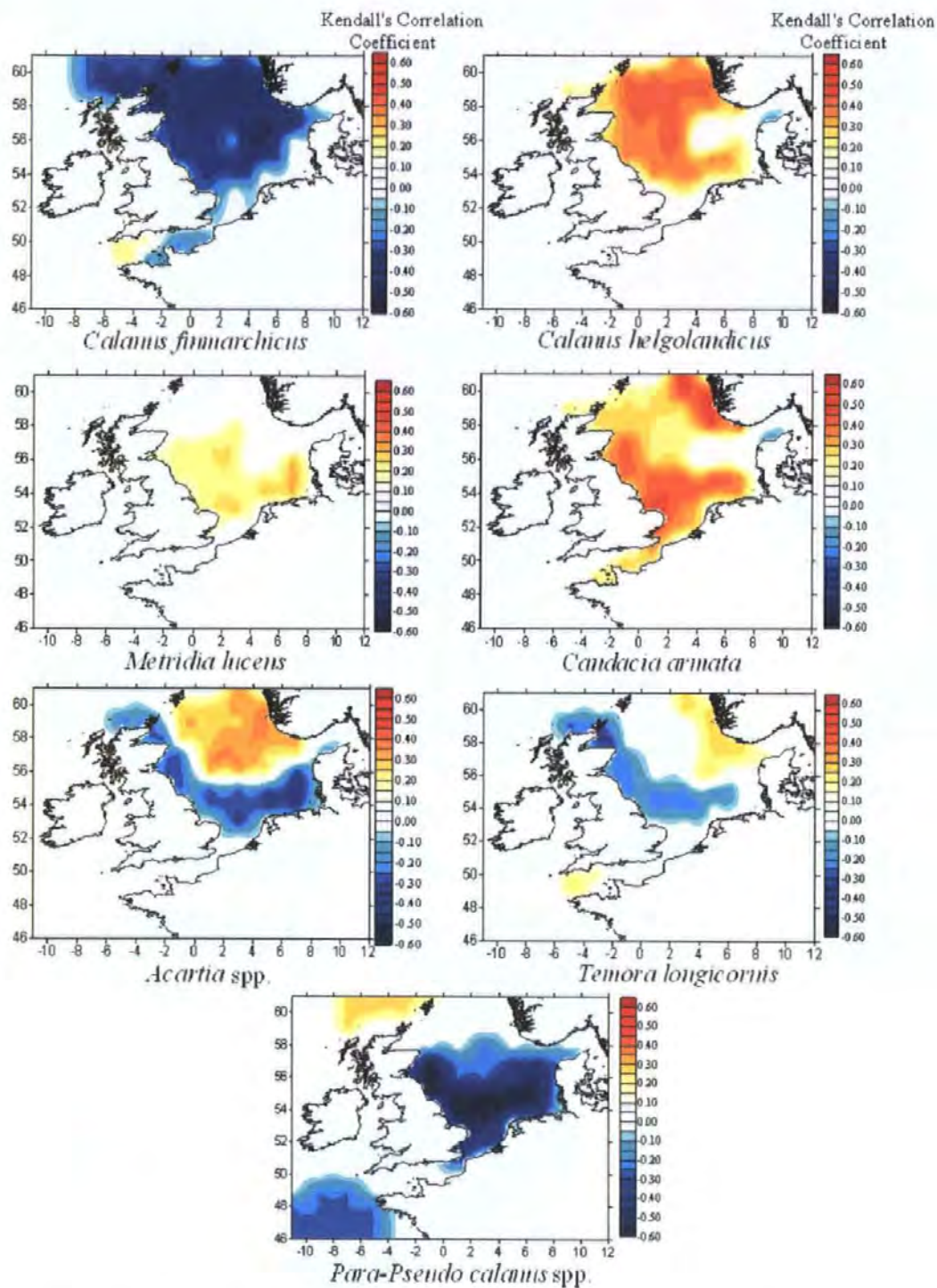


Figure 5.6. Kendall's rank correlation coefficient identifying long-term trends in zooplankton indicator species over the period 1958-2003 (5% significant level: $\tau > 0.201$).

species significantly increased in most of the regions of the North Sea (Fig. 5.6), their relationship with the oceanic inflow varied geographically with the source of the inflow considered. *M. lucens* and *C. armata* showed a positive correlation with both southern and northern inflows in most of the regions of the North Sea (Table 5.4), but *M. lucens* was negatively correlated with the southern inflow in regions 12 and 13 (Table 5.4) and with the northern inflow in region 3 (Table 5.4).

Table 5.4. Results of Spearman's correlation analysis between the cumulative sums of time series of plankton species indicators of oceanic inflow and the modelled (N) northern and (S) southern inflow over the period 1958-2003. Black and grey areas represent significant ($p < 0.05$) positive and negative correlations, respectively. White areas correspond to non-significant correlations. Due to the scarce observation of some species in the North Sea, when there were only zeros in the area the analysis was not performed (-). * The considered inflow does not influence this region.

Species	Inflow	1	2	3	4	5	6	7	8	9	10	11	12	13
<i>Aetideus armatus</i>	S	*	*	*	*	*	*	*	-	-	-	-	■	
	N	■	■	■	■	-	-	-	-	*	*	*	*	*
<i>Candacia armata</i>	S	*	*	*	*	*	*	*	■		■		-	-
	N	■							-	-	*	*	*	*
<i>Ceratium hexacanthum</i>	S	*	*	*	*	*	*	*	-	-	-	■	■	■
	N	-	-	-	-	-	-	■	-	*	*	*	*	*
<i>Clausocalanus</i> spp.	S	*	*	*	*	*	*	*	■	■	■			
	N	-	■	-	■	■	■	■	-	-	*	*	*	*
<i>Subeucalanus crassus</i>	S	*	*	-	*	*	*	*	-	-	-	■		-
	N	-	■	-	■	-	-	-	-	*	*	*	*	*
<i>Paraeuchaeta hebes</i>	S	*	*	*	*	*	*	*	-	-	-	■	-	-
	N	-	-	-	■	-	-	-	*	*	*	*	*	*
<i>Metridia lucens</i>	S	*	*	*	*	*	*	*	■		■		■	■
	N	■	-	■	-	■	■	■	■	*	*	*	*	*
<i>Pleuromamma</i> spp.	S	*	*	*	*	*	*	*	-	-	-	■	■	■
	N	-	-	■				■	-	*	*	*	*	*
<i>Rhincalanus nasutus</i>	S	*	*	*	*	*	*	*	-	-	-	-	■	-
	N	■		-	■	■	■	■	-	*	*	*	*	*

A few other species, including species of phytoplankton (*i.e.* *Ceratium hexacanthum*) and zooplankton (*i.e.* *Aetideus armatus*, *Clausocalanus* spp., *Subeucalanus crassus*, *Paraeuchaeta hebes*, *Pleuromamma* spp., and *Rhincalanus nasutus*), appear occasionally in the northwestern North Sea and seem to be related to the Atlantic inflow (Lindley *et al.* 1990, Corten 1999). Those species have significantly increased in regions 2 and 7, and were correlated to the northern inflow in the western North Sea (Table 5.4). In addition, in most of the English Channel, the southern inflow was positively related to these species (Table 5.4). However, some of these species also

increased in other regions of the North Sea: *P. hebes* increased in regions 1 to 8 and *Clausocalanus* spp. and *S. crassus* increased in the English Channel (Table 5.4). However, only *Pleuromamma* spp. singularly showed a different relation with the inflows, i.e. negative correlation with the southern and northern inflow (Table 5.4).

5.C.5. Decadal changes in the North Sea pelagic community composition

Within the North Sea, decadal-scale trends in community composition varied depending on the region of study and between phytoplankton and zooplankton. Using ANOSIM, the existence of significant difference between decades in the assemblage of key copepod and phytoplankton species was determined. On the assumption of a regime shift in the 1986-1988 (Reid et al. 2001; Beaugrand 2004), the difference in phytoplankton between the two regimes (i.e. 1958-1987 and 1988-2004) was tested; a significant difference was only evident in regions 1 ($r = 0.32$, $p < 0.01$) and 9 ($r = 0.27$, $p < 0.02$). In contrast to the phytoplankton, significant differences between the pre- and post-regime shift assemblages (1958-1987 and 1988-2004) was apparent in regions 2 ($r = 0.26$, $p < 0.01$), 3 ($r = 0.30$, $p < 0.01$), 4 ($r = 0.27$, $p < 0.02$), 6 ($r = 0.27$, $p < 0.01$), and 7 ($r = 0.39$, $p < 0.01$).

The variables (i.e. SST, NAO, salinity, phosphate, nitrate, and inflows of Atlantic waters) are likely to explain the fluctuations observed in phytoplankton and zooplankton species in the North Sea. However, their contribution to the plankton fluctuations was not consistent across regions (Table 5.5), although for phytoplankton species, northern inflow, NAO, and SST are included in the combination of variables in most of the regions. In regions 1, 5, 6, and 7 the fluctuations in phytoplankton were explained by the northern inflow as a single variable. In addition, SST, alone, best explains as a single variable the phytoplankton variations of regions 2 and 4, and is included in the combination of variables explaining the changes in regions 5, 6, and 7 (Table 5.5). Finally, phosphate and NAO best explain as single variables the variations observed in coastal regions 3 and 9, and 8 and 10, respectively. Different results were obtained for copepod species, with SST best explaining the changes as a single variable in regions 2, 4 to 7, and 9. In contrast, in regions 3 and 10 (northeastern and southernmost North Sea) the southern inflow best explained, as a single variable, the variability observed. In addition, phosphate and northern inflow best explained, as single variables, the fluctuations observed in regions 8 and 1, respectively.

Table 5.5. Result of BIOENV analysis between environmental/hydrologic variables (i.e. SST, NAO, salinity, phosphate, nitrate and inflows of Atlantic waters), phytoplankton indicator species and copepods. The single variable best explaining the patterns within the biotic matrix is underlined and the corresponding weighted Spearman correlation coefficient is indicated.

Region	Phytoplankton			Copepods		
	Environmental and hydrological variables	Best single r1	Best combination rbest	Environmental and hydrological variables	Best single r1	Best combination rbest
1	<u>Northern Inflow</u> , NAO	0.154	0.178	<u>Northern Inflow</u>	0.162	-
2	<u>SST</u> , Salinity	0.143	0.145	<u>SST</u> , NAO	0.175	0.180
3	<u>NAO</u> , Northern Inflow, Phosphate	0.079	0.115	<u>Southern Inflow</u> , NAO, SST	0.192	0.242
4	<u>SST</u>	0.121	-	<u>SST</u> , Northern Inflow	0.081	0.103
5	<u>Northern Inflow</u> , Nitrate, SST	0.287	0.422	<u>SST</u> , Nitrate	0.179	0.232
6	<u>Northern Inflow</u> , SST	0.182	0.229	<u>SST</u> , Phosphate, Southern Inflow	0.175	0.198
7	<u>Northern Inflow</u> , SST	0.104	0.127	<u>SST</u>	0.304	-
8	<u>Phosphate</u> , Salinity, NAO	0.091	0.109	<u>Phosphate</u> , Northern Inflow, Nitrate	0.042	0.070
9	<u>NAO</u>	0.205	-	<u>SST</u> , Salinity, Nitrate	0.081	0.127
10	<u>Phosphate</u> , NAO	0.157	0.273	<u>Southern Inflow</u> , SST	0.176	0.208

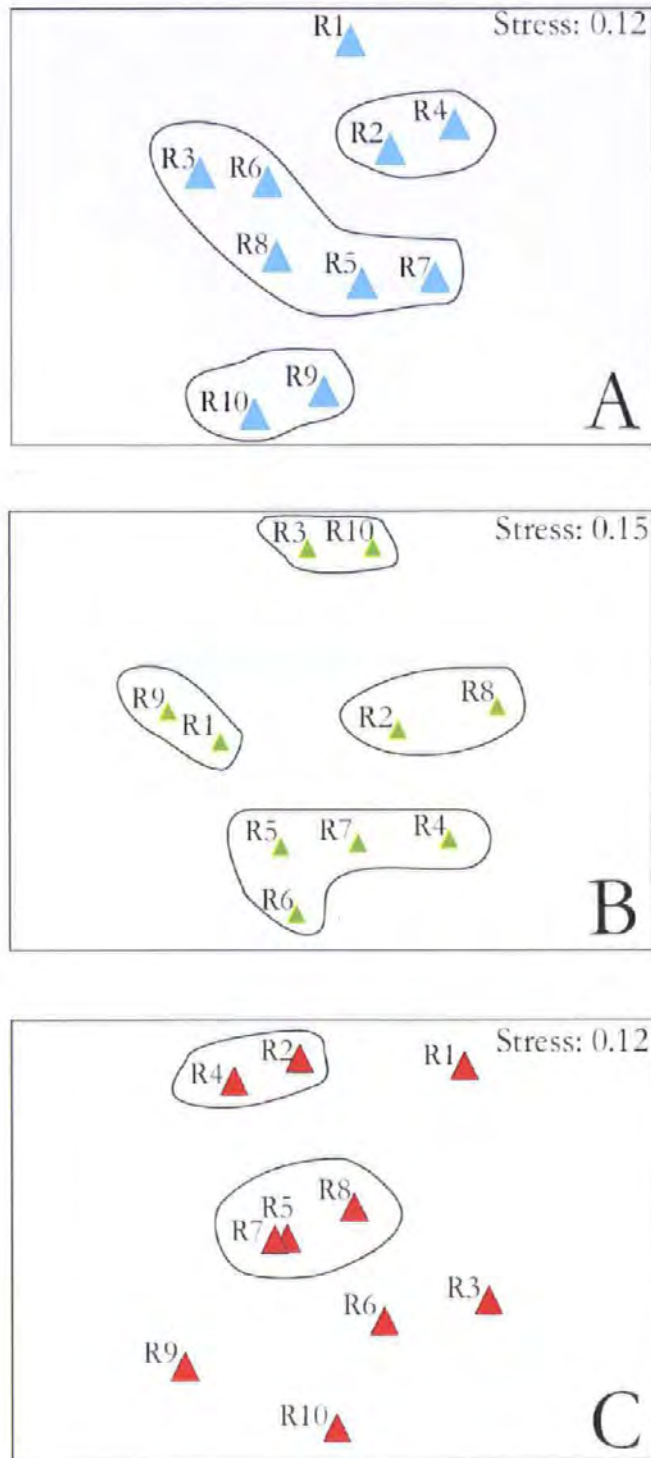


Figure 5.7. Second stage Multi-Dimensional Scaling ordinations for similarity matrices of (A) environmental variables, (B) phytoplankton indicator species and (C) copepods in each region of the North Sea (R1-R10).

The second stage MDS enabled a grouping of regions by similarity in order to assess consistency of patterns of change over time within multivariate data matrices. From the analysis using environmental variables (*i.e.* SST, NAO, salinity, phosphate, nitrate, and inflows of Atlantic waters), three groupings can be identified (Fig. 5.7a). The first group corresponds to regions 2 and 4, the second gathers regions 3 and 5 to 8 and the third group assembles regions 9 and 10. The same analysis was conducted using key phytoplankton species (*C. furca*, *C. fusus*, *C. horridum*, *C. lineatum*, *C. tripos*, *P. alata alata*, *R. hebetata semispina*, *R. styliformis*, *T. nitzschioides*, *Thalassiosira* spp., and *T. longissima*) and four groups were identified (Fig. 5.7b). The first group gather regions 3 and 10, the second brings together regions 4 and 5 to 7, the third group gathers regions 2 and 8, and the fourth group corresponds to regions 1 and 9. Using copepod species (*Acartia* spp., *C. finmarchicus*, *C. helgolandicus*, *Para-Pseudocalanus* spp., and *T. longicornis*), only two groups of regions were identified (Fig. 5.7c). The first group brings together regions 2 and 4, and the second group gathers regions 5, 7 and 8. The groups of regions identified using the different variables (*i.e.* phytoplankton, copepods, or environmental variables) were rarely the same, implying that the underlying patterns of environmental change do not result in similar plankton assemblages. However, the groups identified in the environmental variable analysis (Fig. 5.7a) were most similar to those for copepod species (Fig. 5.7c), suggesting that copepods are reflecting more closely than phytoplankton species the physico-chemical changes within the pelagic environment.

5.D. Discussion

5.D.1. Long-term fluctuations of Atlantic Waters inflow into the North Sea

Between 1958 and 2003, the inflow of Atlantic Waters into the North Sea has significantly increased through the English Channel, but no significant trend was observed for the northern inflow. Modelled flows indicate higher inflow into the northern North Sea from the west in the region of the Fair Isle Channel, between the Orkney and Shetland Isles, in the late 1980s and early 1990s, but decreased inflow from the Norwegian Sea, east of Shetland (Stephens *et al.* 1998). As the northern inflow used in our study combined the inflows via the east of the Shetland Islands and the Fair Isle Channel, this would explain why no long-term fluctuations were observed in overall northern inflow. The regime shifts observed in northern and southern inflows during the 80s have already been suggested by Corten (1999) and Reid *et al.* (2003). This is also consistent with previous statements that the inflow of species associated to the oceanic

inflow into the North Sea appears to have been greater in the late 1980s and 1990s than previously (Lindley & Batten 2002). Their biological observations have been supported by hydrographic data, such as the anomalously high salinity in the late 1980s and early 1990s recorded in the Skagerrak (Danielssen *et al.* 1996), the Southern Bight (Laane *et al.* 1996) and in the northern North Sea (Heath *et al.* 1991). In our study, salinity revealed a long-term increase only in the northwestern North Sea and a significant relationship was observed between salinity and the northern and southern inflows in regions 2 and 11, respectively. Decadal changes have also been observed in nutrients, with positive long-term trends in nitrate in regions 1, 6, 8, and 9 and in phosphate in regions 2, 6, and 9. In the Southern Bight of the North Sea (*i.e.* region 8 and 9), the increase in nutrients reflects the eutrophication (*i.e.* the increase in the rate of supply of organic matter (Nixon 1995) of the area (Lancelot *et al.* 1997, Druon *et al.* 2004). In region 6, the increase in nutrients might reflect changes in the circulation of the North Sea. During positive phases of NAO, the increase in westerly winds results in an intensification of the cyclonic circulation in the North Sea (Schrum 2001). The transport of water masses along the Southern Bight is then enhanced, as well as the sweep of rich nutrient water towards the east of the North Sea.

A significant relationship was observed between the NAO and both northern and southern inflows, but the relationship between the NAO and the southern inflow was weaker than with the northern inflow. The inflow via the Fair Isle Channel is mainly wind-driven and significantly positively correlated to the NAO during the winter (Planque & Taylor 1998). In addition, a smaller wind-driven flow enters through the Strait of Dover, with warmer saltier properties that are significant for the temperature and salinity distributions in the Southern Bight of the North Sea (Pingree 2005). However, the east Shetland inflow current seems to be more density-driven (Svendsen *et al.* 1991), at least during summer months, with a tendency for topographic stirring of flow from far field forcing (Pingree & Le Cann 1989). The wind-driven component of the oceanic inflow is associated with the different phases of the NAO. Positive phase NAO is associated with southwesterly winds that increase wind-driven inflow through the northern North Sea (Fig. 5.8). Greater inflow of oceanic water following southwest or northwest winds has already been observed (Furnes 1992, Svendsen & Magnusson 1992). In addition, Schrum (2001) showed that the inflow of saltier North Atlantic water increased strongly with increasing westerly winds. On the other hand, a negative phase of NAO is associated with southeasterly winds (Fig. 5.8), resulting in less inflow for the same wind stress

(Pingree 2005). Southeasterly winds will have a negative impact on the wind-driven inflow via the Fair Isle Channel but little or no impact on the wind-driven southern inflow through the Strait of Dover. The strength of the wind during positive phases of NAO will determine the inflow and imply a greater entrance of warmer water into the North Sea and, consequently, an increase in SST and salinity. In most of the North Sea, long-term changes have been observed in SST and these have been related to the northern inflow. In addition, significant positive relationships have been observed between SST and the southern inflow in regions 9 and 10. The regime shifts observed in SST and northern inflow occur during the same period (1985-1990) which led to the hypothesis that decadal fluctuations of SST in the North Sea are highly influenced by the oceanic inflows (Becker & Pauly 1996). However, stratification and surface heat fluxes that are also important factors influencing the variations of SST have not been taken into account in this study.

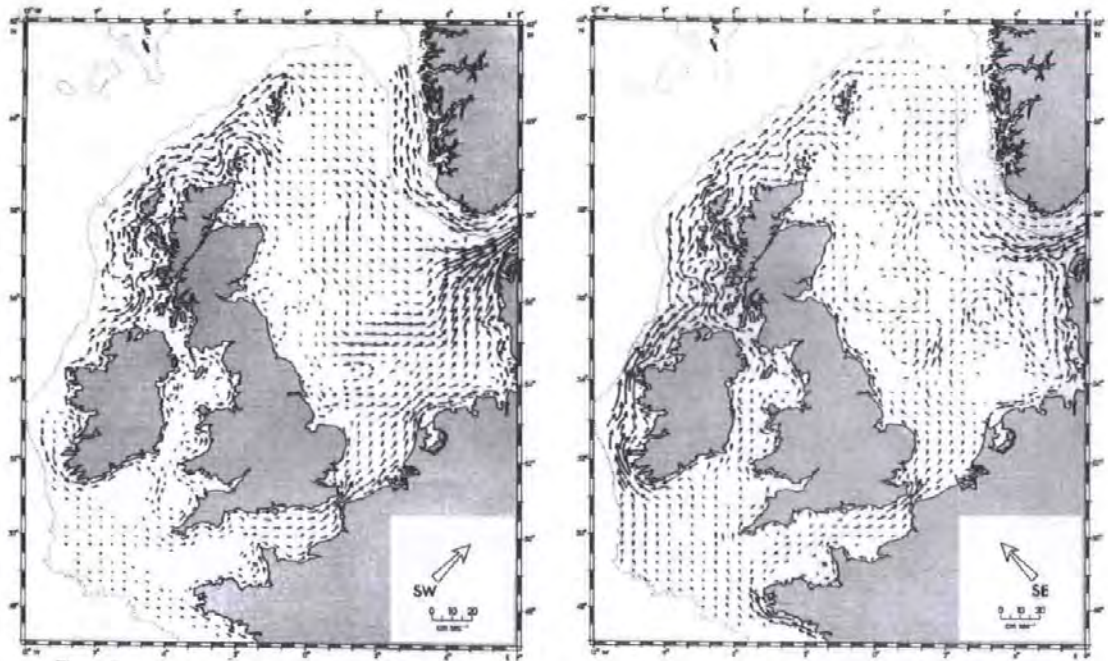


Figure 5.8. Wind-driven residual currents resulting from a uniform southwest and southeast wind stress of $1.6 \text{ dynes cm}^{-2}$. The length of a current vector determines the strength of the current at its central point. The current arrows are slightly curved to conform to the direction of current flow (after Pingree & Griffiths 1980).

5.D.2. Decadal changes in species indicative of Atlantic inflow

As decadal changes have been observed in the inflow of Atlantic Waters into the North Sea, the occurrence of plankton species considered as the best indicators of oceanic waters (Corten 1999) would be expected to show the same fluctuations. This is indeed the case for *Metridia lucens* and *Candacia armata* that demonstrated long-term increases between 1958 and 2003 (Fig. 5.6). Both species usually appear in the North Sea in the second half of the year, and survive for several months before they decline (Corten 1999). They are associated with the inflow of oceanic/mixed warm waters into the central and southern North Sea and have shown an increase in the western and southern North Sea (Table 5.4). Moreover, *C. armata* increased in the northeastern North Sea. As plankton species are highly influenced by the flux of water masses, *C. armata* is dependent on oceanic inflows and circulation within the North Sea. As the abundance of *C. armata* increased in western and southern North Sea regions, the currents towards the northeastern North Sea might have entrained more individuals than usual and caused the increase of *C. armata* in the northeastern North Sea.

In addition, the relationship of *M. lucens* and *C. armata* with the oceanic inflow varied according to the region and the source of the inflow considered, but they were mainly positively correlated to both southern and northern inflow in the North Sea. However, *M. lucens* was negatively correlated with the southern inflow in the English Channel and eastern Atlantic, and with the northern inflow in the northeastern North Sea. Some environmental parameters inherent to those areas might have had a negative impact on *M. lucens*. In particular, SST and NAO have been observed influencing copepods fluctuations in the northeastern North Sea. A few other species, including phytoplankton (*i.e. C. hexacanthum*) and zooplankton (*i.e. A. armatus*, *Clansocalanus* spp., *S. crassus*, *P. hebes*, *Pleuromamma* spp., and *R. nasutus*) species, have also been described as indicative of Atlantic inflow (Lindley *et al.* 1990, Corten 1999). However, in contrast to *M. lucens* and *C. armata*, those species (*e.g. P. hebes*) have only significantly increased in the regions directly influenced by the northern inflow (*e.g. regions 1, 2, 4, and 7*). In addition, they have been reported as showing up in the North Sea only during episodes of exceptional input of Atlantic water (Corten 1999). If these species were not observed in the central and southern North Sea, it might be because they cannot adjust to North Sea conditions and disappear soon after entering the North Sea. An exceptional event is then needed for those species to be observed in the North Sea by the CPR survey.

5.D.3. Long-term fluctuations in the plankton community

Between 1958 and 2003, decadal-scale changes have been observed within phytoplankton and zooplankton communities, but these trends were not consistent across the whole sea, indicating the importance of processes acting at the below-sea scale.

Firstly, diatoms significantly increased in southeastern (*i.e.* *P. alata alata*, *R. hebetata semispina*, *R. styliformis*, *T. longissima*, and *Thalassiosira* spp.) and northeastern (*i.e.* *T. longissima*) North Sea regions. *T. longissima* and *Thalassiosira* spp. were positively correlated to both southern and northern inflow in this area. *T. longissima* is a typical Atlantic diatom which usually declines rapidly after entering the North Sea (Reid *et al.* 1992, Corten 1999). However, due to the increase in the cyclonic circulation of the North Sea associated to the increase in westerly winds (Schrum 2001), *T. longissima* might have drifted further, towards the eastern North Sea causing the increase in abundance of that species not usually observed in this part of the basin (Reid *et al.* 1992). On the opposite, *Thalassiosira* spp. are typical species of the NE Atlantic and the North Sea (Continuous Plankton Recorder Team 2004). The increases in *Thalassiosira* spp. in the southeastern North Sea then does not seem to be related to changes in the inflows or in the circulation of the North Sea, but to local processes inherent to this region. In particular, during positive phases of the NAO, the increase in precipitation over Northern Europe is associated with an increase in river runoff (Drinkwater *et al.* 2003). In the south North Sea, Belgium, Dutch and German rivers discharge lots of nutrients (Hickel *et al.* 1995). The increased nutrient stocks in the southeastern North Sea might then be responsible for the increase in *Thalassiosira* spp.

Secondly, dinoflagellates (*i.e.* *Ceratium* spp.) significantly increased in the northeastern North Sea; *Ceratium* spp. was positively correlated to the northern inflow in this area. Edwards *et al.* (2006) suggested that the increase in the abundance of the genera *Ceratium* spp. off the coast of Norway was related to hydroclimatic changes. Schrum (2001) showed that the outflow of the fresher North Sea water along the Norwegian coast increased. The long-term decreasing trend in salinity is probably caused by the increase in precipitation and substantial increase in runoff associated with positive values of the NAO (Sætre *et al.* 2003). As the NCC flow has increased between 1958-2003 (Kendall correlation test, $\tau = 0.26$, $p < 0.05$), low-salinity water input from the Baltic, as well as transport of freshwater discharged by rivers draining the continental areas, might have increased, causing more frequent stratification along the western Norwegian coasts. Beare *et al.* (2002) indeed observed a freshening of the North Sea waters west of 5°E between

1958 and 1998 and an increase in stratification. According to Margalef's (1975) hypothesis, the growth of dinoflagellate species should be enhanced during stratification, which is congruent with our observations.

However, significant decreases have also been observed in diatoms (e.g. *P. alata alata*) and dinoflagellates (e.g. *Ceratium* spp.) in the northwestern and central North Sea. As the northwestern area (i.e. regions 1 and 4) is directly under the influence of the northern inflow, this area is most representative of North Atlantic conditions. Moreover, some indicator species did not follow the same trend as their main taxa: the diatom *Rhizosolenia* spp., for example, significantly increased in the southeastern North Sea and the English Channel, but significantly decreased in the central and southwestern North Sea (Fig. 5.5). However, it was not possible to determine the mechanisms underlying those changes.

Finally, significant decadal changes have been observed in copepods (i.e. *C. finmarchicus*, *C. helgolandicus*, and *Para-Pseudocalanus* spp.). *C. helgolandicus* significantly increased in most regions of the North Sea and was positively related to both inflows. *C. helgolandicus* is characteristic of warmer shelf-edge Atlantic water (Continuous Plankton Recorder Team 2004) advected into the North Sea via the English Channel and Fair Isle current. Positive phases of NAO are associated with southwesterly winds that increase the wind-driven inflow through northern North Sea (i.e. Fair Isle current) and then induce an increase in *C. helgolandicus* in the North Sea. Even if that species has Atlantic water origins, it can now effectively reproduce in the North Sea, spread over large parts of it and behave like indigenous North Sea species (Corten 1999). By contrast, significant decreases of *Para-Pseudocalanus* spp. and *C. finmarchicus* populations have occurred in most regions; they significantly increased, however, in the northwestern North Sea and in the western English Channel, respectively. *C. finmarchicus* and *Para-Pseudocalanus* spp. were negatively related to northern and southern inflows in most of the regions of the North Sea. On the opposite, they were positively related to the southern inflow in the English Channel. *C. finmarchicus* is mainly advected through the east Shetland inflow current (Beare et al. 2002) which seems to be predominantly density-driven (Svendsen et al. 1991). The fluctuations in wind-regimes associated with the NAO phases should only have a minor influence on this current. However, during positive NAO phases in the late 1980s and early 1990s, the inflow through the east of Shetland decreased (Stephens et al. 1998). A reduction in Atlantic inflow via the East Shetland is one scenario that might explain the long-term changes observed in *C. finmarchicus* (Beare et al. 2002). In addition, the fluctuations of *C. finmarchicus* have been linked

to the increase in SST in the North Sea associated to the increasing trend in Northern Hemisphere Temperature (Beaugrand *et al.* 2002). However, the fluctuations of SST are also highly influenced by the oceanic inflows. The abundance of *C. finmarchicus* in the North Sea seems then to be driven by (i) a decrease in the inflow through the east Shetland inflow current, (ii) changes in temperature related to the fluctuations of the inflow and (iii) the increasing trend in Northern Hemisphere temperature (Beaugrand *et al.* 2002).

Other species, like *Acartia* spp. and *T. longicornis*, significantly increased in the northern and central North Sea and decreased in the western and southern North Sea regions. *T. longicornis* was negatively correlated to the northern inflow in the western and southern North Sea regions, but positively related to southern inflow in the central North Sea and the English Channel. Conversely, *Acartia* spp. was positively correlated to the southern inflow in the English Channel and negatively correlated in the Straits of Dover, whilst its relationship with the northern inflow was essentially positive, except in the northwestern North Sea. *Acartia* spp. enters the northern North Sea mainly with the mixed oceanic and coastal waters which flow around the Scottish north coast (i.e. through the Fair Isle Channel), and also into the southern North Sea through the English Channel. This taxa therefore decreases in the regions directly influenced by the northern inflow, whereas *T. longicornis* increases when the Atlantic influence becomes minimal. *T. longicornis* is a coastal species usually encountered at maximum abundance in the southern and western North Sea, whereas *Acartia* spp. is an oceanic species (Continuous Plankton Recorder Team 2004), predominantly found offshore that drift from southern latitudes into the North Sea along with temperate waters of the NE Atlantic Current (Krause *et al.* 1995). Being a coastal species, typical of the North Sea (Continuous Plankton Recorder Team 2004), *T. longicornis* can may be not adapt to the changes in water characteristics associated to the northern inflow. In contrast, *Acartia* spp. might not be able to adapt to North Sea water conditions and disappear soon after entering in the North Sea.

5.D.4. Decadal changes and regime shifts in the North Sea pelagic community composition

Within the North Sea, decadal-scale trends in community composition varied depending on the region of study and between phytoplankton and zooplankton components. Under the assumption of a regime shift in 1986-1988 (Reid *et al.* 2001, Beaugrand 2004), a regime shift in phytoplankton (1958-1987 and 1988-2004) was only evident in northwestern and southwestern North Sea regions. Edwards *et al.* (2006) showed that regime shifts were less evident in

phytoplankton species than for the PCI. In contrast to the phytoplankton, significant differences between the pre- and post-regime shift copepod assemblages (1958-1987 and 1988-2004) were apparent in northern, western, and eastern North Sea regions. The regime shifts identified in the phytoplankton and zooplankton do not therefore seem to be related. We did not identify regime shifts in every region of the North Sea, but only in specific areas, directly influenced by the oceanic inflows or by the NCC. In addition, differential regime shifts were also identified in the northern inflow in 1988 and in the southern inflow in 1982; however, the regimes identified had similar phases, with a low and high inflow characterised respectively by the decrease and increase in cumulative sums. This suggests that the regime shift identified in phytoplankton and zooplankton species is related to a shift in the oceanic inflow towards the North Sea. These observations are in agreement with the work of Reid *et al.* (2001).

However, other environmental or hydrological variables (*i.e.* SST, NAO, salinity, phosphate, nitrate, and inflows of Atlantic waters) might also be involved in the changes observed in plankton. The best explanatory variables were not consistent across regions, although for phytoplankton species, northern inflow, NAO, and SST are included in the combination of variables in most of the regions (Table 5.5). We obtained different results for copepod species, with SST best explaining the changes as a single variable in most of the regions of the North Sea. In conclusion, zooplankton seems to be under the influence of one major single variable (*i.e.* SST) while phytoplankton appears to be under the influence of different environmental variables according to the region of study. This is congruent with the results of Beaugrand *et al.* (2002) that demonstrated the major influence of the Northern Hemisphere temperature on copepod assemblages.

Chapter 6

IMPACT OF CLIMATE AND MESOSCALE PHYSICAL PROCESSES ON PHYTOPLANKTON DISTRIBUTION IN THE NORTHWEST ATLANTIC OCEAN

Part of this chapter has been included in the following:

Leterme S.C. & Pingree R.D. (in press) The Gulf Stream, Rings and North Atlantic Eddy structure from remote sensing (Altimeter and SeaWiFS). *Journal of marine Systems*.

Leterme S.C. & Pingree R.D. (2005) Impact of mesoscale physical processes on phytoplankton distribution in the Northwest Atlantic Ocean. ASLO Summer Meeting, June 2005, Santiago de Compostela, Spain.

Leterme S.C. & Pingree R.D. (submitted) Structure of phytoplankton (Continuous Plankton Recorder and SeaWiFS) and impact of climate in the Northwest Atlantic Shelves. *Ocean Science*.

6.A. Introduction

The intense hydrodynamic activity observed in the Northwestern Atlantic Shelves Province (Longhurst 1998) makes this region especially intriguing from the point of view of physical-biological interactions. This area is under the influence of the cold southward inflow of Labrador Sea Water (LSW) and the warm northward flow of the Gulf Stream. The Gulf Stream flows from the continental slope off Cape Hatteras and travels eastward, meandering until the tail of the Grand Banks (Stommel 1958). Meanders which separate northward of the stream develops into anticyclonic (warm core) eddies and those separating southward produce cyclonic (cold core) eddies (Richardson 1983, Tomczak & Stuart 2003). Those rings usually move westward when they are not touching the Gulf Stream meanders and eastward when they are attached to them (Fuglister 1972, Richardson 1980). Because of its highly dynamic nature, this environment is a perfect candidate to assess the role on physical-biological interactions in the control of the biological processes by their physical environment.

Frontal and upwelling regions, and their related enrichment processes, are widely acknowledged to be favourable for the rapid growth of phytoplankton (e.g. Wyatt & Horwood 1973) as they represent areas where 'auxiliary energy' (Margalef 1978) fluctuates rapidly in space and time (Legendre & Demers 1984, Legendre *et al.* 1986). Pingree *et al.* (1979) also established that eddies have an influence on the transfer and growth of the phytoplankton. More recently, Gonzalez *et al.* (2001) have shown that mesoscale features are important sources of organic carbon to the pelagic ecosystems in oligotrophic areas and thus greatly influence the plankton community. More specifically, Gulf Stream warm core and cold core rings have been shown to influence surface phytoplankton distributions via the entrainment of the surrounding water masses around and into the rings (Kennelly *et al.* 1985, Garcia-Moliner & Yoder 1994, Ryan *et al.* 1999, Ryan *et al.* 2001). Gulf Stream warm-core rings have also been shown as strongly influencing water mass and chlorophyll distributions along the southern flank of Georges Bank (Ryan *et al.* 2001, Bisagni *et al.* 2001). This area is also under the influence of the North Atlantic Oscillation through modification of the surface and deepwater circulation patterns of the North Atlantic, and more specifically the transport of Labrador Current (Marshall *et al.* 1997). The related fluctuations in the inflow of LSW along the Scotian shelf have been associated with changes in coastal water characteristics (i.e. SST, salinity and nutrient concentration) and zooplankton abundance (Greene & Pershing 2000).

In this context, the first part of this chapter will investigate the relationship between spatial and temporal structures of eddies (via Sea Surface Heights) and chlorophyll *a* (from the Sea-viewing Wide Field-of-view Sensor, SeaWiFS) along the Gulf Stream axis. In particular, identified physical structures are followed and compared with phytoplankton distribution. Then, on the basis of a route continuously sampled by the CPR between Norfolk (Virginia, USA; 39°N, 71°W) and Argentia (Newfoundland; 47°N, 54°W) over the period 1995-1998, the second part of this chapter specifically assesses the relation between phytoplankton and altimetry data on the Georges Bank, with a special focus on the fluctuations in PCI and SeaWiFS data in relation with hydroclimatic variability.

6.B. The Gulf Stream, Rings and North Atlantic Eddy structures from remote sensing (Altimeter and SeaWiFS)

6.B.1. Introduction

In order to determine the relationship between spatial and temporal structures of phytoplankton and eddies along the Gulf Stream axis, the first part of the chapter 6 examines and compares: (i) the spatial and seasonal structure of SeaWiFS chlorophyll *a* along the spring bloom boundary in the North Atlantic near 35°N in relation to eddy structure, (ii) the seasonal cycles of SeaWiFS Chl *a* along a mean Gulf Stream path, (iii) the speed and propagation of Gulf Stream rings and (iv) eddy and SeaWiFS Chl *a* spatial structures along the Gulf Stream route.

6.B.2. Methods and data

6.B.2.a. Sea level anomaly

The purpose of Topex/Poseidon is to measure the sea surface height (SSH), with an exceptional accuracy of less than 5cm precision. Sea level anomaly (SLA) heights have been measured by the ERS 1/2 and Topex Poseidon satellites since the 22 October 1992 at 10 day intervals. Radar altimeters on board the satellite continually transmit signals at high frequency to Earth and receive reflected signals from the sea surface. The data have been processed according to Le Traon *et al.* (1998) with SLA data spatially interpolated to 0.25° in both latitude and longitude.

Maps of SLA were derived for the North Atlantic to compare with monthly SeaWiFS chlorophyll *a* concentration. The SLA is composed of mesoscale structures imposed on seasonal changes with eddy or Rossby wave structures usually dominant. The annual or seasonal signal corresponds, in part, to the rise and fall of the sea surface that arises from the expansion and contraction of the ocean due to its seasonal heating up and cooling down. In addition, the SLA is influenced by an annual cycle due to ocean circulation. The region of maximum variance of sea surface height in the North Atlantic will be along a mean Gulf Stream route (Pingree, pers. comm.). Along the Gulf Stream route, annual buoyancy and circulation changes can result in a maximum annual elevation signal change of ± 20 cm. Since I am interested in elevation structure that matches or correlates with non-seasonal SeaWiFS structure, the annual component and any residual mean elevation was removed from the SLA data using Fourier analysis. Although relatively small in this context, tidal aliasing due to the semi-diurnal tide was also removed. I refer to the resulting data as SLA residuals.

The Gulf Stream route selected follows closely the maximum annual amplitude of Sea Level Anomalies (Fig. 6.1). The chosen path (Fig. 6.2) is in concordance with former Gulf Stream studies (Watts 1983, Brown *et al.* 1986, Lee & Cornillon 1996, Schoellart *et al.* 2004). The downstream path was also followed closely by an ALACE (25976) subsurface float at ~ 600 m depth (Pingree & Sinha 2001) moving with the Gulf Stream in 2002 and an ALACE subsurface float (25972, at ~ 150 m depth) moving from the Florida Strait ($\sim 25.9^\circ\text{N}$, 79.7°W , near Miami) in 2005 which gave a consistent upstream position ($\sim 37.1^\circ\text{N}$, 70.6°W) off Cape Hatteras 20 days later (a mean speed of 1.2 ms^{-1} between the positions).

Altimeter and SeaWiFS Chl *a* data were extracted every 0.25° along the Gulf Stream route (corresponding to 92 stations sampled over a distance of 2080 km; Fig. 6.2). SeaWiFS chlorophyll (Chl *a*) data have been processed and analysed along this route from September 1997 to August 2002 (5 years period). Sea Level Anomalies (SLA) were derived along the same route from January 1993 to December 2000 (8 years period) and time changes of sea surface elevation residuals along the Gulf Stream route are plotted on a Hovmöller diagram. An overlapping time window of SeaWiFS Chl *a* and altimeter anomalies is compared between September 1997 and December 2000.

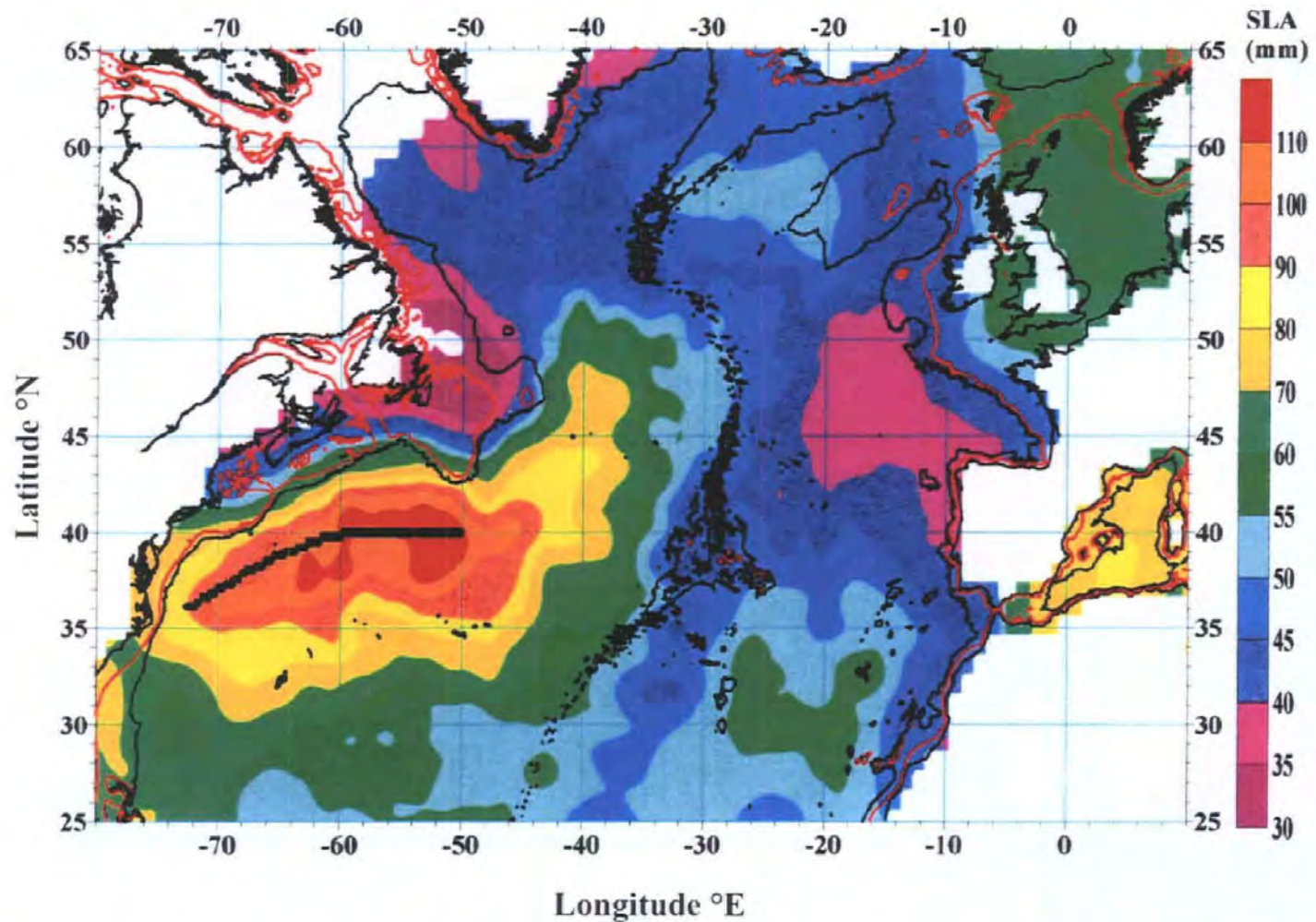


Figure 6.1. Annual Sea Level Anomaly amplitude (mm) in the North Atlantic. The Gulf Stream route selected (marked black) starts along the continental slope off Cape Hatteras and then follows the maximum amplitude region.

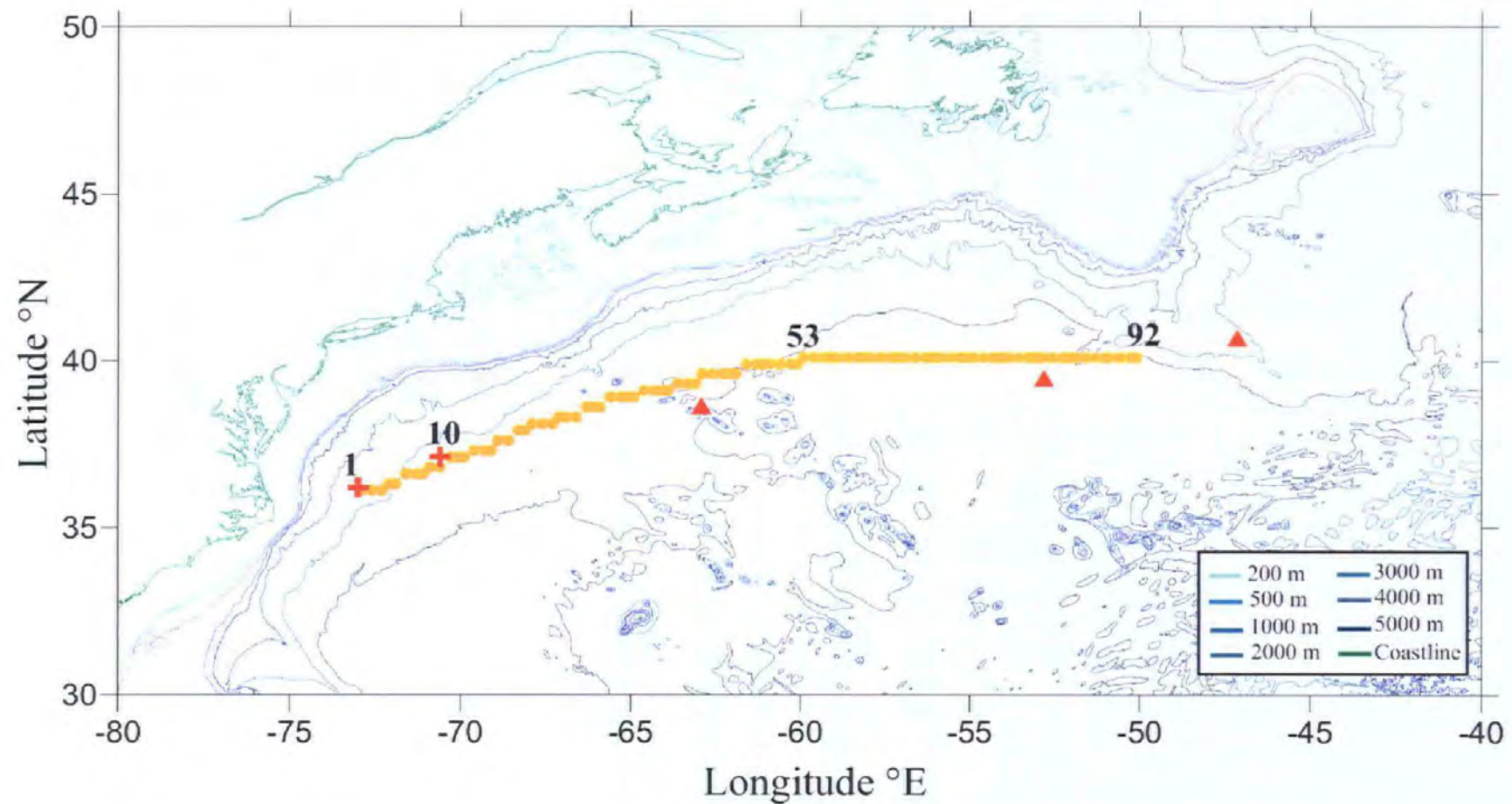


Figure 6.2. Topography of the studied area and position of the Gulf Stream axis (marked orange) adopted in this present study. Station positions 1, 10, 53 and 92 are marked. Red cross at station 1 is a Gulf Stream position based on HMS Hecla XBT section (May 1996). Red cross at station 10 marks the position of the ALACE float 25972 at ~150 m depth moving from Florida Current to the Gulf Stream (September 2005). Red triangles are positions of the ALACE float 25976 at ~600 m depth moving in the Gulf Stream (May - August 2002).

6.B.2.b. SeaWiFS Chlorophyll *a*

SeaWiFS is a spectroradiometer that measures radiance in specific bands of the visible light spectrum (Mueller & Austin 1995). The satellite spectroradiometer offers the possibility of observing and investigating the oceans from a global point of view and provides information on chlorophyll *a* on a daily, weekly, monthly and annual basis. As species of phytoplankton contain dissimilar concentrations of chlorophyll, they can be detected by SeaWiFS as they appear as different colours to this sensitive instrument. SeaWiFS data produced by the SeaWiFS project were obtained from the Goddard Distributed Active Archive Centre under the auspices of NASA. Use of these data is in accord with the SeaWiFS Research Data Use Terms and Conditions Agreement. Processing of SeaWiFS data to final chlorophyll *a* concentration (C_a) used the SeaDAS (SeaWiFS Data Analysis System) software, and C_a was also estimated from the ratio of radiances measured in band 3 (480-500 nm) and band 5 (545-565 nm) according to the following NASA algorithm:

$$C_a = \exp[0.464 - 1.989 \ln(L_{WM,490}/L_{WM,555})] \quad (1)$$

Monthly composite SeaWiFS maps for the North Atlantic were derived. For deriving the 5 year mean seasonal cycles, the SeaWiFS Chl *a* data were spatially averaged over ± 25 km in both latitude and longitude, and missing data due to cloud coverage interpolated.

SeaWiFS Chl *a* structure along the spring bloom boundary near 35°N in April 1999 was matched with the SLA map of elevation (or eddy structure) for April 1999 to determine the influence of eddies on the spatial scale. Eddy orbital velocities were determined using the geostrophic relation. Direct measurements were obtained from the track of ARGOS (Airborne Remote Geographic/Oceanographic System) buoy 1811 moving westward in a cyclonic eddy on the chlorophyll frontal boundary in April 1999.

To examine the chlorophyll structure along the Gulf Stream route, seasonal cycles of SeaWiFS Chl *a* were derived and a mean cycle (based on 5 years of data) was removed from the data to produce SeaWiFS anomalies or residuals between September 1997 and December 2000 and for comparison with SLA residuals.

6.B.3. Results

6.B.3.a. Structure of Chl *a* and SLA in the Subtropical Atlantic Ocean near 35°N

In April 1999, the spring bloom boundary stretches across the North Atlantic from Cape Hatteras to Western Europe at $\sim 35^\circ\text{N}$ (Fig. 6.3). The monthly composites show that during April the spring bloom boundary in the central North Atlantic near 35°N is northward at a speed of about 250 km per month (see also Campbell and Aarup (1992) using CZCS data). The boundary is not regular but has perturbations due to eddy structures.

The North Atlantic altimeter SLA map for April 1999 shows the corresponding mesoscale eddy field (Fig. 6.4.a-e). By matching the altimeter spatial structure with the SeaWiFS boundary spatial structure, it reveals that the SeaWiFS Chl *a* protrusions (a, b, c, d, e, Fig. 6.3) result from the southern components of eddy motions which draw elevated Chl *a* values from the north to the south. Hence, although eddy spatial structure is evident in the SeaWiFS Chl *a* spatial structure, the main influence of eddies in the open ocean is one of advection or redistribution of the Chl *a* field as the spring bloom boundary propagates (by growth) northward. The SeaWiFS Chl *a* perturbation structure has a scale that is about two times the eddy scale. Based on the SeaWiFS Chl *a* protrusions (Fig. 6.3.a-e), a scale, $l \sim 430$ km, was estimated for the perturbation wavelength or about two times the eddy scale, L (c.f. $L \sim 220$ km at 34°N for the NE Atlantic, given in Pingree (2002)).

The track of ARGOS buoy 1811 in March and April 1999 is superimposed on the SeaWiFS Chl *a* and SLA fields for April (Fig. 6.3 and 4). The buoy made 11 loops in the same eddy between January and June 1999 near 35°N . The westward speed of the eddy was 5 km.d⁻¹. The buoy movement in the cyclonic eddy centred near 34.7°N , 53°W in April gives some direct measurements of the flow component between eddies (see section 6.B.3.e).

The region near 35°N can be considered as northern subtropical water and the seasonal cycle of SeaWiFS Chl *a* concentration for this region (Fig. 6.5) shows a spring bloom peak in March with a mean maximum SeaWiFS Chl *a* concentration of ~ 0.3 mg.m⁻³. This cycle contrasts with those representative of NE Atlantic temperate regions ($\sim 45^\circ\text{N} - 50^\circ\text{N}$), since Chl *a* levels start to increase in the autumn-winter period (after September) as the mixed layer deepens due to winter mixing (with nutrient renewal). The Sea Surface Temperature (SST) from ARGOS buoy 1811 showed that the bloom maximum occurred near the winter minimum temperature of 18°C (in March). SeaWiFS Chl *a* concentrations are elevated above a

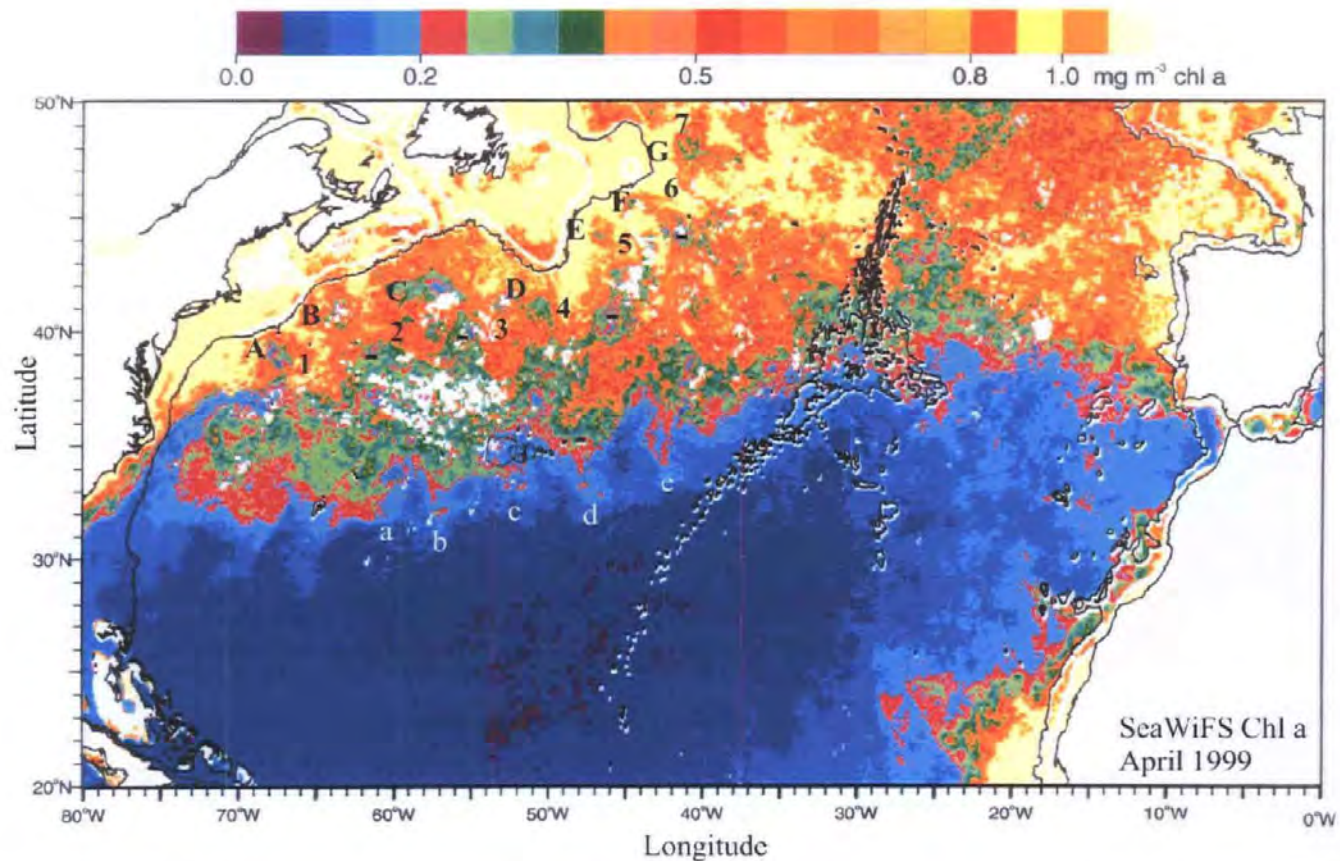


Figure 6.3. SeaWiFS Chl *a* distribution in the North Atlantic Ocean during the spring bloom in April 1999. Black line contour shows 2000m depth. A value of 0.2 mg.m^{-3} Chl *a* (red) has been chosen to show the structure along the frontal boundary of the North Atlantic spring bloom. Plumes extending southward along the spring bloom boundary are labelled a to e. In the Gulf Stream region, cyclonic structures labelled 1 to 7 (see Fig. 6.4) are associated with higher levels of Chl *a*. Anticyclonic eddies to the north of the Gulf Stream axis labelled A to G (see Fig. 6.4) are generally associated with lower Chl *a* levels. Low values of Chl *a* near the Gulf Stream route are marked with - sign (these correspond with warm core rings marked with + in Fig. 4)

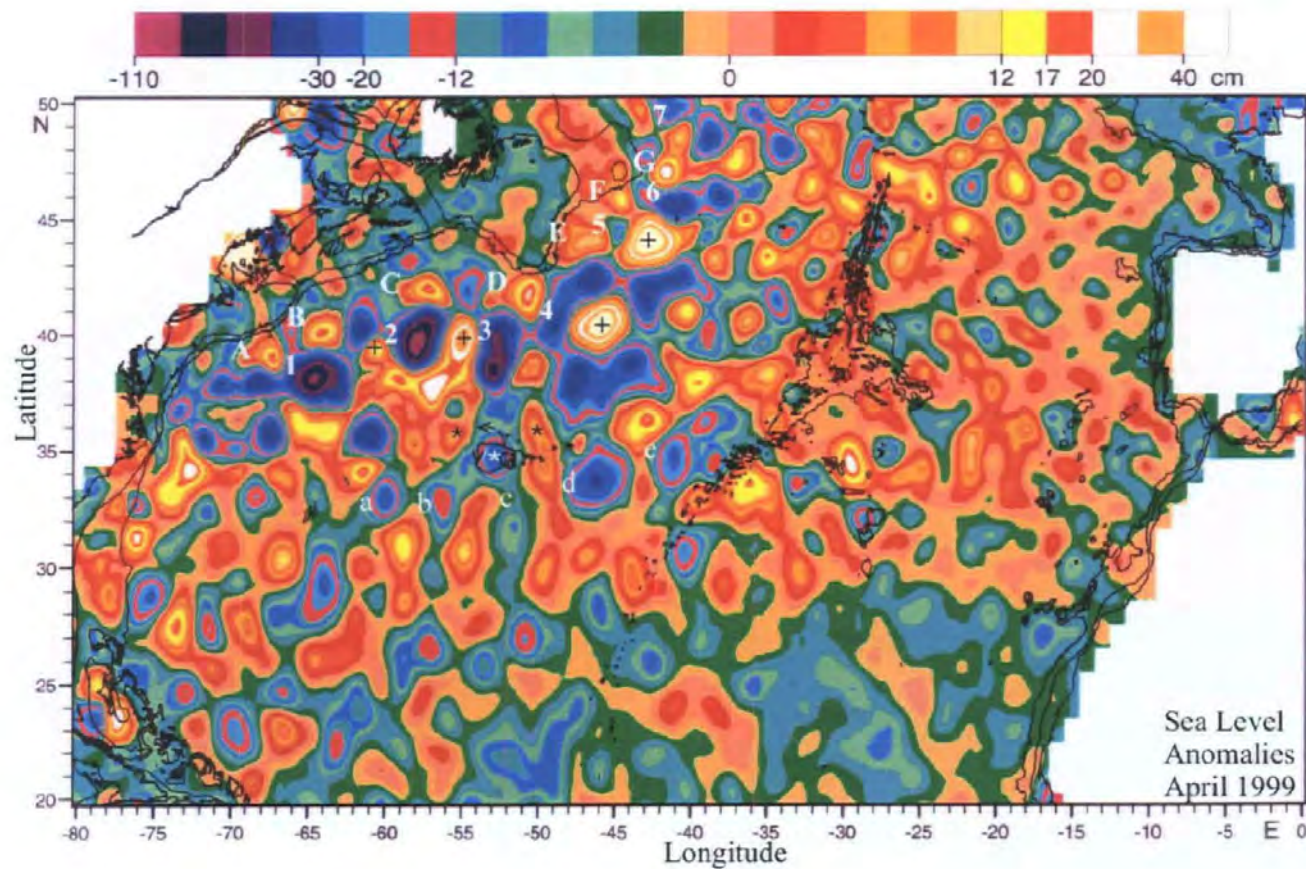


Figure 6.4. Sea level anomalies (cm) for the North Atlantic Ocean for April 1999. Positive and negative anomalies match the spring bloom boundary near 35°N. Labels a to e correspond to the plumes on chlorophyll frontal boundary and are associated with the southerly component of an adjacent cyclonic eddy. Argos buoy track moving anticlockwise around cyclonic eddy between two adjacent anticyclonic structures indicated (marked with stars). More intense mesoscale activity, warm core rings (yellow/white) and cold core rings (blue) can be identified in the Gulf Stream region. Some cold rings are labelled 1 to 7 (numerals placed to the left of the eddy) and 7 warm core eddies to the north of the Gulf Stream axis are labelled A to G. Positive SLA values representing warm core rings between cold core rings near the Gulf Stream axis are marked with + sign.

mean level from about November to May and structure due to advection, or mixing by eddies, is evident for these monthly SeaWiFS concentration maps. By examining the monthly maps for any tendency for regular zonal structure, a separation or wavelength scale of $L = 480 \pm 40$ km was estimated for $\sim 35^\circ\text{N}$ (with about half of the maps showing some structure).

6.B.3.b. Fluctuations of Chl *a* and SLA along the Gulf Stream route

Inspection of both Sea Level Anomalies and SeaWiFS Chl *a* maps shows more intense spatial structure in the Gulf Stream region. The mean values of SeaWiFS Chl *a* variance and SLA variance were determined every 0.25° along the Gulf Stream route (Fig. 6.6 and 7). There is a significant difference between the Chl *a* values obtained between stations 1 and 17 and those obtained between stations 18 and 92 (Wilcoxon-Mann-Witney, $z = 3.621$ $p < 0.01$). The mean Chl *a* values are lower for stations 1 to 17 ($\bar{x}_{Chl a} \pm \sigma = 0.23 \pm 0.02$ mg.m^{-3} Chl *a*) than for stations 18 to 92 ($\bar{x}_{Chl a} \pm \sigma = 0.35 \pm 0.03$ mg.m^{-3} Chl *a*). The difference in Chl *a* is likely due to the changing properties along the route. Between stations 1-17, at the beginning of the Gulf Stream route, the water corresponds to Subtropical Water, low in Chl *a* and inorganic nutrients. Further downstream, meanders or eddies result in elevated mean Chl *a* levels as Atlantic Temperate Slope Water (ATSW) and Subpolar Water are sampled.

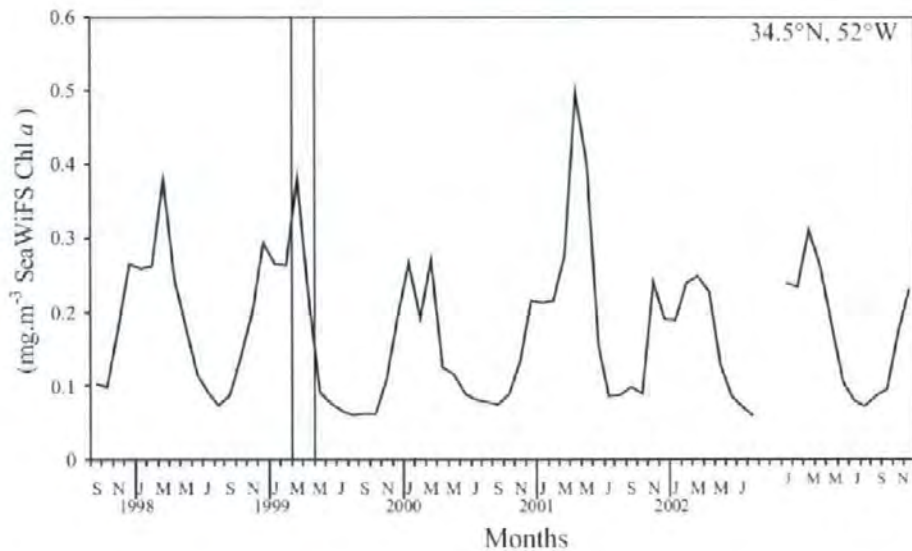


Figure 6.5. Seasonal cycles of SeaWiFS Chl *a* (mg.m^{-3}) at 34.5°N , 52°W over a 5 year data period. Start of the year and first letter of alternate months annotated. The time window corresponding to the buoy track in March (M) and April 1999 is indicated.

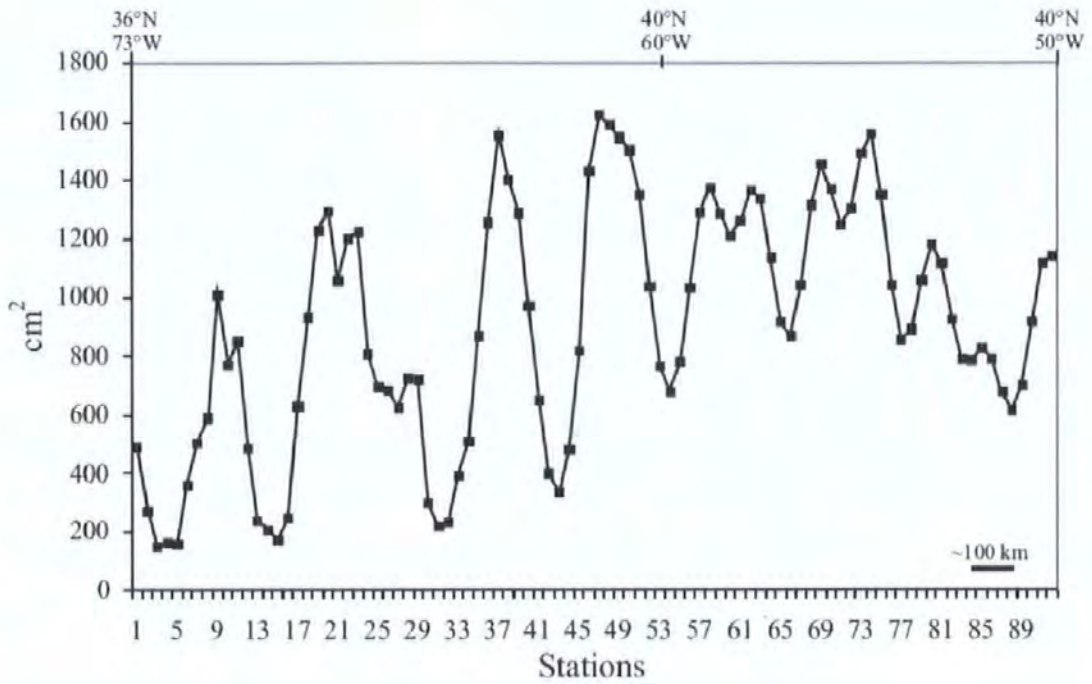


Figure 6.6. Variance (annual component removed) of Sea Level Anomalies (cm^2) along the route of the Gulf Stream for an 8 years period.

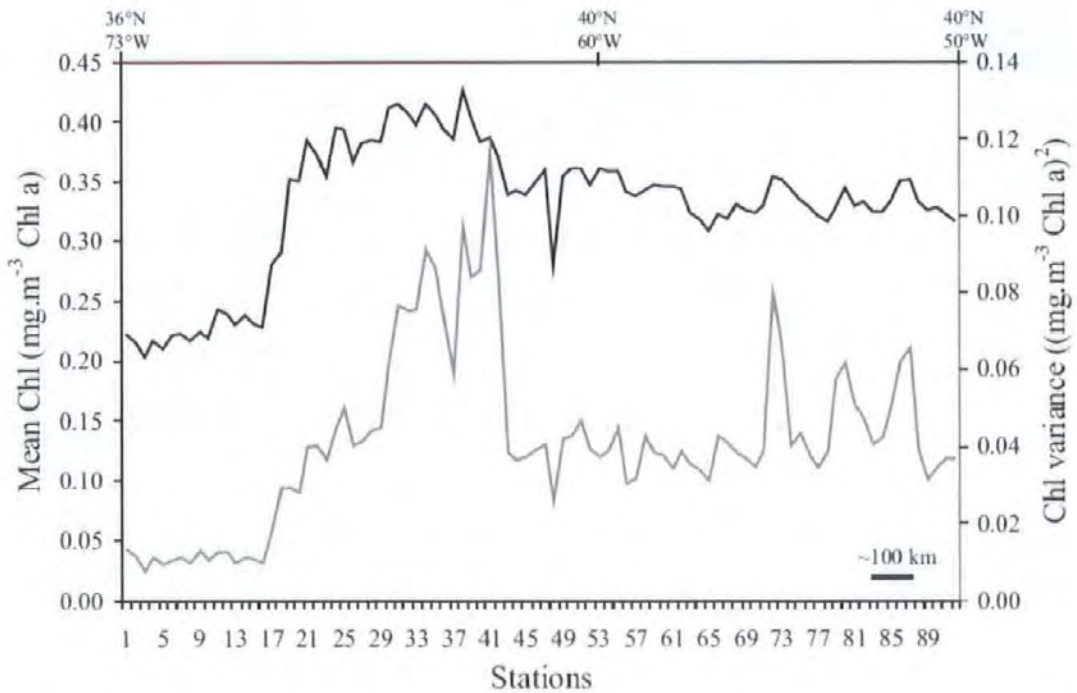


Figure 6.7. Mean of SeaWiFS Chl a ($\text{mg}\cdot\text{m}^{-3}$; black) and variance (seasonal cycle removed) of SeaWiFS Chl a ($[(\text{mg}\cdot\text{m}^{-3})^2]$; grey) along the route of the Gulf Stream for a 5 years period.

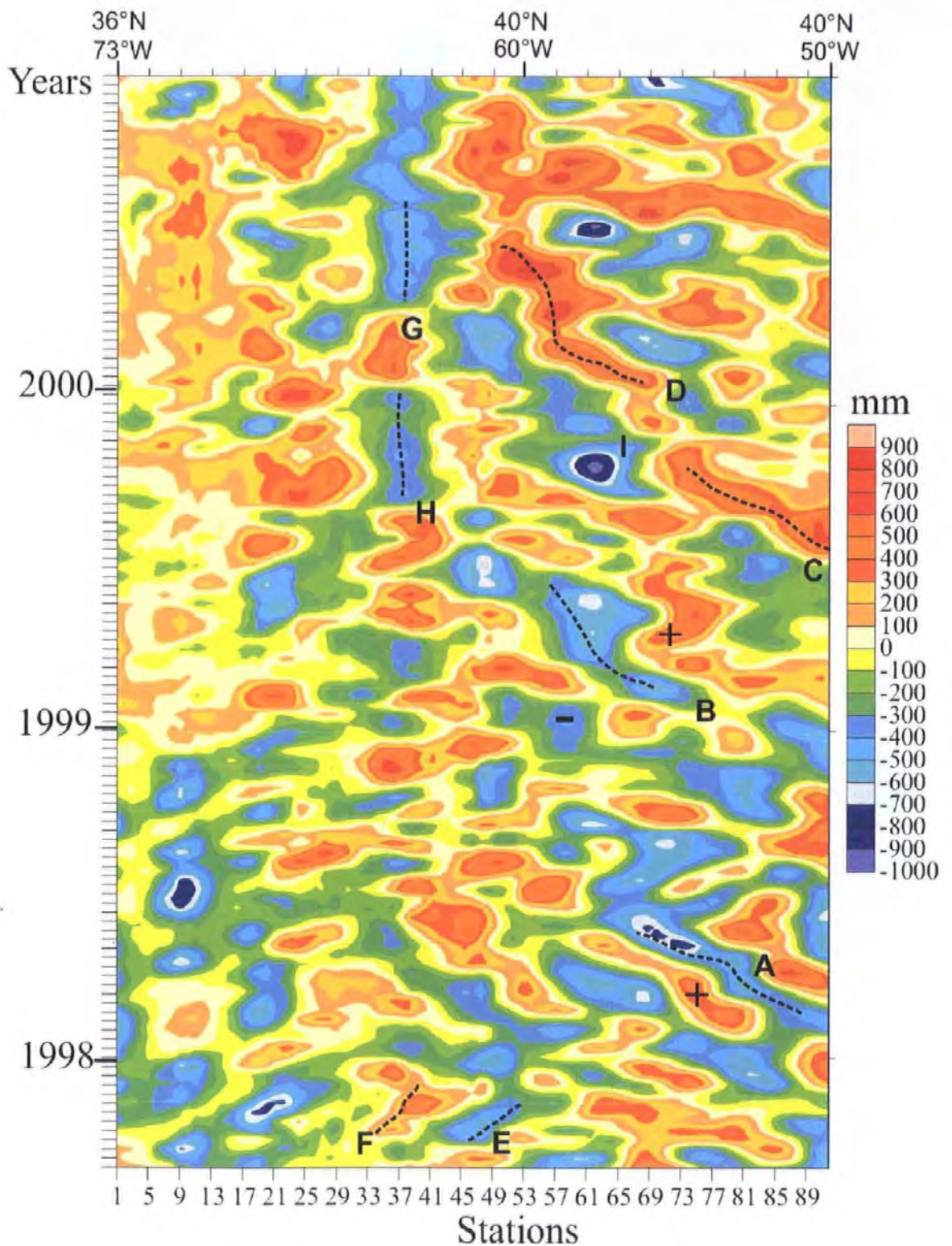


Figure 6.8. Hovmöller diagram of SLA residuals along the route of the Gulf Stream between September 1997 and December 2000. The altimeter signal is the SLA (mm) with the annual signal removed. Anticyclonic (C, D and F) and cyclonic (A, B, E, G, H and I) eddies have been followed in time and space. Negative sign indicates position of a low SLA associated with elevated Chl *a* anomaly (+ in Fig. 6.10). Positive sign indicates position of a high SLA associated with lower Chl *a* anomaly (- in Fig. 6.10).

The variance signal obtained for SLA shows high fluctuations with an average spatial scale of ~ 260 km along the route and a mean variance of $\overline{\mathcal{N}_{SLA}^2} \pm \sigma = 1030 \pm 450 \text{ cm}^2$ (Fig. 6.6). The maximum variance of $\sim 1600 \text{ cm}^2$ corresponds to a root mean squared fluctuation of sea level of $\sim \pm 40$ cm on the Gulf Stream axis. The SLA variance spatial scale is not reflected in the SeaWiFS Chl *a* structure (Fig. 6.7) and if not due to sub-sampling in space and time (see Le Traon *et al.*, 1998), then the minimum values represent a regular pattern of nodes (where the cross axis component of current may increase) or a meander scale extending 1000 km from near Cape Hatteras. To seek a relationship between SeaWiFS Chl *a* structure and SLA variations in the absence of any variance correspondence it will be necessary to take account of phase (*i.e.* time) using the Hovmöller diagrams.

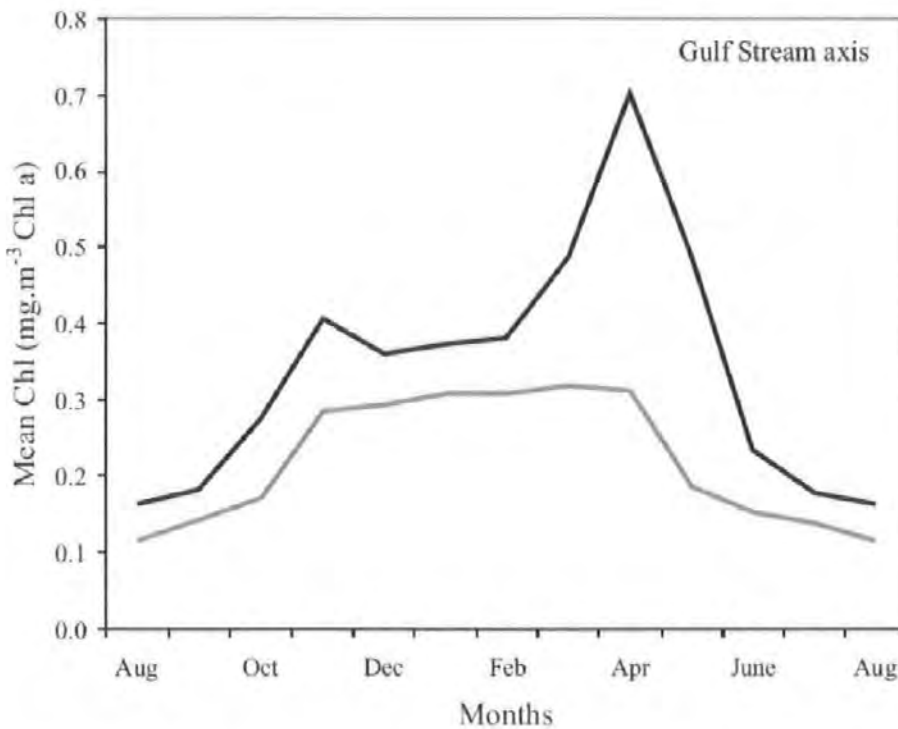


Figure 6.9. SeaWiFS Chl *a* (mg.m^{-3}) seasonal cycle (determined with 5 years of data) along the Gulf Stream route for stations 1-17 (grey) and for stations 18-92 (black).

6.B.3.c. Propagation of eddies over the study period

The SLA residuals have the local annual component removed and the mean value at a point is zero. Intense mesoscale activity, warm core rings (yellow/white) and cold core rings (blue), can be identified along the route of the Gulf Stream (Fig. 6.8). The propagation of these rings over time varies according to their location. Cyclonic (Fig. 6.8, A and B) and anticyclonic (C and D)

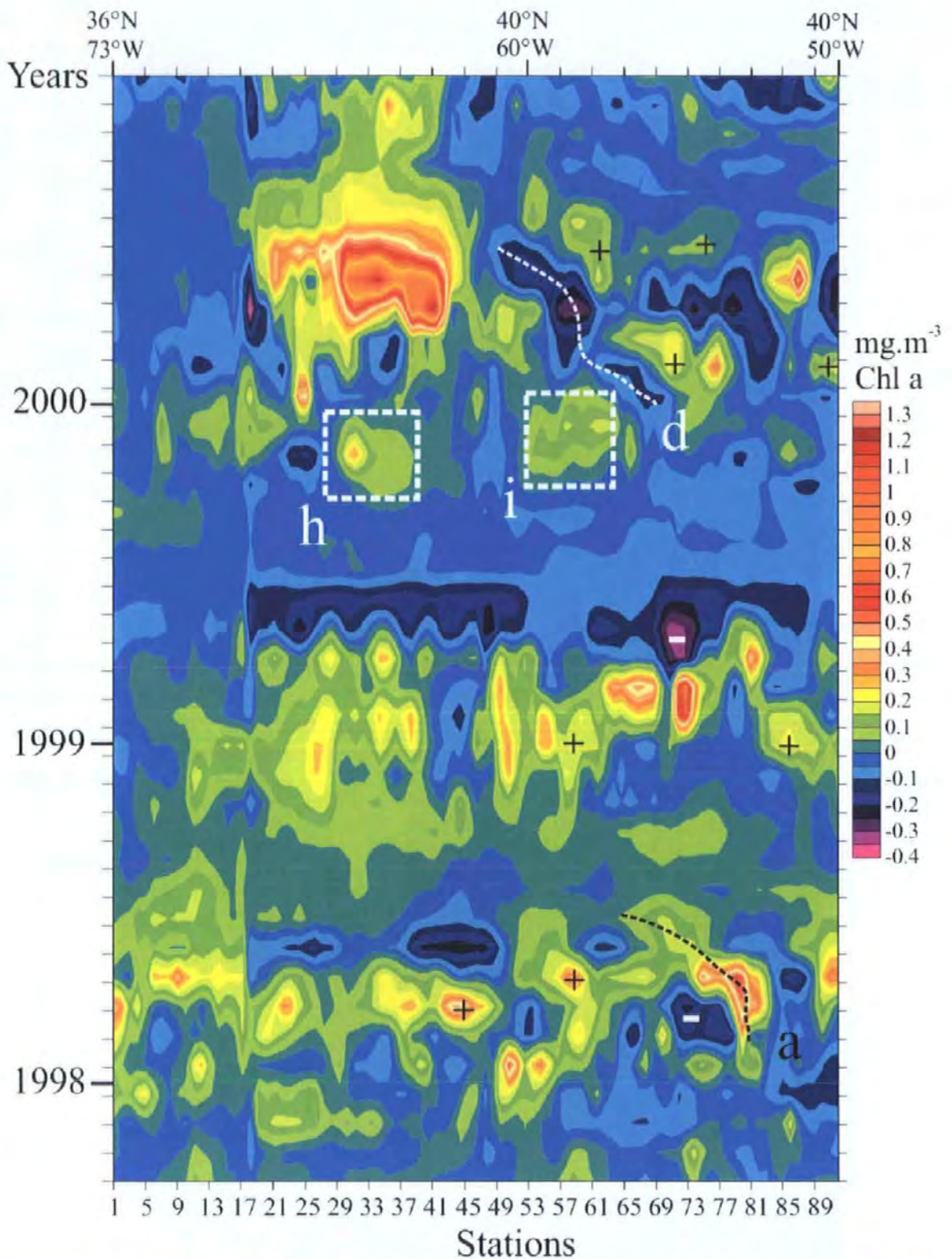


Figure 6.10. Hovmöller diagram of SeaWiFS Chl *a* residuals along the route of the Gulf Stream between September 1997 and December 2000. The Chl *a* signal is the SeaWiFS Chl *a* ($\text{mg}\cdot\text{m}^{-3}$) with the seasonal cycle removed. a, h and i (high Chl *a*) correspond to cyclonic eddies (A, H and I, Fig. 6.8) and d (low Chl *a*) corresponds to an anticyclonic eddy (D, Fig. 6.8). Positive sign indicates position of elevated Chl *a* anomaly associated with low SLA (- in Fig. 6.8). Negative sign indicates position of lower Chl *a* anomaly associated with high SLA (+ in Fig. 6.8).

eddies moving upstream in the path of the Gulf Stream have respectively an average speed between 3.3 – 5.2 km.day⁻¹ and 2.4 – 4.8 km.day⁻¹. Cyclonic (E) and anticyclonic (F) eddies moving downstream along the axis of the Gulf Stream have an average speed of 3.5 km.day⁻¹ and 2.6 km.day⁻¹ respectively. Some eddies (G and H) do not move over time. Other eddies leave the path of the Gulf Stream; anticyclonic eddies were observed to have a westward speed of 3.8 km.day⁻¹ and cyclonic eddies had westward speed of 4.5 km.day⁻¹.

A scale (L) for eddies or rings on the Gulf Stream axis was estimated by measuring the separation distance between positive or negative anomalies along the eastern half of the route where the anomaly structures were more marked. A separation, or anomaly wavelength, was determined as $2L = 440 \pm 65$ km from Figure 6.8, but extended for an 8 year period.

6.B.3.d. Comparison of SLA and SeaWiFS Chl *a* structures along the Gulf Stream route

SeaWiFS structure in space and time may be masked by a dominant seasonal cycle so the SeaWiFS anomalies or residuals are defined as differences from the mean seasonal cycle. These seasonal cycles obtained for stations 1 to 17 and stations 18 to 92 are shown in Figure 6.9. For stations 1 to 17 the bloom occurs from November until April, reflecting nutrient limitation in Subtropical Water, with a maximum value in March (0.31 mg.m⁻³ Chl *a*) and a minimum value in August (0.12 mg.m⁻³ Chl *a*). These results are typical of the Mid-Atlantic Bight water masses that have a simple annual cycle in chlorophyll concentration consisting of a broad peak during winter and minimum concentrations during summer (Yoder *et al.* 2001). For stations 18 to 92, two blooms can be observed, the first in April (0.70 mg.m⁻³ Chl *a*) and the second in November (0.41 mg.m⁻³ Chl *a*); the minimum occurs in August with a value of 0.16 mg.m⁻³ Chl *a*. The spring bloom might result from increased light levels and the autumn bloom might be a response to nutrient availability due to increased vertical mixing and seasonal thermocline erosion.

Removing the mean SeaWiFS seasonal cycle for stations 1-17 from these stations and, similarly, mean SeaWiFS seasonal cycle for stations 18-92 from this set of stations gives the anomaly time series, or SeaWiFS residuals, along the Gulf Stream route (Fig. 6.10).

There is a significant overall inverse relationship between SeaWiFS Chl *a* (Fig. 6.10) and SLA residuals (Fig. 6.8) ($\rho_s = -0.34$, $p < 0.001$). Warm core (anticyclonic) rings generally correspond

to areas of low Chl *a* concentration. For example, the anticyclonic eddy marked D (Fig. 6.8) corresponds to the low Chl *a* pattern marked d (Fig. 6.10). Cold core (cyclonic) rings generally correspond to high Chl *a* concentration structure; the cyclonic eddy marked A (Fig. 6.8) corresponds to the high level Chl *a* pattern marked a (Fig. 6.10). Other lower SLA residuals (marked – in Fig. 6.8) are associated with higher Chl *a* values (marked + in Fig. 6.10). The linear regression equation between Chl *a* ($\text{mg}\cdot\text{m}^{-3}$) and SLA (cm) is :

$$\text{Chl}a = -0.0017 (\text{sla}) + 0.0167$$

When the relationship between SeaWiFS Chl *a* and SLA residuals is analysed for the two different water masses sampled along the route, a higher correlation is found for the Subtropical Water, for stations 1 and 17 ($\rho_r = -0.55$, $p < 0.001$; Fig. 6.11), than for the other part of the route, *i.e.* stations 18 to 92 ($\rho_r = -0.41$, $p < 0.001$; Fig. 6.11). Values also vary for different months in both water regions (Fig. 6.12). Maximum negative correlation for stations 18 and 92, occurred in May ($\rho_r = -0.66$) when the seasonal values are falling, and in August ($\rho_r = -0.61$) when the minimum levels occur. In the Subtropical Water (stations 1-17), a maximum negative value occurred in February with $\rho_r = -0.74$.

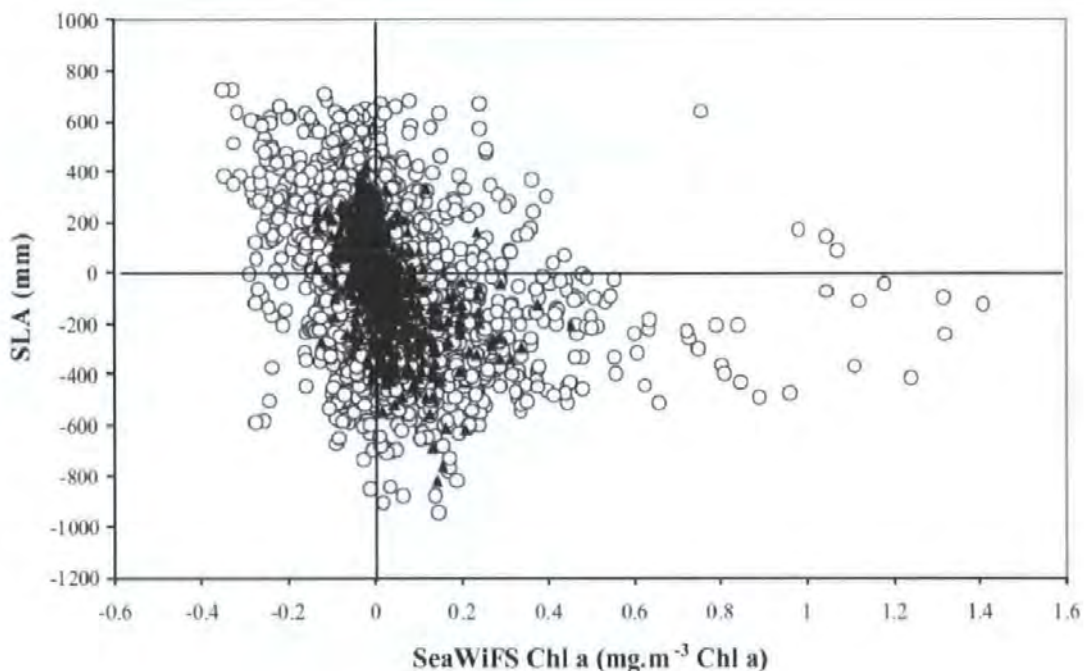


Figure 6.11. Correlation between SeaWiFS Chl *a* and SLA residuals in the different water masses sampled along the route. Black triangles represent stations 1–17 and stations 18–92 are in white dots.

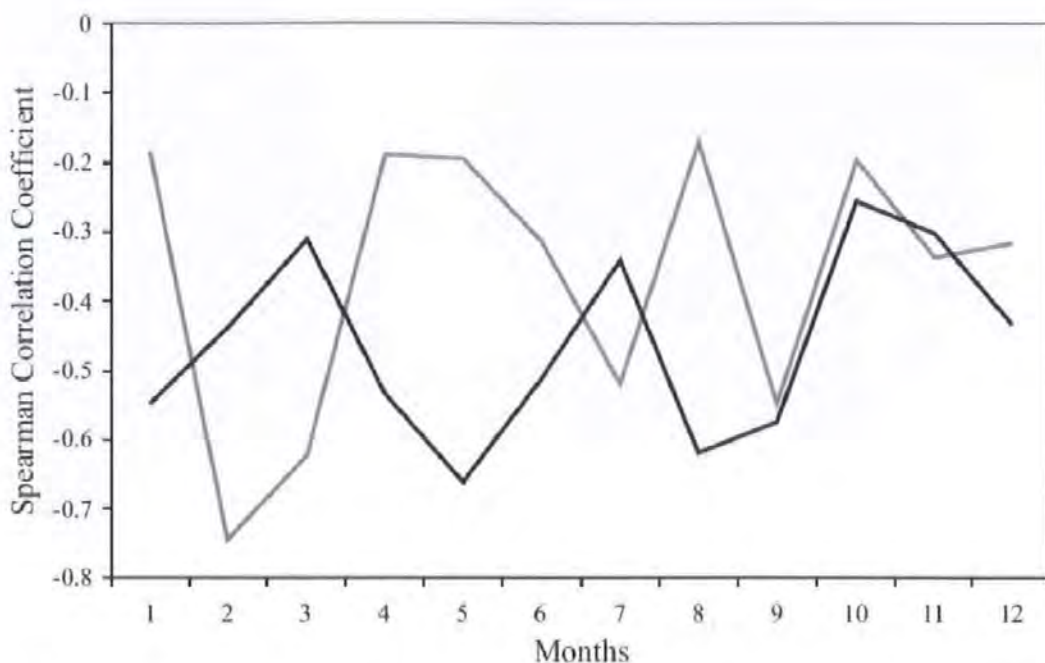


Figure 6.12. Monthly correlation coefficient between SeaWiFS Chl *a* anomalies and SLA residuals in the different water masses sampled along the route. The results for stations 1–17 are in grey and in black for stations 18–92.

The overall correlation coefficient, $\rho_s = -0.34$ ($p < 0.05$), shows that the chlorophyll scale or anomaly wavelength along the Gulf Stream axis matches the separation scale between SLA residuals or eddies of the same sign ($2L = 440 \pm 65$ km). However, the SeaWiFS structure (Fig. 6.10) was too broken or fragmented for an estimate of scale along the Gulf Stream axis. Instead, a wavelength value was determined from monthly SeaWiFS concentration maps for occasions when a repeating concentration structure was evident along the Gulf Stream route. This method gave an independent value of $2L = 460 \pm 50$ km, based on 17 monthly occurrences when there was a tendency for a repeating structure or oscillation wavelength along the Gulf Stream route (see Fig. 6.13A, for example).

6.B.3.e. Advection of Chlorophyll structure by eddies

In the central region of an eddy, the currents move with the eddy and so turn the chlorophyll structure at a near constant radius within the eddy. For external regions, chlorophyll structure can be moved between eddies and so is mixed from regions of higher concentration. For eddy

currents, to show a significant redistribution of a phytoplankton bloom, the eddy swirl currents must be able to advect phytoplankton concentrations at rates comparable or greater than the propagation rates of concentration structures due to phytoplankton growth dynamics.

The velocity of tangential flow due to eddies can be determined by applying the geostrophic relation to maps of SLA (e.g. Figs. 6.4 and 6.13.B):

$$fv = -g \frac{\nabla p}{\rho} \quad (2)$$

Where f is the Coriolis parameter, v is the horizontal tangential swirl velocity, ∇p is the horizontal pressure gradient and ρ is the density of seawater. Applying (1) to eddies C/G or G/D (see Fig. 6.13.B) gives maximum speeds between eddies of

$$v = \frac{g}{f} \frac{dn}{dx} \sim 1 \text{ m.s}^{-1} \quad (3)$$

where g is the gravitational acceleration, dn is the elevation change over a distance change dx .

In the Gulf Stream region, chlorophyll levels are elevated towards the slope and shelf region and eddy currents could produce curved chlorophyll plume structures of a few hundred kilometres in a several days.

For eddies, to be able to produce the chlorophyll structures a, b, c, d and e along the spring bloom frontal boundary (see Fig. 6.3), it is necessary to show that the eddy current structure can result in southward flow speeds that are as fast, or faster, than the northward propagation speed of the chlorophyll structure. Using the geostrophic relation (2), the maximum flow between the cyclonic eddy marked with a white star in Figure 6.4 and the adjacent anticyclonic eddies (marked with black stars, Fig. 6.4) is $\sim 20 \text{ cm.s}^{-1}$ southwestward and $\sim 25 \text{ cm.s}^{-1}$ northeastward. These values can be compared with a direct southward flow measurement of $\sim 18 \text{ cm.s}^{-1}$ and a northward flow of $\sim 35 \text{ cm.s}^{-1}$ derived from the track of the Argos buoy in the same cyclonic eddy in April 1999. Campbell and Aarup (1992) show that the bloom boundary moves seasonally almost sinusoidally by 11° (30°N - 41°N) at a latitude near 35°N . This gives a maximum northward progression of $(2\pi \times 5.5)/12$ degrees of latitude per month or 12 cm.s^{-1} . Hence, southward eddy speeds of $\sim 12 \text{ cm.s}^{-1}$ could locally stall or arrest the northward progression. The observed southward flow measurements are greater than 12 cm.s^{-1} and the southward component of the flow between eddy pairs account for the scale and structure of the SeaWiFS chlorophyll features a, b, c, d and e observed in April 1999 near 35°N .

6.B.4. Discussion

In open ocean conditions of the North Atlantic (32°N-40°N, 30°W-60°W), SeaWiFS chlorophyll (Chl *a*) concentration is redistributed at the eddy scale by the eddy surface swirl currents. Estimates of eddy surface currents derived from altimeter sea level anomalies (SLA), and direct measurement from an ARGOS buoy, show that chlorophyll structure may be introduced between eddies of opposite sign. The zonal scale for chlorophyll perturbations was determined at ~ 430 km (Fig. 6.3) in April near 35°N. The mixing effect of eddies redistributing chlorophyll concentrations will be most marked where there is a gradient in concentration, as for example for the zonal structure of the spring bloom in the North Atlantic in April. Structure with a similar scale ($\sim 480 \pm 40$ km) was observed for the productive period (November to May) when levels of chlorophyll are elevated.

The Gulf Stream represents the boundary between Subtropical Water (*i.e.* with high dynamic heights and lower Chl *a* levels) and Slope and Subpolar Waters (*i.e.* with low dynamic heights and elevated Chl *a* levels) and sea elevation changes or SLA variance levels are a maximum as eddies and meanders cross the mean route. Gulf Stream meanders and rings carry different water types across the mean Gulf Stream position. Bower and Rossby (1989) related meander circulation to cross-frontal exchange with rings providing a mechanism for exchange of both nutrients and biota among Slope and Sargasso Sea Water (Gould & Fryxell 1988). In this study, a wavelength scale from one cold ring to another along the axis of the Gulf Stream was determined as $\sim 440 \pm 65$ km, giving a ring scale of ~ 220 km.

The rings have shown two distinct types of movement. Firstly, both anticyclonic and cyclonic rings have been observed moving upstream. Ring-population studies by Bisagni (1976), Lai and Richardson (1977), Haliwell and Mooers (1979), Richardson (1983) and Brown *et al.* (1986) have shown that several warm-core rings can be found moving westward in the Slope Water with speeds between 2 and 15 cm.s⁻¹. Cold core rings well separated from the Gulf Stream generally move westward at about 5 cm.s⁻¹ (The Ring Group 1981). Speeds measured in this study for warm-core and cold-core rings are included within the range of speeds recorded in former studies. Secondly, both anticyclonic and cyclonic rings have been observed moving downstream. Rings can be partially reattached to and interacts with the Gulf Stream, their movement is then parallel to, and with, the Gulf Stream (The Ring Group 1981).

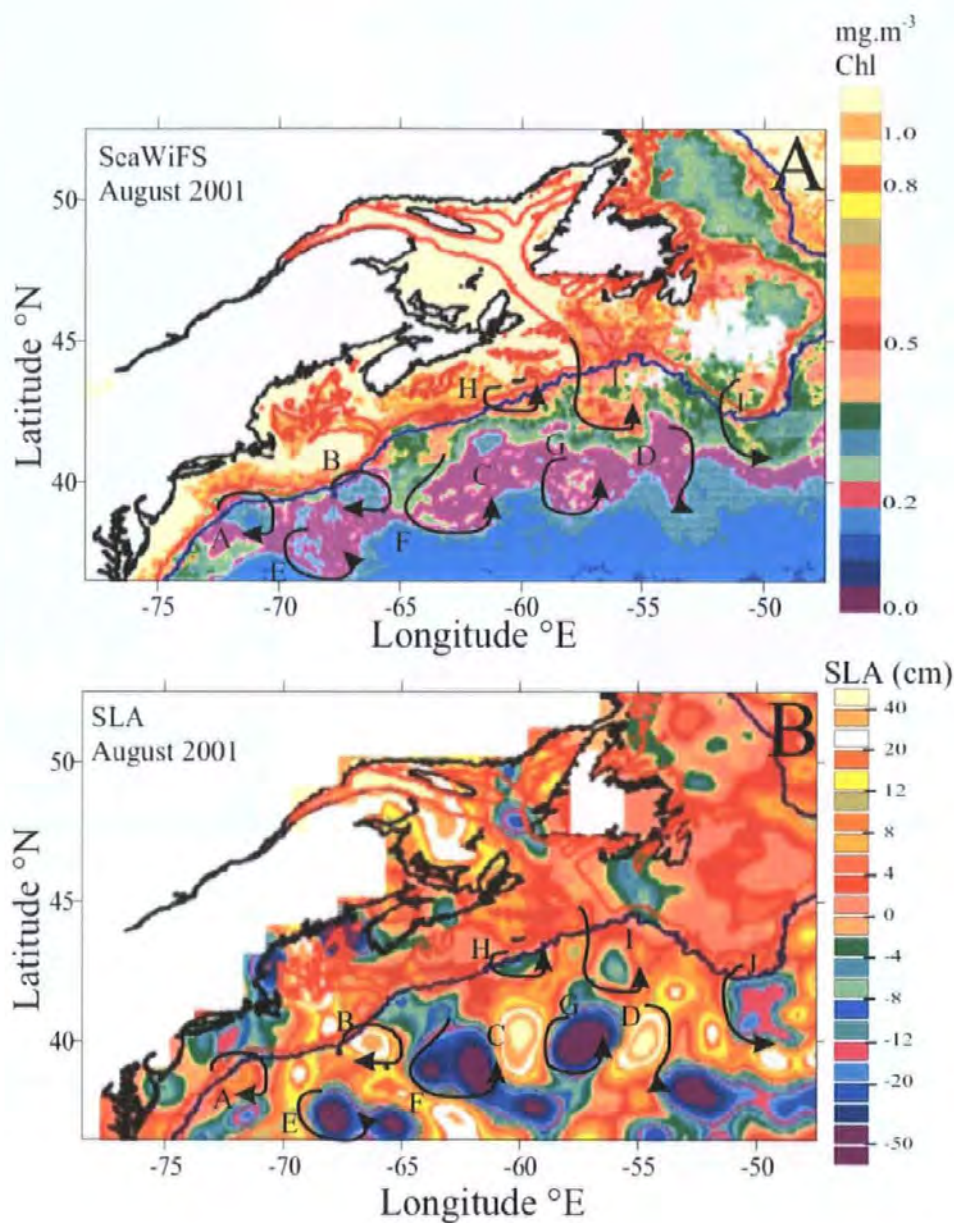


Figure 6.13. Examples of (A) SeaWiFS Chl *a* and (B) SLA structures for August 2001. Warm-core rings are labelled A, B, C, D and cold core rings E, F, G and weaker negative anomalies H, I, J. The arrows represent the currents associated with eddy structure and the sea level slopes between eddies C, G, D have been used to determine the velocity of the flow between the eddies

It is shown that SLA residuals are correlated negatively with chlorophyll residuals with a monthly correlation coefficient $-0.7 < \rho_s < -0.2$. In general, the positive elevation anomalies are low in chlorophyll with a core of Subtropical Water. Seven anticyclones can be seen in Figure 6.4; all these positive eddies along the north of the Gulf Stream axis have low

chlorophyll concentration (labelled A-G, Fig. 6.3). Anticyclonic eddies are associated with depressed isotherms and low levels of inorganic nutrients. On the Gulf Stream axis, lower chlorophyll concentration (marked with – sign, Fig. 6.3) is associated with positive SLA or anticyclonic structure (marked with + sign, Fig. 6.4). Cyclonic eddies have higher levels of inorganic nutrients, the isotherms are domed upwards and localised upwelling may introduce new nutrients into the euphotic zone, which could cause higher primary production in their core (Hitchcock *et al.* 1993, Aristegui *et al.* 1997). The cold core rings are thus generally higher in Chl *a* and cyclonic rings marked 1, 2, 3 along the Gulf Stream route (Fig. 6.4) have elevated chlorophyll concentrations (Fig. 6.3).

The eddy currents may also redistribute surface Chl *a* levels, drawing out plumes of locally increased Chl *a* from regions of higher Chl *a*. This effect can be seen in some SLA maps and SeaWiFS monthly composites: August 2001 (Fig. 6.13) for example, where the eddy current structure draws out plumes (Fig. 6.13, near anticyclonic ring D, or around cyclone F, for example) and in the Hovmöller diagrams (Figs. 6.8 and 10). Between November and October 1999, from stations 33 to 41 there is a marked negative anomaly (marked H, Fig. 6.8). Near the same area and for the same period, a SeaWiFS positive anomaly can be observed in Figure 6.10 (labelled h). However, the SeaWiFS positive anomaly is displaced to the west of the negative SLA anomaly and not centred on it with a maximum near station 31 and as such will tend to reduce the correlation between anomalies. Other decorrelating structures, like the more marked spring bloom conditions extending to the Gulf Stream from the shelf and slope regions in May 2000 (Fig. 6.10), are independent of Gulf Stream conditions. Overall, the correlation coefficient between SeaWiFS Chl *a* structure and SLA residuals along the selected Gulf Stream axis was $\rho_r = -0.34$ and the SeaWiFS Chl *a* spatial variation, or meander wavelength, was $\sim 460 \pm 50$ km, or equal to the altimeter SLA separation determined between cold core or warm core rings.

6.C. Impact of climate and mesoscale physical processes on phytoplankton (Continuous Plankton Recorder and SeaWiFS) along the E-route

6.C.1. Introduction

This section assesses the impact of the LSW changing flow along the Scotian Shelf and the influence of Gulf Stream rings along Georges Bank. A specific CPR route (E-route; between Norfolk (Virginia, USA; 39°N, 71°W) and Argentia (Newfoundland; 47°N, 54°W)) has then been used to investigate (i) the consistency between PCI and SeaWiFS Chl *a* measurements in this area, (ii) the fluctuations of phytoplankton biomass and its geographical distribution, (iii) the potential links between PCI, SST and NAO, and (iv) the relation between phytoplankton and altimetry (i.e. Sea Level Anomalies (SLA) and eddies) over the period 1995-1998.

6.C.2. Methods and data

The visual estimation of the total phytoplankton biomass, known as the Phytoplankton Colour Index (PCI), was determined for each of 15 stations along the E-route, corresponding to the stations most continuously sampled over the period of study (Fig. 6.14). Hovmöller diagrams of PCI were used to compare PCI space-time structure with those observed from space (i.e. Sea Level Anomaly and Sea Surface Temperature (SST)).

6.C.2.a. Sea level anomaly

Fourier analysis and filtering of SLA in time has been used (i) to determine the periods of dominant structure (i.e. annual signal) along the CPR route and (ii) to remove the annual signal and any residual mean elevation (which should be zero). Being in a shelf break area, tidal aliasing due to the semi-diurnal tide was also removed through Fourier filtering. SLA has already been shown to allow the tracking of propagating features (Sinha *et al.* 2004, Leterme & Pingree, in press). These data have then been used to estimate the presence and nature of anomalies in the area of study between January 1995 and December 1998. Elevation and depression of the sea surface are plotted on a Hovmöller diagram (i.e. changes of property in space and time).

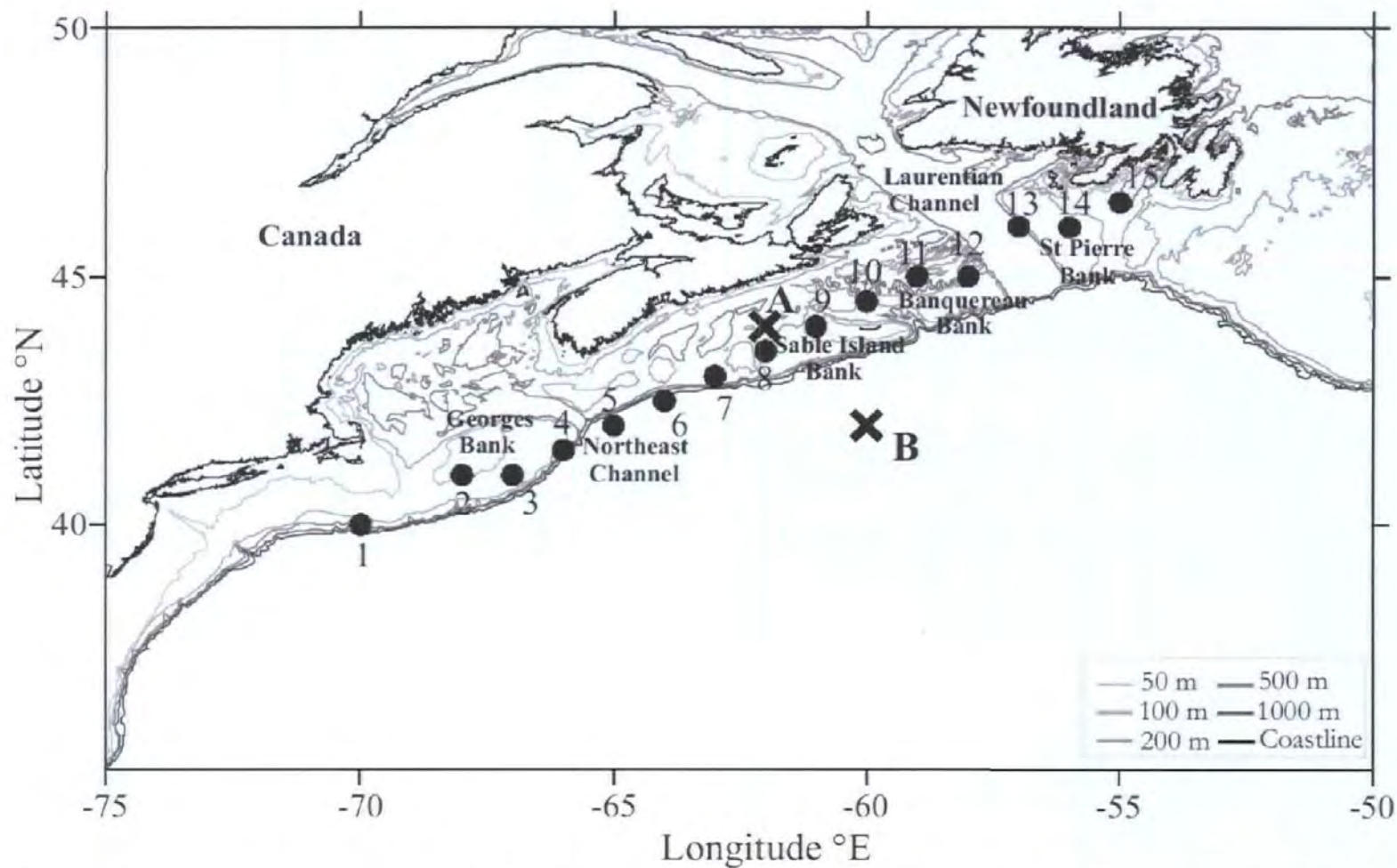


Figure 6.14. Bottom topography of the study area and the position of the 15 stations sampled along the CPR route (black dots). Stations A and B have been chosen as representative of the shelf and the open ocean, respectively, in order to determine the fluctuations in geostrophic flow along the Shelf Break.

6.C.2.b. SeaWiFS Chlorophyll *a*

SeaWiFS Chl *a* data were spatially averaged over ± 25 km in both latitude and longitude. Missing data due to cloud coverage have been interpolated (see chap. 6.B.2). The SeaWiFS chlorophyll *a* concentration data allow the comparison of the structure and seasonality of phytoplankton along the E-route in the overlapping PCI time window between September 1997 and December 1998.

6.C.2.c. Climatic indices

Several indices have been developed to quantify the state of the North Atlantic Oscillation, but the most widely used is Hurrell's NAO index (Hurrell 1995a). Monthly indices of the NAO, based on the difference of normalised sea level pressures between Ponta Delgada, Azores and Stykkisholmur/Reykjavik, Iceland, are available since 1865. In order to take into account the monthly variability, monthly-time series of NAO have been used as a climatic index. The Sea Surface Temperature (SST; HadISST 1.1 from the British Atmospheric Data Centred, data were used to provide additional climatic information likely to influence phytoplankton growth and abundance.

6.C.2.c. Data analyses

Trends in monthly time series of PCI were examined at each station by calculating Kendall's coefficient of rank correlation, τ , between the series and the time in months in order to detect the presence of a linear trend (Kendall & Stuart 1966). The relationship between phytoplankton and climate indices was tested through Spearman rank correlation analysis performed at each station between monthly time series of PCI and (i) the NAO and (ii) the Sea Surface Temperature. As the environmental changes induced by the NAO do not occur instantaneously, the possibility of a lagged response from the phytoplankton has been taken into account and conducted the correlations between PCI and NAO with a lag of zero to 3 months. However, as the response of phytoplankton to SST fluctuations is quick, the correlation between SST and PCI was not performed at different lags.

To detect changes, intensity and duration of any changes in the value of PCI, the cumulative sums method (Ibañez *et al.* 1993) was used. It consists of subtracting a reference value (here the

mean of the PCI anomalies time series at each station) from the data; these anomalies are then successively added, forming a cumulative function. This analysis was performed on the time series of monthly anomalies of PCI at each station along the route. The cumulative sum method was also used on the altimetry and SST anomaly data. This method is useful for data where high frequency variance may obscure longer-term trends. The relationship between PCI and SeaWiFS was also tested through Spearman rank correlation analysis performed at each station between (i) original data (4 years time series) and (ii) mean seasonal cycles (12 months time series) of PCI and SeaWiFS Chl *a*. The structure (i.e. mean, amplitude and phase) of PCI and SeaWiFS Chl *a* seasonal cycles (12 month time series) was compared.

6.C.3. Results

6.C.3.a. Comparison of temporal structures of two phytoplankton estimators

Seasonal cycles of SeaWiFS and PCI (Fig. 6.15) identified distinct regimes for Georges Bank (stations 2 and 3), Shelf Break and Sable Island (stations 6, 7, 8 and 9) and St Pierre Bank (stations 13 and 14). A decrease (non-significant at 5% significance level) in SeaWiFS Chl *a* is observed along the E-route towards Newfoundland. Along the CPR route, monthly time-series of PCI and SeaWiFS chlorophyll *a* showed significant correlation in only 20% of the stations, with a maximum positive correlation of 0.69 (Table 6.1). In contrast, significant relationships between seasonal cycles of PCI and SeaWiFS Chl *a* were observed in 53% of the stations along the CPR route (Table 6.1, Fig. 6.15), with a maximum positive correlation of 0.92 (Table 6.1). There is, finally, a significant correlation ($\rho_r = 0.65$, $p < 0.05$) between the averaged seasonal cycles of these two estimators of phytoplankton (Fig. 6.16).

6.C.3.b. Phytoplankton Colour Index and climate indices

No significant trends were observed in PCI time series along the CPR route. Mostly significant inverse relationships occur along the route between the PCI data and SST (Table 6.2). This is consistent with the shift occurring between their seasonal cycles, with a minimum SST in March occurring near the maximum of PCI (i.e. Spring Bloom period). However, no significant relationships were found between PCI residuals and SST residuals. Finally, no correlations were found between PCI and NAO (Table 6.2). However, positive significant correlations were observed between PCI and monthly NAO (with a lag of 2 months) (Table 6.2).

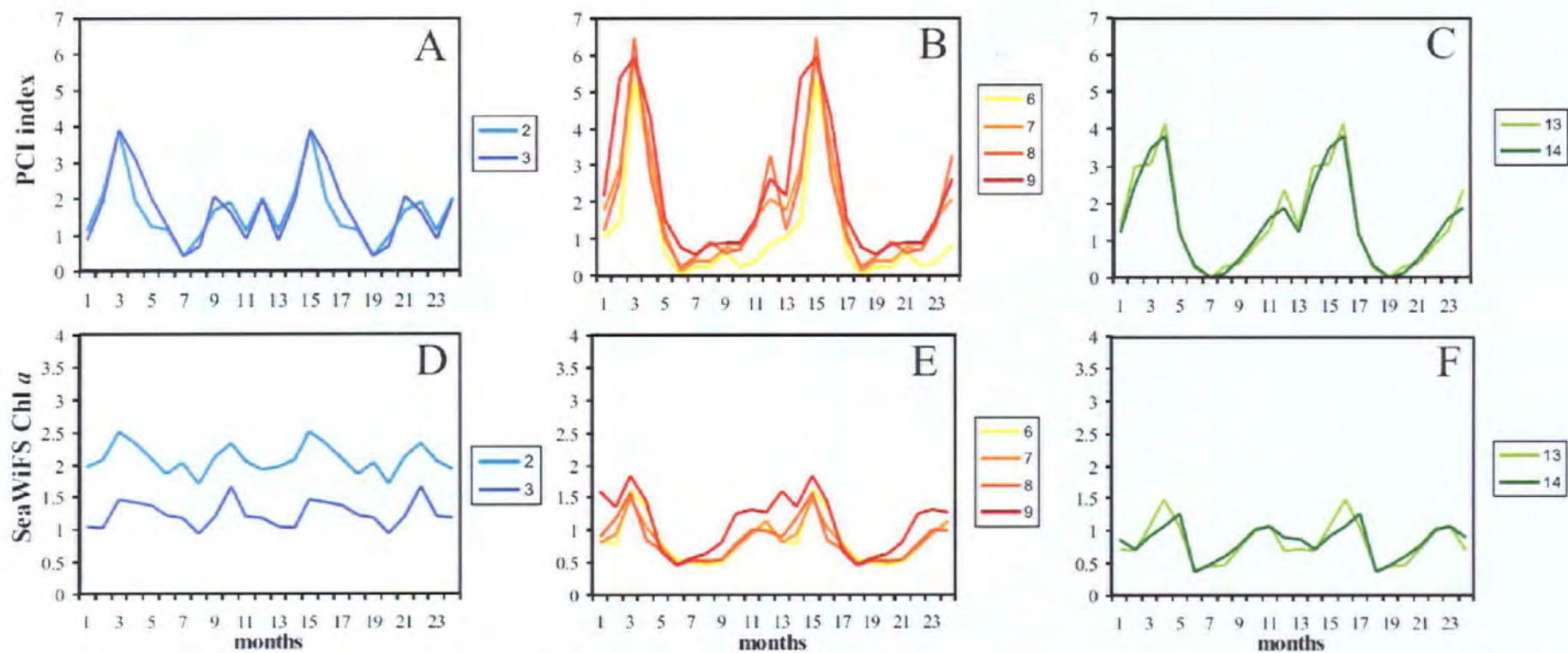


Figure 6.15. Seasonal cycles of Phytoplankton Colour Index (A, B, C) and SeaWiFS chlorophyll *a* ($\text{mg}\cdot\text{m}^{-3}$ Chl *a*; D, E, F) along the CPR route (15 stations). The cycles that were significantly correlated were observed on Georges Bank (stations 2 and 3), Shelf Break (Stations 6 and 7), Sable Island (stations 8 and 9) and St Pierre Bank (stations 13 and 14); see Table 6.C.2.

The spring bloom usually observed between February and May (Riley 1941) was not detected on Georges Bank in 1997, and an unusual autumn bloom was observed in 1996 (Fig. 6.17a). At the other stations along the E-route, the usual bloom was observed but during an extended period of time (November 1996-June 1997). Those changes were also visible on the PCI cumulative sums diagram (Fig. 6.17d). The PCI anomaly cumulative sums analysis revealed different short-term trends in the time series, with a change of slope in winter 1996/1997 for stations 1 to 5. For stations 6 to 10, the cumulative sums of PCI increased from December 1996 until March 1997 and decreased afterwards. Changes were also observed in SST, with negative anomalies observed between June 1996 and June 1997 on the SST Hovmöller diagram (Fig. 6.18c). Conversely, no specific trends were observed for stations 6 to 15. The SST anomalies cumulative sums analysis (Fig. 6.18d) revealed different trends depending on the location along the continental shelf. In stations 1 to 5, the cumulative sums of SST increased until December 1995 and then decreased.

Table 6.1. Spearman correlation analysis between the monthly time series of PCI and SeaWiFS (original data) and between seasonal cycles of PCI and SeaWiFS over the period 1997-1998. *5% significance level.

Stations	Original data	Seasonal cycles
1	0.56*	0.54
2	-0.23	0.58*
3	-0.43	0.58*
4	0.30	0.36
5	0.16	0.52
6	0.03	0.78*
7	0.02	0.92*
8	0.51*	0.86*
9	0.43	0.89*
10	0.41	0.42
11	0.69*	0.33
12	0.22	0.45
13	0.34	0.67*
14	0.37	0.60*
15	0.22	0.37

6.C.3.c. Phytoplankton and mesoscale physical processes

The annual component of altimeter Sea Level Anomaly (SLA) and tidal aliasing (Fig. 6.19b) revealed the alternation between positive and negative SLA with annual periodicity. This corresponds to the rise and fall of the sea surface resulting from the expansion and contraction of the ocean due to seasonal heating and cooling. There was a lag of two months in the

maximum rise and fall of the water level between stations 1 and 15. The amplitude of the annual component is reduced northward along the route where the surface water is cooler.

Table 6.2. Results of Spearman correlation analysis between the monthly time series of PCI and NAO index and between both original and residual (seasonal cycle removed) time series of PCI and SST over the period 1995-1998. *5% significance level.

Stations	monthly PCI-NAO				original data	residual
	no lag	1 month lag	2 months lag	3 months lag	PCI-SST	PCI-SST
1	0.20	0.29*	0.17	-0.09	-0.38*	0.11
2	0.07	0.27	0.34*	0.12	-0.25	0.08
3	-0.18	0.12	0.23	0.14	-0.24	0.07
4	0.08	0.24	0.20	-0.02	-0.21	0.15
5	0.01	0.03	0.15	0.06	-0.39*	0.08
6	0.00	0.25	0.39*	-0.02	-0.50*	0.03
7	0.08	0.25	0.34*	0.10	-0.56*	0.02
8	0.10	0.35*	0.22	-0.04	-0.48*	0.06
9	0.07	0.10	0.17	0.13	-0.59*	-0.02
10	-0.14	0.23	0.36*	0.18	-0.71*	-0.17
11	-0.10	0.23	0.45*	0.11	-0.69*	-0.13
12	0.04	0.23	0.36*	0.19	-0.70*	0.11
13	-0.05	0.22	0.35*	0.13	-0.63*	0.05
14	-0.02	0.22	0.24	0.19	-0.59*	0.01
15	-0.07	0.28	0.20	0.13	-0.67*	0.02

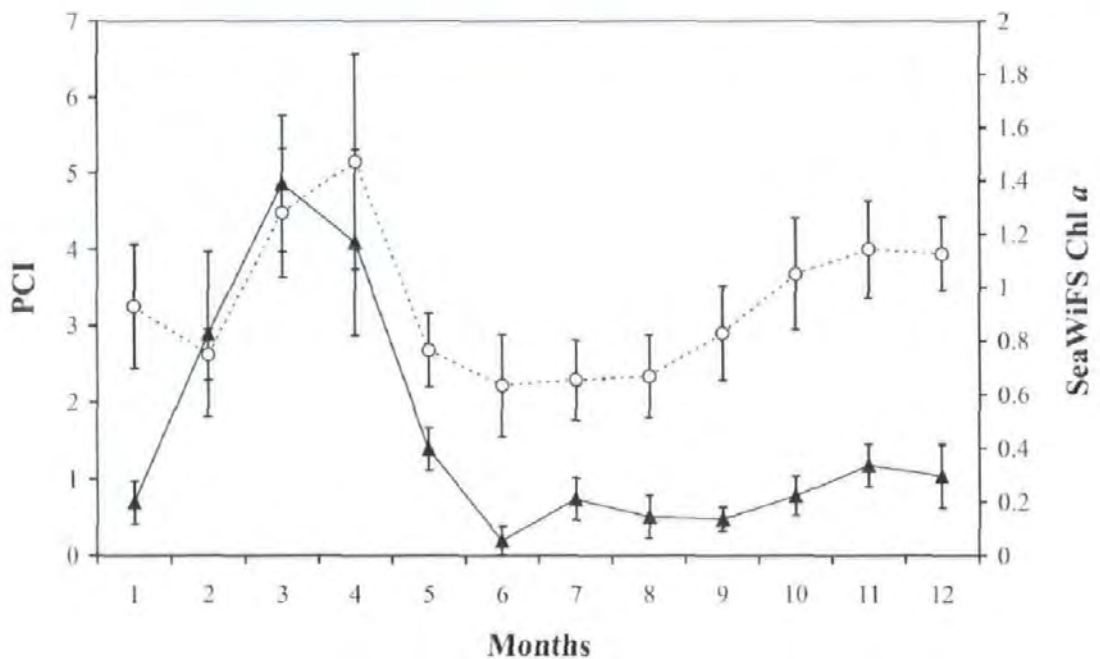


Figure 6.16. Mean seasonal cycles of PCI (black triangles) and SeaWiFS chlorophyll a ($\text{mg}\cdot\text{m}^{-3}$ Chl a ; open dots) over the period 1997-1998 along the CPR route. The error bars are the standard deviation.

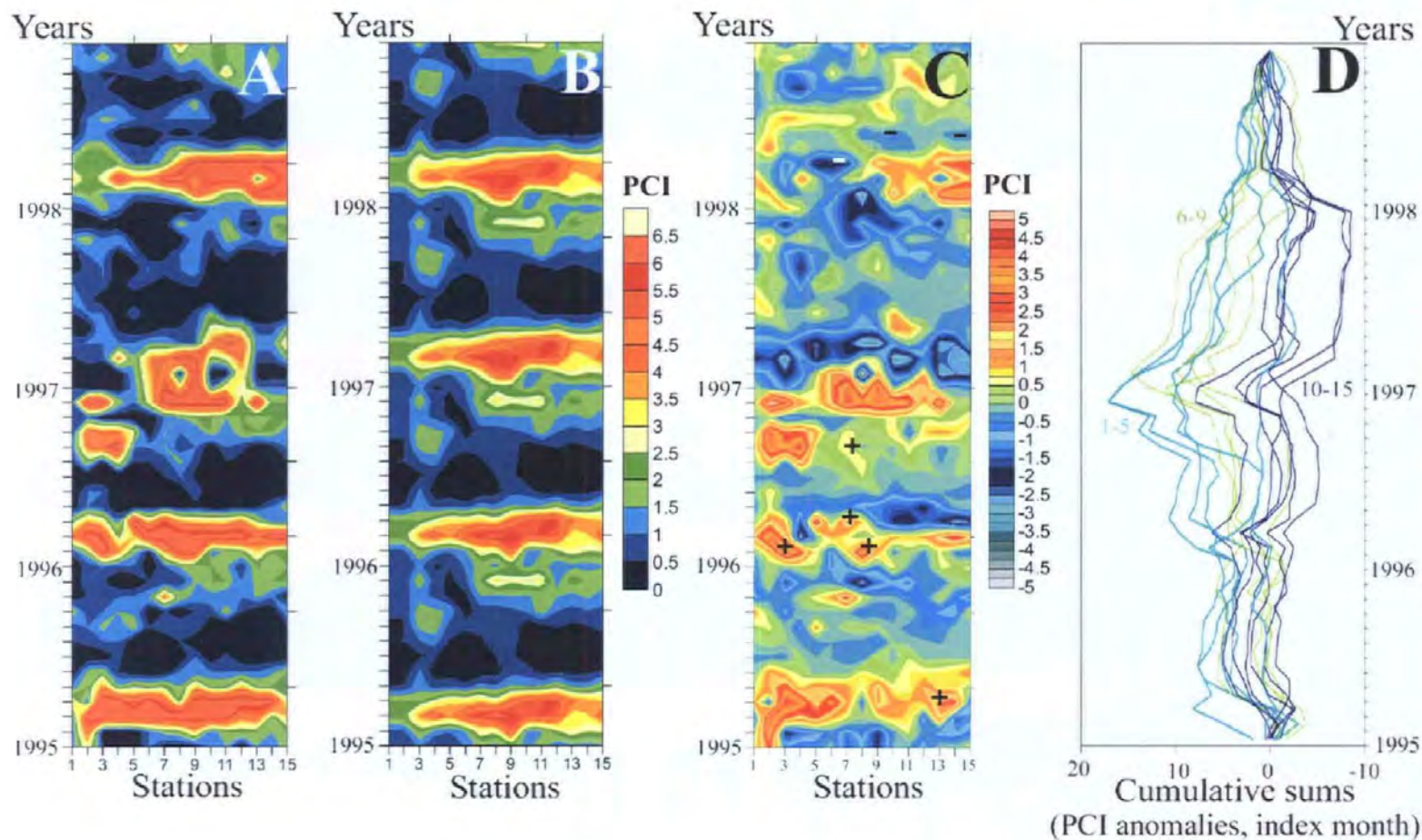


Figure 6.17. Hovmöller diagram of original data (A), seasonal cycle (B) and anomalies after removing the seasonal cycle (C) of Phytoplankton Colour Index (PCI) for the 15 stations sampled on the CPR route between January 1995 and December 1998. Cumulative sum analysis was performed on PCI anomalies for all the stations (D), over the period 1995-1998. Low (high) values of PCI are marked with - (+) sign, corresponding to positive (negative) anomalies marked with + (-) in Fig. 6.19.

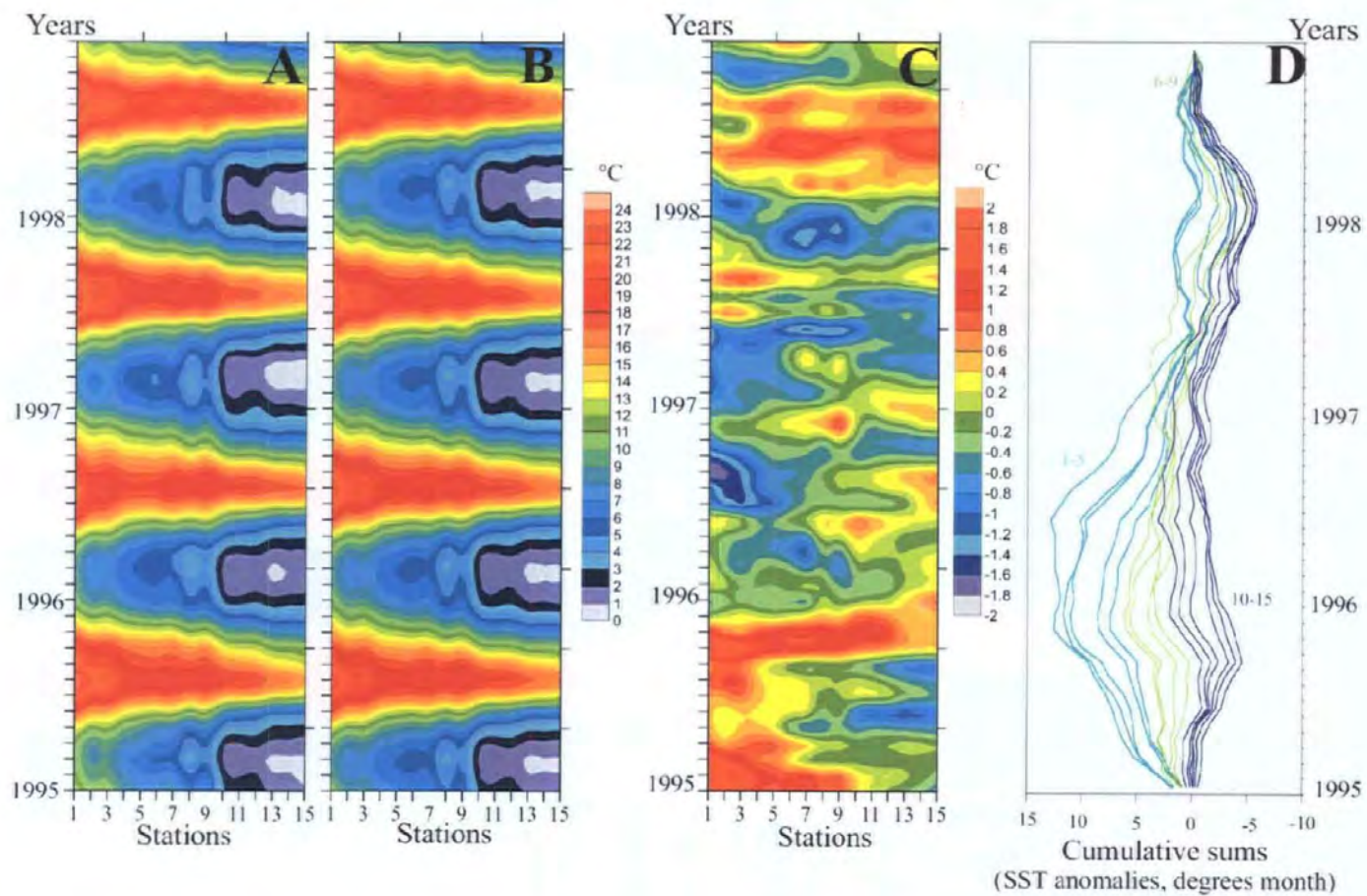


Figure 6.18. Hovmöller diagram of original data (A), seasonal cycle (B) and anomalies after removing the seasonal cycle (C) of Sea Surface Temperature (SST) for the 15 stations sampled on the CPR route between January 1995 and December 1998. Cumulative sum analysis was performed on SST anomalies for all the stations (D), over the period 1995-1998.

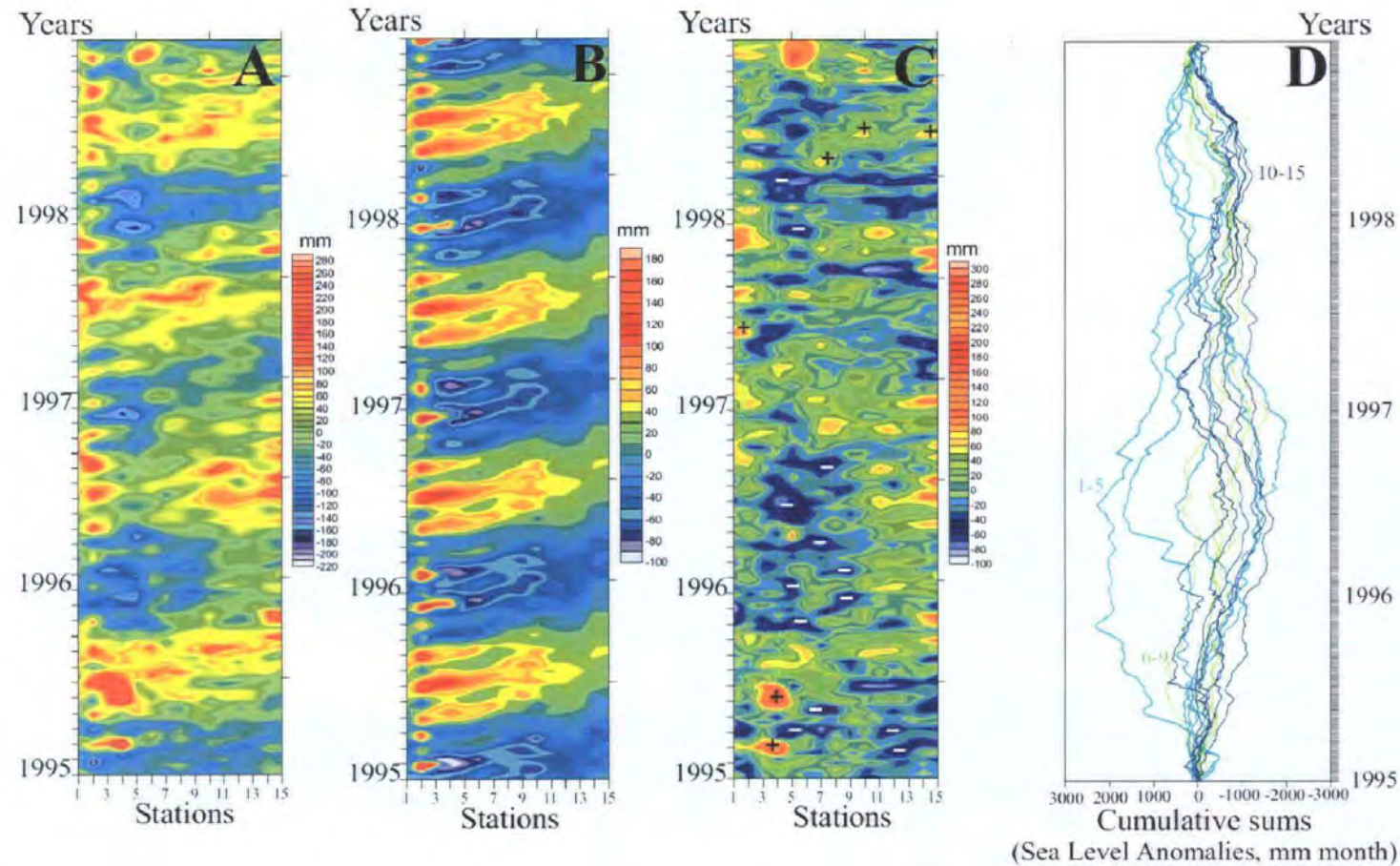


Figure 6.19. Hovmöller diagram of original data (A), seasonal cycle (B) and anomalies after removing the seasonal cycle (C) of Sea Surface Heights (SSH) for the 15 stations sampled on the CPR route between January 1995 and December 1998. Cumulative sum analysis was performed on the residuals of Sea Level Anomalies (SLA) for all the stations (D), over the period 1995-1998. Negative (positive) anomalies of SLA are marked with - (+) sign, corresponding to high (low) values of PCI marked with + (-) in Fig. 6.17.

Positive and negative anomalies have been identified in the SLA residuals on Hovmöller diagram (e.g. marked +/-, Fig. 6.19c). These anomalies can influence the spatial structure of PCI (see first part of this chapter). In particular, PCI anomaly structures corresponding to the SLA residuals structures were identified. Lower/higher SLA residuals (identified respectively by signs - and + in Fig. 6.19c) are associated with higher/lower Chl *a* values (identified respectively by signs - and + in Fig. 6.17c). However, there was no statistically significant correlation between residuals of PCI and SLA for the whole region.

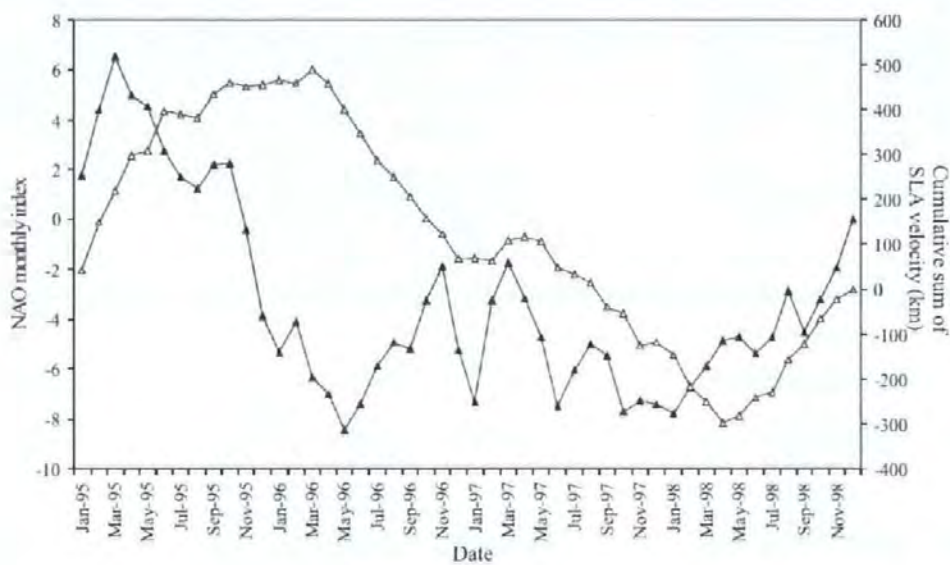


Figure 6.20. Cumulative NAO (index month; black triangles) and cumulative geostrophic current (white triangles) derived from altimeter sea level anomaly (km) over the period 1995-1998.

Changes in geostrophic surface flow can be derived from altimetry data. This was done by measuring the difference in SLA residuals between 2 locations specifically chosen as representative of the shelf area (A; 44°N 62°W) and the open ocean (B; 42°N 60°W; Fig. 6.14) and removing the annual component and tidal aliasing for a 9 years period 1992-2001. Between October 1992 and July 1995, the geostrophic flow moving northeast between the two stations increased by about 1 cm.s⁻¹ (~ 1 km.day⁻¹). Then, after July 1995, the main flow was reduced by about 3 km.day⁻¹ until June 1998. The cumulative sums of geostrophic current (from SLA data effectively giving a distance of travel) was positively correlated with NAO monthly index (Fig. 6.20) ($\rho_t = 0.60$, $p < 0.0001$).

6.C.4. Discussion

6.C.4.a. Seasonal cycles of Phytoplankton Colour Index and SeaWiFS chlorophyll *a*

Along the E-route, a significant relationship has been observed between the seasonal cycles of two estimators of phytoplankton biomass (*i.e.* PCI and SeaWiFS chlorophyll *a*) in 53% of the stations, with a maximum positive correlation of $\rho_s = 0.92$. A similar comparison, based on monthly time series of PCI and SeaWiFS over the period 1997-2002, made for the Central NE Atlantic and the North Sea (*i.e.* 1585 samples), gave a Pearson's correlation coefficient of 0.79 (Raitsos *et al.* 2005). However, based on monthly time series, only 20% of the stations investigated here showed a significant relationship. This strongly suggests that the relationship between PCI and SeaWiFS varies spatially (*i.e.* the average distance between 2 stations along the E-route is 100 km) and that the most part of the observed variability is driven by small-scale processes. Finally, as Raitsos *et al.* (2005) took into account CPR sampling stations located all over the Central NE Atlantic and the North Sea, and did not compare individual stations, they smoothed the above-mentioned spatial variability that could have been present in the relationship.

Table 6.3. Structure of the seasonal cycles of Phytoplankton Colour Index (PCI) and SeaWiFS chlorophyll *a* over the period 1997-1998.

	Annual		Semi-annual		Mean	Ratio of the amplitudes (Semi-annual / Annual)
	Amplitude	Phase (°)	Amplitude	Phase (°)		
PCI	1.57	74	1.10	170	1.57	0.70
SeaWiFS (mg m ⁻³ Chl <i>a</i>)	0.20	28	0.23	215	0.94	1.15

In addition to the moderate level of association between the seasonal cycles of PCI and SeaWiFS (Table 6.1), the structure of the seasonal cycle also differs (Table 6.3). Fundamentally, a seasonal cycle can be thought as a simple three component model, *i.e.* the sum of the mean, the fundamental component (annual component) and its first distorting harmonic (semi-annual component). Except in 1996, no autumn blooms were identified for PCI on the Hovmöller diagram (Fig. 6.17). However, the annual and semi-annual components resulting from a Fourier filtering procedure lead to the identification of spring and autumn blooms for both PCI and SeaWiFS data (Table 6.3). The combination of phases and amplitudes of the annual and semi-annual components estimated for PCI (Table 6.3; see also Fig. 6.16) leads to a magnification

and a dampening of the spring and autumn blooms, respectively. In contrast, this results in a magnification of both spring and autumn blooms for SeaWiFS data (Fig. 6.16). In addition, the phases of the PCI and SeaWiFS dominant annual and semi-annual cycles similarly differ by ca. 45° (Table 6.3), indicating a ca. 1.5 months lag between the maximum values of each blooms (i.e. spring and autumn) of the two data sets. This reveals another difference between PCI and SeaWiFS measurements, a discrepancy in the timing of phytoplankton spring and autumn blooms. Finally, the difference between the ratio of the mean to the annual component (SeaWiFS ~ 5 , PCI ~ 1) suggests a clear divergence in the two methods for assessing chlorophyll *a* levels. According to these arguments, further examination of the seasonal cycle observed along the E-route suggests a more significant contribution of the semi-annual component to both PCI and SeaWiFS signals on Georges Bank (Fig. 6.15a, d) when compared to Shelf Break and Sable Island (Fig. 6.15b, e) and St Pierre Bank (Fig. 6.15 c, f). The differences in amplitude between PCI and SeaWiFS signals is a consistent feature along the E-route (see Fig. 6.15). The comparison of PCI and SeaWiFS seasonal cycles thus leads to the conclusion that :

- the global picture given for a mean seasonal cycle is the same;
- the correlation between these parameters depends on the observation scale (i.e. spatial and temporal). As marine ecosystems are highly heterogeneous in space and time over a wide range of scales (Legendre & Demers 1984, Mackas et al. 1985), it is critical to use plankton estimators that will reflect the most closely the variability of the environment at scales the most relevant of the population dynamics. In particular, for phytoplankton as it represents the first level of the food web.
- the detailed structure of PCI and SeaWiFS mean seasonal cycles completely differs.

In order to determine which estimator is the most accurate, it would be necessary to conduct a comparison between those estimators and Chl *a* concentration estimated from bulk phase seawater.

6.C.4.b. Influence of the climate

Along the CPR route, phytoplankton was significantly correlated with monthly NAO (with a lag of 2 months). PCI anomaly cumulative sums analysis revealed changes in trends of the time series, with a change in slope between December 1996 and March 1997 for stations 2 to 13. In addition, there was no spring bloom on Georges Bank in 1997 (Fig. 6.17a). Finally, a decrease

in SST was observed between June 1996 and June 1997 on the Scotian Shelf (Fig. 6.20). This period (winter 1995-96) corresponds to the most negative value observed in NAO winter index since 1970s (Hurrell 1995a). After the NAO index's large drop in 1996, the Labrador Subarctic Slope Water (LSSW, *i.e.* cool, fresh water poor in nutrients; Petrie & Yeats (2000)) advanced along the shelf break, displacing the Atlantic Temperate Slope Water (ATSW, *i.e.* relatively warm and salty) offshore and penetrating to the southwest as far as the Middle Atlantic Bight (Mercina 2001). Between October 1992 and July 1998, the geostrophic flow was observed moving northeast (*i.e.* corresponding to ATSW flowing along the continental shelf). This flow towards Newfoundland increased by $\sim 1 \text{ km day}^{-1}$ until July 1995, then decreased by about 3 km day^{-1} until June 1998. It is then suggested that the ATSW was progressively replaced along the shelf by LSSW from September 1997 to February 1998, in accordance with previous observations (Greene & Pershing 2003). These water masses movement are also associated to decrease in surface salinity on Georges Bank between 1995 and 1997 (Smith *et al.* 2001). The movement of water masses along the Scotian Shelf is then strongly influenced by the different phases of NAO.

There is strong evidence that production rates of the copepod *Calanus finmarchicus* were limited by the lack of food on the southern flank of Georges Bank during April 1997 (Campbell *et al.* 2001). This observation is consistent with the absence of phytoplankton spring bloom in 1997 on the Georges Bank (Fig. 6.17a). The timing and development of density stratification on Southern Georges Bank have, however, also been shown to influence the growth and recruitment of copepods (Bisagni 2000). The changes in seawater characteristics (*i.e.* temperature and salinity) following the inflow of LSSW might then have modified the timing and development of density stratification on Georges Bank and consequently the development of the spring bloom early 1997. It is finally suggested that such modifications in the ecosystem might have a strong impact on the higher levels of the food web. This is especially critical in a region like Georges Bank that is a large retention area for Atlantic herring, cod, haddock, hake and flounder (Backus 1987).

6.C.4.c. Influence of mesoscale physical processes

The annual component of Sea Level Anomalies (SLA) has shown two structures along the CPR route:

- a lag of two months in the rise and fall of the water level between stations 1 and 15 (Fig. 6.19b);
- a decrease in the amplitude of the annual component northward along the route (Fig. 6.19b), where the surface water is cooler.

The expansion and contraction of the water column, represented by the annual component, is associated to the seasonal changes in atmospheric temperature. Moving northward along the E-route, the mean temperature of the seawater is cooler, and the heat necessary to expand the water column as much as in the southward stations is greater. So, for a same temperature the expansion and contraction of the water column will be much smaller towards Newfoundland than near Georges Bank.

More specifically, positive and negative values have been identified in SLA on the Hovmöller diagram (Fig. 6.19c). Specific structures have also been identified in PCI. Negative anomalies visually correspond to areas of high chlorophyll *a* concentration and positive anomalies are associated with low SeaWiFS chlorophyll *a* concentrations. Negative SLA anomalies, corresponding to cyclonic eddies, are associated with high levels of inorganic nutrients reintroduced in the water column by localised upwellings (Hitchcock *et al.* 1993, Arístegui *et al.* 1997). In contrast, positive anomalies corresponding to anticyclonic eddies are associated with depressed isotherms and low levels of inorganic nutrients. These processes are thus likely to modify the development of localised phytoplankton blooms and then influence the concentration in SeaWiFS chlorophyll *a* observed at the same location. However, there was no significant overall correlation between residuals of PCI and SLA. On the Shelf, SLA may not be related to eddies, but result from different causes (*e.g.* wind set-up, circulation, tidal aliasing, surges) that may not correlate directly with Chl *a*. Moreover, Chl *a* anomalies are likely to have a maximum signal in the productive season due to variations in the timing of the spring bloom whereas SLA anomalies are not seasonally constrained. Those observations lead to the conclusion that except in the open ocean, it is difficult to state unambiguously that there is a relation between eddy structures and phytoplankton structures.

Even if Gulf Stream rings have been identified as moving towards the Scotian shelf between September 1997 and December 2000 (see section 6.B.3.c), none of them (based on looking at the centre of the eddy) was actually observed crossing the shelf break. As a consequence, the positive and negative anomalies identified in SLA between 1995 and 1998 do not seem to be related to Gulf Stream rings. However, a positive SLA observed on the southern flank of the

Georges Bank (i.e. our stations 2 and 3) in May-June 1997 (Fig. 6.20) has been identified by Ryan *et al.* (2001) as a warm-core ring (anticyclone). Low SeaWiFS Chl *a* features related to anticyclonic eddies were observed near Georges Bank in February and March 1999, but could only influence the stations 1 and 4 of the E-route. In addition, two such anticyclonic eddies were also observed at Station 4 in 1995 near Georges Bank (see figure 6.19c). These observations corroborate the possible observation of anticyclonic rings on the southern flank of the Georges Bank. A more extended analysis of sea level anomalies showed that a few of these relatively smaller anticyclonic eddies could move cyclonically around a larger cold core negative anomaly or Gulf Stream Ring in the ocean region and reached the continental slope region near Station 6 (> 200m depth). From here they tended to move southward along the slope region around Georges Bank as far as Station 1. Corresponding SeaWiFS Chl *a* structures showed that the centre of the anticyclonic structure was low in chlorophyll *a* and two such anticyclonic features influencing the Georges Bank region in August 2001 are shown in the first part of this chapter (e.g. marked B on Fig. 6.13). The shelf Chl *a* was thus entrained to the ocean by the ocean eddies from outer regions (see Figs. 6.3 and 6.13). The interactions of anticyclonic rings with shelf water masses, via eddy swirl currents, then likely modify the distributions of phytoplankton and zooplankton species, as well as the retention of fish larvae on the southern flank of the Georges Bank and might have critical implications for fisheries (Ryan *et al.* 2001).

6.D. Conclusion

The aim of this chapter was to investigate the relationship between spatial and temporal structures of eddies (using SLA) and chlorophyll *a* (i.e. PCI and SeaWiFS Chl *a*) in the Northwest Atlantic. In particular, the impact of the Gulf Stream rings on phytoplankton distributions and the fluctuations of physical processes and phytoplankton distribution were compared to climate indices (i.e. monthly time series of SST and NAO) along the E-route.

In the North Atlantic open ocean conditions, SeaWiFS Chl *a* is redistributed at the eddy scale by the eddy surface swirl currents. This led to a significant overall inverse relationship between SeaWiFS Chl *a* and SLA residuals. More specifically, Gulf Stream anticyclonic and cyclonic rings have been observed moving upstream at speed ranging between 2.4 and 5.2 km day⁻¹. In contrast, anticyclonic and cyclonic rings moved downstream respectively at 3.5 km day⁻¹ and 2.6 km day⁻¹. Those eddies were identified on the Hovmöller diagrams and anticyclonic and

cyclonic rings generally corresponded respectively to areas of low and high Chl *a* concentration (see Figs. 6.8 and 6.10). Anticyclonic rings are associated with depressed isotherms and low levels of inorganic nutrients. On the Gulf Stream axis, those rings are associated to low chlorophyll concentration (marked with ‘-’ sign in Fig. 6.3). In contrast, cyclonic rings are associated to high chlorophyll concentration (marked with ‘+’ sign in Fig. 6.3). Cyclonic rings have domed isotherms and the related localised upwellings may bring nutrients into the euphotic zone, which could fuel primary production in their core (Hitchcock *et al.* 1993, Aristegui *et al.* 1997). These mesoscale features can then modify the spatial distribution of phytoplankton in the open ocean by causing localised bloom in the core of an eddy or redistribute the phytoplankton around the eddy via eddy swirl currents.

Along the E-route, the phytoplankton structures were not significantly influenced by the mesoscale features of the Gulf Stream, but were mainly impacted by the changes in surface flow along the Scotian Shelf:

- Firstly, no significant relationship was found between the SLA and PCI structures along the E-route. On the Shelf, SLA may not be related to eddies, but instead result from different causes (*e.g.* wind set-up, circulation, tidal aliasing, surges) that may not correlate directly with Chl *a*. It is therefore difficult to affirm if there is a relation between eddy structures and phytoplankton structures.
- Secondly, although positive anomalies were observed on Georges Bank could be related to the warm-core ring identified by Ryan *et al.* (2001) in spring 1997 on the southern flank of the Georges Bank (stations 2 and 3), no eddies were observed actually crossing the Shelf Break. Over their lifespan, the shape of the eddies is modified by the movement of the surrounding water masses. As some eddies get to a diameter of ~200-250 km (see Chapter 6), it is suggested that their edge could easily be on the shelf break but not their centre. The current associated to the edge of the eddy (*i.e.* eddy swirl current) would then modify the distribution of phytoplankton and zooplankton species, as well as the retention of fish larvae on the southern flank of the Georges Bank and have important implications for fisheries oceanography and shelf carbon budgets (Ryan *et al.* 2001).
- Finally, changes were identified in the flow of Atlantic Temperate Slope Water along the Scotian Shelf. This change in water mass circulation caused a drop in temperature and salinity along the Scotian Shelf and then induced changes in phytoplankton and zooplankton abundance. In particular, these changes in phytoplankton and zooplankton

might have an impact on the recruitment of fish larvae, such as cod and haddock that use Georges Bank as a spawning ground (Campbell *et al.* 2001).

The Western North Atlantic is then highly influenced by the hydrodynamic processes. In particular, Gulf Stream mesoscale features modify the spatial distribution of phytoplankton in the open ocean. In addition, the fluctuations in flow along the Scotian Shelf influence the characteristics of seawater (i.e. temperature and salinity) and then the plankton dynamics.

Chapter 7

GENERAL DISCUSSION

The Continuous Plankton Recorder (CPR) survey has measured the presence and abundance of ca. 500 phytoplankton and zooplankton taxa since 1931 and has provided a visual assessment of total phytoplankton biomass through the Phytoplankton Colour Index (PCI, Colebrook & Robinson 1965) since 1946. The aim of this estimator is to provide an estimation of total phytoplankton biomass. However, some studies have shown that the relationship between PCI and other estimators of phytoplankton abundance is variable.

The first comparison between PCI and fluorometrically measured chlorophyll was undertaken by Hays & Lindley (1994). They showed a good relationship between PCI and chlorophyll concentration, but only when the number of cells retained by the CPR mesh was small. This implies that the relationship, and thus the use of PCI, was significant only in oligotrophic and non-bloom conditions. Batten *et al.* (2003b), however, compared simultaneous fluorometric measurements of Chl *a*, phytoplankton cell abundance and PCI from the Iberian margin, Western Europe. The relationships between fluorometrically determined chlorophyll, cell abundance and PCI were all significant, with PCI showing a better relationship to chlorophyll than to cell abundance. This supports previous research (Colebrook & Robinson 1965, Hays & Lindley 1994) suggesting that the PCI is a useful index of phytoplankton standing stock and, furthermore, may be a measure of cells (like small naked flagellates) that are not preserved or counted in the routine microscopic processing of CPR samples. The relationship between PCI and chlorophyll nevertheless appeared to vary seasonally (Batten *et al.* 2003b), although more extensive data are needed to quantify this variability. The Batten *et al.* (2003b) study also compared the PCI and fluorometer data with chlorophyll values obtained from Sea-viewing Wide Field-of-view Sensor (SeaWiFS) for the Iberian margin. Significant correlations were found during a 15-month time-series between these three estimates of phytoplankton concentration. This result demonstrates that the ~50 year time-series of PCI for the North Atlantic can provide valuable information on changes in phytoplankton standing stock. However, as the relation between PCI and chlorophyll varies seasonally, the interpretation of any results based on PCI data only should be taken with great caution.

The most recent comparison of the PCI with another estimate of phytoplankton abundance was achieved by Raitsoo *et al.* (2005) using SeaWiFS data. They found a significant relationship between PCI and SeaWiFS data in the Northeast Atlantic and the North Sea. In this thesis, PCI was compared with SeaWiFS data along the E-route, in western North Atlantic, and there was a significant relationship between the two estimators. Although the characteristics of the seasonal cycles (see Table 6.3) of PCI and SeaWiFS are correlated at 53% of the stations along the E-route, the structure of the seasonal cycle differs for these measurements. For example, the

secondary late autumn peak observed in PCI has a much smaller amplitude relative to the spring bloom, which is not the case in SeaWiFS data (see Fig. 6.17). In addition, the ratio of the mean to the annual component (SeaWiFS ~ 5 , PCI ~ 1) shows a large discrepancy in the two methods for assessing Chl *a* levels, particularly for assigning a value of near zero Chl *a* concentrations. It is thus suggested that the PCI is less reliable than the SeaWiFS data as it is only a semi-quantitative index while SeaWiFS data are continuous. PCI must then be only considered as 'an estimation of phytoplankton biomass' that requires additional data in order to quantify the fluctuations in phytoplankton community.

As a conclusion, it can be stated that the PCI index has shown some limitations: (i) the relation between phytoplankton abundance and biomass is not constant (Hays & Lindley 1994), (ii) the relation between PCI and chlorophyll appears to vary seasonally (Batten *et al.* 2003b), (iii) Chl *a* is an imperfect measure of phytoplankton biomass (see e.g. Seuront *et al.* 2006, Figs. 3 and 5) and (iv) PCI does not provide relevant information on the structural changes occurring in phytoplankton communities that are likely to influence phytoplankton biomass.

The study of space-time dynamics of phytoplankton communities therefore require further analysis of the diatom and dinoflagellate assemblages. Diatoms and dinoflagellates are the two most important groups of primary producers in the North Atlantic Ocean (Raymont 1980, Lalli & Parsons 1997) and are the two most recorded taxonomic groups in the CPR survey. These data have subsequently been used as corollary variables of PCI. A comparison of potential differences in the space-time dynamics of the PCI, diatom and dinoflagellate abundance was thus undertaken (see Chapters 3 and 4). In particular these three parameters respond in a different way to the modifications of their environment caused by the fluctuations of the NAO. There was a high variability in the trends of PCI, diatom abundance and dinoflagellate abundance observed in the same (or different) region(s) of the North Atlantic basin. PCI is then not always an appropriate assessor of the fluctuations of phytoplankton biomass at the different spatial and temporal scales considered in this work.

Barton *et al.* (2003) reported positive long-term trends in PCI time series across the continental shelf areas in the NE and NW Atlantic, as well as a narrow transition zone between the subarctic and subpolar Central North Atlantic over the period 1948-2000. This increasing trend in the PCI had previously been shown in the North Sea (Reid & Edwards 2001), in the area west of the British Isles (Edwards *et al.* 2001) and over the Scotian Shelf and Georges Bank in the NW Atlantic (Sameoto 2001). In the present work, increasing trends of PCI are evident in

the NE, SC and SW North Atlantic. However, dinoflagellates significantly increased only in the SW and no long-term trends were observed in diatoms between 1958 and 2002 (see Chapter 3). These observations indicate that the PCI does not reflect fluctuations in the dinoflagellates and diatoms found on the CPR silk. More detailed analyses have highlighted that the significance of trends observed for the PCI depends on the month and the geographical area (see Table 3.3). The trends observed in monthly time series of dinoflagellates and diatoms also vary temporally and spatially, but the PCI still does not reflect the changes in dinoflagellates and diatoms.

More specifically, the fluctuations of PCI, diatoms and dinoflagellates were compared with the SST across the North Atlantic basin (see Chapter 3). This showed that the relationship between phytoplankton and the SST varies depending on the area: a stronger relationship between SST and PCI and dinoflagellates has been observed in the eastern part of the ocean (see Table 3.2). The opposite has been observed for diatoms, with a stronger correlation in the NW Atlantic, suggesting the potential influence of different forcing factors across the North Atlantic basin. Drinkwater *et al.* (2003) showed that the physical response to NAO forcing varies spatially across the North Atlantic basin. In particular, there is a regionally variable component to the NAO-climate relationship (Smayda *et al.* 2004). In the north-western Atlantic from the Gulf of Maine southward, there is positive correlation between NAO and sea temperature anomalies (Smayda *et al.* 2004). By contrast, along the North European coastal zone there is a negative correlation between NAO and the sea temperature anomalies.

Even if the PCI is increasing in NE and NW Atlantic, and shows higher correlation with SST in the NE, the taxa leading to these correlations are not the same on both sides of the Atlantic. Diatoms and dinoflagellates have shown different trends, and correlations with SST, in the NE and NW Atlantic, thus seemingly responding in different ways to the same changes occurring in their environment. In addition, the environmental factors (i.e. currents, wind regime, SST and precipitation) that are under the influence of the NAO can fluctuate differently according to the location in the North Atlantic basin. Different adaptive strategies are required to deal with varying combinations of these factors, embodied mainly in the physiological differences between diatoms and dinoflagellates (Margalef 1973). Dinoflagellates possess an undulating flagellum that improves the chances for nutrient uptake in nutrient depleted waters (Margalef 1997). In contrast, diatoms, with their relatively low surface-to-volume ratios need nutrient-rich conditions for growth (Chisholm 1992). In oligotrophic, stratified and/or low turbulent waters, it pays to invest energy in swimming to be able to position the cell in the most favourable environment. This optimisation is however useless in eutrophic and/or turbulent waters, where nutrients are homogeneously distributed and/or redistributed in the water column.

As a consequence, in stratified water (poor and rich in nutrients), dinoflagellates may be dominant; conversely, in turbulent and/or nutrient rich water, diatoms would be dominant. In the NE Atlantic, warmer surface temperatures related to the increasing NAO winter index promoted earlier, or more intense, stratification of the upper water-column (Drinkwater *et al.* 2003). According to Margalef's (1975) hypothesis, all these factors would create an environment favouring the growth of dinoflagellates over the growth of diatoms in both parts of the eastern North Atlantic. This is congruent with the observations regarding the differential relationships found between dinoflagellates, diatoms and the NAO (see Table 3.3, 3.4).

In the NW Atlantic, phytoplankton measures (i.e. PCI, total diatoms and dinoflagellates) have significantly increased between 1958-2003, but during different periods of the year (see Chapter 3). These observations correspond to an increase in the occurrence of diatoms and dinoflagellates during the first month of the period in which they are usually present, and/or an earlier appearance of these taxa during the year. Edwards and Richardson (2004) have previously observed changes in the phenology of these taxa in the central North Sea. They stated that diatoms showed the largest variations in phenology, with particular taxa occurring both earlier and later during the spring and autumn respectively. This study suggests that changes in the timing of the blooms of those taxa in the North Atlantic could be associated with the variations of physical processes along the Scotian Shelf associated to the NAO.

During positive phases of the NAO (Fig. 7.1a), convection is deeper and more intense in the Labrador Sea and a relatively cool, fresh and thick layer of LSW is formed (Dickson *et al.* 1996). This results in higher salinity and temperature on the Scotian Shelf and in the Gulf of Maine (Petrie & Drinkwater 1993) and in higher nutrient concentrations (Gatien 1976). Higher salinity and temperature associated with higher nutrient concentrations can create favourable conditions in spring for the growth of dinoflagellates such as *C. lineatum* and *C. tripos*, typical of mixed Atlantic waters (see Chapter 3). In contrast, diatom species typical of oligotrophic waters, such as *Rhizosolenia* spp., encounter favourable conditions from the end of the summer when low nutrient conditions prevail. These large-sized diatoms adopt a strategy of buoyancy-mediated vertical migration to access nutrient-enriched waters located below the nutricline and then return to the surface to photosynthesise (Villareal 1992, Villareal *et al.* 1993, Villareal *et al.* 1999). This behavioural adaptation prevents direct competition with the dominant nanoplankton size classes (usually encountered in oligotrophic water conditions) for nutrients and allows their survival despite the disadvantages of large size (Singler & Villareal 1995).

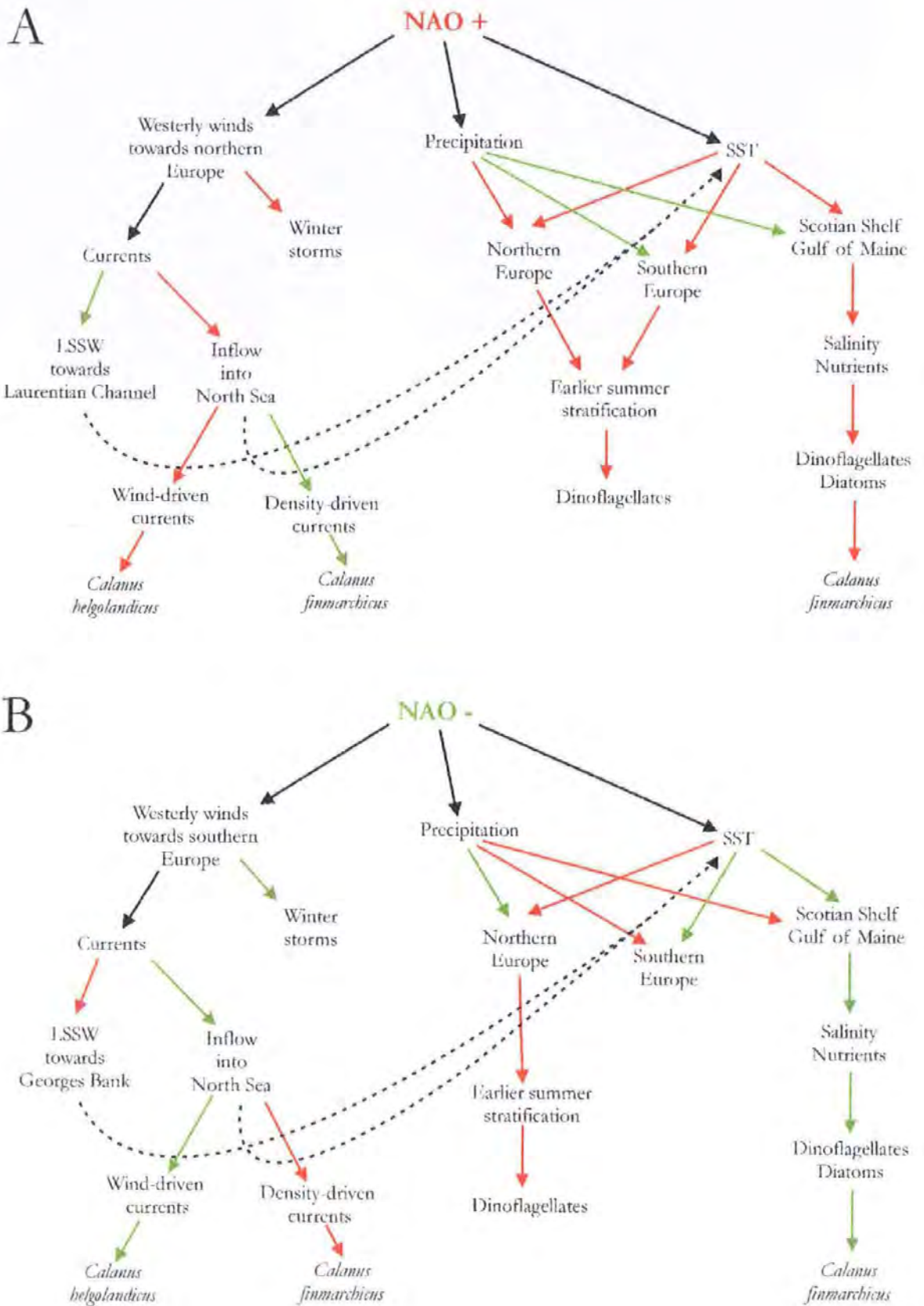


Figure 7.1. Mechanisms linking the positive (A) and negative (B) phases of the North Atlantic Oscillation (NAO) to the variability in physical processes and planktonic ecology. Red/green arrows imply an increase/decrease in the parameter. The dashed arrows illustrate the relationship between NAO and Sea Surface Temperature (SST) via the currents in Northeast and Northwest Atlantic.

During negative phases of the NAO (Fig. 7.1b), the Labrador Basin convection is weaker, the LSW export is diminished and the transport of Labrador Subarctic Slope Water (LSSW, i.e., cool, fresh water poor in nutrients (Petrie & Yeats 2000)) along the continental shelf is enhanced (Pickart *et al.* 1999). During the winter of 1995/1996, the NAO index became strongly negative and LSSW moved southward along the Scotian Shelf (Thomas *et al.* 2003). LSSW advanced along the shelf break, displacing Atlantic Temperate Slope Water (ATSW) offshore (Mercina 2001). Changes in surface flow were estimated from the altimeter data between the 2 stations located on the shelf and in the open ocean, respectively (see Chapter 6). Between October 1992 and July 1998, the geostrophic flow moving northeast (i.e. corresponding to ATSW flowing along the continental shelf) was determined. This flow towards Newfoundland increased by $\sim 1 \text{ km day}^{-1}$ until July 1995, then was reduced by about 3 km day^{-1} until June 1998. The ATSW was progressively replaced along the shelf by LSSW from September 1997 to February 1998 (Greene & Pershing 2003). In this work, changes in the environment of the Scotian Shelf have been observed, as the SST decreased between June 1996 and June 1997, as well as in phytoplankton as there was no spring bloom in 1997 on Georges Bank (see Chapter 6). The decrease in temperature and the changes in water characteristics (i.e. salinity and nutrients) associated to the inflow of LSSW along the Scotian Shelf might have modified the growth of phytoplankton and subsequently the higher level of the pelagic food web. For instance, there is strong evidence that production rates of the copepod *C. finmarchicus* were limited by the lack of food on the southern flank of Georges Bank during April 1997 (Campbell *et al.* 2001). If phytoplankton limitation on the southern flank is interannually variable, as suggested above, then there is the potential for interannual variation in *C. finmarchicus*, with potentially significant consequences for the growth and survival of fish larvae on the Bank. Ultimately, these changes in phytoplankton and zooplankton might have an impact on the recruitment of fish larvae, such as cod and haddock, that use Georges Bank as a spawning ground (Campbell *et al.* 2001).

Water masses and chlorophyll distribution of Georges Bank have been observed as being influenced by mesoscale eddies with Gulf Stream origins (warm-core ring, WCR, Ryan *et al.* 2001). The Gulf Stream represents the boundary between Subtropical Waters (i.e. with high dynamic heights and lower Chl *a* levels) and both Slope and Subpolar origin waters (i.e. with low dynamic heights and elevated Chl *a* levels). Fuglister and Worthington (1947) discovered that rings are generated from the cut-off of Gulf Stream meanders. These meanders, which separate northward of the stream, develop into anticyclonic eddies and those separating southward produce cyclonic eddies (Richardson 1983, Tomczak & Stuart 2003). Those eddies

usually move westward when they are not touching the Gulf Stream and eastward when they are attached to it (Fuglister 1972, Richardson 1980). Even if these rings have been identified as moving towards the shelf break (westward) between September 1997 and December 2000 (see Chapter 6), none of them (based on looking at the centre of the eddy) has been observed crossing the shelf break. Over their life duration, the shape of the eddies is modified by the movement of water masses surrounding them. As some eddies get to a diameter of ~200-250 km (see Chapter 6), it is suggested that their edge could easily be on the shelf break and not their centre. In that case, the edge of the eddy can have an impact on the area it is entering on the Shelf. In particular, along the E-route (mainly located on the Shelf break), a positive anomaly that was observed on Georges Bank in May-June 1997 (see Fig. 6.21) could be related to the warm-core ring (anticyclone) identified by Ryan *et al.* (2001) in spring 1997 on the southern flank of the Georges Bank. This confirms the above-mentioned hypothesis stating that the centre of eddies might not cross the shelf break, while their edge might and thus influence the water masses surrounding them.

The Gulf Stream rings redistribute the surface Chl *a* and then modify the spatial patterns of Chl *a* (see Chapter 6). Gulf Stream anticyclonic (warm core) and cyclonic (cold core) rings have thus been shown to influence surface phytoplankton distributions via the entrainment of the surrounding water masses around and into the rings (Kennelly *et al.* 1985, Garcia-Moliner & Yoder 1994, Ryan *et al.* 1999, Ryan *et al.* 2001). Chlorophyll structure can be stirred between eddies and then mixed from regions of higher concentration with area of lower concentrations, modifying, for example, the boundaries of a bloom. To show a significant redistribution of a phytoplankton bloom, the eddy-swirled currents must be able to advect phytoplankton concentrations at rates comparable to, or greater than, the propagation rates due to phytoplankton growth dynamics. Moreover, rings provide a mechanism for exchange of both nutrients and biota among Slope and Sargasso Sea waters (Gould & Fryxell 1988, McGillicuddy *et al.* 1997) and cross-frontal exchange related to meander circulation has been demonstrated by Bower and Rossby (1989). Two scenarios can be observed (Fig. 7.2). First, many plants and animals that are translocated by the rings die as the ring ages (The Ring Group 1981). Second, some species might successfully exploit these unusual environments and a successful exchange between slope and Sargasso Sea water species communities can be achieved (Fig. 7.2). Eddies could then be seen as an individual microcosm within which plankton species would be different from the one observed in the 'outside-eddy' environment. Depending on the size and persistence of the eddy, those species would survive and reproduce in this 'independent' water mass. According to the location of the disappearance of the eddy,

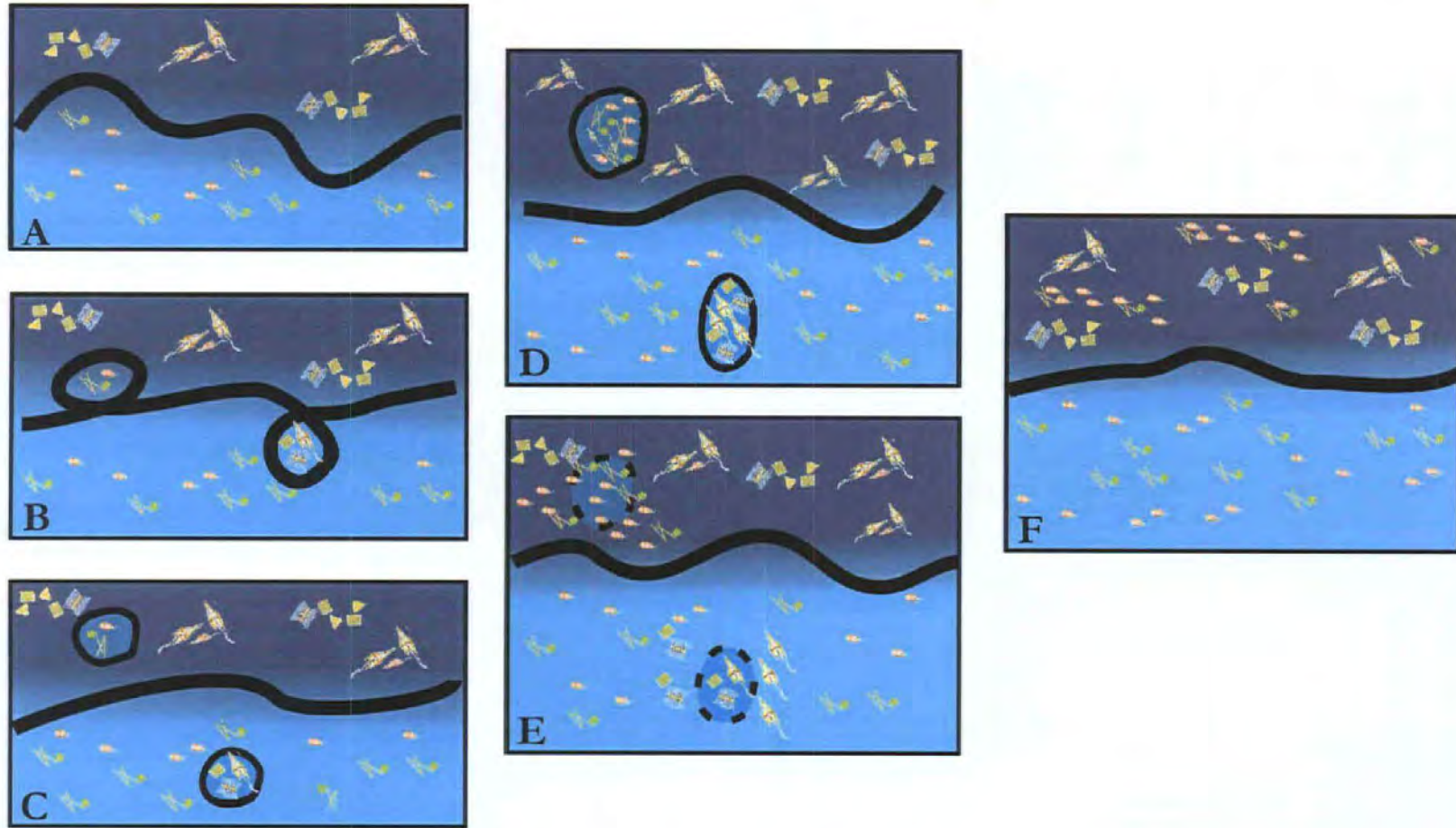


Figure 7.2. Schematic eddy formation from the Gulf Stream meanders and mechanism of plankton and nutrient exchange across the frontal boundary between Subtropical Waters (light blue) and both Slope and Subpolar origin waters (dark blue). Species from Subtropical Waters could be exported toward Slope waters and if they can adapt to this new environment (and there is enough nutrient), survive in those waters. However, it will be more challenging for Slope water species to be exported and survive in Subtropical Waters that are very poor in nutrients.

those species would then be observed in regions from where they are usually absent. Ultimately, if the translocated species manage to survive in their new environment, this could impact the ecosystem by introducing new competitive species and then modify the state of the ecosystem.

In the NE Atlantic, three states of the phytoplanktonic ecosystem have been identified, suggesting differential temporal and spatial dynamics of the phytoplankton communities in geographically adjacent oceanic domains. These states have been related to the fluctuations in the NAO (see Chapter 4). In particular, in the South NE Atlantic and northern North Sea, a currently evolving ecosystem was determined, with an increasing contribution of dinoflagellates. This increase is in contrast to a stable diatom population in the South NE Atlantic and a decreasing contribution of diatoms in the northern North Sea.

These patterns can be related to the specific circulation patterns characterising these areas. The South NE Atlantic and the northern North Sea are indeed both highly influenced by the North Atlantic water inflow (Corten 1999). During the late 1980s, the NAO index was strongly positive and the strength of the westerly winds increased in the NE Atlantic, leading to an increase in the oceanic inflow into the North Sea (Drinkwater *et al.* 2003). Turrell *et al.* (1992) suggested that the Atlantic inflow makes a major contribution to the input of generally warmer, nutrient-rich water into the northern North Sea. The resulting relatively warmer surface temperatures promote earlier, or more intense, stratification of the upper water column (Drinkwater *et al.* 2003), which, according to Margalef's (1975) hypothesis, would create an environment favouring the growth of dinoflagellates over the growth of diatoms. The fluctuations observed in these two phytoplankton taxonomic groups are likely to impact the dynamics of the whole food web through herbivorous copepods and carnivorous zooplankton: Richardson and Schoeman (2004) have shown a dominant bottom-up control within the plankton community in the NE Atlantic over time and space as the result of sea surface warming. The space–time differences in taxonomic group contributions could, for instance, have an effect on zooplankton populations through their trophodynamics. Different hypotheses have been formulated on the effect of diatoms and dinoflagellates on copepod growth and reproduction. In particular, copepods' reproduction has been shown to be influenced by their diet. First, some diatom monodiets induce teratogenic effects (i.e. 'birth defects') in newly hatched copepod nauplii, which then have asymmetrical bodies and reduced numbers of feeding appendages (Poulet *et al.* 1995). Second, rather than showing that they were toxic, Jones and Flynn (2005) showed that some diatoms have lower nutritional value than dinoflagellates. The presence of dinoflagellates or other phytoplankton taxa that would

supplement a purely diatom diet would then maximise copepod growth (Jones & Flynn 2005). Finally, Irigoien *et al.* (2002) observed that under natural environmental conditions, there is no negative effect of diatoms on copepod hatching success. The different results obtained in these studies might be due to interspecific variability and be relevant in specific regions of the North Atlantic basin. However, changes in the phytoplankton community structure like the one observed in this work might induce dramatic changes in copepods and then strongly impact the sustainability of higher levels of the food web. This cascade of reaction would then affect the entire ecosystem via oxygen production, carbon sequestration, and biogeochemical cycling.

The observed different ecosystem states are clearly related to a regime shift in the abundance and/or composition of phytoplankton communities. During the last two decades, “regime shift” has been defined in many different ways. The term was first introduced to describe the concurrent alternations between sardines and anchovies in several parts of the world (Lluch-Belda *et al.* 1989). Scheffer *et al.* (2001) defined it as an abrupt shift from one dynamic regime to another. Some oceanographers and ecologists choose, therefore, to define regime shifts on the basis of changes in the ecosystem as a whole rather than simply on the basis of abrupt changes in time series. Laws (2004), for example, stated that regime shifts occur when a system transitions from one stable configuration to another, specifying that such abrupt changes in biological communities may reflect small changes in environmental conditions such as temperature, oxygen concentration, or irradiance. In addition, Reid *et al.* (2001) used the term “regime shift” to describe large, decadal-scale switches in the abundance and composition of plankton and fish; this definition will be used hereafter. In my analyses (see Chapter 4), only the PCI provided evidence for the regime shift observed in the North Sea during the period 1982 to 1988 (Reid *et al.* 2001, Beaugrand 2004). Dinoflagellates showed a shift in 1985, but only in the northern North Sea, and diatoms did not exhibit any evidence of a regime shift over this period. The observed discrepancy therefore suggests that the changes seen in PCI do not reflect changes in the community structure of major taxa. In addition, the features suggested to explain the regime shift in the North Sea by Beaugrand (2004) are acknowledged to influence the whole North Sea. This study shows, however, that the dynamics of the northern North Sea clearly differ from those of the central and southern North Sea. To investigate this issue more thoroughly, the presence and/or absence of a regime shift was tested in even smaller regions within the North Sea (see Chapter 5). Under the assumption of the regime shift observed in 1986-1988 (Reid *et al.* 2001, Beaugrand 2004), significant differences between the pre- and post-regime shift copepod assemblages (1958-1987 and 1988-2004) were apparent in northern, western, and eastern North Sea regions. Looking at phytoplankton in the same areas, this

regime shift was only apparent in northwestern and southwestern North Sea regions. This suggests that different driving processes might control the dynamics of the phytoplankton and zooplankton community at different locations within the North Sea. By looking at smaller spatial scales, the explanatory mechanisms identified to explain changes in pelagic ecosystems are different than at larger scales. This implies that local and regional processes play an important role in the control of the abundance and community structure of phytoplankton.

This work allowed to observe that changes are occurring in pelagic ecosystems at different temporal and spatial scales. These changes have been illustrated by the spatial variability induced by eddies and/or currents but also by the regional variability of the hydro-climatic processes, influencing in different ways SST, wind-regimes and mixing of local environments. Several different aspects of the NAO impact on pelagic ecosystems have been highlighted:

- In the northeast Atlantic, NAO fluctuations imply changes in (i) SST in northern Europe (Chapter 3), (ii) wind regimes, (iii) Atlantic Water inflow into the North Sea (Chapter 5).
- On the other hand, in the northwest Atlantic, the variations of NAO imply changes in (i) SST on the Scotian Shelf (Chapters 3 and 6), (ii) coastal currents (Chapter 6), and (iii) inflow of Labrador Sea Slope Water (LSSW) towards the Scotian Shelf and Georges Bank (Chapter 6).

These changes in environmental processes impact phytoplankton production, abundance (Chapters 3, 4 and 5), spatial distribution (Chapter 6), community structure (Chapter 4), phenology (Chapter 3) and ultimately would impact trophodynamics processes. It is, however, still difficult to explain unambiguously all the mechanisms that are involved in the control of the observed patterns. As most of the processes affecting the physiology, the biology, and ultimately the ecology of phytoplankton communities are typically occurring at the scale of individual organisms, future work is still needed to reconcile micro- and macroscale observations to critically assess the impact of environmental fluctuations on the growth and sustainability of phytoplankton species, and in the end pelagic ecosystems.

Literature cited

- Aebischer, N. J., J. C. Coulson, J.M.Colebrook. 1990. Parallel long-term trends across four marine trophic levels and weather. *Nature* **347**: 753-755.
- Aristegui, J., P. Tett, A. Hernández-Guerra, G. Basterretxea, M.F. Montero, K. Wild, P. Sangra, S. Hernandez-Leon, M. Canton, J.A. Garcia-Braun, M. Pacheco, E.D. Barton. 1997. The influence of island-generated eddies on chlorophyll distribution: a study of mesoscale variation around Gran Canaria. *Deep-Sea Res.* **44**: 71-96.
- Backus, R.H. 1987. Georges Bank. MIT Press, Cambridge, Massachusetts. 593 pp.
- Barton, A.D., C.H. Greene, B.C. Monger, A.J. Pershing. 2003. The Continuous Plankton Recorder survey and the North Atlantic Oscillation: Interannual- to multidecadal-scale patterns of phytoplankton variability in the North Atlantic Ocean. *Prog. Oceanogr.* **58**: 337-358.
- Batten, S.D., A.G. Hirst, J. Hunter, R.S. Lampitt. 1999. Mesozooplankton biomass in the Celtic Sea; a first approach to comparing and combining CPR and LHPR data. *J. Mar. Biol. Assoc. of the U.K.* **79**: 179-181.
- Batten, S.D., R. Clark, J. Flinkman, G. Hays, E. John, A.W.G. John, T. Jonas, J.A. Lindley, D.P. Stevens, A. Walne. 2003a. CPR sampling: the technical background, materials and methods, consistency and comparability. *Progr. Oceanogr.* **58**: 193-215.
- Batten, S.D., A.W. Walne, M. Edwards, S.B. Groom. 2003b. Phytoplankton biomass from continuous plankton recorder data: assessment of the phytoplankton colour index. *J. Plankton Res.* **25**: 697-702.
- Beare, D.J., S. Batten, M. Edwards, D.G. Reid. 2002. Prevalence of boreal Atlantic, temperate Atlantic and neritic zooplankton in the North Sea between 1958 and 1998 in relation to temperature, salinity, stratification intensity and Atlantic inflow. *J. Sea Res.* **48**: 29-49.
- Beaugrand, G. 2004. The North Sea regime shift: evidence, causes, mechanisms and consequences. *Progr. Oceanogr.* **60**: 245-262.
- Beaugrand, G., P.C. Reid, F. Ibanez, J.A. Lindley, M. Edwards. 2002. Reorganization of North Atlantic marine copepod biodiversity and climate. *Science* **296**: 1692-1694.
- Beaugrand, G., K.M. Brander, J.A. Lindley, S. Souissi, P.C. Reid. 2003. Plankton effect on cod recruitment in the North Sea. *Nature* **426**: 661-664.
- Becker, G.A., M. Pauly. 1996. Sea surface temperature changes in the North Sea and their causes. *ICES J. Mar. Sci.* **53**: 887-898.
- Belgrano, A., O. Lindahl, B. Hemroth. 1999. North Atlantic Oscillation primary productivity and toxic phytoplankton in the Gullmar Fjord, Sweden (1985-1996). *Proc. R. Soc. Lond. B* **266**: 425-430.

- Bisagni, J.J. 1976. Passage of anticyclonic Gulf Stream eddies through Deepwater Dumpsite 106 during 1974 and 1975. NOAA Dumpsite Evaluation Report 76-1, U.S. Dept. of Commerce Pub. 39 pp.
- Bisagni, J.J. 2000. Estimates of vertical heat flux and stratification from Southern Georges Bank, interannual variability, 1985-1995. *Cont. Shelf Res.* **20**: 211-234.
- Bisagni, J.J., K.W. Seemann, T.P. Mavor. 2001. High-resolution satellite-derived sea-surface temperature variability over the Gulf of Maine and Georges Bank region, 1993-1996. *Deep-Sea Res. II* **48**: 71-94.
- Bishop, C.A., D.V. Weseloh, N.M. Burgess, J. Struger, R.J. Norstrom, K.A. Logan. 1992. *An Atlas of Contaminants in Eggs of Fish-eating Colonial Birds of the Great Lakes (1970-1988)*, Vol.1. Technical Report Series n° 152, Canadian Wildlife Service, Ontario Region. 318 pp.
- Blumberg, A., G. Mellor. 1980. A description of a three-dimensional coastal ocean circulation model. In N. Heaps [ed.], *Three-dimensional Coastal Ocean Models*, vol. 4. American Geophysical Union, Washington DC, USA, p. 1-16.
- Bonzek, C.F., P.J. Geer, H.M. Austin. 1995. VIMS juvenile fish trawl survey. Juvenile indices 1979-1994. Virginia Sea Grant Marine Advisory n° 57. Virginia Sea Grant Marine Advisory Program, College of William and Mary, VIMS/SMS, Gloucester Pt., VA 23062. 15 pp.
- Bower, A.S., T. Rossby. 1989. Evidence of cross-frontal exchange processes in the Gulf Stream based on isopycnal float data. *J. Phys. Oceanogr.* **19**: 1177-1190.
- Brown, O.B., P.C. Cornillon, S.R. Emmerson, H.M. Carle. 1986. Gulf Stream warm-core rings: a statistical study of their behavior. *Deep-Sea Res. I* **33**: 1459-1473.
- Cadée, G.C., J. Hegeman. 1993. Persisting high levels of primary production and declining phosphate concentrations in the Dutch coastal area (Marsdiep). *Neth. J. Sea Res.* **31**: 147-152.
- Campbell, J.W., T. Aarup. 1992. New production in the North Atlantic derived from seasonal patterns of surface chlorophyll. *Deep-Sea Res.* **39**: 1669-1694.
- Campbell, R.G., J.A. Runge, E.G. Durbin. 2001. Evidence for food limitation of *Calanus finmarchicus* production rates on the southern flank of Georges Bank during April 1997. *Deep-Sea Res. II* **48**: 531-549.
- Chapman, W.L., J.E. Walsh. 1993. Recent variations of sea ice and air temperature in high latitudes. *Bull. Am. Meteorol. Soc.* **74**: 33-47.
- Chisholm, S.W. 1992. Phytoplankton size. In P.G. Falkowski and A.D. Woodhead [eds.], *Primary Production and Biogeochemical Cycles in the Sea*. Plenum, New-York, p. 213-237.
- Clarke, K.R. 1993. Non-parametric multivariate analyses of changes in community structure. *Austral. J. Ecol.* **18**: 117-143.

- Clarke, K.R., M. Ainsworth. 1983. A method of linking multivariate community structure to environmental variables. *Mar. Ecol. Progr. Ser.* **92**: 205-219.
- Clarke, K.R., R.M. Warwick. 2001. *Change in Marine Communities: An Approach to Statistical Analysis and Interpretation*, 2nd edition. PRIMER-E, Plymouth, UK, 172pp.
- Cloern, J.E. 2001. Our evolving conceptual model of the coastal eutrophication problem. *Mar. Ecol. Progr. Ser.* **210**: 223-253.
- Colebrook, J.M. 1960. Continuous Plankton Records: methods of analysis, 1950-1959. *Bull. Mar. Ecol.* **5**: 51-64.
- Colebrook, J.M. 1975. The Continuous plankton recorder survey: automatic data processing methods. *Bull. Mar. Ecol.* **8**: 123-142.
- Colebrook, J.M. 1982. Continuous plankton records: persistence in time-series and the population dynamics of *Pseudocalanus elongatus* and *Acartia clausi*. *Mar. Biol.* **66**: 289-294.
- Colebrook, J.M., G.A. Robinson. 1965. Continuous Plankton Records: seasonal cycles of phytoplankton and copepods in the northeastern Atlantic and the North Sea. *Bull. Mar. Ecol.* **6**: 123-139.
- Continuous Plankton Recorder Team. 2004. Continuous Plankton Records: Plankton Atlas of the North Atlantic Ocean (1958–1999). II. Biogeographical charts. *Mar. Ecol. Progr. Ser. Suppl.* 11-75.
- Corten, A. 1986. On the causes of the recruitment failure of herring in the central and northern North Sea in the years 1972-1978. *J. Cons. int. Explor. Mer.* **42**: 281-294.
- Corten, A. 1990. Long-term trends in pelagic fish stocks of the North Sea and adjacent waters and their possible connection to hydrographic changes. *Neth. J. Sea Res.* **25**: 227-235.
- Corten, A. 1999. Evidence from plankton for multi-annual variations of Atlantic inflow in the northwestern North Sea. *J. Sea Res.* **42**: 191-205.
- Corten, A. 2001. *Herring and Climate: Changes in the Distribution of the North Sea Herring due to Climate Fluctuations*. Ponsenand Looijen Wageningen edition. 280pp.
- Cox, M., K. Bryan. 1984. A numerical model of the ventilated thermocline. *J. Phys. Oceanogr.* **14**: 674-687.
- Danielssen, S., E. Svendsen, M. Ostrowski. 1996. Long-term hydrographic variation in the Skagerrak based on the section Torungen-Hirthals. *ICES J. Mar. Sci.* **53**: 917-925.
- Dickson, R.R., J. Lazier, J. Meincke, P. Rhines, J. Swift. 1996. Long-term coordinated changes in the convective activity of the North Atlantic. *Progr. Oceanogr.* **38**: 241-295.
- Drinkwater, K.F., D.B. Mountain, A. Herman. 1999. *Variability in the Slope Water Properties off Eastern North America and their Effects on the Adjacent Shelves*. ICES C.M. 1999/O:08. 26 pp.

- Drinkwater, K.F., A. Belgrano, A. Borja, A. Conversi, M. Edwards, C.H. Greene, G. Ottersen, A.J. Pershing, H. Walker. 2003. The response of marine ecosystems to climate variability associated with the North Atlantic Oscillation. In J.W. Hurrell, Y. Kushnir, G. Ottersen and M. Visbeck [eds.], *The North Atlantic Oscillation: Climate Significance and Environmental Impact*. Geophysical Monograph Series, p. 211-234.
- Druon, J.-N., W. Schrimpf, S. Dobricic, A. Stips. 2004. Comparative assessment of large-scale marine eutrophication: North Sea and Adriatic Sea as case studies. *Mar. Ecol. Progr. Ser.* **272**: 1-23.
- Edwards, M. 2001. Large-scale temporal and spatial patterns of marine phytoplankton in the north-east Atlantic. PhD, University of Plymouth. pp.220.
- Edwards, M., A.W.G. John, H.G. Hunt, J.A. Lindley. 1999. Exceptional influx of oceanic species into the North Sea late 1997. *J. Mar. Biol. Assoc. of the U.K.* **79**: 737-739.
- Edwards, M., P.C. Reid, B. Planque. 2001. Long-term and regional variability of phytoplankton biomass in the Northeast Atlantic (1960-1995). *ICES J. Mar. Sci.* **58**: 39-49.
- Edwards, M., G. Beaugrand, P.C. Reid, A.A. Rowden, M.B. Jones. 2002. Ocean climate anomalies and the ecology of the North Sea. *Mar. Ecol. Progr. Ser.* **239**: 1-10.
- Edwards, M., A.J. Richardson. 2004. Impact of climate change on marine pelagic phenology and trophic mismatch. *Nature* **430**: 881-884.
- Edwards, E., D.G. Johns, S.C. Leterme, E. Svendsen, A.J. Richardson. 2006. Regional climate change and harmful algal blooms in the northeast Atlantic. *Limnol. Oceanogr.* **51**: 820-829.
- Eisma, D. 1987. The North Sea: an overview. *Phil. Trans. R. Soc. Lond.* **B 316**: 461-485.
- Farran, G.P. 1910. Résumé des observations sur le plancton des mers explorées par le conseil pendant les années 1902-1908. Copepoda. *Bull. Trim. Cons. Explor. Mer. Bull. Plankton* **1**: 60-79.
- Fox, M.F., D.R. Kester, J.A. Yoder. 2005. Spatial and temporal distributions of surface temperature and chlorophyll in the Gulf of Maine during 1998 using SeaWiFS and AVHRR imagery. *Mar. Chem.* **97**: 104-123.
- Fransz, H.G., J.M. Colebrook, J.C. Gamble, M. Krause. 1991. The zooplankton of the North Sea. *Neth. J. Sea Res.* **28**: 1-52.
- Fraser, J.H. 1952. The Chaetognatha and other zooplankton of the Scottish area and their value as biological indicators of hydrographical conditions. *Mar. Res. Scotl.* **2**: 1-52.
- Fraser, J.H. 1969. Variability in the oceanic content of plankton in the Scottish area. *Progr. Oceanogr.* **5**: 145-159.
- Fromentin J.-M., N.C. Stenseth, J. Gjosaeter, T. Johannessen, B. Planque. 1998. Long-term fluctuations in cod and pollack along the Norwegian Skagerrak coast. *Mar. Ecol. Progr. Ser.* **162**: 265-278.

- Fuglister, F.C., L.V. Worthington. 1947. Hydrography of the Western Atlantic; meanders and velocities of the Gulf Stream. *Woods Hole Oceanogr Inst Tech Rep No WHOI: 47-9*.
- Fuglister, F.C., 1972. Cyclonic rings formed by the Gulf Stream 1965-1966. In A. Gordon [ed.], *Studies in Physical Oceanography: A Tribute to George Wüst on his 80th Birthday*. Gordon and Breach, New York, p. 137-168.
- Furnes, G.K. 1992. Climatic variations, oceanographic processes in the North European Sea: a review of the 1970's and 1980's. *Cont. Shelf Res.* **12**: 235-256.
- Garcia-Moliner, G., J.A. Yoder. 1994. Variability in pigment concentration in warm core rings as determined by coastal zone color scanner satellite imagery from the Mid-Atlantic Bight. *J. Geophys. Res.* **99**: 14277-14290.
- Gatien, M. 1976. A study in the slope water region south of Halifax. *J. Fish. Res. Board of Canada* **33**: 2213-2217.
- Gould, R.W., G.A. Fryxell. 1988. Phytoplankton species composition and abundance in a Gulf Stream warm core ring, I. Changes over a five month period. *J. Mar. Res.* **46**: 367-398.
- Godfrey, D. 1999. Carribean Conservation Corporation (CCC) Celebrates 40 Years of Sea Turtle Conservation. CCC Newsletter, Velador, winter 1999.
- Gonzalez, N., R. Anadon, B. Mourino, E. Fernandez, B. Sinha, J. Escanez, D. de Armas. 2001. The metabolic balance of the planktonic community in the North Atlantic Subtropical Gyre: The role of mesoscale instabilities. *Limnol. Oceanogr.* **46**: 946-952.
- Greene, C.H., A.J. Pershing. 2000. The response of *Calanus finmarchicus* populations to climate variability in the Northwest Atlantic: basin-scale forcing associated with the North Atlantic Oscillation. *ICES J. Mar. Sci.* **57**: 1536-1544.
- Greene, C.H., A.J. Pershing. 2003. The flip-side of the North Atlantic Oscillation and modal shifts in slope-water circulation patterns. *Limnol. Oceanogr.* **48**: 319-322.
- Greene, C.H., A.J. Pershing, A. Conversi, B. Planque, C.G. Hannah, D. Sameoto, E. Head, P.C. Smith, P.C. Reid, J.W. Jossi, D.G. Mountain, M.C. Benfield, P.H. Wiebe, E.G. Durbin. 2003. Trans-Atlantic responses of *Calanus finmarchicus* populations to basin-scale forcing associated with the North Atlantic Oscillation. *Progr. Oceanogr.* **58**: 301-312.
- Haliwell, G.R., C.N.K. Mooers. 1979. The space-time structure and variability of the shelf water-slope water and Gulf Stream surface temperature fronts and associated warm-core eddies. *J. Geophys. Res.* **84**: 7707-7725.
- Harris, G.P. 1986. *Phytoplankton Ecology: Structure, Function and Fluctuations*. Chapman and Hall, London. 384 pp.
- Hasegawa, D., H. Yamazaki, R. Lueck, L. Seuront. 2004. How islands stir and cultivate the ocean. *Geophys. Res. Letters* **31**. L16303, doi:10.1029/2004GL020143.

- Haury, L.R., J.A. McGowan, P.H. Wiebe. 1978. Patterns and processes in the time-scales of plankton distributions. In J.H. Steele [ed.], *Spatial Patterns in Plankton Communities*. Plenum press, New York, p. 277-327.
- Hays, G.C., A.J. Warner. 1993. Consistency of towing speed and sampling depth for the continuous plankton recorder. *J. Mar. Biol. Assoc. of the U.K.* **73**: 967-970.
- Hays, G.C., J.A. Lindley. 1994. Estimating chlorophyll a abundance from the 'PCI' recorded by the Continuous Plankton Recorder survey: validation with simultaneous fluorometry. *J. Plankton Res.* **16**: 23-34.
- Hays, G.C., A.J. Warner, A.W.G. John, D.S. Harbour, P.M. Holligan. 1995. Coccolithophores and the continuous plankton recorder survey. *J. Mar. Biol. Assoc. of the U.K.* **75**: 503-506.
- Hays, G.C., D.R. Clark, A.W. Walne, A.J. Warner. 2001. Large scale patterns of zooplankton abundance in the NE Atlantic in June and July 1996. *Deep-Sea Res. II* **48**: 951-961.
- Heath, M.R., E.W. Henderson, G. Slessor, E.M.S. Woodward. 1991. High salinity in the North Sea. *Nature* **352**: 116.
- Heath, M.R., W. Robertson, J. Mardaljevic, W.S.G. Gurney. 1997. Modelling the population dynamics of *Calanus* in the Fair Isle Current off northern Scotland. *J. Sea Res.* **38**: 381-412.
- Hickel, W., M. Eickhoff, H. Spindler. 1995. Long-term investigations of inorganic nutrients and phytoplankton in the German Bight. *Deut. Hydrogr. Z.* **5**: 197-211.
- Hitchcock, G.L., A.J. Mariano, T. Rossby. 1993. Mesoscale pigment fields in the Gulf Stream: observations in a meander crest and trough. *J. Geophys. Res.* **98**: 8425-8445.
- Holligan, P.M. 1987. The physical environment of exceptional phytoplankton blooms in the northeast Atlantic. *Tirés-à-part Rapp. P.-v. Reun. Cons. int. Explor. Mer.* **187**: 9-18.
- Hurrell, J. W. 1995a. Decadal trends in the North Atlantic Oscillation: Regional temperatures and precipitation. *Science* **269**: 676-679.
- Hurrell, J.W. 1995b. Transient eddy forcing of the rotational flow during northern winter. *J. Atm. Sci.* **52**: 2286-2301.
- Hurrell, J.W., Y. Kushnir, G. Ottersen, M. Visbeck. 2003. An Overview of the North Atlantic Oscillation. In J.W. Hurrell, Y. Kushnir, G. Ottersen and M. Visbeck [eds.], *The North Atlantic Oscillation: Climate Significance and Environmental Impact*. Geophysical Monograph Series, p. 1-36.
- Ibañez, F., J.M. Fromentin, J. Castel. 1993. Application de la méthode des sommes cumulées à l'analyse des séries chronologiques océanographiques. *Compte Rendus de l'Académie des Sciences de Paris, Sciences de la vie/Life sciences* **316**: 745-748.
- Irigoien, X., R.P. Harris, R.N. Head, D. Harbour. 2000. NAO and spring bloom phytoplankton composition in the English Channel. *J. Plankton Res.* **22**: 2367-2371.

- Irigoien X., R.P. Harris, H.M. Verheye, P. Joly, J. Runge, M. Starr, D. Pond, R. Campbell, R. Shreeve, P. Ward, A.N. Smith, H.G. Dam, W. Peterson, V. Tirelli, M. Koski, T. Smith, D. Harbour, R. Davidson. 2002. Copepod hatching success in marine ecosystems with high diatom concentrations. *Nature* **419**: 387-389
- Johns, D.G., M. Edwards, A. Richardson, J.I. Spicer. 2003. Increased blooms of a dinoflagellate in the NW Atlantic. *Mar. Ecol. Prog. Ser.* **265**: 283-287.
- Jonas, T.D., A. Walne, G. Beaugrand, L. Gregory, G.C. Hays. 2004. The volume of water filtered by a CPR sample: the effect of ship speed. *J. Plankton Res.* **26**: 1499-1506.
- Jones, R.H., K.J. Flynn. 2005. Nutritional status and diet composition affect the value of diatoms as copepod prey. *Science* **307**: 1457-1459.
- Kaiser, M.J., M.J. Attrill, S. Jennings, D.N. Thomas, D.K.A. Barnes, A.S. Brierley, N.V.C. Polunin, D.G. Raffaelli, P.J. Williams. 2005. *Marine Ecology: Processes, Systems and Impacts*. Oxford University Press. 0-19-924975-X, 584 pp.
- Kendall, M. 1976. *Time-series*, 2nd ed. Charles Griffin and Co Ltd.
- Kendall, M., A. Stuart. 1966. *The Advanced Theory of Statistics*. Hafner.
- Kennelly, M.A., R.H. Evans, T.M. Joyce. 1985. Small scale cyclones on the periphery of a Gulf Stream warm core ring. *J. Geophys. Res.* **95**: 8845-8857.
- Koski M, J. Engstrom, M. Viitasalo. 1999. Reproduction and survival of the calanoid copepod *Eurytemora affinis* fed with toxic and non-toxic cyanobacteria. *Mar. Ecol. Prog. Ser.* **186**: 187-197.
- Krause, M., J.W. Dippner, J. Beil. 1995. A review of hydrographic controls on the distribution of zooplankton biomass and species in the North Sea with particular reference to a survey conducted in January-March 1987. *Progr. Oceanogr.* **35**: 81-152.
- Kushnir, Y., V.J. Cardone, J.G. Greenwood, M. Cane. 1997. On the recent increase in North Atlantic wave heights. *J. Climate.* **10**: 2107-2113.
- Laabir, M., I. Buttino, A. Ianora, G. Kattner, S.A. poulet, G. Romano, Y. Carotenuto, A. Miralto. 2001. Effect of specific dinoflagellate and diatom diets on gamete ultrastructure and fatty acid profiles of the copepod *Temora stylifera*. *Mar. Biol.* **138**: 1241-1250.
- Laane, R.W.P.M., G. Groeneveld, A. de Vries, A.J. Bennekom, J.S. Sydow. 1996. Nutrients (P, N, Si) in the Channel and the Dover Straits: seasonal and year-to-year variation and fluxes to the North Sea. *Oceanol. Acta* **16**: 607-616.
- Lai, D.Y., P.L. Richardson. 1977. Distribution and movement of Gulf Stream rings. *J. Phys. Oceanogr.* **7**: 670-683.
- Lalli, C. M., and T. R. Parsons. 1997. *Biological Oceanography, an Introduction* 2nd ed. Butterworth Heinemann. 314pp.

- Lancelot, C., V. Rousseau, G. Billen, D. van Eeckhout. 1997. Coastal eutrophication of the Southern Bight of the North Sea: assesment and modelling. *NATO-ASI Series*: 439-454.
- Laws, E. 2004. Export flux and stability as regulators of community composition in pelagic marine biological communities: implications for regime shifts. *Progr. Oceanogr.* **60**: 343-354.
- Lee, A. 1970. The currents and water masses of the North Sea. *Oceanogr. Mar. Biol. Ann. Rev.* **8**: 33-71.
- Lee, T., P.C. Cornillon, 1996. Propagation of Gulf Stream meanders between 74° and 70°. *J. Phys. Oceanogr.* **26**: 205-224.
- Legendre, L., S. Demers. 1984. Towards Dynamic Biological Oceanography and Limnology. *Can. J. Fish. Aquat. Sci.* **41**: 2-19.
- Legendre, L., S. Demers, D. Lefaivre. 1986. Biological production at marine ergoclines. In J.C.J. Nihoul [ed.], *Marine Interface Ecohydrodynamics*. Elsevier, Amsterdam, p. 1-29.
- Legendre, P., L. Legendre. 1998. *Numerical Ecology*. 2d english edition. Elsevier science B.V. 853pp.
- Leterme, S.C., M. Edwards, L. Seuront, M.J. Attrill, P.C. Reid, A.W.G. John. 2005. Decadal basin-scale changes in diatoms, dinoflagellates, and phytoplankton color across the North Atlantic. *Limnol. Oceanogr.* **50**: 1244-1253.
- Leterme, S.C., R.D. Pingree. 2006. The Gulf Stream, Rings and North Atlantic Eddy structure from remote sensing (Altimeter and SeaWiFS). *J. Mar. Syst.*, in press.
- Le Traon, P.Y., F. Nadal, N. Ducet. 1998. An improved mapping method of multisatellite altimeter data. *J. Atm. Oceanic Technol.* **15**: 522-534.
- Li, W.K.W. 2002. Macroecological patterns of phytoplankton in the northwestern North Atlantic Ocean. *Nature* **419**: 154-157.
- Lindley, J.A., R. Williams. 1980. Plankton of the Fladen Ground during FLEX 76. II. Population dynamics and production of *Thysanoessa inermis* (Crustacea: Euphausiacea). *Mar. Biol.* **57**: 79-86.
- Lindley, J.A., J. Roskell, A.J. Warner, N. Halliday, G. H. Hunt, A.W.G. John, T.D. Jonas. 1990. Doliolids in the German Bight in 1989: evidence for exceptional inflow into the North Sea. *J. Mar. Biol. Assoc. of the U.K.* **70**: 679-682.
- Lindley, J.A., S.D. Batten. 2002. Long-term variability in the diversity of North Sea zooplankton. *J. Mar. Biol. Assoc. of the U.K.* **82**: 31-40.
- Lindley, J.A., P.C. Reid, K. Brander. 2003. Inverse relationship between cod recruitment in the North Sea and young fish in the Continuous Plankton Recorder survey. *Sci. Mar.* **67**: 191-200.

- Longhurst, A. 1998. *Ecological Geography of the Sea*, edited by Academic Press Ltd, London. 398pp.
- Lluch-Belda, D., R. J. M. Crawford, T. Kawasaki, A. D. McCall, R. H. Parrish, R. A. Schwartzlose, P. E. Smith. 1989. Worldwide fluctuations of sardine and anchovy stocks: The regime problem. *South African J. Mar. Sci.* **8**: 195-205.
- Mackas, D.L., K.L. Denman, M.R. Abbot. 1985. Plankton patchiness : biology in the physical vernacular. *Bull. Mar. Sci.* **37**: 652-674.
- Margalef, R. 1975. Assessment of the effects on plankton. In E.A. Pearson and E. De Fraja Frangipane [eds.], *Marine Pollution and Marine Waste Disposal Proceedings of the 2nd International Congress*, San Remo 17-21 dec. 1973, p. 301-306.
- Margalef, R. 1978. What is an upwelling ecosystem? In R. Boje and M. Tomczak [eds.], *Upwelling Ecosystems*. Springer-Verlag, Berlin, p. 12-14.
- Margalef, R. 1997. Turbulence and marine life. *Sci. Mar.* **61**: 109-123.
- Marshall, J., Y. Kushnir, D. Battisti, P. Chang, J. Hurrell, M. McCartney, M. Visbeck. 1997. A white paper on Atlantic climate variability. <http://geoid.mit.edu/accp/avehtml.html>
- McGillicuddy, D.J., A.R. Robinson. 1997. Eddy induced nutrient supply and new production in the Sargasso Sea. *Deep-Sea Res.* **144**: 1427-1449.
- MERCINA. 2001. Gulf of Maine/Western Scotian Shelf ecosystems respond to changes in ocean circulation associated with the North Atlantic Oscillation. *Oceanography* **14**: 76-82.
- Moser, H. G., R. L. Charter, P. E. Smith, D. A. Ambrose, W. Watson, S. R. Charter, E. M. Sandknop. 2001. Distributional atlas of fish larvae and eggs in the Southern California Bight region: 1951-1998. CalCOFI atlas n°38.
- Mueller, J.L., R.W. Austin. 1995. Ocean optics protocols for SeaWiFS validation, Revision 1, SeaWiFS Technical Report Series, Vol. 25. S.B. Hooker, E.R. Firestone and J.G. Acker [eds.], *NASA Technical Memorandum 104566*. Greenbelt, Maryland, 67pp.
- Nixon, S.W. 1995. Coastal marine eutrophication: a definition, social causes, and future concerns. *Ophelia* **41**: 199-219.
- Oceanographic Laboratory Edinburgh. 1973. Continuous Plankton Records: a plankton atlas of the North Atlantic and the North Sea. *Bull. Mar. Ecol.* **7**:1-174
- Ohman, M.D., H.J. Hirche. 2001. Density-dependent mortality in an oceanic copepod population. *Nature* **412**: 638-641.
- Otto, L., J.T.F. Zimmermann, G.K. Furnes, M. Mork, R. Sætre, G. Becker. 1990. Review of physical oceanography of the North Sea. *Neth. J. Sea Res.* **26**: 161-238.
- Petrie, B., F.F. Drinkwater. 1993. Temperature and salinity variability on the Scotian Shelf and in the Gulf of Maine 1945-1990. *J. Geophys. Res.* **98**: 20079-20089.

- Petrie, B., P. Yeats. 2000. Annual and interannual variability of nutrients and their estimated fluxes in the Scotian Shelf-Gulf of Maine region. *Can. J. Fish. Aqu. Sci.* **57**: 2536-2546.
- Pickart, R.S., T.K. McKee, D.J. Torres, S.A. Harrington. 1999. Mean structure and interannual variability of the slope water system south of Newfoundland. *J. Phys. Oceanogr.* **29**: 2541-2558.
- Pingree, R.D., P.M. Holligan, G.T. Mardell. 1979. Phytoplankton growth and cyclonic eddies. *Nature* **278**: 245-247.
- Pingree, R.D., D.K. Griffiths. 1980. Currents driven by a steady uniform wind stress on the shelf seas around the British Isles. *Oceanol. Acta* **3**: 227-236.
- Pingree, R.D., B. Le Cann. 1989. Celtic and Armorican slope and shelf residual currents. *Progr. Oceanogr.* **23**: 303-338.
- Pingree, R.D., B. Sinha, 2001. Westward moving waves or eddies (Storms) on the Subtropical / Front near 32.5°N ? Interpretation of the Eulerian currents and temperature records at moorings 155 (35.5°W) and 156 (34.4°W). *J. Mar. Syst.* **29**: 239-276.
- Pingree, R.D. 2002. Ocean structure and climate (Eastern North Atlantic) : in situ measurement and remote sensing altimeter. *J. Mar. Biol. Assoc. of the U.K.* **82**: 681-707.
- Pingree, R.D. 2005. North Atlantic and North Sea Climate Change: curl up, shut down, NAO and Ocean Colour. *J. Mar. Biol. Assoc. of the U.K.* **85**: 1301-1315.
- Planque, B., A.H. Taylor. 1998. Long-term changes in zooplankton and the climate of the North Atlantic. *ICES J. Mar. Sci.* **55**: 644-654.
- Poulet, S.A., M. Laabir, A. Ianora, A. Miralto. 1995. Reproductive response of *Calanus helgolandicus*. I. Abnormal embryonic and naupliar development. *Mar. Ecol. Prog. Ser.* **129**: 85-95.
- Rae, K.M. 1952. Continuous Plankton Records: explanation and methods, 1946-1949. *Hull Bull. Mar. Ecol.* **3**: 135-155.
- Rae, K.M., J.H. Fraser. 1941. Continuous Plankton Records: the copepods of the Southern North Sea, 1932-37. *Hull Bull. Mar. Ecol.* **1**: 171-238.
- Rae, K.M., C.B. Rees. 1947. Continuous Plankton Records: the copepods in the North Sea, 1938-39. *Hull Bull. Mar. Ecol.* **2**: 95-132.
- Raitsos, D.E., P.C. Reid, S.J. Lavender, M. Edwards, A.J. Richardson. 2005. Extending the SeaWiFS chlorophyll data set back 50 years in the northeast Atlantic. *Geophys. Res. Letters* **32**: L06603, doi:10.1029/2005GL022484.
- Ramp, S.R. 1986. The interaction of warm core rings with the shelf water and shelf-slope front south of New England. Ph.D. Thesis, University of Rhode Island.
- Reid, P.C. 1975. Large scale changes in North Sea phytoplankton. *Nature* **257**: 217-219.

- Reid, P.C. 1978. Continuous Plankton Records: Large-scale changes in the abundance of phytoplankton in the North Sea from 1958 to 1973. *Rapp. P.-v. Reun. Cons. int. Explor. Mer.* **172**: 384-389.
- Reid, P.C., G.A. Robinson, H.G. Hunt. 1987. Spatial and temporal patterns of marine blooms in the Northeastern Atlantic and North Sea from the Continuous Plankton Recorder survey. *Rapp. P.-v. Reun. Cons. int. Explor. Mer.* **187**: 27-37.
- Reid, P.C., S.C. Surey-Gent, H.G. hunt, A.E. Durrant. 1992. *Thalassiothrix longissima*, a possible oceanic indicator species in the North Sea. *ICES Mar. Sci. Symp.* **195**: 268-277.
- Reid, P.C., M. Edwards, H.G. Hunt, A. J. Warner. 1998. Phytoplankton change in the North Atlantic. *Nature* **391**: 546.
- Reid, P.C., M. Edwards. 2001. Long-term changes in the pelagos, benthos and fisheries of the North Sea. *Senckenbergiana Maritima* **31**: 107-115.
- Reid, P.C., M. Borges, E. Svendsen. 2001. A regime shift in the North Sea circa 1988 linked to changes in the North Sea horse mackerel fishery. *Fish. Res.* **50**: 163-171.
- Reid, P.C., M. Edwards, G. Beaugrand, M.D. Skogen, D. Stevens. 2003. Periodic changes in the zooplankton of the North Sea during the twentieth century linked to oceanic inflow. *Fish. Oceanogr.* **12**: 260-269.
- Richardson, A.J., D.S. Schoeman. 2004. Climate impact on plankton ecosystems in the Northeast Atlantic. *Science* **305**: 1609-1912.
- Richardson, A.J., A.W. Walne, A.W.G. John, T.D. Jonas, J.A. Lindley, D.W. Sims, D. Stevens, M. Witt. 2006. Using continuous plankton recorder data. *Progr. Oceanogr.* **68**: 27-74.
- Richardson, K. 1997. Harmful or exceptional blooms in the marine ecosystem. *Adv. Mar. Biol.* **31**: 301-385.
- Richardson, P.L. 1980. Gulf Stream ring trajectories. *J. Phys. Ocean.* **10**: 90-104.
- Richardson, P.L., 1983. *Gulf Stream Rings*. In A.R. Robinson [ed.], *Eddies in Marine Science*. Springer-Verlag, Berlin, p. 19-45.
- Riley, G.A. 1941. Plankton studies. V. Georges Bank, *Bulletin of the Bingham Oceanographic Collection* **7**: 1-73.
- Robertson, A. E. 1968. The continuous plankton recorder: a method for studying the biomass of calanoid copepods. *Bull. Mar. Ecol.* **6**: 185-223.
- Robinson, G.A., A.R. Hiby. 1978. The Continuous Plankton Recorder survey. In A. Sournia [ed.], *Phytoplankton manual*. UNESCO. 337pp.
- Rodriguez, J., J. Tintore, J.T. Allen, J.M. Blanco, D. Gomis, A. Reul, J. Ruiz, V. Rodriguez, F. Echevarria, F. Jimenez-Gomez. 2001. Mesoscale vertical motion and the size structure of phytoplankton in the ocean. *Nature* **401**: 360-363.

- Rogers, J.C. 1990. Patterns of low frequency monthly sea level pressure variability (1899-1986) and associated wave cyclone frequencies. *J. Clim.* **3**: 1364-1379.
- Ryan, J.P., J.A. Yoder, J.A. Barth, P.C. Cornillon. 1999. Chlorophyll enhancement and mixing associated with meanders of the shelf break front in the Mid-Atlantic Bight. *J. Geophys. Res.* **104**: 23479-23493.
- Ryan, J.P., J.A. Yoder, D.W. Townsend. 2001. Influence of a Gulf Stream warm-core ring on water mass and chlorophyll distributions along the southern flank of Georges Bank. *Deep-Sea Res. II, Top. Stud. Oceanogr.* **48**: 159-178.
- Saetre, R, J. Aure, D.S. Danielssen. 2003. Long-term hydrographic variability patterns off the Norwegian coast and in the Skagerrak. *ICES Mar. Sci. Symp.* **219**: 150-159.
- Sameoto, D. 2001. Decadal changes in phytoplankton color index and select calanoid copepods in continuous plankton recorder data from the Scotian Shelf. *Can. J. Fish. Aquat. Sci.* **58**: 749-761.
- Scheffer, M., S. Carpenter, J.A. Foley, C. Folke, B. Walker. 2001. Catastrophic shifts in ecosystems. *Nature* **413**: 591-596.
- Scherrer, B. 1984. *Biostatistique*. G. Morin [ed.], Québec, Canada. 850pp.
- Schollaert, S.E., T. Rossby, J.A. Yoder. 2004. Gulf Stream cross-frontal exchange: possible mechanisms to explain interannual variations in phytoplankton chlorophyll in the Slope Sea during the SeaWiFS years. *Deep-Sea Res. II* **51**: 173-188.
- Schrum, C. 2001. Regionalization of climate change for the North Sea and Baltic Sea. *Clim. Res.* **18**: 31-37.
- Seuront, L., S. Souissi. 2002. Climatic control of *Phaeocystis* spring bloom in the Eastern English Channel (1991-2000). *La Mer* **40**: 41-51.
- Seuront, L., D. Vincent, J.G. Mitchell. 2006. Biologically induced modification of seawater viscosity in the eastern English Channel during a *Phaeocystis globosa* spring bloom. *J. Mar. Syst.*, in press.
- Sims, D.W., P. Reid. 2002. Congruent trends in long-term zooplankton decline in the North-east Atlantic and basking shark (*Cetorhinus maximus*) fishery catches off west Ireland. *Fish. Oceanogr.* **11**: 59-63.
- Singler, H.R., T.A. Villareal. 1995. Nitrogen inputs into the euphotic zone by vertically migrating *Rhizosolenia* mats. *J. Plankton Res.* **27**: 545-556.
- Sinha, B., B. Topliss, J. Harle. 2004. Eastward propagating surface anomalies at ocean gyre boundaries. *J. Geophys. Res.* **109**: doi:10.1029/2004JC002393.
- Skogen, M., E. Svendsen, J. Berntsen, D. Aksnes, K. Ulvestad. 1995. Modelling the primary production in the North Sea using a coupled 3 dimensional physical chemical biological ocean model. *Estuar. Coast. Shelf Sci.* **41**: 545-565.

- Skogen, M., E. Svendsen, M. Ostrowski. 1997. Quantifying volume transports during SKAGEX with the Norwegian ecological model system. *Cont. Shelf Res.* **17**: 1817-1837.
- Skogen, M., H. Soiland. 1998. *A user's guide to NORWECOM v2.0. The NORWegian ECOlogical Model system*. Tech. Rep. Fisker og Havet 18/98. Institute of marine Research, Pb.1870, N-5024 Bergen. 42pp.
- Smayda, T., D. Borkman, G. Beaugrand, A. Belgrano. 2004. Ecological effects of climatic variations in the North Atlantic. In N. Stenseth, G. Ottersen, J. Hurrell, A. Belgrano [eds.], *Marine Ecosystems and Climate Variation*, Oxford University Press, p. 49-58.
- Smith, P.C., R.W. Houghton, R.G. Fairbanks, D.G. Mountain. 2001. Interannual variability of boundary fluxes and water mass properties in the Gulf of Maine and on Georges Bank 1993-1997. *Deep-Sea Res. II* **48**: 37-70.
- Soiland, H., M. Skogen. 2000. Validation of a 3-D biophysical model using nutrient observations in the North Sea. *ICES J. Mar. Sci.* **57**: 816-823.
- Sokal, R.R., F.J. Rohlf. 1995. *Biometry*, 3d ed. Freeman. 850pp.
- Somerfield, P.J., K.R. Clarke. 1995. Taxonomic levels, in marine community studies, revisited. *Mar. Ecol. Progr. Ser.* **127**: 113-119.
- Stephens, J.A., M.B. Jordan, A.H. Taylor, R. Proctor. 1998. The effects of fluctuations in North Sea flows on zooplankton abundance. *J. Plankton Res.* **20**: 943-956.
- Stockton, C.W., M.F. Glueck. 1999. Long-term variability of the North Atlantic oscillation (NAO). *Proc. Amer. Met. Soc. Tenth Symp. Global Change Studies, 11-15 January, 1999, Dallas, TX*, 290-293.
- Stommel, H. 1958. *The Gulf Stream*. Cambridge University Press, London. p. 202.
- Svendsen, E., R. Sætre, M. Mork. 1991. Features of the northern North Sea circulation. *Cont. Shelf Res.* **11**: 493-508.
- Svendsen, E., A.K. Magnusson. 1992. Climatic variability in the North Sea. *ICES Mar. Sci. Symp.* **195**: 144-158.
- Svendsen, E., A. Aglen, S.A. Iversen, D.W. Skagen, O. Smestad. 1995. Influence of climate on recruitment and migration of fish stocks in the North Sea. In R.J. Beamish [ed.], *Climate change and northern fish population*. *Can. Spe. Publ. in Fish. and Aqu. Sci.* **121**: 641-653.
- Sverdrup, H.U. 1953. On conditions of the vernal blooming of phytoplankton. *J. Cons. Int. Explor. Mer* **18**: 287-295.
- Sy, A., M. Rhein, J.R.N. Lazier, K.P. Koltermann, J. Meincke, A. Putzka, M. Bersch. 1997. Surprisingly rapid spreading of newly formed intermediate waters across the North Atlantic Ocean. *Nature* **386**: 675-679.

- Taylor, A.H., J.A. Stephens. 1998. The North Atlantic Oscillation and the latitude of the Gulf Stream. *Tellus* **50A**: 134-142.
- The Ring Group, 1981. Gulf Stream cold core rings: their physics, chemistry, and biology. *Science* **212**: 1091-1100.
- Thomas, C.R. 1997. *Identifying Marine Phytoplankton*. Academic Press Limited, London.
- Thomas, A.C., D.W. Townsend, R. Weatherbee. 2003. Satellite-measured phytoplankton variability in the Gulf of Maine. *Cont. Shelf Res.* **23**: 971-989.
- Thompson, D.W.J., J.M. Wallace. 1998. The arctic oscillation signature in the wintertime geopotential height and temperature fields. *Geophys. Res. Letters* **25**: 1297-1300.
- Tomczak, M., J.S. Godfrey. 1994. *Regional Oceanography*, Pergamon, Elmsford, NY. 442pp.
- Tomczak, M., G. Stuart. 2003. *Regional Oceanography: an introduction*. 2nd ed., Daya Publishing House, Delhi. 382 pp.
- Turrell, W.R., E.W. Henderson, G. Slesser. 1990. Residual transport within the Fair Isle Current observed during the Autumn Circulation Experiment (ACE). *Cont. Shelf Res.* **10**: 521-543.
- Turrell, W.R., E.W. Henderson, G. Slesser, R. Payne, R.D. Adams. 1992. Seasonal changes in the circulation of the Northern North Sea. *Cont. Shelf Res.* **12**: 257-286.
- Turrell, W.R., G. Slesser, R. Payne, R.D. Adams, P.A. Gillibrand. 1996. Hydrography of the East Shetland Basin in relation to decadal North Sea variability. *ICES J. Mar. Sci.* **53** : 899-916.
- van der Spoel, S., 1994. The basis for boundaries in pelagic biogeography. *Progr. Oceanogr.* **34**: 121-133.
- Villareal, T.A. 1992. Buoyancy properties of the giant diatom *Ethmodiscus*. *J. Plankton Res.* **14**: 459-463.
- Villareal, T.A., M.A. Altabet, C. Rymaszak. 1993. Nitrogen transport by vertically migrating diatom mats in the North Pacific Ocean. *Nature* **363**: 709-712.
- Villareal, T.A., C. Pilskaln, M. Brzezinski, F. Lipschultz, M. Dennett, G. Gardner. 1999. Upward transport of oceanic nitrate by migrating diatom mats. *Nature* **397**: 423-425.
- Visbeck, M., E.P. Chassignet, R. Curry, T. Delworth, B. Dickson, G. Krahnmann. 2003. The Ocean's Response to North Atlantic Oscillation Variability. In J.W. Hurrell, Y. Kushnir, G. Ottersen and M. Visbeck [eds.], *The North Atlantic Oscillation: Climate Significance and Environmental Impact*. Geophysical Monograph Series, p. 113-146.
- Walker, G.T., E.W. Bliss. 1932. World weather V. *Mem. Roy. Meteor. Soc.* **4**: 53- 84.
- Walsh, J.E., W.L. Chapman, T.L. Shy. 1996. Recent decrease of sea level pressure in the central Arctic. *J. Clim.* **9**: 480-486.

- Warner, A.J., G.C. Hays. 1994. Sampling by the continuous Plankton Recorder survey. *Progr. Oceanogr.* **34**: 237-256.
- Watts, D.R., 1983. Gulf stream variability. In A.R. Robinson [ed.], *Eddies in Marine Science*. Springer Verlag, p. 115-144.
- Williams, R., J. A. Lindley. 1980. Plankton of the Fladen Ground During FLEX 76. I. Spring development of the plankton community. *Mar. Biol.* **57**: 73-78.
- Witbaard, R., G.C.A. Duineveld, P.A.W.J. De Wilde. 1997. A long-term growth record from *Arctica islandica* (Mollusca, Bivalva) from the Fladen Ground (northern North Sea). *J. Mar. Biol. Assoc. of the U.K.* **77**: 801-816.
- Wyatt, T., J. Horwood. 1973. Model which generates red tides. *Nature* **244**: 238-240.
- Yoder, J.A., J.E. O'Reilly, A.H. Barnard, T.S. Moore, C.M. Rusham. 2001. Variability in Coastal Zone Color Scanner (CZCS) chlorophyll imagery of ocean margin waters off the U.S. east coast. *Cont. Shelf Res.* **21**: 1191-1218.
- Zar, J.H. 1996. *Biostatistical analysis*, 3rd ed. Printice-Hall, Inc. 718 pp.

Copyright statement

This copy of the thesis has been supplied on condition that anyone who consults it is understood to recognise that its copyright rests with its author and that no quotation from the thesis and no information derived from it may be published without author's prior consent.